The Role and Function of Clusterin in Normal and Fibrotic Lung.

By Lizzy Peix

A thesis submitted to University College London for the degree of Doctor of Philosophy

Centre for Inflammation and Tissue Repair,
UCL Respiratory,
Rayne Institute, University College London,
5 University Street, London, WC1E 6JF.

DECLARATION

I, Lizzy Peix, confirm that the work presented in this thesis is my own. Where information has been derived from other sources, I confirm that this has been indicated in this thesis.

Lizzy Peix

30/03/2017

Date

ABSTRACT

Pulmonary fibrosis is a progressive scarring disorder of the lung with a dismal prognosis and no curative therapy. Clusterin, a multifunctional glycoprotein with extracellular chaperone activity and involved in regulating cell function, is reduced in bronchoalveolar lavage fluid of patients with pulmonary fibrosis. However, its distribution and role in normal and fibrotic lung are incompletely characterised. Immunohistochemical localisation of clusterin in human lung revealed strong staining associated with fibroblasts in control lung and morphologically normal areas of fibrotic lung but weak or undetectable staining in fibroblasts in fibrotic regions and particularly fibroblastic foci. Clusterin also co-localised with elastin in vessel walls and additionally with amorphous elastin deposits in fibrotic lung. Analysis of primary lung fibroblast isolates *in vitro* confirmed the down-regulation of clusterin expression in fibrotic compared with control lung fibroblasts and further demonstrated that TGF-β_1 is capable of down-regulating fibroblast clusterin expression. shRNA-mediated down-regulation of clusterin did not affect TGF-β_1-induced fibroblast-myofibroblast differentiation but inhibited fibroblast proliferative responses and sensitised to apoptosis. Together, these data demonstrate that clusterin promotes lung fibroblast proliferation and survival. Down-regulation of clusterin in fibrotic lung fibroblasts at least partly due to increased TGF-β_1 may, therefore, represent an appropriate but insufficient response to limit fibroproliferation. Reduced expression of clusterin in the lung may also limit its extracellular chaperoning activity contributing to dysregulated deposition of extracellular matrix proteins. Alveolar macrophages express clusterin receptor LRP2, suggesting that these cells are responsive to altered clusterin in the lung. *In vitro* studies with human alveolar and blood-derived macrophages, demonstrate that exogenous clusterin induces the secretion of pro-inflammatory cytokines/chemokines, including TNFα, suggesting a clusterin-mediated polarisation towards an “M1-like” phenotype. Reduced levels of secretory clusterin in the fibrotic lung may, therefore, benefit polarisation towards “M2-like” macrophages, which produce pro-fibrotic mediators, including TGF-β_1, resulting in further clusterin reduction and progression of pulmonary fibrosis.

ACKNOWLEDGEMENTS

Firstly, I wish to express my sincerest gratitude to my primary supervisor Professor Robin McAnulty for his scientific guidance, motivating reliance, and patience throughout the duration of this project. Robin's support, supervision and many discussions with him have helped me to grow as a scientist, apply critical thinking and further strengthened my passion for science. Moreover, I would like to express my special thanks to Robin for appraising this thesis.

Dr Toby Maher, my secondary, academic supervisor for his preliminary research that has let to this project and his helpful scientific feedback on the project. I would also express my special thanks to my secondary, industrial supervisor Dr Juliet Simpson, for her guidance and humble support in several aspects for my projects at GSK laboratories.

Special thanks are due to my GSK laboratory supervisors Dr David Budd, Dr Susan Boyce, and Dr Sarah Hotee for their support and guidance during the project at GSK. My group and colleagues at UCL for all their positivity and support, assistance and scientific feedback, including David Pearce, Dr Iona Evans, Jo Barnes and researchers of the Centre for Inflammation and Tissue Repair, these include in no specific order: Manuela Platè, Jessica Eley, Deborah Chong, Sofia Da Silva Lourenco, Pascal Durrenberger, Robert Alexander, Hannah Woodcock, Noura Al-Juffali, Sharada Karanam, Ricardo Jose and Ellen Forty.

I would like to thank Catherine King and the Cancer Institute Cancer Genome Engineering Facility, UCL for the provision of lentiviral stocks and Professor David Abraham and the Centre for Rheumatology and Connective Tissue Diseases, UCL for the provision of primary SSc lung fibroblasts. The research presented in this thesis was founded by the Biotechnology and Biological Sciences Research Council (BBSRC) and GlaxoSmithKline (GSK).
Finally, I would like to thank my parents, Mathias and Christiane for their motivation and support throughout my studies and this PhD project.

Last but definitely not the least, I would like to thank my fiancé, Wilhelm, for his unfailing support, encouragement, and his immense patience during those four years.

To Wilhelm

TABLE OF CONTENTS

LIST OF FIGURES

LIST OF TABLES

ABBREVIATIONS

ATS	American Thoracic Society
AE	Acute exacerbation
BALF	Bronchoalveolar lavage fluid
BCA	Bicinchoninic acid
BEAS-2B	Immortalised human bronchial epithelial cells
BLAST	Basic Local Alignment Search Tool
BMP1	Bone morphogenic protein 1
bp	Base pairs
BSA	Bovine serum albumin
COPD	Chronic obstructive pulmonary disease
COX	Cyclooxygenase
Ct	Threshold cycle
DAB	3,3'-diaminobenzdine
DAPI	4',6-diamidino-2-phenylindole
ddH_2O	Double-distilled water
DEPC	Diethylpyrocarbonate
DMEM	Dulbecco's modified eagle's medium
DMSO	Dimethyl sulfoxide
DNA	Deoxyribonucleic acid
DPBS	Dulbecco's phosphate-buffered saline
DTT	Dithiothreitol
ECM	Extracellular matrix
EDTA	Ethylenediaminetetracetic acid
EGF	Epidermal growth factor
ELISA	Enzyme-linked immunoassay
ER	Endoplasmic Reticulum
ERS	European Respiratory Society
FasL	Fas ligand
FBS	Foetal bovine serum
FLS	Fibroblast-like synoviocytes
HBEC	Human bronchial epithelial cells
HBSS	Hank's Balanced Saline Solution
HDAC	Histone deacetylase
HPLC	High pressure liquid chromatography

HRCT	High-resolution computed tomography
HRP	Horseradish-peroxidase
HUVEC	Human umbilical vein endothelial cells
IFN	Interferon
IFNγ	Interferon gamma
IGF	Insulin-like growth factor
IL	Interleukin
ILD	Interstitial ling disease
IPF	Idiopathic Pulmonary Fibrosis
kDa	Kilo Dalton
LAP	Latency-associated peptide
LLC	Large latency complex
LPS	Lipopolysaccharides
LRP2	Low-density lipoprotein-related protein 2
LTGF	Latent TGF-beta binding protein
M-CSF	Macrophage colony-stimulating factor
M1	M1 like macrophage phenotype
M2	M2 like macrophage phenotype
MAPK	Mitogen activated protein kinase
MCP-1	Monocyte chemoattractant protein-1
MIF	Macrophage migration inhibitory factor
MIP-1α/β	Macrophage Inflammatory Proteins alpha/ beta
MMP	Matrix metalloproteinases
MOI	Multiplicity of infection
OD	Optical density
PASMC	Pulmonary artery smooth muscle cells
PBMC	Peripheral blood mononuclear cell
PBS	Phosphate buffered saline
PDE	Phosphodiesterase
PDGF	Platelet-derived growth factor
PF	Pulmonary fibrosis
PFA	Paraformaldehyde
PG	Prostaglandin
PGE_2	Prostaglandin E2
PI3K	Phosphatidylinositol-3 kinase
PSMC	Pulmonary artery smooth muscle cells

PVDF	Polyvinylidene difluoride
QC	Quality control
qRT-PCR	Real-time quantitative reverse transcription polymerase chain reaction
RANTES	Regulated on activation, normal T cell expressed and secreted
RIN	RNA integrity number
RIPA	Radioimmunoprecipitation assay buffer
RISC	RNA Interference Specificity Complex
RNA	Ribonucleic acid
ROS	Reactive oxygen species
RT	Room temperature
RT-PCR	Reverse transcription polymerase chain reaction
SDS	Sodium dodecyl sulphate
SDS-PAGE	Sodium dodecyl sulphate polyacrylamide gel electrophoresis
SEM	Standard error of mean
shRNA	Short hairpin RNA
siRNA	Small interfering RNA
TBS	Tris-buffered saline
TBST	Tris-buffered saline tween
TdT	Terminal deoxynucleotidyl transferase
TGF-β_1	Transforming growth factor beta 1
TIMP	Tissue inhibitors of matrixmetalloproteinases
TMB	Tetramethylbenzidine
TNFα	Tumour necrosis factor alpha
UIP	Usual interstitial pneumonia
UV	Ultraviolet
v/v	Volume/volume per cent
VEGF	Vascular endothelial growth factor
VSMC	Vascular Smooth muscle cells
w/v	Weight/Volume per cent
αSMA	Alpha smooth muscle actin
EtOH	Ethanol
HCL	Hydrogen chloride
HEK 293 cells	Human Embryonic Kidney 293 cells

1 Introduction

1.1 Lung structure and function

The human lungs are located in the chest on either side of the heart and vessels in the chest cavity. Their main function is to supply the body with oxygen and remove carbon dioxide from the circulation. To deliver oxygen to the body, air is inhaled and guided by structural passageways of the lung through a branching system consisting of trachea, bronchi, bronchioles and alveoli.

1.1.1 Alveolar capillary unit

The lung is essential for gas exchange by introducing oxygen (O_2) into the body and by removing carbon dioxide (CO_2). The gas exchange takes place in minuscule air sacs, called alveoli. These small respiratory sacs are located at the end of bronchioles, surrounded by pulmonary capillaries. Figure 1.1 shows a schematic of the alveolar-capillary unit where gas exchange takes place. Besides gas exchange, this unit is essential for oxygen sensing, the redistribution of the pulmonary blood flow, as well as fluid balance and serves as a physical barrier against environmental toxins and pathogens. Physical or chemical damage of this unit is frequently occurring throughout life and is opposed by tightly regulated cellular mechanisms orchestrated to induce wound repair via key molecules involved in tissue homeostasis. However, when these repair mechanisms fail to contribute to the functional reconstruction of the alveolar structure, gas exchange is impaired, with life threatening consequences. The destruction of the alveolar structure is, therefore, discussed as one of the earliest events leading to a large number of pulmonary diseases, including pulmonary fibrosis (Maher et al. 2007; Chambers 2008; Datta et al. 2011), chronic obstructive pulmonary disease (COPD) (Chilosi et al. 2012), emphysema (Rennard et al. 2006) and asthma (Shifren et al. 2012). The following sections focus on the cellular and matrix structures of the alveolar-capillary unit that have been associated with the pathogenesis of pulmonary fibrosis.

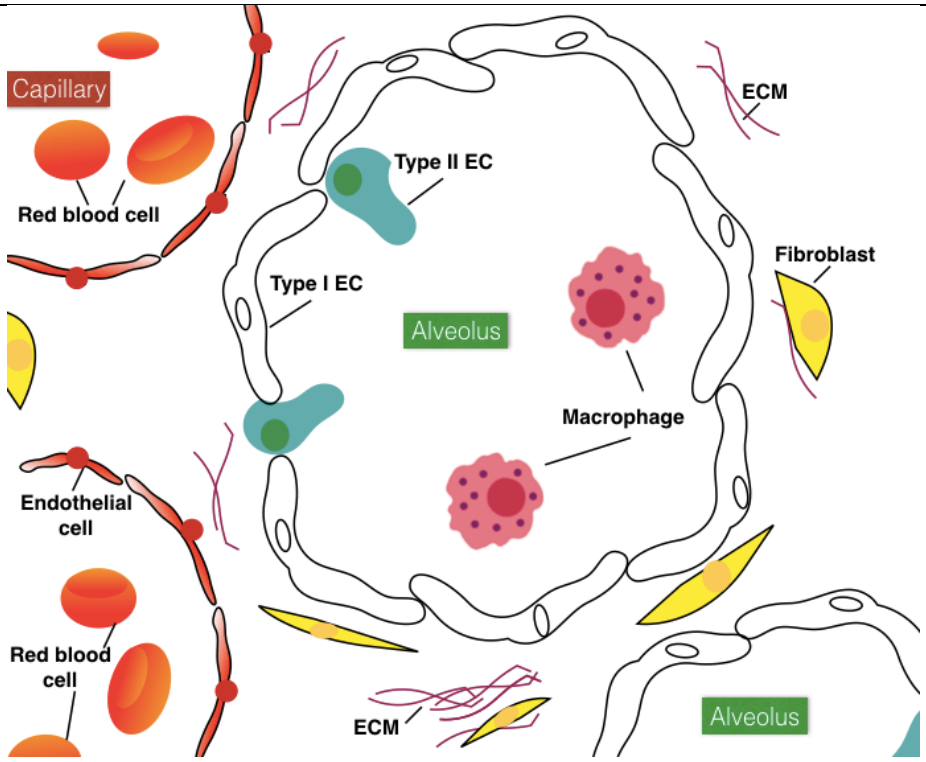

Figure 1.1 Schematic cross section of the alveolar-capillary unit.

The alveolar capillary unit is compromised of three primary components: the epithelium, the endothelium, and the basement membrane with different cellular and extracellular interstitial constituents (Simionescu 1980). These components form a thin lining between blood and air, allowing the reverse diffusion of O_2 and CO_2. 95 % of the alveolus is lined by EC type I cells and 5 % are cuboidal type II EC. The other component of the blood air barrier is formed of flattened extensions of capillary endothelial cells connected via tight junctions to form a fluid barrier. Alveolar macrophages are located in the alveolar space closely associated with EC type I cells and are involved in the defence mechanism of the lungs. The alveolar wall also contains fibroblasts, and occasionally mononuclear cells and ECM proteins. EC - epithelial cell, ECM - extracellular matrix (David Kaminsky 2011).

1.1.2 Extracellular matrix

The blood-air barrier consists of epithelial and endothelial cells and basement membrane. Respiratory gases located in the alveolar space, have to conquer the surface lining surfactant, alveolar epithelium, basement membrane, and the microvascular endothelium before entering the blood stream and *vice versa*. It is noteworthy that the gas transfer occurs passing a distance of 0.2 to 0.6 µM (Adds et al. 2001). Due to the fragile structure of thin alveolar walls, it is relevant that the basement membrane is constituted of extracellular matrix that is highly resistant to physical and mechanical stress. The extracellular matrix is a term for

acellular components of the basement membrane and interstitial tissue. The composition of the extracellular matrix (ECM) and the interaction with cellular components is essential to maintain the function of the lung: The ECM forms a three-dimensional network to provide structural support for cells but also supports various cellular responses including cytoskeletal formation for adhesion and focal contacts as well as cell differentiation, the formation of stress fibres, proliferation, and migration (Dunsmore & Rannels 1996).

The ECM of the basement membrane is predominantly formed by type IV collagen, laminin, entactin and proteoglycans, while the pulmonary interstitium encompasses constituents such as fibrillar collagens, elastic fibres and proteoglycans (Dunsmore & Rannels 1996). During development and wound repair, other components such as fibronectin and tenascin form a provisional matrix (Dunsmore & Rannels 1996). Collagen is the most abundant fibrous ECM constituent (Frantz et al. 2010) and provides tensile strength to the lung tissue. Collagen exists in 28 different types, however, collagen type I and III form 95 % of the lung parenchymal collagen (Last & Reiser 1984). Collagen also locates to the tracheobronchial tree, and alveolar interstitium (Hance et al. 1976). As outlined in **Figure 1.2**, collagen biosynthesis involves the formation of a triple helix and crosslinking for the formation of collagen fibrils (Chen & Raghunath 2009). Collagen and elastin are the most frequent non-cellular structural proteins in the lung (Townsley 2013). Similarly to collagen, elastin has an important role in the formation of new alveoli, by promoting alveolar wall resiliency and patency (Dunsmore & Rannels 1996), and its assembly and crosslinking into a functional polymer are essential for the functionality of the ECM (Kozel et al. 2006). Elastin provides elasticity and flexibility to the lung tissue since each elastin molecule uncoils into a more extended conformation when the fibre is stretched and recoils spontaneously when the force declines (Alberts et al. 2014). Although both collagen and elastin require lysyl oxidase for the crosslinking steps, the chemistry underlying these crosslinks is distinct for each protein (Alberts et al. 2014). Both elastin and collagen are important components of the airways, vessel walls and the lung parenchyma, while elastin is also located to the outermost lamina of small vessel walls or in alveolar septal walls (Townsley 2013).

(A) Fibrillar collagen	(B) Elastin
Transcription	
Synthesis of procollagen chains	Synthesis of tropoelastin chains
Posttranslational Modification: prolyl hydroxylation, glycosylation, disulfide bond formation	Posttranslational Modification: prolyl hydroxylation
Formation of triple helix with chaperone HSP47	No helix formation
Secretion of procollagen into the extracellular space	Secretion of tropoelastin into the extracellular space
Propeptidases cleave the C- and N-terminals of the procollagen chains	No cleavage
Covalent crosslinking of collagen molecules via lysyl oxidases	Oxidative deamination of lysine residues via lysyl oxidase

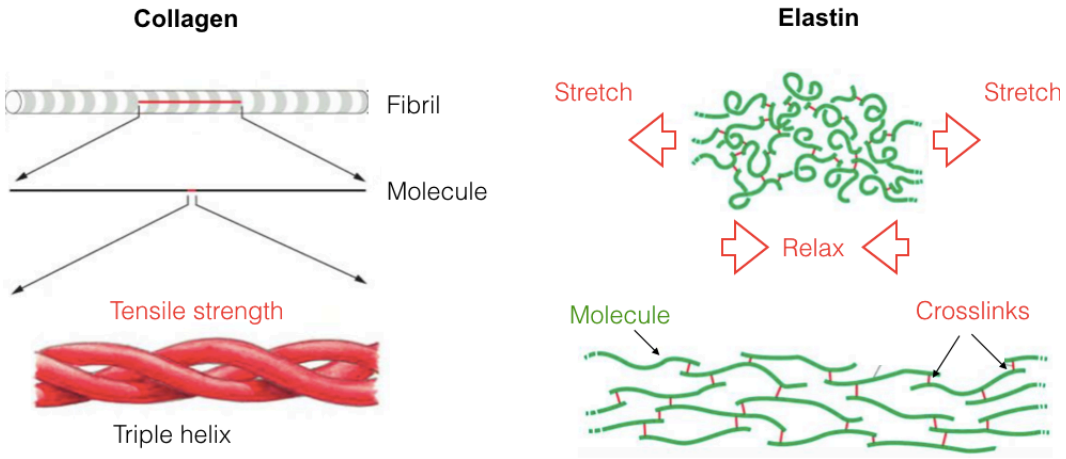

Figure 1.2 Collagen and elastin synthesis.

(A) Collagen is formed as triple helix, which is cross-linked in the extracellular space to form collagen fibrils with high tensile strength. (B) Similarly to collagen, elastin polypeptide chains are cross-linked in the extracellular space to form a microfibrillar scaffold. Modified from (Alberts et al. 2014) and (Chen & Raghunath 2009).

The synthesis and degradation of ECM proteins, including collagen I and elastin is tightly regulated in normal human lungs: The degradation of lung ECM proteins is mediated by matrix metalloproteinases (MMPs), serine proteases and plasmin (Mutsaers et al. 1997). All members of the MMP family are zinc-dependent endopeptidases, which together are able to degrade all ECM proteins. MMPs are up-regulated in patients with IPF and MMPs and their inhibitors, tissue inhibitor of MMPs (TIMPs) have been demonstrated to regulate pulmonary fibrosis in multiple murine model systems (Craig et al. 2015). An imbalance of MMPs and TIMPs could influence the balance between ECM accumulation and degradation and result in aberrant tissue repair (Manoury et al. 2007). In the event of uncontrolled matrix deposition for example when MMPs are aberrantly expressed, the functional pulmonary architecture can be distorted by excessive ECM deposition and result in severe diseases such as pulmonary fibrosis, COPD (Clarke et al. 2013), and airway remodelling in asthma (Royce et al. 2009). *In vitro* assays that recapitulate the supramolecular assembly of collagen into fibrils under molecular crowding conditions (Chen et al. 2009) provide a useful tool to assess the potential of compounds that modulate the processing and deposition of collagen.

1.1.3 Respiratory epithelial cells

The respiratory epithelium provides a shield against environmental toxins and pathogens and is permanently exposed to physical forces during lung ventilation. Therefore, the respiratory epithelium is involved in mucociliary clearance, reduction of surface tension in the alveoli and clearance of pathogens and allergens (Whitsett & Alenghat 2015). This can be accommodated by different cell types of lung epithelium across the bronchial tree. An overview of representative epithelial cell types and their distribution in the lung is shown in Figure 1.3.

Human bronchial epithelium in the large and smaller airways are involved in regulating the immune response, by secretion of pro- and anti-inflammatory mediators such as cytokines, chemokines, growth factors, and arachidonic acid metabolites (Van Der Velden et al. 1998). Thus, they impact directly on the recruitment, differentiation and activation of immune cells and mesenchymal cells. Although bronchial epithelial cells release cytoprotective molecules e.g. to activate myofibroblast in the lamina reticularis, they can account for a chronic

cycle of inflammation and injury (Hamilton et al. 2001). Bronchial epithelial cells are key therefore players in the regulation of inflammation and contribute to airway remodelling in the event of tissue damage.

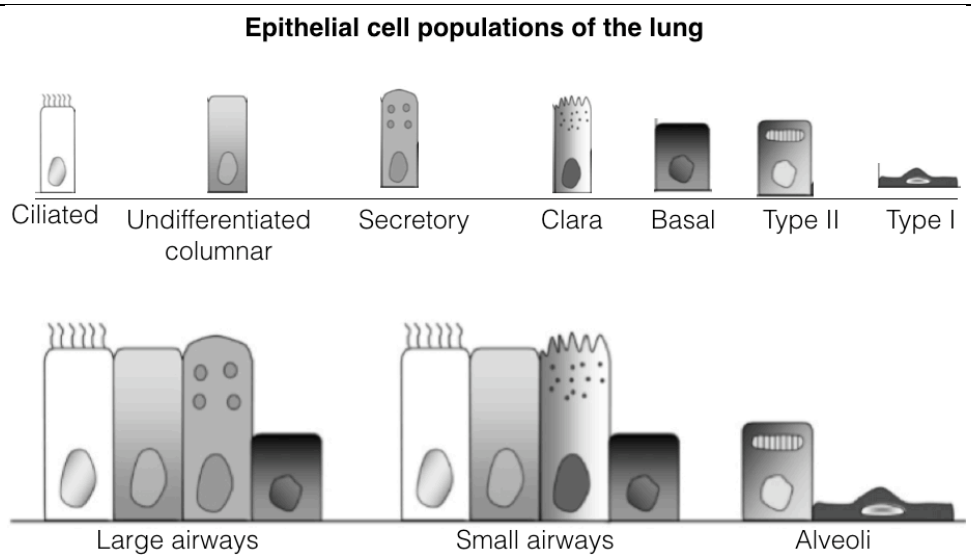

Figure 1.3 Cell types of the lung epithelium adapted from (Crystal et al. 2008).

The most representative epithelial cell populations in the large airways are ciliated, undifferentiated columnar, secretory or basal cells. In the small airways, the number of ciliated cells increases and Clara cells replace secretory epithelial cells gradually. In the terminal alveoli type I and type II pneumocytes represent the main group of respiratory epithelium.

Alveolar epithelial cells, on the contrary, are involved in the process of gas exchange and decrease of surface tension within the alveoli. Two main cell populations encompass the alveolar epithelium: alveolar type I and type II pneumocytes. Squamous type I pneumocytes comprise up to 95 % of the alveolar surface area (Haschek & Rousseau 1997) and are connected via tight junctions. Due to their squamous cell shape (flattened and thin structure) and their cytoplasmic plates, type I pneumocytes provide a large surface area for gas exchange (Ward & Nicholas 1984). In contrast type II pneumocytes, act as supporter cells in the alveolus, by supplying progenitor cells for both type I and type II cells and are, therefore, essential for the regeneration of alveolar cells in the event of lung injury (Castranova et al. 1988). Moreover, type II epithelial cells produce surfactant, a lipid-protein film to reduce stiffness and protect the patency of alveoli. Surfactant consists of phospholipids, neutral lipids, and surfactant proteins, to reduce surface tension and prevent alveolar collapse (Zhao et al.

2010). In addition, type II pneumocytes have been reported to be involved in preventing the accumulation of alveolar fluid but maintaining a fluid layer on the alveolar surface. This is achieved by sodium transporters that regulate apical to basolateral fluid transport (Eaton et al. 2004; Selman & Pardo 2006; Shannon & Hyatt 2004). The delicate structure of the alveolar wall is essential for gas exchange but makes it vulnerable to damage and inhaled toxins and pathogens.

1.1.4 Pulmonary/alveolar macrophages

Pulmonary macrophages, represent a heterogeneous cell population with phagocytic, antigen processing and immunomodulatory functions (Gordon & Read 2002). Pulmonary macrophages occur throughout the respiratory system, are key effector cells in the front line of cellular defence against respiratory pathogens (Busse & Lemanske 2001). All lung macrophages originate from precursor cells in haemopoietic organs and transit to the lung via blood or lymph as monocytes. Once monocytes leave the circulation to enter the lung tissue they develop a macrophage phenotype depending on the location and state of activation (Gordon & Read 2002). This macrophage phenotype is predominantly dependent on chemo- and cytokines derived from bronchial epithelial cells, type II pneumocytes or the composition of the surfactant (Striz et al. 2001; Gordon & Read 2002; Hussell & Bell 2014a).

In order to protect and clear respiratory spaces of inhaled particles and pathogens, pulmonary macrophages migrate through bronchioles, pulmonary interstitium, and alveoli, where they are called alveolar macrophages. Alveolar macrophages represent 95 % of the cell burden in BALF (bronchoalveolar lavage fluid) of normal lungs (Gordon & Read 2002), whereas interstitial macrophages are located in the lung parenchyma. Both cell types are involved in modulating immune responses and are important for the phagocytosis of apoptotic cells, cellular debris and pathogens (Hussell & Bell 2014a). To accommodate different macrophage functions alveolar macrophage phenotypes are highly plastic depending on the tissue context (Hussell & Bell 2014b). Similarly, to the nomenclature of pro- and anti-inflammatory lymphocytes, the following dichotomy has been suggested for macrophage activation: Macrophages that mediate inflammation have been classified as “M1”-like whereas macrophages with tissue remodelling / pro-fibrotic activity have been classified as “M2”-like and are defined by their expression of cell markers and the secretion of pro- or anti-inflammatory cytokines (Martinez & Gordon 2014; Wermuth & Jimenez 2015).

When using this terminology it has to be acknowledged, however, that studies with alveolar macrophages demonstrated that most macrophages do not accurately fit in this classification (Hussell & Bell 2014a). This suggests the existence of dynamic macrophage populations, with intermediate polarisation states (N. Wang et al. 2014; Hussell & Bell 2014b; Aggarwal et al. 2014). The classification scheme for human macrophage population subsets is outlined in **Table 1**. However, for simplicity reasons traditional macrophage polarisation nomenclature was used, within this thesis (M1-like and M2-like) to describe a general polarisation towards a pro-inflammatory or anti-inflammatory/profibrotic macrophage stage.

Table 1 Simplified classification of main macrophage polarisation subsets - modified from Wermuth & Jimenez 2015 and Röszner 2015.

	Inflammatory	Tissue remodeling/profibrotic		
	M1	M2a	M2b	M2c
Differentiating agent	IFNγ, TNFα, LPS	IL-4, IL-13, IL-4 + LPS	LPS	IL-10 TGF-β_1 IFN-β
Cytokines produced	TNF-α IL-1β IL-6 IL-12 IL-23 CCL8	IL-10 TGF-β IL-1ra	IL-4 IL-6 IL-10 TNF-α	IL-10 TGF-β
Chemokine /receptor	IL-8, MIG, IP-10, MIP-2α, MIP-2β,	Eotaxin 2	CCL1	CCR2

Classification scheme for monocyte/macrophage subsets demonstrating differentiating agents and the production of main cyto- and chemokines.

Due to the close proximity of alveolar macrophages and airway epithelial cells, both cell types may amplify the cytokine production *in vivo* to mediate inflammation or tissue repair. Hence, *in vitro* studies focussing on lung pathologies, often study the effects on macrophage polarisation and inflammation in co-culture systems with macrophages and bronchial epithelial cells (Fujii et al. 2002; Tao & Kobzik 2002; Chuquimia et al. 2013; Moon et al. 2015). Together, these studies suggest that the interplay of macrophages and epithelial cells in the lung tissue may contribute to a pro-inflammatory or pro-fibrotic environment with

potential consequences for the development of chronic lung disease or tissue fibrosis.

1.1.5 Lung fibroblasts

Fibroblasts, present in the pulmonary parenchyma are essential for the functionality of the lung. Together with the components of the extracellular matrix, lung fibroblasts provide structural and functional integrity for the alveolar-capillary unit and interstitium. Particularly, the interaction of fibroblast cytoskeletal proteins and the ECM facilitate cell motility and the generation of contractile forces essential during wound healing (Moises Selman & Barrios 1991; McAnulty 2007). Furthermore, lung fibroblasts, among other cells are the major source of ECM-proteins, including collagen I and III but also regulate ECM degradation through the production of matrix metalloproteinases (Greenlee et al. 2007). Together, lung fibroblasts are fundamental for maintaining the integrity of the lung tissue and for orchestrating tissue repair processes (Darby et al. 2014).

Under normal conditions lung (proto-) fibroblasts exhibit cell-cell or cell-matrix contacts (Tomasek et al. 2002). However, in response to mechanical stress or tissue injury, lung fibroblasts become activated, migrate to the wound site, and differentiate into so-called (proto-) myofibroblasts expressing α-smooth muscle actin (αSMA) (schematic of differentiation towards myofibroblast detailed in Figure 1.4).

Fibroblast differentiation is mediated through mechanical stress and cytokines released from tissue resident cells or recruited cells at the wound site and involves multiple steps: Firstly, interstitial fibroblasts are activated by extracellular stress arising from mechanical properties of the ECM (Hinz et al. 2007; Tomasek et al. 2002) and differentiate into so-called proto-myofibroblasts, a fibroblast differentiation stage which has been demonstrated to be present in normal alveolar septa (Hinz et al. 2007). Proto-myofibroblasts express stress fibres including ED-A fibronectin and filamentous actin, as well as focal adhesion molecules in order to conquer mechanical stress and to strengthen the wound. In the event of high levels of active transforming growth factor- beta (TGF-β) proto-myofibroblast differentiate further into myofibroblasts, which express abundant levels of ED-A fibronectin and filamentous actin, and high levels of stress fibres containing αSMA (Skalli et al. 1986), the most reliable marker of the myofibroblast phenotype (Tomasek et al. 2002). With the expression of αSMA in filament bundles or stress fibres, myofibroblast enhance their contractile

properties and contribute to wound contraction in provisional granulation tissue (Hinz 2010; Goffin et al. 2006; Hinz et al. 2001; Zhang et al. 1996).

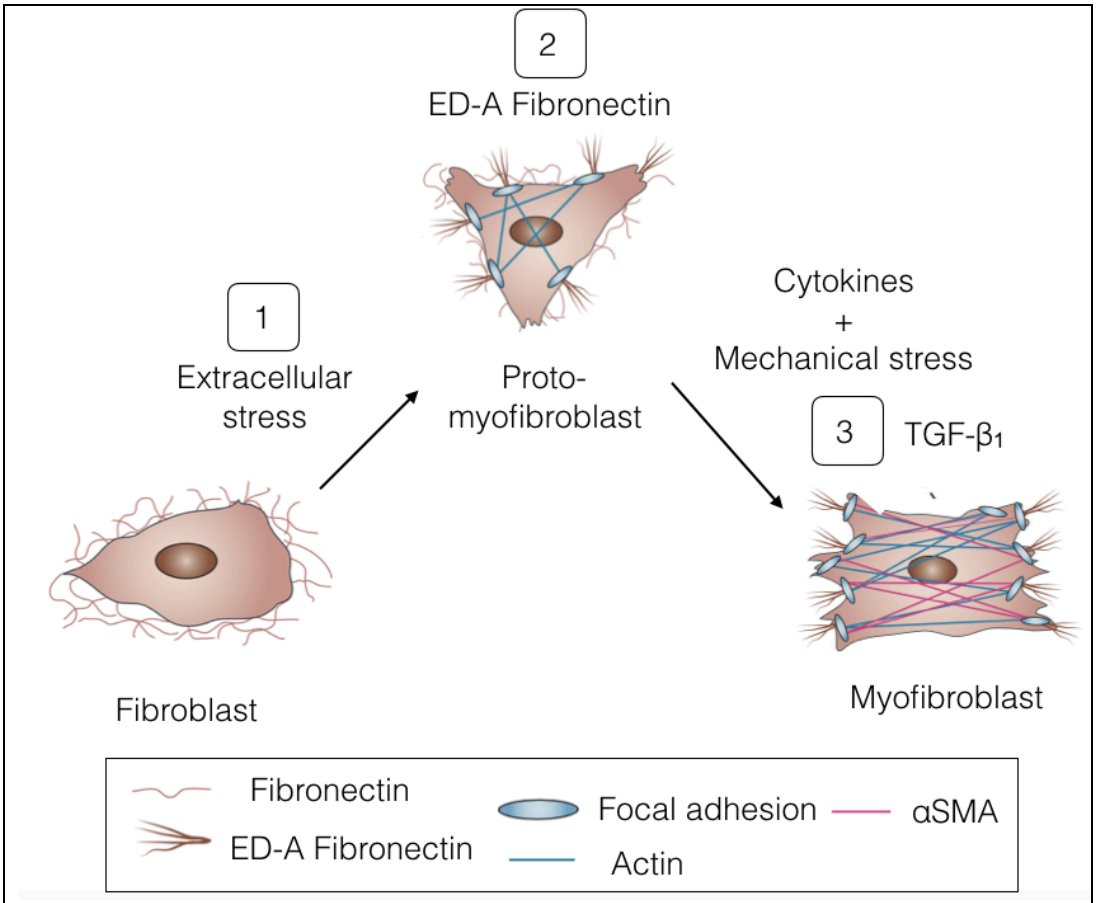

Figure 1.4 Fibroblast to myofibroblast transition modified from (Falke et al. 2015).

Fibroblasts, resident in the pulmonary interstitium, express fibronectin but no filamentous actin. Proto-myofibroblasts express ED-A fibronectin, stress fibres, and focal adhesion proteins. By contrast, myofibroblasts express high levels of ED-A fibronectin, filamentous actin, and αSMA. The differentiation of fibroblasts into myofibroblasts requires three different events: 1) high extracellular stress 2) specialized ECM proteins e.g. ED-A Fibronectin; 3) accumulation of biologically active TGF-β_1 (Hinz et al. 2007).

Apart form the *de novo* synthesis of αSMA, active TGF-β induces the expression of ECM proteins, predominantly fibrillar collagens. Moreover, it has been demonstrated that mechanical forces induce matrix production in fibroblasts. Mechanical stress is sensed by focal ECM-cell contacts and is translated into downstream signalling pathways of multiple receptors (Torday & Rehan 2003;

Sarasa-Renedo & Chiquet 2005; Tamada et al. 2004), a process which is called mechanosensing.

Transforming growth factor-beta (TGF-β) is a potent cytokine responsible for the induction of multiple cellular effects, such as differentiation and collagen production, immunomodulation, and is a key mediator in wound healing. Additionally, TGF-β is a potent mediator of chemotaxis in fibroblasts and myofibroblast and is the key player in mediating a fibroproliferative response (A E Postlethwaite et al. 1987). To date, three TGF-β isoforms are described in the literature TGF-β_1, TGF-β_2, and TGF-β_3, with distinct tissue functions (Shi & Massague 2003; Bottoms et al. 2010). Amongst the three TGF-β isoforms, TGF-β_1 is the most studied isoform. During normal wound healing TGF-β_1 is secreted as inactive latent precursor by monocytes/macrophages (Grotendorst, Smale, et al. 1989), fibroblasts (Kelley et al. 1991), activated leucocytes and stromal cells (Li et al. 2006) as well as endothelial cells (Grotendorst, Soma, et al. 1989). Before TGF-β_1 dimer binds to TβRII to form a complex with TβRI (Penn et al. 2012) it is inactive and non-covalently associated with latency associated peptide (LAP) and forms the large latency complex together with an ECM anchor protein LTBP (latent TGF-beta binding protein) (Miyazono et al. 1991; Taipale et al. 1994). The activation of latent TGF-β_1, involves the separation from its non-covalently linked latency peptide, which dissociates in response to temperature or pH changes *in vitro* (Henderson & Sheppard 2013a). Other, potential mechanisms of TGF-β_1 activation involve ROS (reactive oxygen species), proteases, or shear stress (Brown et al. 1990; Worthington et al. 2011). One of the most recently studied mechanisms of TGF-β_1 activation involve the integrin family, especially αvβ3, αvβ5 and αvβ6 (Araya et al. 2006; Y. Zhou et al. 2010; Scotton et al. 2009; Leask & Abraham 2004; Henderson & Sheppard 2013a), which are expressed by many cells including lung fibroblasts. In the lung, αvβ6 is expressed by the alveolar epithelium and *in vitro* studies show that the activation of TGF-β_1 can be inhibited by αvβ6 blocking antibodies (Munger et al. 1999; Van Aarsen et al. 2008). More recently it has been demonstrated that integrin-mediated activation of TGF-β_1 is induced by mechanical forces generated by these integrins (Shi et al. 2011). The particular role of TGF-β_1 in fibroblast activation and fibroblast-mediated wound healing will be discussed in the next section.

1.2 Wound healing

Normal wound healing involves a sequence of events, tightly regulated by a multitude of mediators, resulting in successful tissue repair and restoration of the normal lung function. Aberrant wound healing has been associated with the pathogenesis of lung disease, particularly in pulmonary fibrosis. In the lung, the mechanisms underlying wound-healing events following injury are poorly understood. These mechanisms are often explained by studies of cutaneous wound healing (Singer & Clark 1999; Clark 1991; Darby et al. 2014). The normal wound healing response requires both tissue resident cells as well as circulating cells and mesenchymal progenitors. Their recruitment, interaction, activation and cytokine profiles are coordinated by a dynamic series of events involving a complex composition of cytokines, chemokines, growth and complement factors, lipid mediators, as outlined in Figure 1.5 (Sinno & Prakash 2013). The wound healing process is driven by four essential, overlapping sequences: The haemostasis phase, inflammatory phase, the proliferative phase (development of the granulation tissue) and the maturation phase, including scar formation, and re-epithelialization (Darby et al. 2014; Micallef et al. 2012).

In the early events following injury during haemostasis, the clotting cascade stops the bleeding process, which results in the formation of a provisional wound matrix, composed of fibrin and fibronectin (Olczyk et al. 2014). Recruited cells, such as lymphocytes, neutrophils, macrophages and endothelial cells use the provisional matrix to exaggerate the inflammatory phase. Macrophages, recruited in the inflammatory phase originate from monocytes, which are differentiated through stimulation e.g. by extracellular matrix components, TGF-β and monocyte chemoattractant protein 1 (MCP-1) (Leibovich & Ross 1975). Moreover, to coordinate the clearance of bacteria and foreign debris, macrophages secrete numerous cytokines and chemokines, interleukins, tumour necrosis factor (TNF) as well as platelet-derived growth factor (PDGF) to stimulate fibroblast fibroproliferation (Clark 1996; Sinno & Prakash 2013). The proliferation phase is characterised by reepithelialisation, neovascularization, and the accumulation of granulation tissue as well as collagen deposition. Neovascularization is critical for the recruitment of additional macrophages and fibroblasts; newly arrived macrophages further secrete growth factors to stimulate fibroplasia.

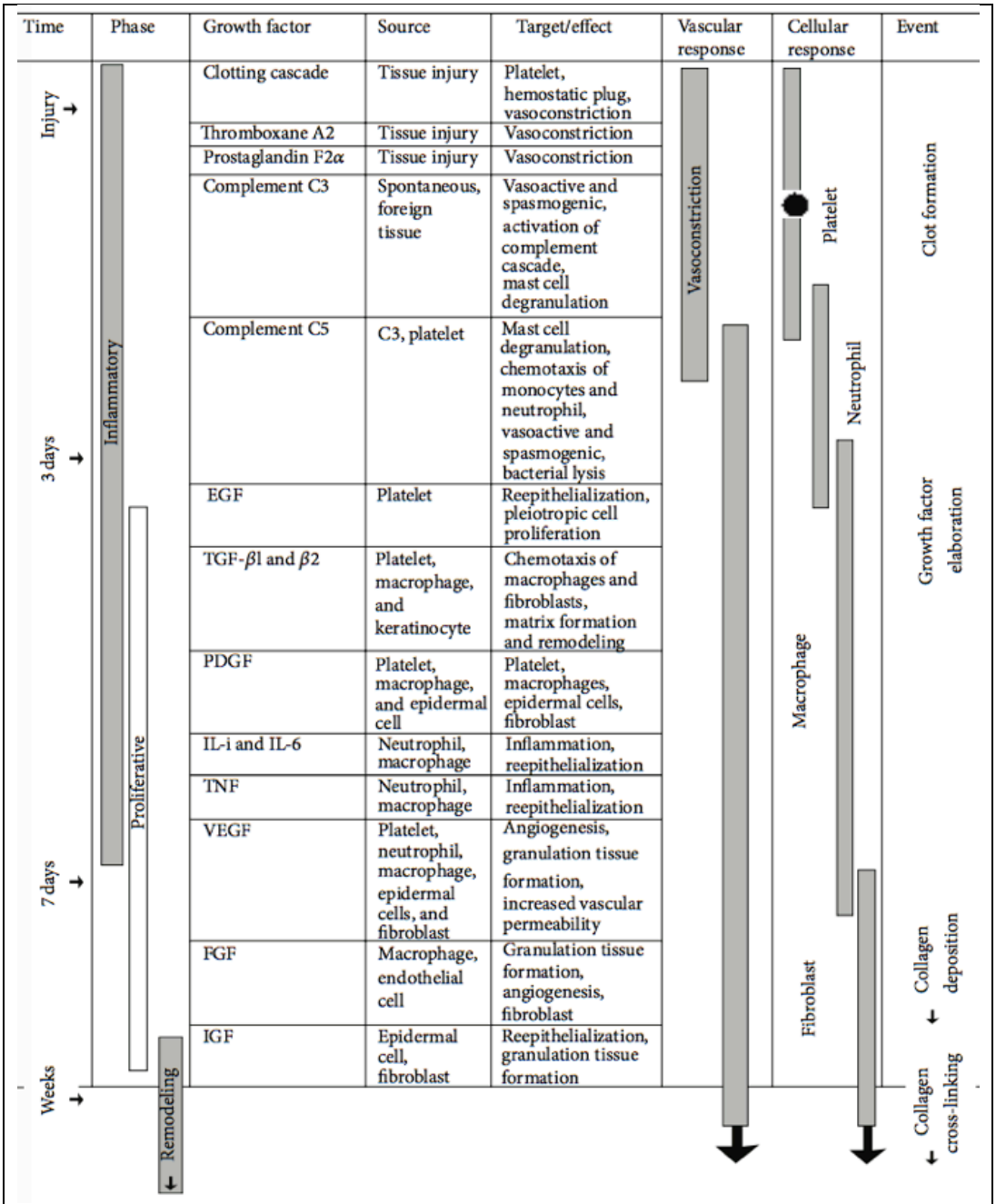

Figure 1.5 Cytokines involved in wound healing modified from (Sinno & Prakash 2013)[1].

Different cytokines and growth factors orchestrate the wound healing response. Complements C3 and C5, epidermal growth factor (EGF), transforming growth factor (TGF), platelet-derived growth factor (PDGF), tumour necrosis factor (TNF), vascular endothelial growth factor (VEGF), and insulin-like growth factor (IGF).

[1] This is an open access article distributed under the Creative Commons Attribution License, which permits unrestricted use, distribution, and reproduction in any medium, provided the original work is properly cited. From http://www.ncbi.nlm.nih.gov/pmc/articles/PMC3741993/.

Additional factors such as PDGF (Risau et al. 1992), TGF-β and extracellular matrix molecules (Xu & Clark 1996) stimulate fibroblast proliferation and differentiation to strengthen the wound. Hence, myofibroblasts become most abundant in the proliferation phase of wound healing (Horowitz & Thannickal 2006). Figure 1.6 outlines the role of lung fibroblasts in normal wound healing.

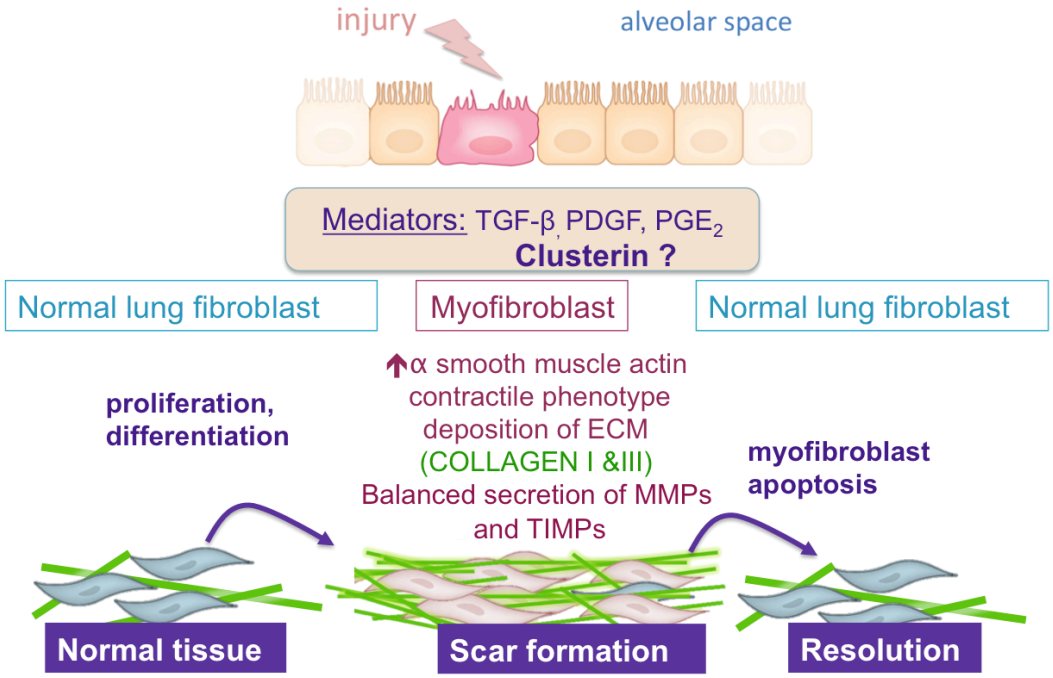

Figure 1.6 Potential role of lung fibroblasts during normal wound healing.

Following epithelial injury, various tissue mediators such as TGF-β, PDGF and PGE_2 are released by resident epithelial cells and recruited immune cells. Those mediators induce fibroproliferation of tissue resident and recruited fibroblasts and differentiation into myofibroblasts, which express high levels of alpha smooth muscle actin (αSMA) and deposit collagen I and III to contribute to the formation of scar tissue. Fibroblasts and myofibroblast secrete MMPs and TIMPs to regulate ECM deposition and degradation. During the resolution phase, fibroblasts undergo apoptosis and ECM is remodelled and reduced which signals the onset of the maturation phase of functional lung tissue.

The maturation phase is marked by the progressive remodelling of the granulation tissue into scar tissue involving further fibroblast activation, differentiation into myofibroblasts, proliferation and extracellular matrix deposition to continuously remodel and eventually replace the provisional matrix (Darby et al. 2014). The expression of αSMA in microfilament and stress fibres and extracellular matrix deposition, including collagen I and III fibrils, assist in wound

contraction and to strengthen the wound site, approximately three weeks after tissue injury. Additionally, (myo-) fibroblasts, secrete matrix metalloproteinases (MMPs) and tissue inhibitors of metalloproteinases (TIMPS) to remodel the granulation tissue (Darby et al. 2014). Furthermore, collagen III is replaced with collagen I and collagen fibres rearranged and cross-linked to further support scar formation. During the resolution phase myofibroblasts progressively undergo apoptosis, which signals the onset of the maturation phase for normal functional tissue (Figure 1.6) (Desmoulière et al. 1995; Horowitz & Thannickal 2006).

1.2.1 Pathological repair in the lung

Dysregulation of the normal wound response has been proposed as one of the earliest events in many diseases (Sarrazy et al. 2011). In internal organs, such as the lung, aberrant wound healing is proposed to be generally similar to processes in pathological cutaneous scar formation. Pathological wound healing often involves a repetitive noxious stimulus that leads to persistent epithelial injury, with continuous ECM deposition resulting in permanent scar formation (Wilson & Wynn 2009; Micallef et al. 2012). In many disease states, as it is proposed for fibrosis, the dialogue between (myo-) fibroblasts and their microenvironment may be altered or disrupted leading to repair defects and continuous production of scar tissue (Darby et al. 2014). Dysregulation of the wound repair-response can affect many fibroblast functions including differentiation into myofibroblasts, proliferation, ECM deposition, and the balance of apoptosis and survival. Consequently, aberrant wound healing can result in uncontrolled fibroblast proliferation and excessive ECM deposition, caused by an imbalance between extracellular matrix synthesis and degradation by myofibroblasts, common pathological features in pulmonary fibrosis and airway remodelling associated with asthma (McAnulty 2007; Chambers 2008; Shifren et al. 2012). Conversely, dysregulation of wound repair response can result in the destruction of the ECM, which is a histopathological hallmark of emphysema (Horowitz et al. 2012). To date, the mechanisms of normal and aberrant wound healing are incompletely understood and key mediators orchestrating the wound healing response, such as TGF-β_1, are in the focus of research.

Apart from (myo-) fibroblasts, M2 macrophages are suggested to be involved in a dysregulated wound response. M2 macrophages secrete high levels of growth factors, including TGF-β_1, driver of fibroblast differentiation (Desmoulière et al. 1993) and PDGF, which stimulate the fibroproliferative response and the

synthesis and deposition of excessive ECM (Falke et al. 2015). Together, M2 polarised macrophages, through the secretion of TGF-β_1 enhance a fibroblast driven aberrant wound repair response (Murthy et al. 2015; Zhang et al. 2016).

The role of TGF-β_1 has been the most studied in the context of pathological wound healing (Fernandez & Eickelberg 2012). As mentioned earlier, TGF-β_1 is secreted by a large number of cells, and the active form exerts pleiotropic functions to drive fibrogenesis. TGF-β_1 does not only induce macrophage chemotaxis, but also their expression of PDGF to enhance fibroblast proliferation (J.-S. Kim et al. 2006; Fernandez & Eickelberg 2012). Moreover, TGF-β_1 stimulates the expression and secretion of profibrotic cytokines, including TNFα, PDGF, IL-1β and IL-13 to perpetuate fibrogenesis (Fernandez & Eickelberg 2012). In addition, TGF-β_1 induces Smad signalling cascades that directly influence the transcriptional activity of collagen genes, including collagen I A1 (Cutroneo et al. 2007) and promotes collagen deposition (Fernandez & Eickelberg 2012).

In contrast to profibrotic mediators including TGF-β_1 and PDGF anti-fibrotic prostaglandin E_2 (PGE_2), the most abundant prostanoid within the lung, a lipid mediator of inflammation and regulator of wound repair is rapidly upregulated upon lung injury and expressed by alveolar epithelial cells, lung fibroblasts and alveolar macrophages (Churchill et al. 1989; Hempel, Monick & Hunninghake 1994; Hempel, Monick, He, et al. 1994; Jordana et al. 1994; Kolodsick et al. 2003). During normal wound healing PGE_2 promotes epithelial proliferation and angiogenesis (Fairweather et al. 2015). In addition, a growing body of evidence suggests that PGE_2, secreted by alveolar epithelial cells promotes the inhibition of fibroproliferation (Lama et al. 2002). Moreover, it has been demonstrated that PGE_2 reduces fibroblast migration (Y. J. Li et al. 2010), proliferation (Bitterman et al. 1986; Elias et al. 1985), collagen synthesis, and induces fibroblast apoptosis (Lama et al. 2002; Huang et al. 2009; Maher et al. 2010).

Aberrant wound healing in the lung is a complex sequence of tightly regulated events. A dysregulation of these events can result in the ignition and progression of many lung diseases.

1.3 Pulmonary Fibrosis

Pulmonary fibrosis is a progressive and ultimately fatal condition that currently affects more than 5 million people worldwide, the incidence is increasing, and there is no known cure (Meltzer & Noble 2008; Hutchinson et al. 2015; Kreuter et al. 2015). Pulmonary fibrosis occurs in association with several lung diseases, either in isolation, as in idiopathic pulmonary fibrosis (IPF) or multi-organ connective tissue diseases such as systemic sclerosis (SSc) (Maher et al. 2007; Varga & Abraham 2007; Herzog, Mathur, Tager, et al. 2014). Other manifestations of pulmonary fibrosis with known aetiology are associated with various triggers including allergens, chemicals, environmental particles or radiation (Wilson & Wynn 2009). Histopathologically, pulmonary fibrosis is defined by excessive extracellular matrix deposition into the parenchyma with consequent destruction of the normal functioning lung architecture. Hence, clinical symptoms involve progressive breathlessness, which often leads to respiratory failure resulting in morbidity and mortality. The most common disorders that lead to the final stage of pulmonary fibrosis are the idiopathic interstitial pneumonias (IIPs). This group of disorders has been partly characterised, however, the aetiology for IIPs remain elusive. Since many IIPs share pathological and clinical characteristics, identification, treatment, and diagnosis of IIPs are demanding (Travis et al. 2013). Moreover, its has been proposed that pulmonary fibrosis associated with SSc shares some features with interstitial lung disease (ILD) and their most common form IPF (Herzog, Mathur, Tager, et al. 2014).

1.3.1 Idiopathic Pulmonary Fibrosis

The most common and aggressive form of pulmonary fibrosis is idiopathic pulmonary fibrosis (IPF), typically described as a specific form of chronic, progressive and fatal scarring ILD with unknown aetiology (Trawinska et al. 2016; Daccord & Maher 2016). The median survival with IPF following diagnosis is less than three years, which is worse than for many cancers (Gribbin et al. 2006) and there are more than 5,000 new patients diagnosed with IPF each year in the UK (Navaratnam et al. 2011). The incidence of IPF increases with age (Trawinska et al. 2016) and is 7.44 per 100,000 in the United Kingdom and is considered as the most common cause of death within the heterogeneous group of progressive

lung disease (Rafii et al. 2013). More recent numbers of the incidence of IPF in Europe and North America were estimated to be 3 – 9 diagnosed patients per 100,000 (Hutchinson et al. 2015). Additionally, the prevalence of IPF is rising in the United Kingdom and the USA (Navaratnam et al. 2011). IPF affects patients predominantly between 40 to 70 years of age and occurs more frequently (twice as often) in man than in woman (Han et al. 2008; Raghu et al. 2006).

Two recently approved treatments, pirfenidone, and nintedanib, slow disease progression (King et al. 2014; Richeldi et al. 2014) but are only indicated for a small proportion of patients, have modest beneficial effects and considerable side-effects. The mechanism by which pirfenidone, a pyridone derivative, exerts its treatment effects is incompletely understood. It has been suggested that pirfenidone decreases fibroblast proliferation and TGF-β downstream signalling in primary human lung fibroblasts (Conte et al. 2014; Inomata et al. 2014). Nintedanib is a compound that inhibits many receptor-associated tyrosine kinases, including receptors for vascular endothelial growth factor (VEGF) and PDGF blocking profibrotic signalling cascades that contribute to fibroblast proliferation, migration, differentiation, and the secretion of ECM (Richeldi et al. 2014; Wollin et al. 2015). These treatment options may slow down disease progression, and the rate of decline of pulmonary function but, in some cases lung transplants are considered as only treatment option (Lynch et al. 2016; Kistler et al. 2014). There, therefore, remains a significant unmet clinical need and a requirement to further characterise the pathogenesis of pulmonary fibrosis and develop more effective treatments.

1.3.2 IPF diagnosis

Clinically, IPF is characterised by the histological pattern, described as usual interstitial pneumonia (UIP) with the exclusion of other alternative aetiologies, including connective tissue disease, drug toxicity or environmental insults (Herzog, Mathur & Tager 2014; Raghu et al. 2011). Other symptomatic features of IPF include cough, dyspnoea, bilateral interstitial infiltrates visible on radiographs or computed tomographic (CT) scans, progressive fibrosis and destruction of the lung parenchyma (Lynch et al. 2016). Due to common features with other interstitial lung diseases (ILDs), specialists urge that the diagnosis IPF, should be based on the histological evaluation of UIP or when a classical high-resolution CT (HRCT) scan supports the diagnosis of IPF (Lynch et al. 2016;

Raghu et al. 2011). There is, however, an unmet need for non-invasive diagnostic tools since many patients are too unwell for lung biopsies, which makes the diagnosis of IPF inaccessible. Genomic techniques together with advanced sampling methods, including transbronchial cryobiopsies, biomarkers and improved imaging techniques (micro-CT) could influence diagnosis in the future to help improve therapeutic efforts (Richeldi 2016).

1.3.3 Histopathology of IPF

As mentioned previously, the international, multidisciplinary ATS/ERS consensus for diagnostic criteria for IIPs suggests the diagnosis of IPF, based on the histological phenomenon UIP (ATS/ERS 2002). UIP is heterogeneous and is characterised by areas of active lung injury, inflammation, fibroproliferation, extracellular matrix remodeling, areas of apparently normal lung structure alongside dense fibrotic tissue with irreversible distortion of the lung architecture (Lynch et al. 2016). Additionally, hyperplastic, cuboidal type II pneumocytes are an additional characteristic of UIP (Kasper & Haroske 1996). Although not prominent, scattered neutrophils, macrophages, or eosinophils are present throughout the fibrotic parenchyma (Lynch et al. 2016) and macrophages infiltrate the lung and form clusters in airspaces and bronchioles. In addition, collagen intermingled with proliferating myofibroblasts and fibroblasts; so-called “fibroblastic foci” are distributed in active fibrotic lesions, which intersperse with areas of almost acellular collagen accumulation and morphologically normal lung. These foci are composed of collagen deposits, and proliferating (myo-) fibroblasts and are overlaid with hyperplastic epithelium (Scotton et al. 2009). In past studies, fibroblastic foci have been suggested to present an organising stage of focal acute tissue injury (Cool et al. 2006; Myers & Katzenstein 1988; Fukuda et al. 1995; Kuhn & McDonald 1991). Cool and colleagues, suggest that fibroblastic foci are the forefront of a highly interconnected, complex reticulum, that originates in the subpleura and expands to nearby parenchyma (Cool et al. 2006). As assessed in various studies the number of fibroblastic foci identified in biopsy specimens is associated with disease severity of IPF, poor survival, and provides a diagnostic tool to assess the progression of the disease (King et al. 2001; Nicholson et al. 2002; Flaherty et al. 2003; Enomoto et al. 2006). It is noticeable that, although fibroblastic foci are a hallmark of IPF, these structures are also present in up to 30 % of patients with SSc-associated ILD (Raghu et al. 2011;

Solomon et al. 2013). In addition, aberrant responses to TGF-β have been observed in both SSc-associated ILD and IPF (Castelino & Varga 2010). This suggests that similar phenotypic changes occur in both IPF and SSc-derived lung fibroblasts (Herzog, Mathur, Tager, et al. 2014).
In summary, fibroblastic foci represent a hallmark of UIP, correlate with disease severity and are focal points of active disease between morphologically normal lung and mature collagen deposits throughout fibrosing tissue that ultimately contribute to the architectural distortion of the normal lung tissue (Cool et al. 2006).

The end stage of IPF is characterised by large cystic airspaces and dense scar tissue, often referred to “honeycomb” structures, a specific hallmark of IPF (Katzenstein et al. 2008). The airspaces of honeycomb-like structures are separated from the fibrotic tissue by bronchialised epithelium. An immunohistochemical comparison between the normal and fibrotic lung architecture is presented in Figure 1.7.

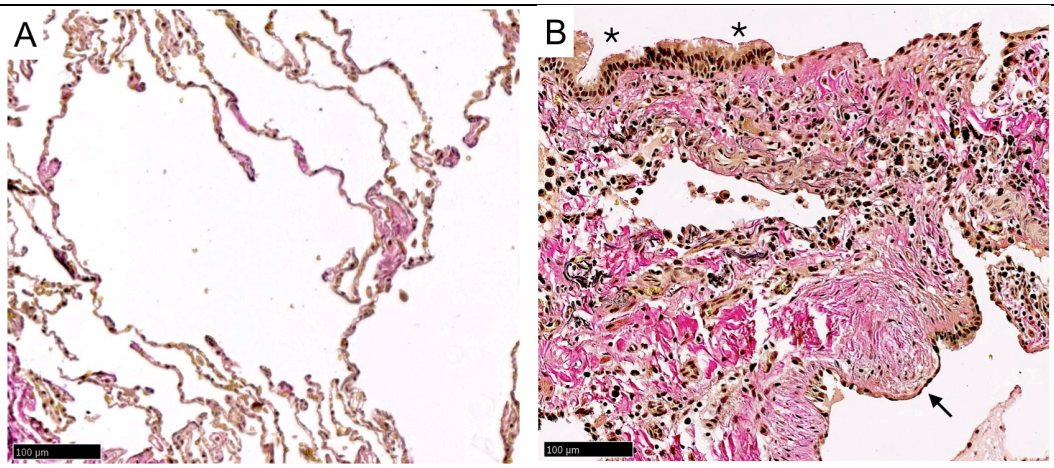

Figure 1.7 Normal lung architecture and distorted architecture in IPF lung.

Elastica van Giesson staining in tissue of normal (A) and IPF lung (B): collagen (pink), elastin (black), and other structures (yellow). In normal lung, alveoli are thin-walled structures with occasionally small amounts of interstitial collagen. By contrast, IPF tissue is characterised by thickened alveolar walls and fibroblastic foci (arrow) as well as dense collagen deposition in the interstitium. Fibroblastic foci are revealed as accumulations of fibroblasts and deposited collagen, with hyperplastic epithelium overlying the foci (arrow). Bronchialised epithelium (*) produces and secretes excessive amounts of mucin, which is deposited in the cystic airspaces of the fibrotic lung.

With increasing disease progression, the lung tissue looses its elasticity, alveoli collapse leading ultimately to impaired gas exchange and breathlessness resulting in high morbidity and mortality (McAnulty 2007; Datta et al. 2011; Yang 2012; Loveman et al. 2015).

1.3.4 Pathogenesis of IPF

The development of pulmonary fibrosis is incompletely understood. Medical and scientific efforts have helped to identify advanced diagnostic tools to improve our understanding of this devastating disease. The mechanisms contributing to the early and progressing events of the disease are predominantly studied in biopsy specimens from IPF patients and a model of bleomycin-induced fibrosis in mice (Williamson et al. 2015). Over the last decades, different theories about the pathogenesis and aetiology have shaped our perception of the disease, with conflicting theories up until today. In the mid 1970s, Crystal and colleagues argued that IPF begins with alveolitis and transitions into an interstitial fibrotic

disease, which could be potentially reversed by therapies targeting inflammatory and immune processes (Crystal et al. 1976). Turner-Warwick later argued that in IPF viral infection could be aetiologically involved (Turner-Warwick 1998). Up until today the inflammation appears to be a prominent feature in the pathogenesis of IPF (Bringardner et al. 2008; Keane 2008; Moore et al. 2014; Balestro et al. 2016), despite the lack of treatment benefits with immunomodulatory drugs (Gross & Hunninghake 2001; Thannickal et al. 2004). The hypothesis that IPF is a chronic inflammatory/autoimmune disease has been further countered with arguments that the presence of inflammatory cells is low when compared with other interstitial lung diseases (Selman et al. 2001). Additional studies with high-dose immunosuppressive therapy demonstrated no benefit regarding disease progression or outcome (Maher & Wells 2008). More recently, a hypothesis emerged, that suggests that the pathophysiology of the disease is more a consequence of fibroblast dysfunction than of dysregulated inflammation. This hypothesis was put forward by Laurent and McAnulty in the early 1980s (Laurent & McAnulty 1983). Abnormal tissue repair mechanisms following alveolar epithelial cell damage (Selman et al. 2001; King Jr. et al. 2011), have been suggested to result in the release of profibrotic mediators, which drive the activation of fibroblasts (Lovgren et al. 2011). Hence, the persistence of wound healing processes, involving increased numbers of fibroblast/ myofibroblast cells driving excessive production of extracellular matrix proteins, are considered to be central to the IPF pathogenesis (McAnulty 2007).

The initiation of the fibrotic process, in the early stages of the disease, is proposed to be induced by recurrent micro-injuries and chronic damage to alveolar epithelial cells, followed by sequential exposure to toxic stimuli. Potential causes for these reoccurring epithelial cell damage may involve various risk factors, such as smoking (Baumgartner et al. 1997; E. B. Meltzer 2008; Selman et al. 2008; Maher 2013; Daccord & Maher 2016), viral infections (Irving et al. 1993; Egan et al. 1995), ER stress (Korfei et al. 2008; Lawson et al. 2008; Kropski et al. 2013; Camelo et al. 2014; Daccord & Maher 2016) and genetic risk factors, 5 % of cases in IPF are familiar (Noble et al. 2012). Other risk factors involve oesophageal reflux (Tobin et al. 1998) and epigenetic factors (Sanders et al. 2008; Yang & Schwartz 2015; Evans et al. 2016). Despite the fact that the detailed mechanisms that lead to the early events in IPF remain unknown, it is noticeable that many observations in IPF share characteristics and mediators of the normal wound healing response.

Studies point towards disrupted basement membranes, damaged, apoptotic and necrotic alveolar and bronchial epithelial cells in IPF tissue (Plataki et al. 2005; Katzenstein 1985; Lovgren et al. 2011) with ultrastructural alterations of alveolar epithelial cells, including hypertrophy and hyperplasia and loss of adhesion molecules (Kasper & Haroske 1996). Albeit, IPF has been traditionally described as an interstitial lung disease, bronchial epithelium in the airways have been proposed to play a role in the pathogenesis of IPF (Sakai & Andrew M. Tager 2013). Bronchial epithelial cells display pro-apoptotic features in IPF (Plataki et al. 2005) but are also considered as a source for profibrotic mediators such as TGF-β in conditions of stress (Tschumperlin et al. 2003). Furthermore, bronchial epithelial cells are associated with chronic airway disease (Kamio et al. 2005) and pathobiology of IPF (Speer et al. 2011). Histologically, bronchialised epithelium lines cystic airspaces in IPF and produce excessive amounts of mucin and matrix metalloproteinases (MMPs), which further promotes ECM remodelling and disruption of the basement membrane in lungs of IPF patients (Lovgren et al. 2011). The persistent damage and apoptosis of epithelial cells and consequent loss of the epithelial cell barrier increases vascular permeability and leads to the recruitment of inflammatory cells (Mora et al. 2006; Chambers 2008; Leppäranta et al. 2012). The continuity of these processes induces the activation of various stress pathways, including ER stress, resulting in further dysfunction of alveolar and bronchial epithelial cells. Epithelial injury is found neighbouring myofibroblasts (Li et al. 2004) and correlates with the sites of fibroblastic foci (Kuhn & McDonald 1991). This suggests that damaged alveolar epithelial cells are involved in the induction of a fibroblast-driven aberrant wound healing response (Puglisi et al. 2016). It has been demonstrated in a bleomycin-induced model of fibrosis in mice that epithelial damage induces the secretion of TGF-β_1 (Kumar et al. 1996). In addition apoptotic bronchial epithelial cells have been reported to produce high levels of TGF-β_1 (Hodge et al. 2002) further perpetuating the profibrotic response.

Originally, fibroblast accumulation in fibrotic lung tissue was described to develop from resident tissue fibroblasts. More recent studies hypothesise that fibroblasts additionally originate from type II pneumocytes by epithelial to mesenchymal transition (EMT) driven by TGF-β (Willis et al. 2005). Other studies suggest that some fibroblasts that contribute to pulmonary fibrosis originate from circulating fibrocytes, which are bone marrow-derived mesenchymal progenitor cells able to differentiate into fibroblasts and myofibroblasts (Strieter et al. 2009). However, it seems more likely that the majority of fibroblasts involved in the pathomechanism

of fibrosis derive from initially quiescent, tissue resident fibroblasts and proto-myofibroblasts in normal alveolar septa (Hinz et al. 2007; Puglisi et al. 2016).
As mentioned earlier activated epithelial cells and recruited inflammatory cells secrete profibrotic mediators, including TGF-β_1 and PDGF both of which regulate proliferation, migration of fibroblasts and their differentiation into myofibroblasts as well as ECM deposition (Yi et al. 1996; Antoniades et al. 1990; Khalil et al. 1991; Chambers 2008; Thompson et al. 2006; Hostettler et al. 2008). Moreover, *in vitro* co-culture experiments have shown that mechanical stress in epithelial cells can promote the activation of TGF-β_1 in the ECM (Morishima et al. 2001). Although all three isoforms of TGF-β are expressed in the lung, TGF-β_1 has been particularly associated with fibrotic development (Coker et al. 1997; Jagirdar et al. 1997). TGF-β_1 has been reported to be elevated in IPF lungs, particularly in lung epithelium and macrophages (Khalil et al. 1991; Khalil et al. 1996) and impacts on fibroblast function in a paracrine manner (Leppäranta et al. 2012). Several lines of evidence support that the phenotype of IPF fibroblasts differs from the one found in fibroblasts derived from healthy lungs: IPF fibroblasts exhibit a invasive fibroproliferative phenotype (Mio et al. 1992; Khalil et al. 2005b; Huang et al. 2014; H. Chen et al. 2016a) and demonstrate enhanced migration when isolated from fibrotic lesions (Suganuma et al. 1995; Pierce et al. 2007). Moreover, in IPF several reports postulate that dysregulated apoptotic mechanisms result in increased epithelial apoptosis, while IPF fibroblasts appear resistant to different pro-apoptotic stimuli, including FasL (Hampel et al. 2005; Tanaka et al. 2002; Moodley et al. 2004; Bühling et al. 2005; Maher et al. 2010; Chang et al. 2010). This phenomenon is called the apoptosis paradox in IPF (Maher et al. 2010).
PGE_2, the major prostaglandin in the lung, counters the profibrotic effects of TGF-β_1, inhibits fibroproliferation (Lama et al. 2002; Bitterman et al. 1986; Elias et al. 1985) and induces apoptosis in fibroblasts (Huang et al. 2009). However, the levels of PGE_2 in IPF-BALF are reportedly decreased (Wardlaw et al. 1989; Borok et al. 1991; Bozyk & Moore 2011) and PGE_2 production and signalling, through its four receptors, E prostanoid (EP) receptors, is reduced (Bozyk & Moore 2011). In particular, TGF-β_1-induced PGE_2 synthesis is reduced in fibroblasts from fibrotic lung due to an impaired upregulation of COX-2 mRNA (Keerthisingam et al. 2001). Keerthisingam and colleagues suggest that decreased antifibrotic PGE_2 may lead to unopposed fibroproliferation and collagen synthesis further perpetuating the development of pulmonary fibrosis. Moreover, reduced levels of PGE_2 have been suggested to contribute to the

apoptosis paradox in IPF (Maher et al. 2010). Maher and colleagues suggest that the lack of PGE_2 is one mechanism capable of being responsible for both increased epithelial apoptosis and reduced fibroblast apoptosis. Together, the mechanisms that contribute to this fibroproliferative and apoptosis-resistant phenotype in IPF fibroblasts remain incompletely understood.

Recruited and tissue-resident macrophages indirectly regulate fibrogenesis by the secretion of growth factors, cytokines, and metalloproteases (Song et al. 2000). Uh and colleagues addressed in the late 1990s if these growth factors, cytokines, and metalloproteases contribute to the progression of IPF and found, that the occurrence of interstitial macrophages in the IPF lung corresponded with the level of clinical deterioration and deposited collagen (Uh et al. 1998). So-called alternatively activated macrophages (M2 macrophages) have been proposed as key effector cells in the advancement of wound healing, tissue remodelling and resolution of inflammation (Martinez et al. 2008; Zhang & Mosser 2008; Martinez et al. 2009). Interestingly, studies with alveolar macrophages derived from IPF patients display the phenotype of alternatively activated macrophages and have also been associated with increased fibroproliferation and collagen deposition in IPF (Prasse et al. 2006; Gong et al. 2012; Stahl et al. 2013; Murthy et al. 2015; Lech & Anders 2013; Byrne et al. 2016). Furthermore, M2 macrophages have been associated with acute exacerbation (AE), a phase of enhanced progression of respiratory symptoms and deterioration of pulmonary function in IPF (Schupp et al. 2015). Schupp and colleagues described that in AEs, M2 cytokines such as IL-1ra, MCP-1, CCL17, MIP-4, and CCL22 were increased, further implying that M2 cytokines are involved in exaggerating the progression of the disease. The role of macrophage-derived MMPs and endogenously derived tissue inhibitors of metalloproteinases (TIMPs) have been discussed in association with the IPF pathogenesis. MMPs are known to be elevated in IPF lungs and play a role in extracellular matrix remodelling and basement membrane disruption (Pardo & Selman 2012). Although it is challenging to predict the effects of MMPs in IPF lung due to their cleavage and activation of cytokines (Lech & Anders 2013) some MMPs may exert anti-fibrotic effects under certain circumstances. MMP-9 has been reported to be elevated in IPF-BALF samples (Henry et al. 2002), is produced by fibroblasts and alveolar and interstitial macrophages (Lemjabbar et al. 1999; Suga et al. 2000; Pardo & Selman 2012) and has been suggested to induce a pro-fibrotic feedback loop via

the activation of TGF-β_1 (Yu & Stamenkovic 2000). It is, however, incompletely understood how MMP-9 secretion is regulated in human alveolar macrophages.
Macrophages play a key role in tissue homoeostasis and wound healing. In the context of IPF M2 macrophage polarisation appears to impact directly on a pro-fibrotic environment that exaggerates the fibroproliferative response via the expression of pro-fibrotic mediators, including TGF-β_1 and the secretion of MMPs, including MMP-9.

In summary, aberrant regulation of multiple pathways involved in inflammation and wound repair have been suggested to contribute to the pathogenesis of IPF, and it is, therefore, likely that multifactorial events contribute to the onset and progression of this devastating disease. Figure 1.8 summarises all discussed cellular processes involved in the development of pulmonary fibrosis. The cause for an altered, pro-fibrotic phenotype in fibrotic lung fibroblasts and sustained M2 macrophage activation remains elusive. It is, therefore, important to assess the cellular role of altered proteins in IPF in order to help improve our understanding of the pathogenesis of this devastating disease. Clusterin, a multifunctional protein expressed by a wide range of cells in the human body is altered in IPF.

The next section summarises what is known about the role of clusterin in the lung and its potential links to the pathobiology of pulmonary fibrosis.

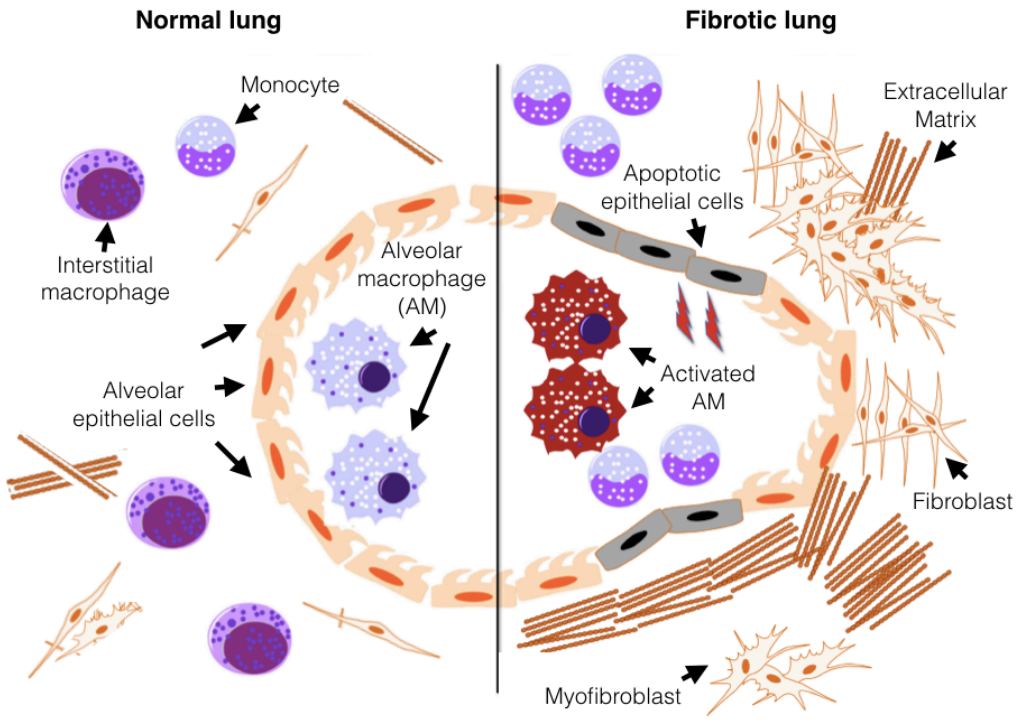

Figure 1.8 Schematic diagram of the normal alveolar architecture and a simplified hypothetical overview of cellular processes involved in the development of pulmonary fibrosis modified from (Byrne et al. 2016).

In normal lung tissue fibroblasts and occasionally myofibroblast contribute to the integrity of the lung. Alveolar macrophages are located in the alveolar space and interstitial macrophages resident in the interstitial parenchyma. In response to tissue injury, and the destruction of the epithelial integrity and alveolar basement membrane, inflammatory cells and mesenchymal progenitor cells are recruited towards the site of injury. Resident and recruited fibroblasts proliferate and differentiate into myofibroblasts; resulting in excessive ECM deposition and form subepithelial fibroblastic foci composed of fibroblast, myofibroblast, and extracellular matrix deposits. Activated epithelial cells and activated macrophages secrete numerous profibrotic mediators, including TGF-β_1 and PDGF and promote fibroproliferation and further perpetuate fibrogenic processes.

1.4 Clusterin

1.4.1 Clusterin in pulmonary fibrosis

Clusterin (also called apolipoprotein J) is a heterodimeric secretory glycoprotein, ubiquitously expressed in human tissues and body fluids. In a proteomic analysis of bronchoalveolar lavage fluid (BALF) Kim and co-workers showed that clusterin levels were approximately 7-fold lower in IPF compared with controls (T. H. Kim et al. 2010). In addition, studies of fibrosis in other organs, including heart, kidney, liver, and in animal models suggest that down- or up-regulation of clusterin enhance or limit the development of fibrosis respectively (Jung et al. 2012; Gangadharan, Bapat, Rossa, R Antrobus, et al. 2012; Greer et al. 2006; Rosenberg & Silkensen 1995; Klahr & Morrissey 1997) suggesting that clusterin may play an important role in the pathogenesis of fibrosis.
However, the localisation of clusterin in normal and fibrotic lung, the mechanisms contributing to its down-regulation in IPF-BALF and its role in the pathogenesis of pulmonary fibrosis have not been investigated.

The next sections summarise what is known about clusterin in human and rodent lung, its role in tissue injury and disease and its biosynthesis, regulation and multifunctional role in different cell types.

1.4.2 Clusterin in the human and animal lung

To date, there is very little information on distribution and function of clusterin in the lung. The following section summarises the current literature on clusterin in the human lung in health and disease and relevant animal models.

Human lung

Clusterin expression in the human lung and human lung fibroblasts, in particular, has been previously described in the context of oxidative stress caused by cigarette smoke extract (Carnevali et al. 2006). In this study Carnevali et al. analysed clusterin expression in bronchial biopsy specimens, of smokers and non-smokers and demonstrated that clusterin was mildly expressed in lung of non-smokers and clusterin immunostaining was markedly increased in the submucosa of lungs from active smokers. In addition, this study demonstrated that the expression of clusterin in lung fibroblasts was increased in response to

2.5 % to 5 % cigarette smoke extract in the culture medium. Although Carnevali and colleagues suggest that clusterin may have a protective effect in the airways of smokers, their report, however, did not outline other cell specific clusterin expression and potential implications in cell function in fibroblasts or the human lung.

Other studies on clusterin in the human lung, focused on its increased expression in lung cancer cells. Clusterin has been reported to be elevated in lung adenocarcinoma cells (X. Chen et al. 2016) and induces treatment resistance in lung cancer cells *in vivo* (Ma et al. 2015). Silencing of secretory clusterin *in vitro* promotes cisplatin anti-tumour activity (Zhang et al. 2014) and inhibits proliferation, migration and promotes apoptosis in non small lung cancer cells (NSLCC) (H. Li et al. 2010; C. Y. Cheng et al. 2012; Yan et al. 2013a). The protective effects of clusterin, which promote treatment resistance in cancer cells, may be attributed to its effects on inhibiting pro-apoptotic protein Bax (Zhang et al. 2005). Phase III and IV clinical trial studies are currently assessing the effects of antisense oligonucleotides targeting the clusterin gene in lung and prostate cancer[2].

Rodent lung

Numerous studies in rodents have assessed the role of clusterin during lung injury. A study investigated the potential protective effects of clusterin in perfused rabbit lungs: Heller and colleagues showed that the administration of clusterin reduced pulmonary hypertension and oedema due to a protective effect of clusterin in fMLP-mediated leukocyte-induced pulmonary injury via complement inhibitory mechanism (Heller et al. 2003). Additionally, clusterin was elevated in rat lungs exposed to systemic pulmonary shunt-induced pulmonary arterial hypertension (PAH). Here, clusterin was identified as a phenotypic modulator of pulmonary artery smooth muscle cells (PASMCs) with an important role in vascular pulmonary remodelling: *In vitro* evidence suggests, that clusterin promotes proliferation, migration and apoptosis resistance in human PASMCs, potentially through the engagement of Erk1/2 and Akt signalling pathways (Liu et al. 2015).

Another model in mice investigated the effect of clusterin-deficiency on house dust mite-induced airway inflammation (Hong et al. 2016). In clusterin-deficient mice the total number of immune cells was increased in BALF and the lung.

[2] www.clinicaltrials.gov NCT01578655 (on-going) and NCT01630733 (recruiting). Status September 2016.

Furthermore, profibrotic mediator CCL-20 was enhanced in BALF from clusterin-deficient mice, suggesting that CCL-20 secretion was negatively regulated by clusterin in bronchial epithelial cells. Moreover, clusterin-deficient mice demonstrated increased levels of Th2 and M2 cytokine IL-4 in BALF. Hence, clusterin was suggested as anti-inflammatory mediator and dysregulation of clusterin expression could be linked to persistent airway inflammation (Hong et al. 2016).

Together, the data suggests that clusterin is protective in smoker's lung but promotes survival in various lung cancer cells. In animal studies focusing on the role of clusterin in the lung, clusterin was suggested to act as an immunomodulator to protect against lung injury in rodents. However, the detailed distribution of clusterin, its immunomodulatory affects associated with fibrosis and its function in the human lung remains unknown.

1.4.3 Clusterin expression in lung disease and response to tissue injury.

Clusterin expression has been reported to be altered in many disease states that are associated with tissue injury and repair. In asthma, clusterin serum levels were significantly increased, and correlated with asthma severity (Kwon et al. 2014). A more recent study describes clusterin sputum levels in childhood asthma were elevated, reflecting airway inflammation and severity of symptoms (Sol et al. 2016). Additionally, clusterin serum levels increased with severity in COPD (severe COPD 167.50 ± 18.13 µg/ml) when compared with healthy controls (121.30 ± 13.56 µg/ml), and clusterin was suggested to be a potential peripheral biomarker of cognitive dysfunction in COPD patients (Li & Huang 2013). In these studies it was solely indicated, that clusterin serum levels were increased with disease severity. However, it remains unknown if altered clusterin levels in lung disease are causative or protective throughout the course of the disease. Another study with 61 Systemic sclerosis (SSc) patients and 24 healthy individuals indicated that serum levels in SSc patients (median, 162.9 µg/ml) were increased when compared with controls (median, 142.2 µg/ml). However, SSc patients with elevated clusterin levels had digital ulcers and pulmonary arterial hypertension less often than those with normal clusterin levels (Yanaba et al. 2012). This suggests that elevated clusterin levels, at least in patients with SSc, could be a protective mechanism to conquer the progression of the disease. In conclusion, clusterin serum levels are altered in various lung-associated

diseases. Yet, the distribution of clusterin in normal lung is incompletely described. Further insights, into cell dependent clusterin expression patterns in health, compared with disease would allow new insights into the role of clusterin in the lung and its impact on disease severity.
In order to better understand the role of clusterin in the lung, it may be of interest to review the literature on clusterin role and function in other organs. Generally, clusterin is reported to be elevated in states of tissue injury (Silkensen et al. 1994), which strongly suggests a role of clusterin in regulating repair and remodelling processes.

In acute head injury, clusterin expression was elevated in astrocytes from 30 min after injury and remained increased at high levels for several weeks after injury, with potential immunoregulatory effects (Troakes et al. 2016). Clusterin has been suggested to be a stress-inducible biomarker (Viard et al. 1999; J. H. Kim et al. 2010; Antonelou et al. 2011). Additional studies in Crohn's disease, suggested that clusterin is increased in crypt epithelial cells to exert a cytoprotective function to prevent further injury (Gassler et al. 2001).
On a cellular level clusterin was induced in many cell types following experimental injury, including VSMC in a model of balloon-injured rabbit aorta (Miyata et al. 2001), in tubular epithelial cells (Girton et al. 2002), astrocytes (Imhof et al. 2006), corneal epithelia cells (Shin et al. 2009) and ventricular myocytes (Swertfeger et al. 1996). Consistent with a protective role, clusterin-deficiency worsens the injury in rodent models of kidney injury (W. Zhou et al. 2010) and attenuates renal fibrosis in response to obstruction (Jung et al. 2012).
In summary, clusterin, a stress-regulated protein appears to be a potential mediator of the response to injury and tissue remodelling (Bailey et al. 2002). However, little has been reported about the role of clusterin in lung injury and potential implications in normal and aberrant wound repair. A detailed analysis of clusterin distribution and function in healthy and fibrotic lung would significantly enhance our understanding of its role in protecting against or contributing to disease severity of lung fibrosis.

1.4.4 Clusterin biosynthesis

Although extensive efforts have been undertaken to understand the biosynthesis and regulation of clusterin in the past decades, only basic information about clusterin's gene expression and regulation have been reported. In humans, the CLU gene (CLU) is a single, nine exon gene, located on chromosome 8 (Wong et al. 1994). This CLU gene organisation is well conserved across species including mouse and rat (Rizzi et al. 2009). The CLU gene expression is tightly regulated and very tissue specific: It is known that the clusterin promoter is highly conserved and contains numerous regulatory elements, which control clusterin expression in a tissue-and stress specific manner (Michel et al. 1995; Wilson 2000; Trougakos 2013). Clusterin expression is linked to environmental cytokine signals and growth factors including TGF-β, nerve growth factor, epidermal growth factor, and heat shock transcription factor 1 (reviewed in Park et al. 2013). Before 2006, it was believed that CLU gene originates a unique transcript (Rizzi et al. 2009). However, more recent reports suggest that more transcripts code for CLU. As listed most recently in the NCBI database the human CLU-gene encodes for at least three different mRNA variants (variant 1: NM_001831.3; variant 2: NR_038335.1 and variant 3: NR_045494.1)[3]. These transcripts are probably originated from two alternative transcriptional initiation start sites and only produced in humans and chimpanzees (Rizzi et al. 2009). All transcripts have a unique exon 1 and share exon 2-9 (Prochnow et al. 2013). Transcript variant 1 (NM_001831.3) is the most abundant of all CLU mRNA variants and its translation initiation starts from an AUG start codon upstream of the ER-signal-peptide-sequence, which results in the translation of a 449 amino acid long precursor protein including an ER-signal peptide (Wong et al. 1993; Prochnow et al. 2013; Mydlarz et al. 2014). In the early stages of its maturation precursor protein appears as an unfolded 48 kDa protein in the rough ER where it is cleaved from its ER-signal peptide before it is folded and glycosylated at six glycosylation sites resulting in a 60k Da sized precursor protein (Figure 1.9). The glycosylated precursor is then processed to the Golgi apparatus for further glycosylation and proteolytic cleavage into α and β subunits (Kirszbaum et al. 1992). The α and β chain are reassembled in an anti-parallel manner and are connected via five disulphide bounds leading to a 75-80 kDa heterodimer (de Silva et al. 1990a), which is then destined for secretion (Figure 1.9). In U251

[3] http://www.ncbi.nlm.nih.gov/gene/1191

human astrocytoma cells, stress-induced retranslocation of clusterin from the ER into the cytosol has been demonstrated (Nizard et al. 2007). In some cells, it has been reported that the unfolded precursor clusterin (pnCLU, Figure 1.9) translocates to the nucleus, where it has been proposed to induce pro-apoptotic effects (Zhang et al. 2005; Shannan et al. 2006). The molecular mechanism of induction of this protein form remains unclear. In some cell lines, it has been reported that precursor CLU is able to escape the secretory pathway using the ER-associated protein degradation pathway to accumulate in the cytosol and mitochondria (Nizard et al. 2007; Li et al. 2013). Cleavage and secretion of mature secretory clusterin are independent of its state of glycosylation (Burkey et al. 1991; Kapron et al. 1997; Charnay et al. 2012).

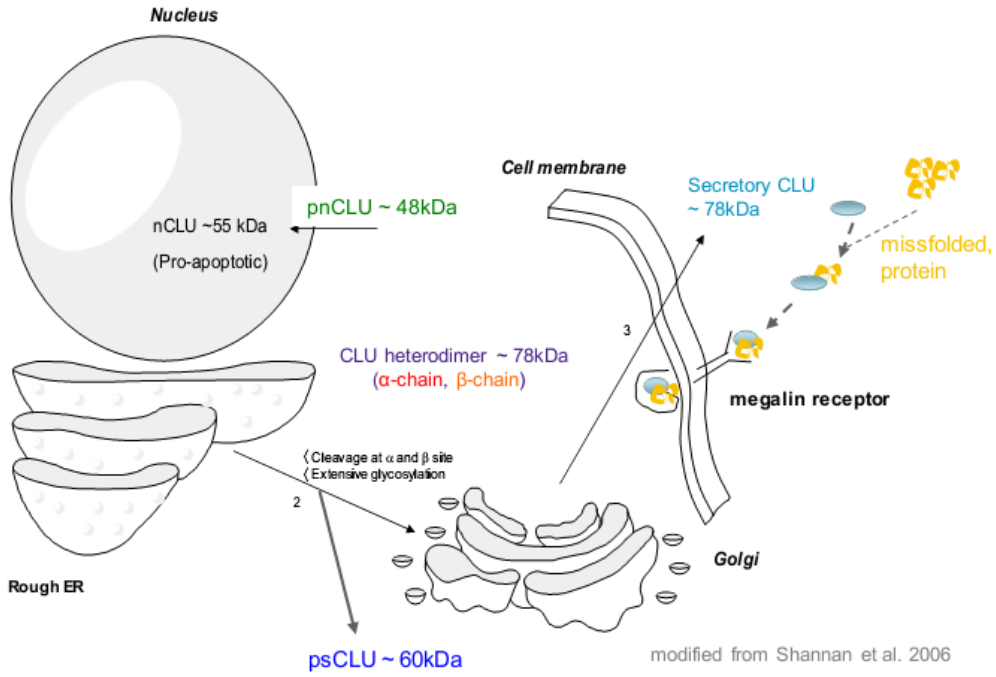

Figure 1.9 Clusterin biosynthesis modified from (Shannan et al. 2006).

Clusterin is translated from the fist AUG start codon upstream of the ER-signal-peptide-sequence resulting in a 60 kDa precursor protein (psCLU). In some cells, alternative transcriptional initiation results in translation of a truncated nuclear form (pnCLU 48 kDa) that translocates into the nucleus to exert pro-apoptotic effects. Cytoplasmic precursor clusterin (psCLU 60 kDa) is glycosylated on six sites, cleaved into α and β, assembled in an antiparallel manner and as protein of ≈ 78 kDa secretory clusterin with five disulphide bonds between the α and β subunit. Secretory clusterin was reported to act as extracellular chaperone. It assembles with misfolded proteins in the extracellular space and is internalised via receptor mediated endocytosis (Stewart et al. 2007). ER – endoplasmic reticulum, CLU - clusterin.

1.4.5 Clusterin regulated by cell stress and TGF-β_1

As previously mentioned clusterin is elevated in response to stress. This was confirmed in several *in vitro* models, where clusterin was upregulated in response to cell stress: Clusterin was induced in response to TNFα in murine fibroblasts (Humphreys D.T et al. 1997), heat shock (Michel et al. 1997), UV (Hsieh et al. 2005) and oxidative stress in human breast cancer cells (Yang et al. 2000). Moreover, clusterin mRNA and protein was induced by TGF-β_1 in a dose-dependent manner in astrocytes (Morgan et al. 1995). TGF-β has been reported to up-regulate clusterin expression in epithelial cells, including mink lung epithelial cells, affecting differentiation and apoptosis (Reddy, Jin, et al. 1996; Itahana et al. 2007; Wegrowski et al. 1999; Reddy, Karode, et al. 1996; Jin & Howe 1999). It is, however, unknown if TGF-β_1 affects clusterin expression in human pulmonary cell types, including lung fibroblasts.

1.4.6 Clusterin regulates cell differentiation and function

Clusterin is a multifunctional protein. Numerous roles have been assigned to clusterin in regulating differentiation, proliferation, migration and survival of various cells. The following sections outline the effects of clusterin on these processes. Insights into clusterin's role in various cell types may help us to understand its potential role in pulmonary cells types with possible implications for clusterin's role in the normal lung and in disease states. The previously identified effects of clusterin in various cell types may provide insights into its potential role in pulmonary cells in the normal and distorted fibrotic lung.

1.4.7 Differentiation

Clusterin has been suggested to be expressed during differentiation processes in the embryonic mouse lung (French et al. 1993; Min et al. 1998), and clusterin staining was located to termini of developing bronchioles (Zheng et al. 2013). However, the role of clusterin in the development of the human lung remains unknown.

Other studies suggest a role for clusterin in mesenchymal cell differentiation: Initial experiments from Thomas-Salgar et al. reported that endogenous clusterin supports the rapid formation of nodules in monolayer cultures of smooth muscle

cells (Thomas-salgar & Albert 1994), similar to its role in differentiation, reorganisation and nodule formation of vascular smooth muscle cells (VSMCs) (Millis et al. 2001). Additional studies using Boyden chambers demonstrated that clusterin promoted VSMC migration (Millis et al. 2001; Miwa et al. 2004). This data suggests that clusterin is a critical player in regulating the phenotype of smooth muscle cells, with important implications for vascular diseases. Alterations of clusterin could hence contribute to the pathogenesis of vascular diseases. Additionally, it has been suggested that clusterin promotes differentiation of pancreatic beta cells into insulin-secreting cells (B. M. Kim et al. 2006). Together, the current literature demonstrates that clusterin may have a potential role in regulating differentiation processes during embryogenesis and in response to injury.

1.4.8 Migration

Reports about the role of clusterin in cell migration appear to be controversial and cell-specific: *In vitro* studies examined the effects of silenced clusterin expression on cell migration and invasion in a human breast cancer cell line, MDA-231. Clusterin knock-down cells demonstrated significantly less cell migration in a wound healing assay than control cells suggesting a role of clusterin in migration and invasion of human breast and renal cancer cells (Li et al. 2012; Niu et al. 2012; X. Wang et al. 2014). These results are consistent, with findings in lung adenocarcinoma cell lines where clusterin silencing resulted in reduced migration and pulmonary infiltration *in vitro* (Chou et al. 2009).

In the context of vascular remodeling, adenovirus-mediated overexpression of clusterin repressed TNF-alpha-stimulated expression of ICAM-1, VCAM-1, and MMP-9, leading to inhibition of VSMC migration (Kim et al. 2009). This conflicts with earlier reports, in which recombinant clusterin (10 μg/ml) was shown to promote VSMC migration (Millis et al. 2001). Similar, studies in human umbilical vein endothelial cells (HUVECs), demonstrate that decreased secretory clusterin levels resulting from radiation lead to inhibition of migration (Hwang et al. 2013).
Apart from cancer and mesenchymal cells, clusterin has been associated with increased migration in monocytes and macrophages of human and murine origin. Checkerboard analysis demonstrated that clusterin-induced the chemotactic migration of human monocyte and murine peritoneal macrophages (Kang et al. 2014). Administration of pertussis toxin or Gβγ inhibitor suppressed clusterin-

induced migration in these cells suggesting that this was G-protein-coupled Gβγ-pathway dependent. Previous studies in murine (Raw264.7) and peritoneal macrophages demonstrated that clusterin-induced chemotactic migration and the secretion of TNFα via ERK, JNK, and PI3K/Akt dependent pathways (Y.-J. Shim et al. 2012). In addition, the same study suggested that clusterin regulated chemotactic cytokines, such as monocyte chemotactic protein-1 (MCP-1), macrophage inflammatory protein-1b (MIP-1b) and regulated upon activation and normal T cell expressed and secreted (RANTES). Another study by Shim and colleagues showed that clusterin induced the expression of matrix metalloproteinase-9 (MMP-9) in macrophages potentially enabling cancer cell invasion via basement membrane breakdown (Shim et al. 2011).
In summary, these studies suggest that clusterin promotes migration and invasion in cancer cell lines, vascular remodelling via enhanced migration of mesenchymal cells and serves as a molecular bridge between inflammation and remodelling via recruitment of immune cells, including macrophages.

1.4.9 Proliferation

Several lines of evidence suggest that clusterin plays a major role in tissue repair via inducing proliferation of various cells after injury. Nguan and colleagues studied the role of clusterin in renal tissue repair after experimental ischemia induced injury. Clusterin-deficient mice demonstrated enhanced tubular damage in response to reperfusion-induced injury, resulting in renal failure. *In vitro* data derived from these studies strongly suggest that clusterin is a mediator of proliferation in tubular epithelial cells (Nguan et al. 2014). Similar data have been demonstrated for reactive astrocytes during brain injury. Shin and colleagues demonstrated that clusterin induced proliferation in astrocytes *in vitro* while targeting clusterin expression via antisense oligonucleotides induced growth arrest in astrocyte cultures (Shin et al. 2006). Apart from beneficial effects of clusterin on proliferation, these effects have also been demonstrated for many cancer cell lines, such as non-small lung and renal, breast and ovarian cell lines (Yan et al. 2013b; Shi et al. 2013; Niu et al. 2012; Fu et al. 2015). However, secretory clusterin and overexpression in VSMC inhibited proliferation *in vitro*, suggesting that clusterin may play a protective role during vascular injury rather than a causative role in the pathogenesis of neointimal hyperplasia (Kim et al. 2009).

In summary, these data strongly support that clusterin is essential in regulating proliferation dependent repair processes in kidney and the brain. However, in the context of the lung, kidney and breast cancer clusterin's pro-proliferative properties may promote uncontrolled proliferation and tumour growth. Clusterin effects on proliferation appear tissue and cell dependent and may be protective against neointimal hyperplasia. The effects of clusterin on (lung) fibroblast proliferation have not been described.

1.4.10 Apoptosis/Survival

Over 500 PubMed articles about the role of clusterin in apoptosis are listed indicating the importance and manifold implications of this protein in this form of cell death. At this moment, the majority of articles focus on the role of clusterin in impaired apoptosis in treatment resistant cancer cells. Clusterin is upregulated by apoptotic triggers and induces treatment resistance in many cancers, including human lung adenocarcinoma, myeloid leukaemia, pancreatic and prostate cancer cells while silencing of clusterin mRNA levels enhances treatment induced apoptosis (Xiu et al. 2013b; July et al. 2004; Wang et al. 2015; Xu et al. 2015; Yamamoto et al. 2015). A potential mechanism by which clusterin exerts its anti-apoptotic effects was demonstrated in studies with prostate cancer cells. Zhang et al. suggest that clusterin inhibits apoptosis by associating with Bax in the cytosol to prevent the initiation of the intrinsic apoptosis pathway in response to pro-apoptotic stimuli such as anti-cancer therapies (Zhang et al. 2005; Muhammad & Saad 2015). More recently it has been reported that cytoplasmic clusterin exerts pro-survival effects through the activation of the AKT pathway in hepatocellular carcinoma cells (Xiu et al. 2013b). Moreover, it has been shown in prostatic cells that overexpression of clusterin protects against tumour necrosis factor-alpha (TNFα)-induced apoptosis via the up-regulation of the phosphorylation of AKT (Ammar & Closset 2008). Due to the promising effects of clusterin gene silencing in cancer progression, an antisense oligonucleotide drug called "custirsen" is currently being assessed in clinical phase III an IV studies in a combination therapy with anti-cancer drugs.[4]

In contrast, TGF-β_1, has been reported to up-regulate clusterin expression in HepG2 hepatocellular carcinoma cells and CCL64 mink lung epithelial cells resulting in induced apoptosis in these cells (Reddy, Jin, et al. 1996; Itahana et

[4] (www.clinicaltrials.gov NCT01578655 and NCT01630733)

al. 2007; Wegrowski et al. 1999; Reddy, Karode, et al. 1996). These effects may be caused by a nuclear isoform of clusterin with pro-apoptotic properties that translocates into the nucleus in response to TGF-β_1 to induce cell death (Reddy, Jin, et al. 1996).

As alluded to earlier clusterin has been suggested to play an important role in pulmonary vascular remodelling in response to injury. Liu and colleagues suggest that clusterin plays a vital role in regulating these processes and to contribute to biological behaviour modification in human PASMCs. Their *in vitro* studies suggest that secretory clusterin induces resistance to apoptosis in human PASMCs, potentially mediated through ERK 1/2 and Akt signalling pathways (Liu et al. 2015). Liu and colleagues also provide evidence for the reverse effect: Clusterin silencing via siRNA induced spontaneous apoptosis in human PASMCs.

However, the effects of clusterin in fibroblast-like synoviocytes (FLS) were in conflict to the effects in human PASMCs. In FLS transgenic overexpression of clusterin-induced apoptosis within 24 hours (Devauchelle et al. 2006), while in human PASMCs clusterin promoted the resistance to apoptosis. Devauchelle and colleagues further suggested that high levels of extracellular and low levels of intracellular clusterin in FLS may enhance NFκB activation and survival of synoviocytes.

Interestingly, clusterin has been suggested to be a biomarker of senescence in human fibroblasts, as a secondary consequence rather than playing a causative role in senescence (Petropoulou et al. 2001) and is upregulated in quiescent skin fibroblasts (Bettuzzi et al. 2002). Furthermore, clusterin has been suggested as a biosensor of oxidative stress in lung fibroblasts (Trougakos & Gonos 2006), and overexpression of clusterin protects against cytotoxicity in response to oxidative stress in WI-38 human embryonic lung fibroblasts (Dumont et al. 2002). In clusterin-deficient mouse embryonic fibroblasts (MEFs) genotoxic stress induced NFκB levels were enhanced, suggesting that clusterin stabilises IκBs to inhibit NFκB signalling (Santilli et al. 2003). Together, this suggests that the effects of clusterin on survival and apoptosis are diverse and may be tissue and cell type specific. However, it is noticeable that clusterin silencing in cancer cells generally induces the same effects while clusterin gene silencing in mesenchymal cells resulted in conflicting effects in response to apoptosis. The effects of clusterin on basal and induced apoptosis in adult human lung fibroblasts have not been described.

1.4.11 Extracellular chaperone

Apart from clusterin's multiple effects on cell differentiation and function, many studies suggest that clusterin acts as an extracellular molecular chaperone involved in promoting the appropriate folding and conformation of extracellular proteins and shielding proteins under conditions of tissue stress (Poon et al. 2000; Aigelsreiter et al. 2009). Secretory clusterin is ubiquitously expressed in most mammalian tissues and body fluids, such as blood plasma, urine, semen, breast milk and cerebrospinal fluid. Strong evidence suggests that secretory clusterin exerts extracellular chaperone activity similar to that of small heat shock proteins intracellularly (Kirszbaum et al. 1992; Poon et al. 2000; Wilson 2000; Lakins et al. 2002). Secretory clusterin assembles with misfolded proteins in the extracellular space via hydrophobic and amphipathic α-helices based at the N-terminus of both α and β chain and the c terminus of the β chain to mediate the interaction with hydrophobic ligands (Law & Griswold 1994). Clusterin chaperone activity has been associated with neurodegenerative diseases such as Alzheimer's disease, since clusterin sequesters with Aβ oligomers and regulates their aggregation and disaggregation (Narayan et al. 2011). Moreover, clusterin chaperone properties were associated with decreased enzymatic MMP-9 activity, to maintain the epithelial barrier in the events of high MMP-9 aggregation (Jeong et al. 2012). The clusterin receptor called LDL receptor family member glycoprotein 330 (LRP2) is the clusterin receptor that has been most frequently studied in association with clusterin endocytosis (Byun et al. 2014; Gil et al. 2013; Park et al. 2013; Marzolo & Farfán 2011). Clusterin has been demonstrated to bind to LRP2 via three independent, discrete binding sites (Lakins et al. 2002; Lakins et al. 2006). It has been reported that secretory clusterin mediates the recognition and disposal of miss-folded, long-lived protein intermediates and damaged proteins via LRP2/megalin receptor-mediated endocytosis (Bartl et al. 2001; Kang et al. 2005; Stewart et al. 2007) followed by lysosomal degradation (Wyatt et al. 2011).

In aged human skin, clusterin has been shown to associate with altered elastic fibres (Janig et al. 2007). It was, therefore, proposed that clusterin may contribute to the clearance of defective and degraded elastin via megalin/gp330 receptor-mediated endocytosis (Bartl et al. 2001; Janig et al. 2007). Nevertheless, the distribution of clusterin in normal and fibrotic lung and its role as extracellular chaperone in the lung has not been described.

1.5 Summary, Hypothesis and Aims

Pulmonary fibrosis is a progressive, diffuse, parenchymal lung disease with dismal prognosis and no curative therapy. Dysregulated repair processes promote the polarisation of macrophages into a profibrotic M2 phenotype secreting pro-fibrotic mediators including TGF-β_1 and PDGF, which results in unopposed fibroproliferation. Dysregulation of fibroblast function in pulmonary fibrosis, involving uncontrolled proliferation, myofibroblast-differentiation and resistance to apoptosis, results in excessive deposition of extracellular matrix, leading to progressive scarring of the lung tissue and impaired gas exchange. Clusterin, a multifunctional glycoprotein with extracellular chaperone activity and which is involved in regulating cell function, is reduced in BALF of patients with pulmonary fibrosis. However, its distribution and role in normal and fibrotic lung, particularly in fibroblast and macrophage biology are incompletely characterised. These observations led to the generation of the hypothesis examined in this thesis; **that clusterin plays an important role in normal human lung homoeostasis and changes in clusterin distribution and expression may be protective against the pathogenesis of pulmonary fibrosis.** To address this hypothesis I will:

1) Determine the expression and localisation of clusterin and its receptor LRP2 in normal and fibrotic human lung.

2) Examine the extracellular protein binding characteristics of clusterin and its functional effects on human lung fibroblast differentiation, proliferation, αSMA expression and collagen synthesis and apoptosis *in vitro* in cells isolated from control and fibrotic lung.

3) Investigate potential mechanisms for the regulation of clusterin and its role in mediating the pro-fibrotic effects of TGFβ_1 in control lung fibroblasts and compared with its effects on fibrotic lung fibroblasts.

4) Examine the regulation of clusterin in and the effect of plasma-derived human clusterin on macrophage phenotype by assessing the secretion of pro- and anti-inflammatory cyto- and chemokines.

5) Investigate the effects of exogenous clusterin on macrophage polarisation towards a pro-inflammatory or pro-fibrotic phenotype.

2 Material and Methods

Materials

2.1 General plastic ware, chemicals, and cell culture reagents

Sterile tissue culture plates and flasks were purchased from Nunc (Roskilde, Denmark) and Corning (Flintshire, UK). Sterile polypropylene centrifuge tubes and pipettes were purchased from Falcon (Fisher Scientific, UK). Whatman cyclopore 0.2 µm polyester syringe filters were purchased from Whatman (UK), sterile 12-well Transwell® (6.5 mm polycarbonate inserts with 8 µm pore size) from Corning (Flintshire, UK), 96-well black tissue culture-treated plates and Staurosporine from VWR International (UK). Deionised water was prepared using a Millipore Water Purification System (Milli-Q Plus; Millipore Ltd, UK) for the preparation of dilutions and buffers. Sterile Dulbecco's Modified Eagle Medium (DMEM; high glucose, sodium pyruvate, no L-glutamine), Roswell Park Memorial Institute (RPMI) 1640 medium, Hank's Balanced Saline Solution (HBSS), penicillin-streptomycin, L-glutamine, 0.25 % trypsin-EDTA, amphotericin B, Foetal Bovine Serum (FBS) and Opti-MEM® Reduced Serum Medium were purchased from Gibco Life technologies (Thermo Fisher Scientific, UK) as well as Histopaque 1077 for PBMC isolation. HEPES buffer was purchased from Lonza (UK). DMSO and L-Ascorbic acid 2-phosphate sesquimagnesium salt hydrate, Hydrogen peroxide solution (30 %, v/v), Triton X, goat serum, puromycin dihydrochloride and polybrene transduction reagent was purchased from Sigma-Aldrich (UK). PBS tablets were ordered from Oxoid Ltd. (Hampshire, UK). INTERFERin siRNA transfection reagent was received from Polyplus Bioscience Ltd (UK). $CD14^+$ MicoBeads (human) and Midi MACS 25 LS columns were purchased from MACS Miltenyi Biotec (Surrey, UK).

2.2 Cytokines, eicosanoids, growth factors, peptides and toxins

Synthetic, cell culture tested PGE_2 was obtained from Cambridge bioscience (UK). PDGF-AB was received from PeproTech EC Ltd. (UK). Recombinant human FasL was purchased form Merck Biosciences (Germany). Purified porcine TGF-β_1, IFNγ, IL-4, PDGF-BB and M-CSF were purchased from R&D systems (Abingdon, UK) and native, exogenous human plasma clusterin[5] from BioVendor

[5] Endotoxin levels < 1.0 EU/ug as measured by LAL.

(Oxford, UK). Lipopolysaccharide (LPS) was purchased from Sigma (Sigma-Aldrich, UK).

2.3 Antibodies

Antibodies used for immunohistochemical localisation studies are listed in Table 2 Polyclonal rabbit isotype IgG (ab37415) and mouse isotype IgG_1 (ab91353) were also purchased from Abcam and used at matching concentrations of primary antibody concentrations.

Table 2 List of antibodies used for immunohistochemical localisation studies.

Antibody target	Antibody type	Source company	Cat.-no	Antigen unmasking method	Final antibody concentration
Clusterin (α,β)	rabbit polyclonal	Santa Cruz	sc-8354	Citrate buffer	0.67 µg/ml
TGF-β_1	rabbit polyclonal	Santa Cruz	sc-146	Proteinase K	1.0 µg/ml
α-SMA	mouse monoclonal	Dako	Clone 1A4 M0851	Citrate buffer	142 ng/ml
LRP2	rabbit polyclonal	Abcam	ab76969	Citrate buffer	1.0 µg/ml

The antibodies used for Western blotting are listed in Table 3. Polyclonal secondary antibodies, goat anti-rabbit, rabbit anti-mouse, rabbit anti-goat were purchased from Dako (Glostrup, Denmark).

Table 3 List of antibodies used for Western blotting.

Antibody target	Antibody type	Source company	Cat.-#	Final antibody concentration
Clusterin (α,β)	rabbit polyclonal	Santa Cruz	sc-8354	267 ng/ml
Clusterin (α)	mouse monoclonal	Santa Cruz	sc-5289	267 ng/ml
αSMA	mouse monoclonal	Dako	M0851	7.10 ng/ml
Vinculin	goat polyclonal	Santa Cruz	sc-7649	267 ng/ml
anti-rabbit	goat polyclonal	Dako	P0448	50 ng/ml
anti-mouse	rabbit polyclonal	Dako	P0260	260 ng/ml
anti-goat	rabbit polyclonal	Dako	P0449	275 ng/ml

The antibodies used for immunocytochemistry are listed in Table 4. Mouse and rabbit IgG isotype controls were purchased from Vector (New Zealand) and mouse IgG_1 was purchased from (ab91353) from Abcam (Cambridge, UK) and (5415S) Cell Signalling Technology (UK). Polyclonal secondary antibodies, goat anti-mouse IgG (H+L) Alexa Fluor® 555 (A-21422), goat anti-mouse IgG (H+L), Alexa Fluor® 488 (A-11001) and goat anti-rabbit IgG (H+L), Alexa Fluor® 647 were purchased from Thermo Fisher Scientific (Ma, US).

Table 4 List of antibodies used for immunocytochemistry.

Antibody target	Antibody type	Source company	Cat.-no	Dilution	Final antibody concentration
Clusterin (α,β)	rabbit polyclonal	Santa Cruz	sc-8354	1 in 100	2.0 µg/ml
Clusterin (α)	mouse monoclonal	Santa Cruz	sc-5289	1 in 100	2.0 µg/ml
αSMA	mouse monoclonal	Denmark	M0851	1 in 600	118 ng/ml
Collagen I	mouse monoclonal	Sigma, Aldrich	C2456	1 in 1000	4.7µg/ml

All antibody-coated magnetic bead performance assays were purchased from R&D Systems and are listed in Table 5.

Table 5 List of single-plex luminex assays.

Target /Kit (human)	Cat.-no.	Dilution of sample required
Human base A kit	LUHM000	N/A
IL-10	LUHM217	1:1
IL-1RA	LUHM280	1:1
IL-4	LUHM204	1:1
IL-6	LUHM206	1:1
IL-8	LUHM208	1:5
MCP-1	LUHM279	1:1
MIP-1α	LUHM270	1:1
RANTES	LUHM280	1:5
TNFα	LUHM210	1:1
IFNγ	LUHM285	1:1
Human MMP base kit	LMPM000	N/A
MMP-8	LMPM908	1:1
MMP-9	LMPM911	1:1

2.4 Kits

BCA™ protein Assay Reagents A & B were purchased from Pierce (USA) and Quick Start™ Bradford Protein Assay form Bio-Rad (UK). Luminata Crescendo Western HRP substrate kit was purchased from Millipore (Darmstadt, Germany). Precision DNase kit was obtained from Primerdesign Ltd. (UK). qScript cDNA SuperMix® kit was purchased from Quanta Biosciences (USA). RT-PCR kit for cDNA synthesis was purchased from Applied Biosystems (Roche, Lewes, UK). Proteinase inhibitor cocktail complete, Mini, EDTA-free was obtained from (Roche, UK) and phosphosafe extraction reagent from Merck Chemicals Ltd. (UK). The human MMP and human base kit A and all magnetic bead-based multiplex Luminex assays were purchased from R&D Systems (Abingdon, UK) and the Human cytokine magnetic 25-plex panel kit from Novex (Thermo Fisher Scientific, UK).

2.5 Human biological samples

The human biological samples were sourced ethically and their research use was in accord with the terms of the informed consents.

Methods

2.6 Patient population and primary cell isolation

Fibrotic lung tissue was obtained from lung biopsies and at transplant surgery (IPF n = 7, aged 62 ± 4 years, four male; SSc n = 7, aged 52 ± 2 years, one male). All IPF samples used in this study were classified using the diagnostic criteria of the American Thoracic Society / European Respiratory Society (ATS/ERS) consensus criteria: namely, a pattern of usual interstitial pneumonia (UIP) (Raghu et al. 2011). All SSc samples were classified using the diagnostic criteria of the American college of rheumatology/European league against rheumatism collaborative initiative (ACR/EULAR) (van den Hoogen et al. 2013).

Control lung tissue was obtained from histologically normal areas of peripheral lung distal to lung cancer resection (uninvolved tissue) or from patients who died as a result of an accident with no signs of lung disease (n = 6, aged 59 ± 7 years, two male). Approval for the use of all material was obtained from the ethics committee of University College London and University College London Hospital and the Royal Brompton & Harefield NHLI. Informed consent was received from each subject. An overview of patient information associated to the used method is presented in Appendix 1. The method used to isolate the fibroblasts from the lungs was the same for each donor and was conducted as previously described (Akers et al. 2000; Keerthisingam et al. 2001).

Briefly, lung tissue was collected from hospital into DMEM and transported to the laboratory on ice. The peripheral lung tissue was trimmed under sterile conditions into sections sized 1 mm^3 or less and fixed on petri dishes with 2 ml of 20 % FBS in DMEM (containing 400 U/ml penicillin streptomycin, 2 mM L-glutamine and 0.1 % amphotericin B). Tissue fragments were allowed to adhere for 24 hours (37 ^oC, 10 % CO_2) before adding a further 8 ml media. Amphotericin B and Penicillin / Streptomycin (1:1 ratio) were replenished at 200 µL every following 2 - 3 days. During 2 - 4 weeks cells were proliferating and growing out of the explant and reached 80 - 90 % confluence before they were washed with 2 mL trypsin - EDTA once, followed by treatment with 2 mL trypsin-EDTA at 37 ^oC. The cells were inspected after approximately three minutes, using an Olympus TCK-2 inverted phase contrast light microscope (Olympus Optical Ltd, UK) for shape change (rounding up) and detachment from the plastic. Once most cells were detached from the plastic dish, trypsin was subsequently neutralised with 10 % FBS in DMEM. The cells were then centrifuged (300 x g, 5 minutes). The

supernatant was discarded, and the pellet was resuspended in 10 % FBS in DMEM. The cells were counted with Millipore Cell Scepter and seeded into tissue culture flasks or transferred into cryogenic vials in freezing medium (40 % DMEM, 40 % FBS and 20 % DMSO) for storage in liquid nitrogen. (Keerthisingam et al. 2001; Maher et al. 2010). Once established, cells were cultured in 75 cm^2 or 175 cm^2 tissue culture flasks (Corning, UK) in DMEM containing 10 % FBS with 50 units/ml penicillin and 50 µg/ml streptomycin at 37 °C in a humidified atmosphere of air containing 10 % CO_2. Media was changed every 72 hours and cells detached with trypsin solution (0.05 % Trypsin–EDTA). Fibroblasts were passaged on reaching confluence approximately every 5 – 7 days and were used for experiments between passage 3 and 12. All tissue culture media and supplements were purchased from Gibco, Life Technologies, UK.

When using lung fibroblasts from explant cultures the following limitations have to be considered: *In vitro* systems do not represent effects of systemic factors, which are present *in vivo.* Actively migrating/apoptosis-resistant cells are positively selected, since they are more likely to extra-migrate from the explant tissue and survive, whilst quiescent fibroblasts remain in the deteriorating tissue and are excluded from the analysis in long term *in vitro* culture.

2.7 Preparation of growth factors and cytokines for *in vitro* experiments

PGE_2 was reconstituted in DMSO at a concentration of 10 mM and was stored at 4 °C. FasL was reconstituted in sterile deionized water at 50 µg/ml and was stored prior to use in aliquots at - 80 °C. Lyophilized human plasma clusterin was dissolved in sterile deionized water at a concentration of 0.5 mg/ml. Staurosporine was reconstituted in DMSO at concentration of 1 mM and stored at - 20°C. PDGF-BB and TGF-β_1 were dissolved in sterile 4mM HCL containing 0.1 % BSA. Prior to use an aliquot of the relevant compound was defrosted on ice and diluted to the required concentration in the appropriate medium. Because of the potential of DMSO to affect cell function, DMSO vehicle alone was added to control wells in each experiment in a concentration equal to that of wells containing growth factors or cytokines. LPS (1mg/ml), IFNγ (100 µg/ml) and IL-4 (10 µg/ml) were reconstituted in RPMI culture medium and stored at -20 °C.

2.8 Clusterin siRNA transfection

Mammalian cell transfection with siRNA (small interfering RNA) is a molecular method, commonly used to transiently knock down gene expression (Elbashir et al. 2001). siRNA duplexes are formed by a guide strand, complementary to the

mRNA target and passenger strand. During transfection, specific siRNA duplexes are introduced into the host cell via transfection reagent. Inside the cell, the siRNA complex unwinds and the guided strand is incorporated into the RNA Interference Specificity Complex (RISC) and exposed to endogenous target mRNA. Following ligation of the guided strand with endogenous specific target mRNA, the mRNA is cleaved and degraded resulting in silencing of gene expression.

In order to transiently knock down clusterin expression, cells were transfected following reverse transfection protocol provided by Polyplus-transfection® (Illkirch, France). Silencer® Select Human siRNA targeting clusterin and the *Silencer*® Select Negative Control No. 1 siRNA (Thermo Fisher Scientific, UK) were reconstituted to 1 µM stock in RNA buffer. A range of siRNA concentrations (1 nM, 5 nM, 10 nM) was tested to optimise the conditions and combined with Interferin transfection reagent (Polypus, UK) as per manufacturer's protocol. Interferin is composed of non-liposomal amphiphilic molecules that form stable complexes with siRNA and transport it into the cell cytoplasm. Interferin can be used in the presence of serum and antibiotics and does not affect cell viability. Primary cells were seeded at 1.5 x 10^5 in 6 well plates in 2 mL 10 % FBS in DMEM and grown to 50 % confluence. The medium was replaced with freshly prepared transfection mix. Cells were then incubated for 24 hours, 48 hours and 72 hours. After each time the medium was removed, and whole cell lysates collected for mRNA and protein analysis.

2.9 Clusterin shRNA lentiviral transduction and silencing

Lentiviral transduction of mammalian cells with shRNA (short hairpin RNA) allows stabile silencing of gene expression *in vitro*. In contrast to siRNA transfection, shRNA are endogenously expressed in the host cell, resulting in a sustained and specific silencing of target mRNA. shRNAs are expressed from polymerase II promoters cloned into plasmids for example lentiviral plasmids (Brummelkamp et al. 2002).

Lentiviral shRNA and vectors (pGIPZ) targeting clusterin expression were provided by the UCL Cancer Institute Cancer Genome Engineering (CAGE) Facility, which houses the GE Life Sciences Human Open Biosystems GIPZ shRNA collection. The non-silencing shRNA construct (scrambled shRNA) served as negative control. All sequences are shown in Table 6.

Table 6 Sequences of shRNA targeting clusterin and non-silencing control.

Target gene	Name	Thermo Scientific Clone ID	Mature Antisense
hCLU	LP 1	V3LHS_337309	5´-TGTATTTCCTGGTCAACCT-3`
hCLU	LP 2	V3LHS_337307	5´-TCTTCTAGGTTGCTGAGCA-3`
hCLU	LP 3	V3LHS_337304	5´-TGAATTTCCTTATTGACGT-3`
No target	LP 4	Non-silencing shRNA control	5´-TCTCGCTTGGGCGAGAGTAAG-3`

All clusterin shRNA sequences were analysed via sequencing and blast search to ensure that they were target-specific. Sequence comparison was performed using the NCBI nucleotide BLAST tools (http://www.ncbi.nlm.nih.gov/tools/primer-blast/).

Consequently, all lentiviral constructs have been designed to give high specificity and increased knockdown efficiency of clusterin. Visual accessibility of knockdown efficiency was granted by Turbo - GFP tag marking cells expressing shRNA (see Figure 2.1).

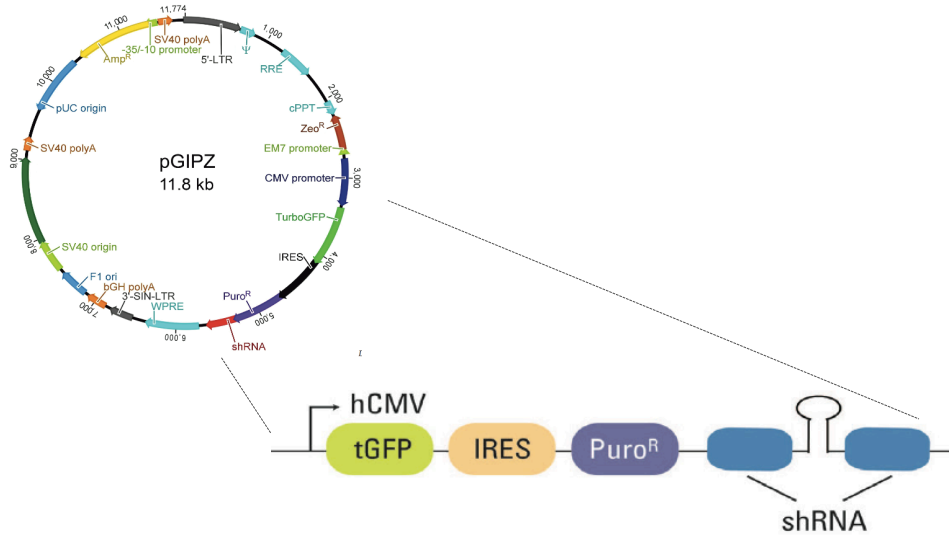

Figure 2.1 Illustration of the pGIPZ vector.

Abbreviations: hCMV (human cytomegalovirus promoter drives strong transgene expression); tGFP TurboGFP reporter for assessment of transduction efficiency; IRES: Internal ribosomal entry site that allows expression of TurboGFP and puromycin resistance genes in a single transcript; PuroR Puromycin resistance permits antibiotic-selective pressure and propagation of stable integrants. Illustration modified from www.thermoscientificbio.com.

For preparation of lentiviral particles, HEK 293T cells were grown in DMEM (10 % FBS) in 10 cm dish. At 70 % confluence the medium was replaced and 8 ml of DMEM were added to the cells.

Cells were co-transfected with 1.5 µg lentiviral construct (pGIPZ) plus 1 µg encapsidation plasmid (p8.91) and 1 µg envelope plasmid (pMDG) in 200 µl Optimem per dish using FuGENE® 6 transfection reagent as per suppliers instructions (Promega, UK) overnight at 37 °C in a humidified atmosphere of air containing 10 % CO_2. The Optimem medium (10 % FBS in DMEM) was changed 18 hours after transfection, and the virus-containing supernatant was harvested 24 , 48 and 72 hours after medium change and filtered through a 0.22 µm syringe filter unit to remove cells debris. Un-concentrated virus particles were stored at 4 °C prior to transduction of fibroblasts. To determine the titre of the lentiviral stocks a four-step one in three dilution was performed and dilutions at 1.5 mL were added to HEK 293T cells on 24 well plates. After 72 hours the GFP-positive fraction was determined via FACS and the titre determined via the following formula:

Transforming units/ ml = fraction cell infected (%) / 100.

The titre was expected to be between 1-20 % GFP^+, according to Catherine King, who performed the lentiviral preparation up until this point.

For transduction of control lung fibroblasts, cells were grown to 80 % confluence in DMEM plus 10 % FBS in T75 flasks and supernatant replaced with media containing 5 MOI (multiplicity of infection) lentiviral particles in 12 mL per T75 flask together with polybrene (10 µg/ml, Millipore UK Ltd.) for 6 hours at 37 °C. The supernatant was removed, and replaced with 10 % FBS (v/v) in DMEM. Transduction efficiency was determined 72 hours after transduction by accessing the proportion of GFP-positive cells via fluorescence microscopy; thereafter, transduced cells were positively selected via resistance to puromycin (3 µg/ml, Sigma, UK) in the culture medium. Non-transduced fibroblasts were not treated with puromycin (see Figure 2.2.).

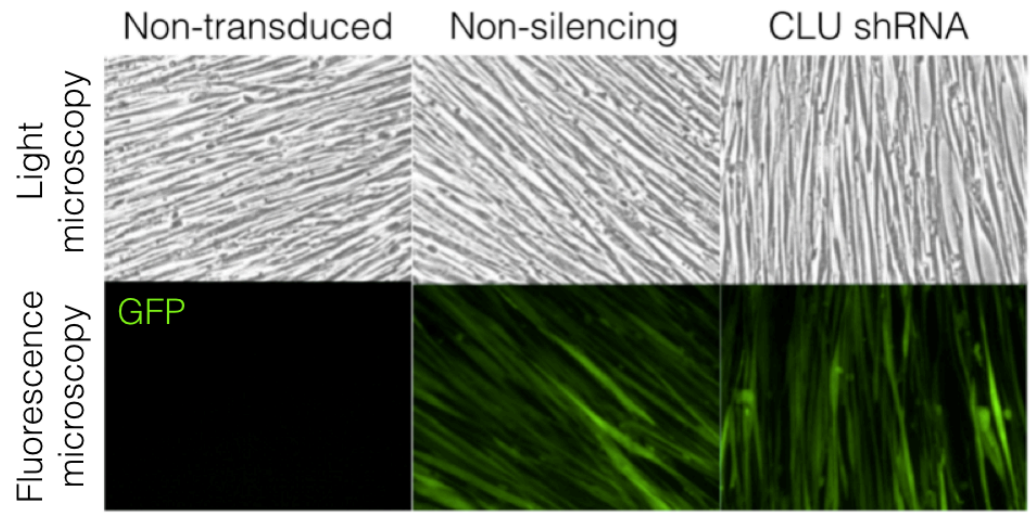

Figure 2.2 Illustration of GFP-positive, puromycin-selected cell population.

Transduced cells were positively selected via puromycin resistance and visualised via pGIPZ lentiviral vector - induced GFP expression.

2.10 Immunohistochemistry

Immunohistochemistry describes a method of localising proteins *in vivo*, within a tissue section by using the principle of antibodies binding specific antigens. Immunohistochemistry was performed on 3 µm thick paraffin-embedded sections of human lung using micro-polymer peroxidase antibody method (Reinhardt et al. 2005).

Table 7 Protocol sequence for dewaxing and rehydration.

Step No.	Solution	Time
1	Dry	30 sec
2	Xylene	3 min
3	Xylene	3 min
4	100 % Ethanol	2 min
5	100 % Ethanol	2 min
6	70 % Ethanol	2 min
7	30 % Ethanol	2 min
8	Wash in dH_2O	∞

Following dewaxing, sections were rehydrated (details in Table 7) and antigen retrieval achieved by either proteinase K digestion (20 µg/ml) for 5 minutes at RT for TGF-β_1 staining or by microwaving/steaming in 10 mM citrate buffer (pH 6) in H_20 for 20 minutes for clusterin, LRP-2 or α-SMA staining.

Sections were washed in TBS (pH 7.6); sections on the slides were outlined via ImmEdge Hydrophobic Barrier Pen (PAP Pen) (Vector Laboratories, Peterborough, UK) and endogenous peroxidase blocked with 3 % hydrogen peroxide (Sigma-Aldrich) for 30 minutes at RT. After another wash sections were incubated with 2.5 % (v/v) horse serum (ImmPRESS, Vector Labs CA) in TBS for 20 minutes at room temperature. Excess serum was removed, and the sections incubated overnight at 4°C with primary antibodies at pre-optimised concentrations in TBS with 1 % BSA: TGF-β_1 (1 µg/ml, sc-146, Santa Cruz Biotechnology), clusterin (0.67 µg/ml, H330 Santa Cruz Biotechnology, α/βchain AB: sc-8354) and α-SMA (142 ng/ml, M0851, Dako, Denmark) and LRP2 (at 1µg/ml, ab76969 Abcam, UK) as demonstrated in Table 8. Non-immune isotype IgG, in place of primary antibody, was used as a negative control (ab37415 or ab91353, Abcam, Cambridge, UK). Sections were washed and incubated with anti-rabbit or anti-mouse Ig reagent as appropriate (ImmPRESS, Vector Labs CA) for 30 min at room temperature. Further washes in TBS were performed, and antibody binding was visualised using Vector NovaRED substrate (Vector Labs Pty) at established times for colour development. Sections were further processed in an Autostainer (Tissue Tek DRS Autostainer, Sakura, USA): Sections were washed in distilled water, counterstained with Mayer's haematoxylin, differentiated in acid alcohol (1% HCL in 70 % Ethanol (v/v) in distilled water), washed in tap water, dehydrated, cleared in xylene and mounted

via Sakura Coveraid cover slipper (Bayer Diagnostics) (details in Table 9). To visualise elastic fibres, sections were stained via Elastica van Giesson staining (Elastic Stain Kit, Sigma-Aldrich, UK) according to the manufacturer's instructions. Section scans were performed with NanoZoomer Digital Scanner and analysis software NDP.view2 (Hamamatsu Corp). Following staining, sections were assessed by two reviewers.

Table 8 Antibodies used for immunohistochemically stained human lung tissue.

Antibody target	Antibody type	Source company	Cat.-no	Pre-treatment	Final antibody concentration
Clusterin (α,β)	rabbit polyclonal	Santa Cruz	sc-8354	Microwave	0.67 µg/ml
TGF-β1	rabbit polyclonal	Santa Cruz	sc-146	Proteinase K	1.0 µg/ml
α-SMA	mouse monoclonal	Dako	M0851	Microwave	142 ng/ml
LRP-2	rabbit polyclonal	Abcam	ab76969	Microwave	1µg/ml

Table 9 Protocol sequence for counterstain with haematoxylin and dehydration.

Step No.	Solution	Time
1	dH_2O	30sec
2	Haematoxylin	10sec
3	Tap Water	20sec
4	1 % HCL in 70 % Eth	5sec
5	Tap Water	2min
6	dH_2O	30sec
7	70 % EtOh	2min
8	100 % EtOH	2min
9	100 % EtOH	2min
10	Xylene	3min
11	Xylene	3min

2.11 Reverse transcription polymerase chain reaction (RT-PCR) and microarray analysis

Samples for microarray analysis were generated by Dr Iona Evans and analysed on a Human HT-12 v4 Expression BeadChip according to supplier's instructions (Illumina Inc. San Diego, California, US). Microarray data was statistically analysed by Cambridge Genomic Services (CGS, UK). All other gene expression analysis was performed via RT-PCR. To perform the analysis of cellular gene expression through quantification of mRNA, cDNA copies of mRNA were generated in a process called reverse transcription (RT). RT-PCR facilitates amplification and simultaneous quantification of a specific-targeted molecule of RNA into its DNA complement. Relative quantification can be achieved using the total copy number normalised to one or more simultaneously measured housekeeping gene. SYBR green was used to label double stranded DNA. As copies of DNA increase with each PCR cycle, SYBR emission increased and was detected via Lightcycler following quantification of copy number. Qualitative analysis was performed by normalising the gene of interest to a simultaneously measured house keeping genes using the $^{\Delta\Delta}$Ct-method (Livak & Schmittgen 2001).

2.11.1 RNA isolation

RNA isolation was performed with molecular biology grade chemicals and DEPC-treated deionised water. Furthermore, equipment used was thoroughly cleaned with RNaseZap (Sigma Aldrich, UK) and nuclease-free, filter pipette tips (Gentaur, UK) were used to prevent RNA degradation as well as contamination with external nuclear material. Cells in 6 well plates or pelleted cells were lysed with 0.5 ml of TRI-reagent (Sigma, UK). TRI-reagent is a solution of phenol and guanidine isothiocyanate, which disrupts cell membranes and dissolves cell components leaving RNA integrity intact. To isolate mRNA, 500 µl TRI-reagent was added to each sample and was incubated for 5 minutes at room temperature and 100 µl of chloroform was added. The mixture was mixed vigorously and left for 10 minutes at room temperature to allow separation of upper aqueous and a lower organic phase. The samples were then centrifuged for 15 minutes ~ 16,000 x g at 4 °C, and the aqueous phase containing RNA was transferred to a new Eppendorf tube containing 250 µL isopropanol. The RNA was allowed to precipitate for 10 minutes at room temperature and was then centrifuged at

~ 16,000 x g for 15 minutes at 4 °C. The supernatants were discarded, and the RNA pellet was resuspended in 80 % ethanol in DEPC-treated deionised water. Following further 15 minutes centrifugation at ~ 16,000 x g at 4 °C, the supernatants were discarded, the pellets air dried and then resuspended in 12.5 µl of nuclease free water (Ambion, UK). Contaminating genomic DNA was removed using PrimerDesign DNAase I kit: 1.5 µL DNase I was added to the total RNA and incubated at 37 °C for 20 minutes. The DNase reaction was terminated by heating the sample to 55 °C. The concentration and purity of the RNA was further quantified using a Nanodrop 8000 spectrophotometer (Thermo Scientific, UK). The ratio of the A_{260}/A_{280} was used as a measure of protein contamination of the sample. A ratio of 2 was considered ideal with a range from 1.7 to 2 considered acceptable.

2.11.2 cDNA synthesis

Complementary DNA (cDNA) was prepared by reverse-transcription (RT) using the qScript cDNA SuperMix kit (Quanta BioSciences, USA). Following the manufacturer's instructions, up to 1 µg of RNA sample was made up to a volume of 16 µL with nuclease-free water. 4 µL of qScript cDNA SuperMix (5 x reaction buffer containing optimised concentrations of $MgCl_2$, dNTPs (dATP, dCTP, dGTP, dTTP), recombinant RNase inhibitor protein, qScript reverse transcriptase and primers, was then added to each sample, to achieve a final volume of 20 µL. Samples were then incubated for 5 minutes at 25 °C, 30 minutes at 42 °C and five minutes at 85 °C. After completion of cDNA synthesis, the cDNA product was diluted one in four with nuclease-free water and frozen in aliquots at -20 °C. RT-PCR was performed with 1.0 µg of cDNA using SYBR green (MESA FAST qPCR MasterMix Plus dTTP for SYBR® Assay (Eurogentec, UK) or Power SYBR® Green PCR Master Mix (ThermoFisher Scientific, UK) and primers (forward and reverse each at a final concentration of 400 nM; 10 µL reaction, Table 10) on an Eppendorf Realplex Mastercycler (Eppendorf, Germany). Cycling conditions were as follows: For MESA FAST SYBR: activation of SYBR Green 95 °C for 10 minutes; cDNA amplification 95 °C for five seconds, 60 °C for 45 seconds for 40 cycles followed up by melting curve analysis. For Power SYBR®: 95 °C for 10 minutes; and 40 cycles of 95 °C (15 s) and 60 °C (45 s).

The efficiency of each primer pair was assessed by determining the relationship of primer crossing point (Cp) values with cDNA concentration using a series of

half-log dilutions of template cDNA. Cp values were defined as the earliest point of the linear region of the logarithmic amplification plot reaching a threshold level of detection. The log of cDNA concentrations was plotted against Cp values, and the slope of the plot was used to ascertain primer efficiency. Primer efficiency was given by the equation: Efficiency= $10^{(-1/slope)}$ and was only used if the slope was close to 1 indicating PCR efficiency greater than 90 %.

To examine the quantitative differences in target mRNA expression in each sample, Ct values were determined from the linear region of the logarithmic amplification plot. Each sample was also tested for the expression of the housekeeping genes B2M, CYC 1 and ATPB5 to normalise between samples. The listed housekeeping genes were selected, as their expression was the most consistent in combination with TGF-ß$_1$ stimulation according to geNORM (Primerdesign, UK) studies conducted by Dr Natalia Smoktunowicz. The Ct values of the housekeeping genes were used to normalise between samples. Statistical analysis was performed using the ΔCt values. Fold-change was subsequently calculated using the standard $2^{-\Delta\Delta Ct}$ approach (Livak & Schmittgen 2001).

The specificity of the products obtained by PCR was confirmed by analysis of the melting curve. Double-stranded DNA has a melting temperature (Tm) defined as a temperature at which half of the DNA is denatured, and its value is primarily dependent on the nucleotide sequence. The melting curve analysis is performed by measuring a decrease in fluorescence due to the dissociation of DNA helix as a function of temperature, and a single melting curve is indicative of a single PCR product.

2.11.3 Primer design

All primers used in RT-PCR studies were designed by Dr Iona Evans, Dr Chris Scotton or myself and using internet based software (Invitrogen custom primers, www.thermofisher.com). Accession numbers were located from http://www.ncbi.nlm.nih.gov/gene. This number was then entered into primer BLAST (www.ncbi.nlm.nih.gov/tools/primer-blast/). The parameters were set at: product size 80-120 bp; primer size 18-23 nucleotides long; primer melting temperature 58 °C to 62 °C with an optimum of 60 °C and a maximum temperature difference of 0.5 °C; primer GC % was 40 % to 60 % with an optimum of 50 %; maximum self-complementary was set at 6.0 and maximum 3’

self-complementarity of 2.0 and finally, the maximum poly-X was set at 3 to avoid same 2 base runs of nucleotides. A BLAST search was also performed to check that the forward and reverse primers were specific for the intended sequence. The primers were manufactured by Invitrogen (UK). Primer sequences are listed in Table 10. In order to verify clusterin primers, PCR products were run on a 1 % agarose gel, bands were visualised by UV transillumination (Syngene, Cambridge, UK) and product size determined. An example of the results obtained is shown in Figure 2.3. Since the resulting product length of primer pair CLU 1° was shorter than CLU 2° all RT-PCR, which enables easy binding to the template at annealing temperatures, experiments were performed with primer pair CLU 1°.

Table 10 Real-time RT-PCR primers

Gene	Forward sequence	Reverse sequence
CLU 1°	5´-CAAGTGCCGGGAGATCTTGT-3`	5´-GTCAACCTCTCAGCGACCTG-3`
CLU 2°	5´-CCAACAGAATTCATACGAGAAGG-3`	5´-CGTTGTATTTCCTGGTCAACCTC-3`
PAI-1	5´-AACTATACTGAGTTCACCACGCC-3`	5´-GAACATGCTGAGGGTGTCCC-3`
α-SMA	5´-AATCCTGTGAAGCAGCTCCAG-3`	5´-TTACAGAGCCCAGAGCCATTG-3`
FN1	5´-CCTCGAAGAGCAAGAGGCAG-3`	5´-GCTTCAGGTTTACTCTCGCA-3`
COL1A1	5´-ATGTAGGCCACGCTGTTCTT-3`	5´-GAGAGCATGACCGATGGATT-3`

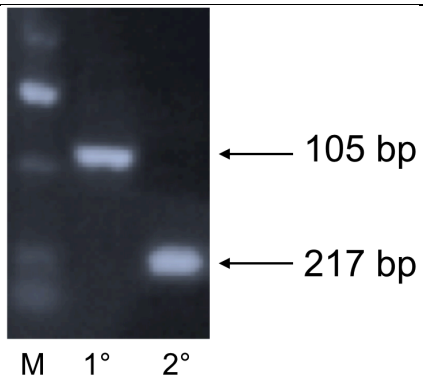

Figure 2.3 Example of PCR products, separated by gel electrophoresis.

Abbreviations; M – marker, 1° - CLU primer no 1., 2° - CLU primer no 2.

2.12 SDS-Polyacrylamide electrophoresis and Western blotting

Western blotting is a well-established method to separate and detect proteins in polyacrylamide electrophoresis gels via specific antibody-antigen interaction after transfer on a nitrocellulose or polyvinylidene difluoride (PVDF) membrane (Reisfeld et al. 1962). To assess fibroblast levels of clusterin and αSMA lung fibroblasts were grown in 6 well plates. On reaching confluence cells were washed twice with PBS and grown in serum-free DMEM for 24 hours before being treated with TGF-β_1 for 20 or 48 hours and lysed in RIPA buffer (1 % Igepal Ca-630, 0.05 % sodium deoxycholate, 0.1% sodium dodecyl sulphate in PBS) containing complete protease inhibitor cocktail (Complete-mini; Roche, UK). Following the addition of lysis buffer samples were frozen and stored at -80 °C. For analysis, following defrosting on ice, lysates were centrifuged at 13 000 x g for 5 minutes at 4 °C to remove insoluble cell debris and the supernatant transferred to a clean centrifuge tube. Prior to analysis, the protein concentration of each sample was measured by BCA protein assay (section 2.12.1).

2.12.1 BCA assay

The assay is based on the biuret reaction where protein reduces Cu^{2+} to Cu^{1+} in an alkaline medium. Two bicinchoninic acid molecules chelate with the reduced cuprous cation, developing an intense purple colour. The BCA-copper complex is linearly proportional to protein concentration and displays strong absorbance at 562 nm. The assay was performed as per manufacturer's instructions and the results compared with an eight-point standard curve of bovine serum albumin with 2 mg/ml as highest concentration (example see Figure 2.4). The assay was conducted in 96-well plate format with 5 µl of sample in duplicate mixed with 100 µl freshly prepared BCA working reagent. The plate was incubated for 30 minutes at 37 ^{o}C and the absorbance measured at 562 nm on a VersaMax™ Microplate Reader (Molecular Devices, USA).

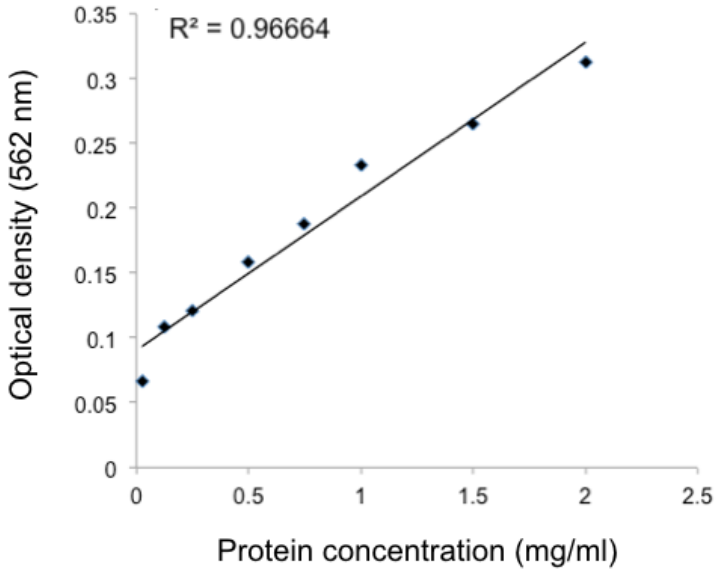

Figure 2.4 BCA standard curve.

A representative standard curve generated for the BCA protein assay. Standards represent serial dilutions of bovine albumin from 0 µg/ml to 2000 µg/ml. Standards and samples were measured, and absorbance calculated 562 nm after the background values were subtracted from all values. Each point represents the mean of two duplicate wells per standard. The line of best fit is demonstrated.

2.12.2 SDS-gel preparation

Samples were adjusted with deionized water to standardise total protein concentrations and proteins reduced and denatured for antibody detection. To achieve this, 5 – 20 µg of total protein was mixed in a 5 : 1 ratio with 5 x Laemmli buffer (100 mM dithiothreitol - DTT, 1M Tris pH 6.8, 10 % w/v sodium dodecyl sulphate (SDS), 20 % w/v glycerol, ddH_2O, bromphenol blue dye) and boiled for 5 minutes at 100 °C. Samples or 5 µl PageRuler Plus protein ladder (Thermo Scientific UK) were then subjected to non-reducing SDS-PAGE using 12.5 % resolving/ 4.8% stacking polyacrylamide gels prepared as indicated in Table 11 in the presence of running buffer (0.25 M Tris-Base, 1.92 M glycine,0.1 % w/v SDS, ddH_2O) and the gel was run at 150V for 45 min.

Table 11 SDS gel preparation for Western blot analysis.

Resolving gel		Stacking gel	
Chemical	Volume	Chemical	Volume
1.5M Tris pH 8.9	2.5 ml	1 M Tris pH 6.8	0.63 ml
30% acrylamide/methylene bisacrylamide solution	4.2 ml	30% acrylamide/methylene bisacrylamide solution	0.8 ml
Water	3.3 ml	Water	3.5 ml
20% SDS	100 µL	20% SDS	50 µL
10 % APS (0.1g/ml)	67 µL	10 % APS (0.1g/ml)	67 µL
TEMED	4 µL	TEMED	10 µL

Electrophoresed proteins were electroblotted onto polyvinyldene difluoride (PVDF, Sigma-Aldrich, UK) membrane at constant voltage of 20 V for one hour in transfer buffer (25 mM Tris, 0.2 M glycine, 1% w/v SDS, 20% v/v methanol) and the quality of transfer was assessed via Ponceau S staining (in 5% acetic acid, Sigma, UK). To reduce unspecific binding the membrane was blocked with and immunodetection was carried out in Tris-buffered saline Tween-20 (TBST), 10 nM Tris pH 8, 150 nM NaCl, 0.1% v/v Tween-20, ddH2O) pH 7.6 with 5 % w/v non-fat milk (Sigma-Aldrich,UK). Polyclonal rabbit anti-human or mouse-monoclonal clusterin (0.267 µg/ml, sc-8354 or sc-5289, Santa Cruz) or mouse monoclonal anti - human α-smooth muscle actin (7.1 ng/ml, M0851, Dako Denmark) and goat polyclonal anti-human vinculin (0.267 µg/ml, sc-7649, Santa Cruz) antibodies in 5 % w/v non-fat milk in 0.1% v/v Tween-20 in ddH_2O were incubated with the membrane over night at room temperature. After washing the membrane 6 x 5 minutes in TBST, secondary antibodies conjugated to HRP (goat anti-rabbit, 50 ng / ml; rabbit anti – mouse, 260 ng/ml; rabbit anti-goat, 110 ng/ml, Dako, Denmark) were applied for 1.5 hours at room temperature. Following 6 x 5 minute washes; signal detection via chemiluminescence (Luminata Crescendo Western HRP substrate, Millipore) was captured via ImageQuant and TL analysis software (GE healthcare, UK). Protein sizes were analysed via PageRuler Pre-stained Protein Ladder (Thermo Fisher Scientific, UK). The optical density of control protein (vinculin) was determined to allow the correction for variability in protein loading for comparison between samples on one membrane. Vinculin was used as high molecular weight loading control for all western blots with clusterin since clusterin α, β chain low molecular weight bands appear as bands were low molecular weight loading controls such as α-tubulin, GAPDH are expected.

2.13 Clusterin Enzyme Immunoassay

Quantification of clusterin was performed using a clusterin DuoSet Enzymeimmunoassay (ELISA) Kit (R&D Systems, Abingdon, UK) according to the manufacturer´s protocol. The R&D assay is sensitive to recombinant, and natural human clusterin in standards and the samples tested. The test principle is based on a sandwich immunoassay. Firstly, polystyrene microplates are coated with a fixed quantity of clusterin specific antibodies (mouse - anti - human clusterin capture antibodies) and unbound capture antibodies are washed away. In the following step clusterin in samples or standards competes for binding sites on all clusterin-specific capture antibodies and unbound materials are washed away. Following this, the plate is incubated with biotinylated mouse anti-human clusterin detection antibody, which is then labelled with streptavidin-HRP (horse radish peroxidase) for amplification and high sensitivity of the target signal. The signal is then detected using TMB (tetramethylbenzidine) solution (Sigma, UK). TMB reacts with peroxidase, which results in the development of a blue coloured solution in proportion to the analyte present in the sample or standard. To avoid saturation of the assay colour development is stopped by addition of acid and the colour of the solution turns yellow. This then permits colourimetric assessment of colour intensity at a wavelength of 450 nm. The ELISA assay detects clusterin in the range between 1 - 200 pg/well (20 and 4000 pg/ml). Briefly, a 96 well plate was coated with capture antibody (2 µg/ml) over night and the plate washed the next day three times with 0.05 % Tween 20 in PBS before 50 µl of cell culture media or clusterin standards were pipetted into appropriate wells. Where necessary, samples were pre-diluted in reagent diluent (1 % BSA in PBS). All clusterin standards were prepared by serial dilution from 4000 pg/ml down to 31.25 pg/ml. All standards were run in duplicate and diluted assay buffer alone was used to determine non-specific binding. Two wells were left as empty blanks. 50 µl of sample or standard were added to all wells except for the blank, and the plate was then incubated for 2 hours at room temperature. After two washing steps with wash buffer (0.05 % Tween in PBS), 50 µl of detection antibody (180 µg/ml) was added to each well and the plate incubated for another 2 hours at room temperature. Wells were washed twice before 50 µl streptavidin conjugated to horseradish-peroxidase (HRP) was added to each well and incubated for 20 minutes at room temperature avoiding direct light. Unbound Steptavidin-HRP was then removed with two washing steps before 50 µl of room temperature equilibrated enzyme substrate (TMB) was added to all wells. Direct exposure to light was avoided during colour development, and the 96-well plate was mixed on

a microplate shaker. The colorimetric reaction was terminated by the addition of 25 µl 2 N H_2SO_4 to each well. Optical density was then determined at an absorbance wavelength of 450 nm on a Fluostar Omega microplate reader (BMG Labtech, Germany). Results were calculated by comparison of sample concentrations to known ones of clusterin standards. A representative standard curve is shown in Figure 2.5.

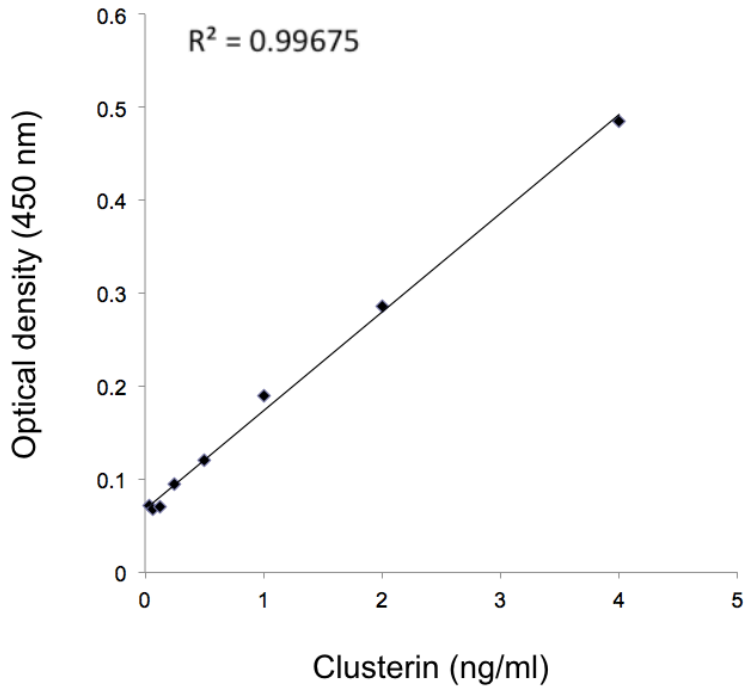

Figure 2.5 Representative standard curve for clusterin DuoSet ELISA.

Each point represents the mean of two duplicate wells per standard. The regression line is shown. Standard concentrations displayed from 4000 pg/ml to 0 pg/ml. Background values were subtracted for all wells.

2.14 Immunocytofluorescence

Immunocytofluorescence is a cell imaging technique based on the use of antibodies, conjugated to fluorescent dyes to label a specific target antigen within cells. Experiments are based on using indirect immunofluorescence. Hereby, a primary antibody binds the specific target antigen and is then detected by a fluorophor conjugated detection antibody. The fluorescent signal is detected via fluorescence microscopy.

2.14.1 Clusterin and αSMA expression and collagen I deposition post TGF-β_1 stimulation

In order to achieve collagen I deposition *in vitro*, experiments were performed under molecular crowding conditions as previously described (Chen et al. 2009). Molecular crowding is based on the "excluded volume effect". Neutral non-aggregating crowders such as Ficoll (here 400k Da and 70 kDa) exclude volume through their mass and reduce the volume, in which potential substrate reactions occur, which increases the frequency of such reactions. Chen et al. suggest that this is in part due to a low bioavailability of an enzyme called procollagen C-proteinase, which is required for the conversion of procollagen to collagen via the removal of C-terminal pro-peptides. To increase the bioavailability and *in vitro* activity of procollagen C-proteinase, ficoll and ascorbic acid were added to the culture medium of lung fibroblasts, with or without TGF-β_1. Briefly, cells were seeded at 1 x 10^4 cells/ well in a 96-well plate and allowed to attach to the plate over night. On the next day cells were serum starved (0.4 % FBS in DMEM) for 16 hours. Crowding of the culture medium was achieved with neutral mixed ficoll (70 kDa ficoll at 37.5 mg/ml^{-1} and 400 kDa 25 mg/ml^{-1}). Additionally, porcine TGF-β_1 (1 ng/ml, R&D Systems) at a concentration previously established (Tiggelman et al. 1997) and L-ascorbic acid (16.6 µg/ml, Sigma-Aldrich) were added to the culture medium (0.4 % FBS/ 2 mM L-Glutamine in DMEM) to induce collagen I expression and deposition. The medium was removed 20 - 48 hours post TGF-β_1-stimulation and cells were processed for immunocytochemistry (section 2.14.2).

2.14.2 Immunocytochemistry

Cells were fixed with ice-cold methanol for 2 minutes following 3 washes in PBS and permeabilisation with 0.1 % Triton-X (Sigma Aldrich, UK) for 90 seconds. In order to avoid unspecific binding cells were blocked with 1 % bovine serum albumin (Merck Millipore UK) and 3 % goat serum (Sigma Aldrich, UK) in PBS for 30 minutes at room temperature. Monoclonal mouse antibodies against collagen type I (Sigma, Aldrich, C2456 at 4.7 µg/ml) or mouse monoclonal against clusterin-α (Santa Cruz, sc-5289, at 2.0 µg/ml) in separate wells were incubated over night at 4° C followed by three washes with 0.05 % (v/v) Tween in PBS (T-PBS). Secondary antibody (AlexaFluor 555 goat anti-mouse: A-21422, Thermo Fisher Scientific, UK) together with 1.43 nM 4′,6- diamidino-2-

phenylindoldilactate (DAPI, ThermoFisher Scientific, UK) to stain nuclei were incubated for 1.5 hours at room temperature and plates washed three times with 0.05 % T-PBS and stored with 200 µl PBS per well at 4 °C until optical analysis (Section 2.14.4).

2.14.3 High – throughput proliferation assay

Fibroblasts were seeded at a density of 4 x 10^3 in 96-well plates in 0.4 % FBS (10 % for PGE_2 experiments) in DMEM. 18 hours after seeding, cells were treated with specific proliferation mediators at indicated concentration and time points for 48 - 72 hours. Thereafter, cells were fixed and stained with 4′,6-diamidino-2-phenylindoldilactate (DAPI) as described in section 2.14.2. Cell numbers were quantified at 48 – 72 hours post treatment by counting DAPI-positive nuclei in a high-throughput immunofluorescence assay (see 2.14.4). Cell numbers were normalised to cell counts of untreated controls and results expressed as proliferation percent relative to untreated control.

2.14.4 Optical analysis

Optical analysis was performed via ImageXpress Micro XLS Widefield High Content Screening System acquiring 6 - 9 images at 20 x original magnification and analysed using the MetaXpress High Content Image Acquisition & Analysis Software (Molecular Devices, Sunnyvale, CA, USA). An integrated Multi Wavelength Cell Scoring method was established to quantify the area of fluorescent collagen I or clusterin staining, data was converted into ‘mean stain integrated intensity’ (total pixel intensity over the stained area, divided by the total number of cells) as shown in Table 12.

Table 12 Module settings for multi wavelength cell scoring module.

Settings	DAPI	Collagen I	α-SMA	Clusterin
Approximate min width in µm	9	11	5	11
Approximate max width in µm	20	50	30	50
Intensity above local background in grey levels	100	2000	800	1200
Min stained area in μm^2	N/A	400	400	400

Non-immune isotype controls at concentrations of primary antibodies were used to determine fluorescent intensity thresholds for background removal. The total number of cells was assessed by nuclear staining with DAPI. Results were compared with untreated controls for each time point. Isotype controls were used to determine the suitable fluorescent intensity thresholds for background removal as demonstrated for clusterin in Figure 2.6.

In order to merge multiple fluorescent raw data channel images in one RGB stack, ImageJ software was used (ImageJ 1.47v, Wayne Rasband, National Institute of Health, USA). In some cases, contrast and brightness were adjusted equally for all images of one experiment.

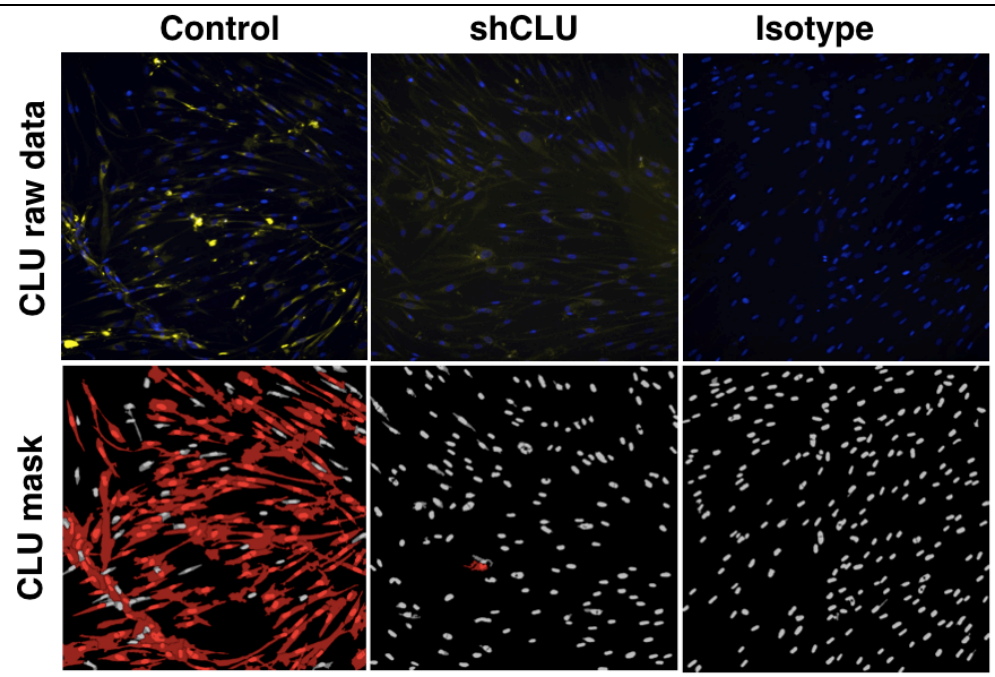

Figure 2.6 Establishment of mask settings for quantification of clusterin signal.

Contrast and brightness were equally adjusted in all images. Control – mock transduced fibroblasts, shCLU – shRNA targeting the clusterin gene. CLU – clusterin.

2.15 Confocal microscopy

Cells seeded in glass chamber slides (density 10,000 cells/ well) were washed three times with PBS and fixed with methanol for 2 minutes or 4 % paraformaldehyde for 20 minutes. The cells were then blocked with 3 % serum (same species as secondary antibody) and 1 % BSA in PBS for 1 hour, followed by incubation with primary antibody (at 4 µg/ml, H330 Santa Cruz Biotechnology, α/βchain AB: sc-8354) diluted in Dulbecco's phosphate-buffered saline (DPBS) with 1% BSA over night. The cells were then washed three times with DPBS, followed by incubation with fluorescently labelled secondary antibody (goat anti-rabbit IgG (H+L), Alexa Fluor® 488) with DAPI for 1 hour at room temperature in the dark. The cells were then washed and mounted with Shandon Immu-mount (Fisher Scientific Ltd, CA). The LSM 700 confocal microscope from Zeiss was used to visualise and capture images.

2.16 Scratch assay

Fibroblasts were seeded into a 96-well plate at a density of 12 x 10^3 cells per well and allowed to adhere for 24 hours. A 96-needle device (Wound Maker™) was used to create a disruption in the cell monolayer, by moving a needle three times through the cell monolayer in each well to create a scratch 800 µm in width. By washing the monolayer three times with media all detached cells were removed from the well, and the scratch area was checked microscopically for remaining cells in the scratch area. Subsequently, medium was added to the cells (0.4% FBS in DMEM) with or without TGF-β_1 (5 ng/ml). The duration of scratch closure was assessed via capturing images of migrated cells every 2 hours and was analysed via image analysis software (IncuCyte ZOOM software®) based on the criteria described in Figure 2.7. The scratch closure was determined as state in which the scratch width was zero. The scratch width was determined as the average distance (µm) between the edges of the scratch mask in each line of resolution within an image and was assessed independently from the initial scratch wound mask.

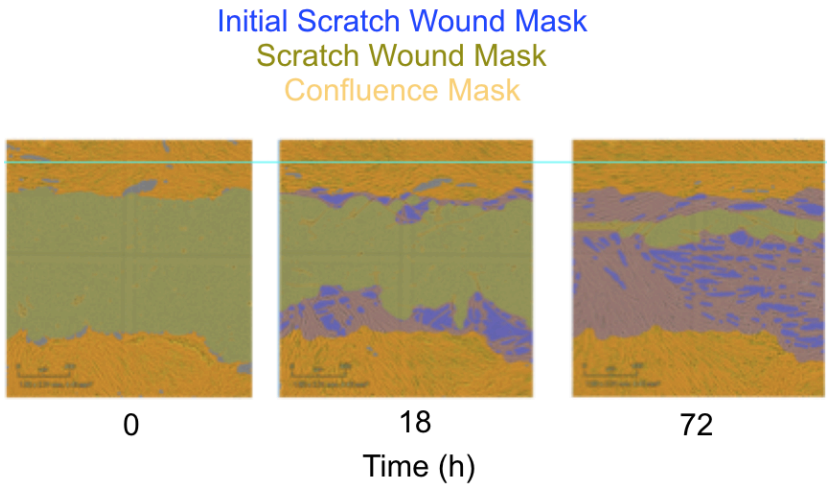

Figure 2.7 Illustration of mask criteria for the scratch assay.

Phase contrast images of disrupted fibroblast monolayer taken 0, 18 and 72 hours after scratch application. Confluence mask (orange overlay) indicate areas of the image that are occupied by cells. The initial scratch wound mask (blue) is superimposed on the phase image and outlines the scratch after scratch application. Scratch wound mask (green) indicating the scratch border locations after 18 and 72 hours and are overlaid on the initial scratch mask.

2.17 Transwell® migration assay

The Transwell® migration assay assesses migratory responses to chemotactic agents *in vitro* and is based on the Boyden chamber assay (Chen 2005): A chamber of two medium-filled compartments, separated by a microporous membrane, through which cells migrate towards a chemotactic gradient. Transwell migration assays were performed with lung fibroblasts as previously described for skin fibroblasts (Rodriguez-Menocal et al. 2012). To assess the effect of clusterin-deficiency on lung fibroblast chemotaxis and/or chemokinesis, primary human lung fibroblasts were seeded at 5 x 10^4 cells in 0.4 % FBS in DMEM into the upper compartment of culture inserts (6.5 mm polycarbonate membrane pore size 8 µm, Corning Inc., NY) and allowed to migrate for 18 hours towards diffusing gradients of PDGF-BB (25 ng/ml, R&D Systems), TGF-β_1 (1 ng/ml, R&D Systems) or human plasma-derived clusterin (1 µg/ml, Biovendor, CR) in the lower chamber prepared in 0.4 % FBS in DMEM. Cells were fixed with methanol and non-migrating cells in the upper chamber were removed with a cotton swab, while migrated cells adhering to the lower surface of the membrane were stained with crystal violet (0.5 % v/v in 10 % methanol in PBS, Sigma Aldrich, Germany). Quantification of migrated cells was performed via elution of crystal violet and spectrophotometric analysis of absorbance at 570 nm.

2.18 *In vitro* induction of apoptosis

Fibroblasts were seeded into 96-well plates at a density of 8.0 x 10^3 cells/well and were grown to 80 % confluence in DMEM supplemented with 10 % FBS. Prior to experiments, the medium was removed, fibroblasts washed with 5 % FBS in DMEM to remove detached cells. Cells were exposed to 0 - 200 ng/ml FasL or exogenous plasma-derived clusterin (10 µg/ml concentration from (Jun et al. 2011)) for 19 hours unless otherwise stated in the figure legends. Apoptosis was either assessed morphologically (see section 2.19) or by Annexin V/DAPI staining detected by flow cytometry. A minimum of five separate wells was used for each treatment condition per experiment.

2.19 Induction and detection of apoptosis

During early apoptosis, a phospholipid named phosphatidylserine (PS), that is usually facing the inner cytoplasmic surface of the cell membrane, flips to the outer surface of the cell membrane. *In vivo,* this provides a signal to nearby and resident inflammatory cells that the affected cell has commenced apoptosis. Fluorescence labelled antibodies targeting Annexin V bind to PS and mark early apoptotic cells. DAPI is a DNA intercalating fluorescent dye that binds to nuclear material. Since it passes the intact cell membranes of live cells less effectively, it predominantly stains nuclei of late apoptotic or necrotic cells. On this basis, Annexin V^- /$DAPI^-$ cells were judged to be non-apoptotic. $Annexin^+$ / $DAPI^-$ cells were considered to be apoptotic, and $Annexin^+$ / $DAPI^+$ cells were recorded as being necrotic (example see Figure 2.10).

To assess if clusterin-deficiency affects levels of basal and FasL-induced apoptosis, fibroblasts were seeded at 8.0 x 10^3 cells/well in 96 well plates and were grown to 80 % confluence in DMEM supplemented with 10 % FBS. The medium was replaced to remove detached cells and replaced with medium containing FasL (Calbiochem, CA; 100 – 200 ng/ml) in 5 % FBS for 19 hours and human plasma-derived clusterin (Biovendor, CR) was added at doses and times indicated in the figure legends. Subsequently after FasL exposure media, including floating cells, were collected from each well. Adherent cells were washed twice with PBS, and the PBS washes, including dislodged cells were added to the media collected from each well. Thereafter the cells were detached with 0.05 % trypsin in EDTA and detachment of cells confirmed visually, followed by neutralization of trypsin by the administration of 10 % FBS in DMEM. Media and cells were then transferred into FACS tubes and pelleted by centrifugation

(300 x g for 5 minutes). The pellet was then resuspended in 100 µL of 1 x Annexin V binding buffer (Becton, Dickinson and Company, UK) in PBS and 5 µL of Alexa Fluor® 647 Annexin V antibody (Cambridge Bioscience, UK) and incubated for 15 minutes at room temperature in the dark. Samples were then transferred on ice before the addition of 1 µg/ml DAPI in 1 x Annexin V binding buffer. Cells were kept on ice and analysed immediately by flow cytometry (Section 2.20.).

Verification of results was performed by morphological assessment of cell nuclei (Maher et al. 2010). Briefly, adherent cells in 96-well plates were fixed in 70 % ethanol for 2 minutes. Cell nuclei were then stained with 1.43 nM DAPI in PBS and analysed by fluorescent microscopy. For each well apoptotic and non-apoptotic cells were counted in six consecutive high power fields. Cells were considered to be apoptotic if nuclei were condensed with fragmented or aggregated DNA (Doonan & Cotter 2008) as shown in Figure 2.8.

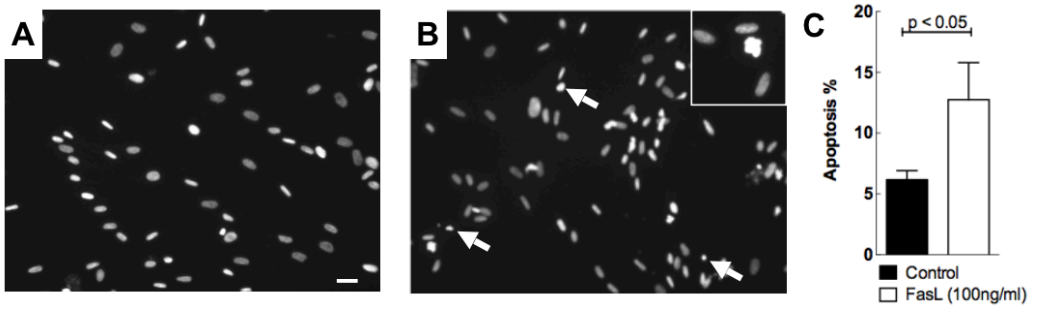

Figure 2.8 Morphological assessment of apoptosis.

Apoptosis was assessed morphologically in fixed, untreated cells that were permeabilised following nuclei staining with DAPI: (A) untreated fibroblasts, (B) FasL- treated fibroblasts (100 ng/ml). Apoptotic nuclei initially demonstrate condensation of chromatin (B, high-power inset) before progressing to form dense, highly fluorescent apoptotic bodies (arrows in B). Scale bar represents 10 µm.

2.20 Flow Cytometry

Flow cytometric analysis was performed on a BD FACS Verse™ flow cytometer using an excitation wavelength of 405 nm, 488 nm and 640 nm band pass filter for DAPI, GFP (transduced cells) and Annexin V detection, respectively. Samples were gated according to forward and side scatter characteristics to exclude cell debris (Figure 2.9). A minimum of 4,000 gated events were collected for each sample analysed. Sample analysis and quantification was performed using the BD FACSuite™ and the FlowJo V10 analysis software. Electronic compensation

was not required due to no overlap of the emission spectra. Samples of cells that were only stained for DAPI or Annexin V and GFP-positive cells were analysed separately by flow cytometry. Readings from these samples were then used to facilitate a selection of positive signal, which determined the thresholds for a positive signal as indicated in Figure 2.10

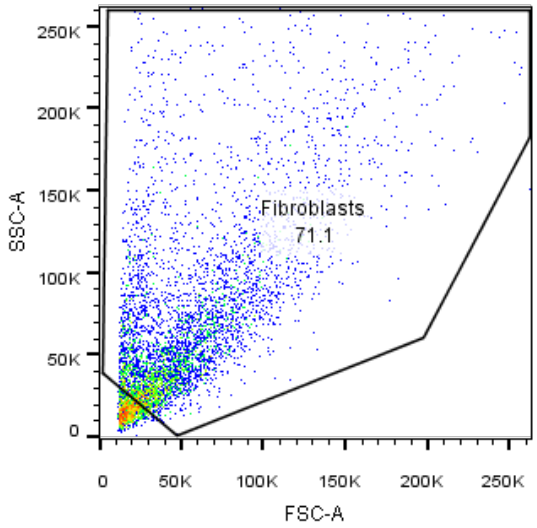

Figure 2.9 Forward scatter (FSC-A) and side scatter (SSC-A) profile of normal human lung fibroblasts.

Gate "Fibroblast" used to select viable cells and exclude cell debris.

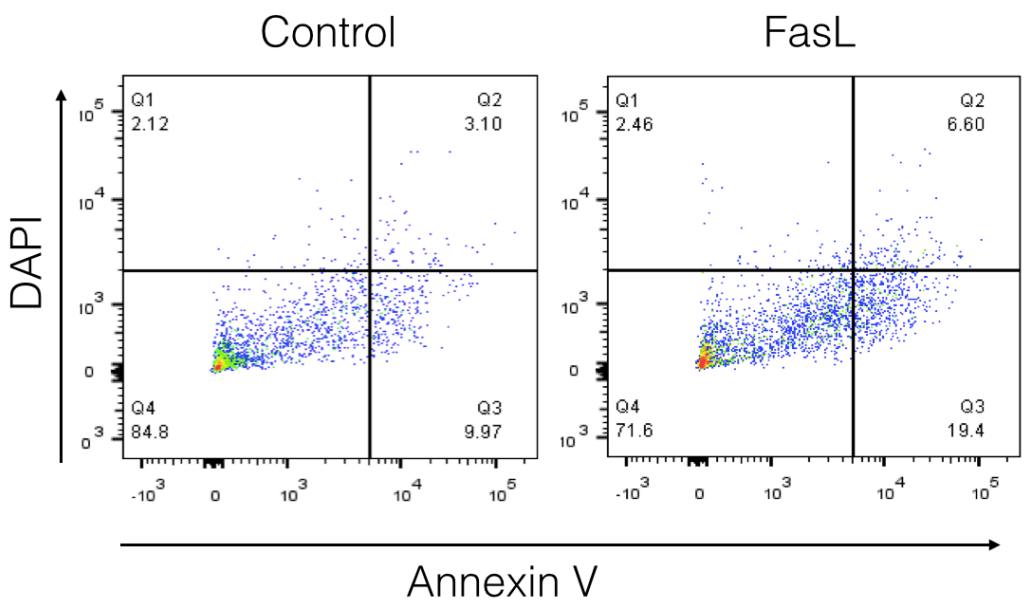

Figure 2.10 Example of flow cytometry analysis of Annexin V / DAPI stained untreated and FasL treated fibroblasts.

Cells in the lower left quadrant are AV^- / $DAPI^-$ (living), cells in the lower right quadrant are AV^+/ $DAPI^-$ (apoptotic) and cells in the upper right quadrant are AV^+/ $DAPI^+$ (late apoptotic/ necrotic).

2.21 Isolation of human alveolar macrophages and co-culture with BEAS-2B cell line

Alveolar macrophages were isolated by Ben Calvert (GSK, Stevenage, UK) from a healthy, male, control lung (donor age 35) received from National Disease Research Interchange (Philadelphia, USA). Briefly, 20 - 30 g lung tissue sections were perfused with PBS to flush out cells, including alveolar macrophages from the airways onto a petri dish. Cells were transferred into a 50 ml falcon tube and centrifuged at 350 x g for 5 minutes at room temperature. The cell pellet was resuspended in 25 ml of RPMI medium supplemented with 10 % FBS and layered onto 15 ml Histopaque® to separate mononuclear cells from red blood cells and platelets in a 50 ml tube and centrifuged at 350 x g for 25 minutes without deceleration. Mononuclear cells were collected at the interface between Histopaque® and serum and transferred to a fresh tube. Cells were washed three times by resuspension in culture medium and centrifugation at 350 x g for 5 minutes and counted (1.4 x 10^7 total cells) and assessed microscopically. Total cells were resuspended in culture medium to obtain 1 x 10^6 cells/ml solution. Cells were seeded onto 96 well plates, and macrophage cell morphology was confirmed microscopically. In order to assess cytokine/chemokine levels released into the medium by macrophages in co-culture with BEAS-2B cells in response to exogenous clusterin (5 µg/ml), 1 x 10^4 cells in 100 µl culture medium were added to the cell monolayer of BEAS-2B cells (section 2.22) per well of a 96-well plate, and monocultures for each cell type were retained throughout the duration of the experiment (Illustration Figure 2.11). 24 hours after adding airway cell isolates to the monolayer of BEAS2B cells, the cell supernatant, including undetached cells, were removed, and culture medium replaced with medium containing clusterin at concentrations of 1 µg/ml or 5 µg/ml or no clusterin. 24 hours after addition of clusterin, supernatants were collected and subjected to luminex analysis (section 2.26).

2.22 Human bronchial epithelial cell (BEAS-2B) culture

Immortalised human bronchial epithelial cells were purchased from ATCC® and cultured as per suppliers instructions. Cells were cultured in 75 cm^2 tissue culture flasks and sub-cultured before reaching confluence to prevent squamous terminal differentiation. For this purpose, culture medium was removed, and replaced with 10 ml PBS to wash away cell debris and detached cells. After removal of PBS, 3 ml TrypLE (Thermo Fisher Scientific, UK) was added to the cells at 37 °C and

cells were observed under an inverted microscope until the cell layer was dispersed (2 - 5 min) and TrypLE was neutralised by adding RPMI culture medium containing 10 % FBS. Cells were centrifuged at 350 x g for 5 min to remove neutralised TrypLE, the cell pellet was resuspended in media and 1 x 10^4 cells were seeded per well into a 96-well plate. The following day alveolar macrophages were added to the monolayer of BEAS-2B cells as described in section 2.21.

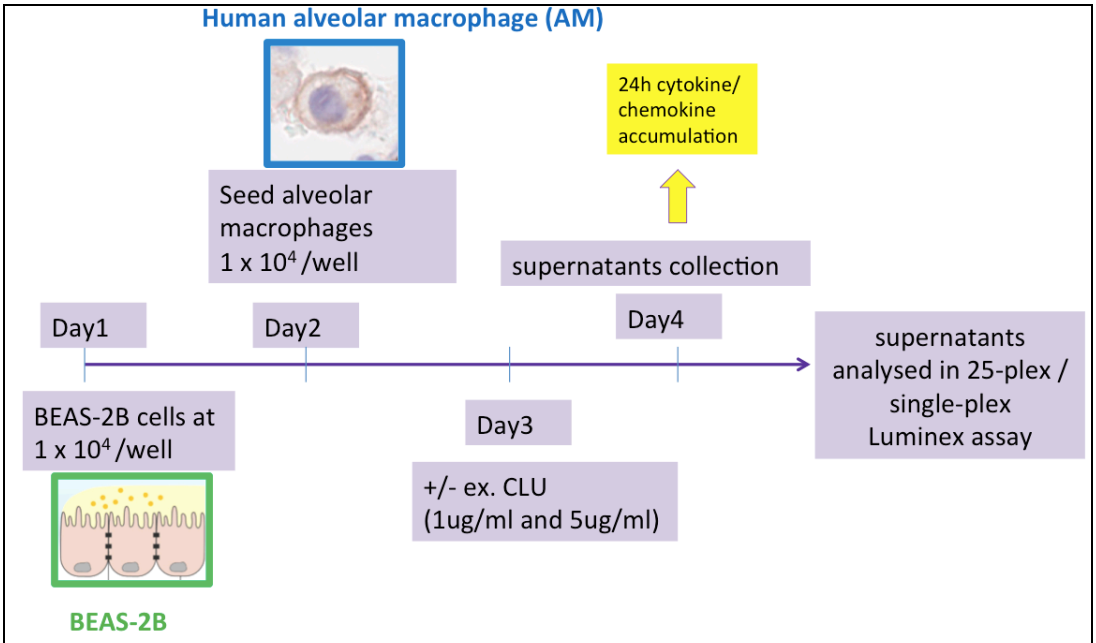

Figure 2.11 Schematic overview of the experimental design for alveolar macrophage – BEAS-2B cell co-culture.

A monolayer of immortalised bronchial epithelia cells (BEAS-2B) cells was established for 24 hours before adding isolated alveolar macrophages (AM) at matching cell number to assess the effect of exogenous clusterin (CLU) on secreted cytokines and chemokines in co- and mono culture of BEAS-2B and AM cells. Detection of cytokines and chemokines in the cell culture medium was assessed by luminex analysis.

2.23 PBMC preparation and $CD14^+$ isolation from human blood cones

PBMC (peripheral blood mononuclear cell) isolation from whole blood results in small PBMC yields due to the restriction of blood volume that can be donated at a time by one individual donor. A novel medical technology called platelet aphaeresis allows the collection of platelets and PBMCs from a larger volume of whole blood while red blood cells and plasma are returned to the donor. This form of blood cell separation can yield large amounts of PBMCs collected in so called blood cones while keeping them sterile for tissue culture and is based on

cell-plasma separation through centrifugation. All blood-derived cells were collected from the Blood Donor Panel at GSK (Stevenage, UK), from individuals who have previously given their informed consent. Blood cones from 4 healthy control donors were processed within a period of a day after blood donation. The content of 1 cone was diluted in sterile PBS to a volume of 40 ml and 20 ml were each layered onto 15 ml of Histopaque®, a polysucrose density gradient solution of 1.077 g/ml and centrifuged at 800 g for 20 minutes without deceleration. The PBMC layer was collected and transferred to a new 50 ml tube topped up with PBS to 50 ml. To remove Histopaque® residues PBMCs were centrifuged at 300 x g for 10 min at room temperature with deceleration and the supernatant removed, and the wash step repeated. The cell pellet was resuspended in 27 ml of PBS and cells were counted using the NucleoCounter nc-3000 (ChemoMetec, Copenhagen) and a total cell number of 3 - 4 x 10^8 total cells were expected with a cell viability ≥ 85%. In order to isolate $CD14^+$ cells (monocytes) cells were pelleted by centrifugation at 365 x g for 5 minutes at room temperature. The supernatant was removed, and the cells were resuspended in 3 ml MACS buffer (0.5 % BSA, 2 mM EDTA in PBS, pH 7.2) and 300 µL $CD14^+$ MicroBeads (magnetic beads conjugated to mouse IgG2a monoclonal anti-human CD14 antibodies) and incubated for 15 minutes at 4 °C after mixing the cell bead suspension by flicking the tube. The cell-bead suspension was then loaded onto three MACS LS columns (1 ml per column), which were subjected to an electric field of a MACS separator. During three wash steps with MACS buffer, which removed unlabelled $CD14^-$ cells, magnetically labelled $CD14^+$ cells remain in the column. Columns are then removed from the magnet and placed onto a 15 ml tube to collect $CD14^+$ cells by eluting labelled cells in 5 ml MACS buffer. All cell suspensions from three columns were merged, and the cell number counted and cell numbers of 2.0 – 2.5 x 10^8 total cells with a cell viability of ≥ 95% were expected.

2.24 Cell culture and polarisation of human blood-derived macrophages

The $CD14^+$ MACS buffer cell suspension (section 2.23) was centrifuged at 365 x g for 5 minutes at room temperature, resuspended in RPMI medium (supplemented with 10 % FBS, 400 U/ml penicillin streptomycin, 2 mM L-glutamine and plated into 96-well plate at a cell density of 1 x 10^5 cells per well. Cells were allowed to differentiate into macrophages in the presence of M-CSF at 100 ng/ml for four days. Thereafter cells were stimulated to differentiate towards

an “M1” phenotype with LPS / IFNγ (at 10 ng/ml for LPS and 50 ng/ml for IFNγ) or an “M2” phenotype with IL-4 (20 ng/ml) in the presence and absence of human plasma-derived clusterin (1 - 30 µg/ml) or remained untreated. Supernatants were collected after 72 hours and secreted proteins analysed via Luminex assay as described in section 2.26.

2.25 Neutralisation of TNFα in the culture medium of human blood-derived macrophages

Human-blood-derived macrophages were isolated and cultured as indicated in sections 2.23 and 2.24. After differentiation of monocytes with M-CSF (100 ng/ml) for four days, supernatants were replaced with culture medium (RPMI with 10 % FBS) as untreated control of medium containing clusterin at 5 µg/ml with or without soluble TNF-α neutralising antibodies at 10 µg/ ml (R&D Systems, AF-210-NA) or isotype control (R&D Systems, AB-108-C) at matching concentrations (R&D Systems, Abingdon, UK). Supernatants were collected after 72 hours and analysed via luminex assay as described in section 2.26.

2.26 Luminex assay

In order to measure multiple cytokines simultaneously in a small sample volume for example cell culture supernatants, multiplex detection assays following a principle that is similar to a traditional ELISA were used. The principle of the multiplex technology relies on analyte-specific antibodies that are coupled to magnetic microparticles that are dyed with fluorophores of differing intensities, which allows the combination and simultaneous identification of individual beads in the same sample.

In order to measure changes of cytokines and chemokines in supernatants of macrophages and bronchial epithelial cells in response to clusterin in the culture medium, 25-plex (Human Cytokine magnetic 25-plex panel, Life Technologies, UK) and/ or combined single-plex luminex assays (listed in Table 5, R&D Systems, Abingdon, UK) were performed according to manufacturer´s protocol.

Briefly, 25 µL (25-plex) or 50 µL (single-plex) antibody coupled beads (of differing specificities) were vortexed and sonicated for 30 seconds and pipetted into each well of a 96 well plate. Analyte-specific standards in a 6 point, 3-fold dilution and samples at 50 µl (25-plex) or 100 µl (single-plex) were added to the wells of a 96-well plate and incubated over night at 4 °C after mixing the plate on an orbital plate shaker at 500 rpm. Next day the 96-well plate was placed on a magnetic

plate separator to keep all magnetic beads including bead-bound substances in the plate while unbound substances were washed away (3 x), by adding and removing 100 µL of provided wash buffer to each well. After discarding the final wash solution from each well 100 µl (25-plex) or 50 µL (single-plex) of biotinylated antibody cocktail, specific to analytes of interest, were added to each well and incubated for 1 hour on an orbital plate shaker at 500 rpm. Thereafter, all wells were washed three times with kit-specific wash buffer after placing the 96-well plate onto the magnetic plate separator to remove unbound biotinylated antibody. To amplify the signal, 100 µl Streptavidin-RPE (25-plex) or 50 µL streptavidin-phycoerythrin conjugate (single-plex) which binds to biotinylated capture antibodies were added to each well and incubated for 30 minutes at room temperature on an orbital shaker at 500 rpm. After washing the 96-well plate on the magnetic plate separator with 100 µl kit-supplied wash solution, the plate was removed from the magnetic plate holder, and magnetic beads including bound analytes were resuspended in 100 µl wash buffer. The plate was mixed on the orbital shaker for 3 minutes before the plate was read via Flexmap 3D system® (Merck-Millipore, UK) and analysed with the Luminex xPONENT software.

2.27 Statistics

All data in figures are presented as mean ± standard error of the mean (SEM) unless otherwise stated. Statistical evaluations were performed by ANOVA and Tukey-Kramer post hoc test for multiple comparisons or unpaired t-tests for single comparisons using GraphPad Prism version 6.0 for Mac OS X (GraphPad Software, San Diego, CA). Non-parametric data were analysed using a Mann-Whitney U test. P-values of less than 0.05 were considered significant.

3 Results

3.1 Overview

All experimental results described in this thesis have been divided into different sections. The first section demonstrates the immunolocalisation of clusterin in normal and fibrotic lung and highlights fibrosis – specific changes in the fibrotic lung. The following section explores the *in vitro* evidence for the role of pro-fibrotic mediator TGF-β_1 in modulating clusterin expression in control lung fibroblasts and discusses the immunolocalisation of clusterin, αSMA, collagen and TGF-β_1 in fibroblastic foci in sections of fibrotic lung tissue. Subsequent sections determine the effect of shRNA-induced clusterin-deficiency in differentiation and function of control fibroblast and compare those to the effects of low clusterin expression in fibrotic lung fibroblasts *in vitro*. The final two sections explore the immunolocalisation of clusterin receptor LRP-2 in tissue of control and fibrotic lungs and discuss the effect of exogenous, human plasma-derived clusterin on cytokine and chemokine secretion in human blood-derived macrophages of differing polarisation states and in alveolar macrophages and bronchial epithelial cells *in vitro*.

3.2 Clusterin distribution in fibrotic compared with control lungs

Clusterin is significantly down-regulated in IPF-BALF of patients when compared with BALF from normal lungs (T. H. Kim et al. 2010). Although clusterin has been described to be altered in smoker's lung when compared with control lungs (Carnevali et al. 2006) the detailed distribution and expression of clusterin in control lung and fibrosis relevant changes remain undescribed. To assess whether lung-associated changes may, at least partly, cause the reduction of measurable clusterin in IPF-BALF and to examine the expression and localisation of clusterin in normal and fibrotic lung immunohistochemical staining was performed as described in section 2.10. For this purpose, paraffin-embedded specimens of IPF lung tissue obtained from patients undergoing surgical biopsy or lung transplantation and control tissue from histologically normal areas of peripheral lung removed at lung cancer resection were used (as described in section 2.6). All tissue was obtained with appropriate consent and its use approved by the relevant local research ethics committee. For all antibodies used during immunohistochemical staining optimal epitope, unmasking procedures were established and optimal antibody concentrations determined as listed in section 2.10. Non-immune isotype Ig controls, at matched concentrations to the primary antibodies

were used as a negative control. Representative images of staining with isotype controls are shown in Appendix 2.

3.2.1 Clusterin distribution and expression in control human lungs.

In normal human lung, clusterin was localised to fibroblast-like cells (Figure 3.1A) and in areas of bronchial epithelial cells (Figure 3.1B). Additional clusterin staining was observed in the alveolar interstitium and vessel walls (Figure 3.1C) and co-localised with elastin as assessed by Elastica van Gieson (EvG) staining (Figure 3.1D). Weak or undetectable immunopositivity was observed in macrophages (Figure 3.1A). Furthermore, clusterin was undetectable in alveolar epithelial cells (Figure 3.1A), endothelial cells and smooth muscle cells (Figure 3.1C).

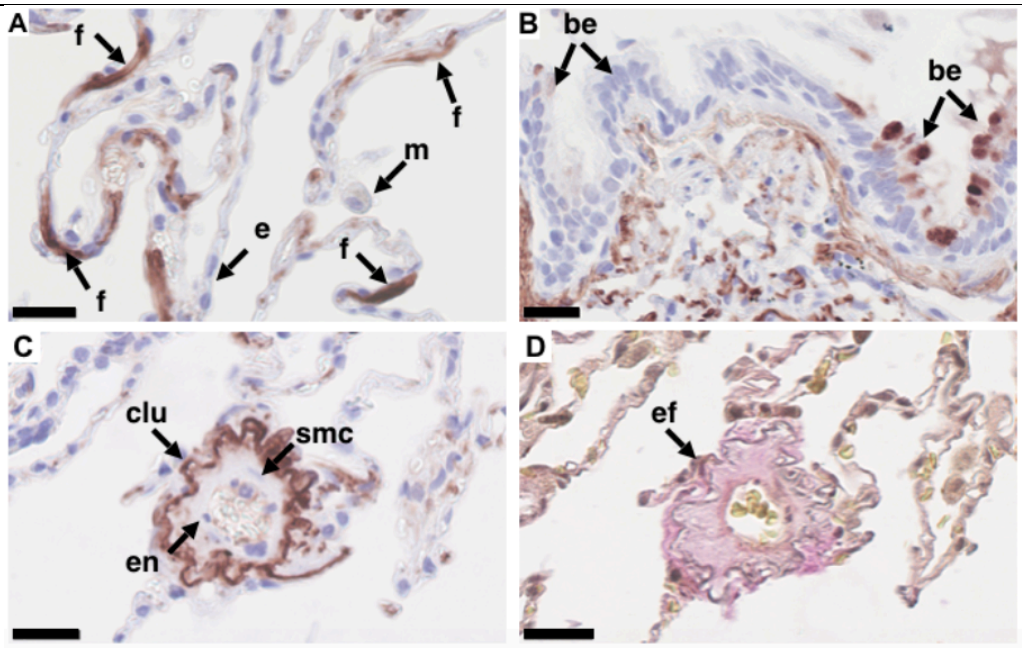

Figure 3.1 Localisation of clusterin in normal human lung.

Representative images of clusterin (A-C, α/βchain AB: sc-8354, brown, nuclei - blue) and elastic fibres (D, dark black) in tissue obtained from control lung. Clusterin localises to fibroblast-like cells (A), to small areas of bronchial epithelia cells (B) and to elastic fibres in blood vessels and alveolar walls (C). Weak or undetectable immunopositivity was observed for macrophages and alveolar epithelial cells (A) and endothelial cells (C). Different cell populations/structures are indicated by arrows: f - fibroblast-like cell, m - macrophage, e – alveolar epithelial cell, be - bronchial epithelial cells, en - endothelial cell, smc – smooth muscle cells, ef - elastic fibres. Scale bar represents 25 μm.

3.2.2 Clusterin distribution and expression in IPF lungs

In contrast, in IPF lung clusterin staining was weak or undetectable in fibroblasts associated with fibrotic regions (Figure 3.2A), whereas fibroblasts in morphologically normal areas of IPF lung showed strong clusterin staining (Figure 3.2B) comparable to that of fibroblast-like cells in control lungs (Figure 3.1A). Hyperplastic epithelial cells overlying fibroblastic foci showed weak or no clusterin staining (Figure 3.2A). Clusterin staining of macrophages, smooth muscle cells and endothelial cells of IPF lungs was weak or undetectable similar to control lungs (Figure 3.2D,E).

Figure 3.2C and Figure 3.3A show a more extensive clusterin staining located to the apical compartment of bronchial epithelium in IPF-lungs compared with controls. It is well known that alveolar macrophages express high levels of TGF-β_1 in pulmonary fibrosis (Corrin et al. 1994). In order to exclude the possibility that positive clusterin staining locates to macrophages associated with the apical surfaces of bronchial epithelial cells, rather than being located to bronchial epithelial cells, staining of serial sections were performed for clusterin and TGF-β_1 (Figure 3.3A, B). Clusterin localised apically in bronchial epithelium while TGF-β_1 was not detectable in bronchial epithelium. On the contrary, TGF-β_1 localised to interstitial tissue macrophages (see also Figure 3.8). This demonstrates that clusterin is expressed by bronchial epithelium in IPF and not in alveolar macrophages that are associated with the luminal bronchial epithelium.

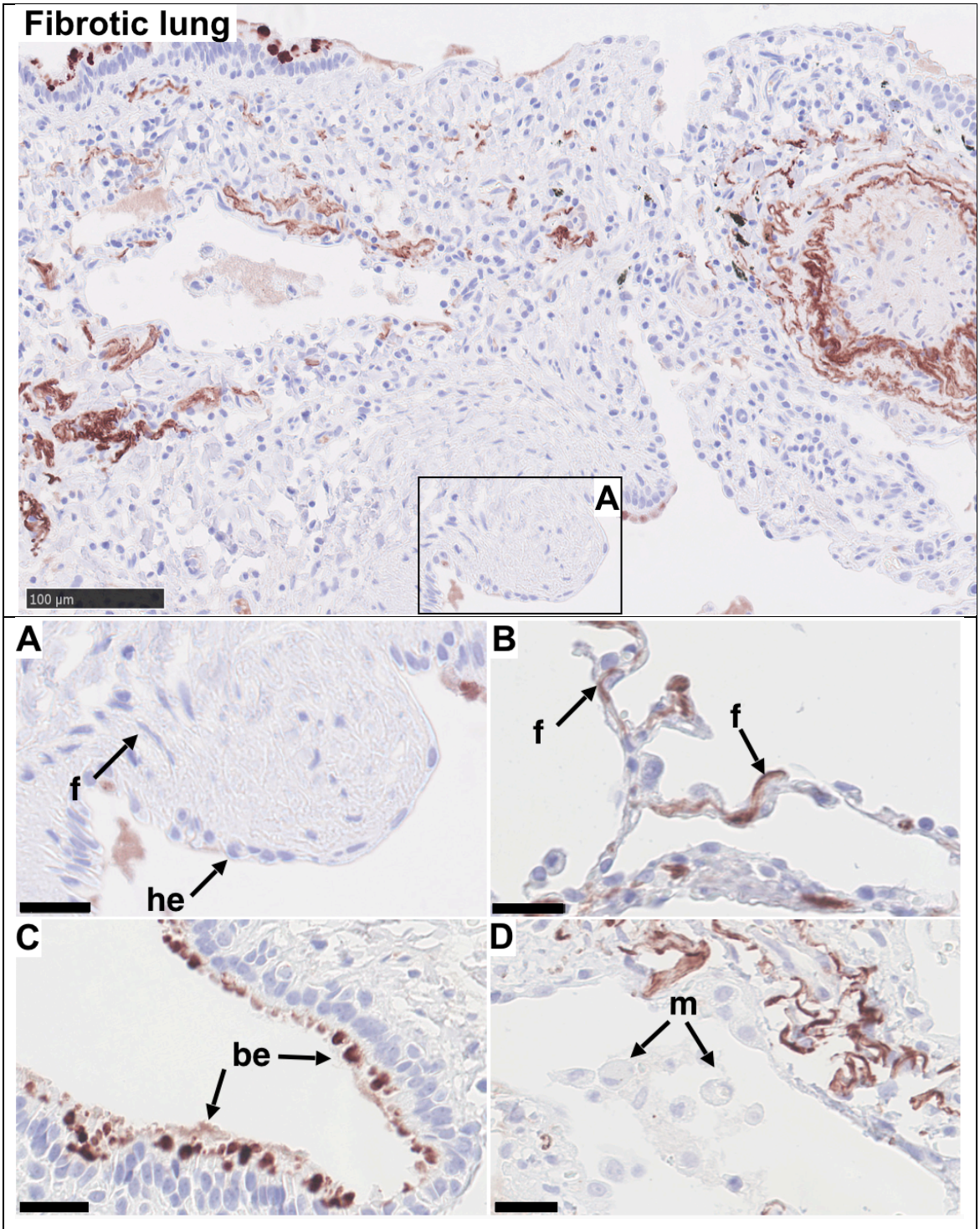

Figure 3.2 Localisation of clusterin in IPF lung (continued over the page).

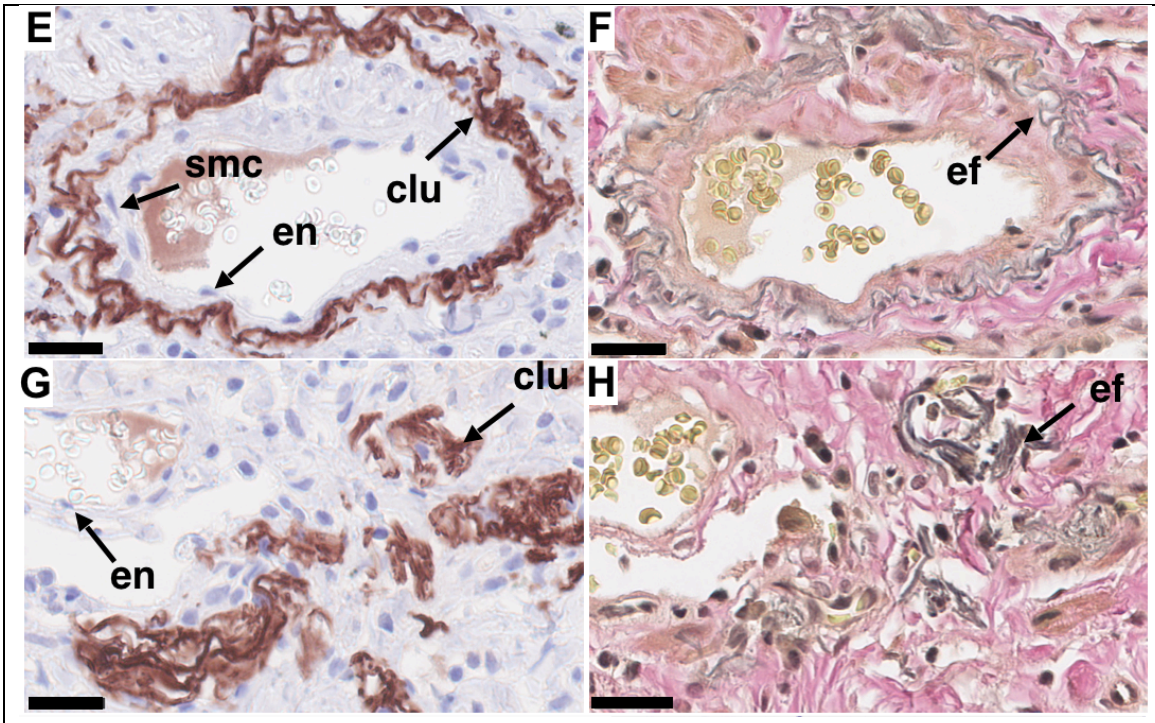

Figure 3.2 Localisation of clusterin in IPF lung.

Immunohistochemical staining of clusterin in IPF lung (overview, A-D, α/βchain AB: sc-8354, E, G, brown, nuclei - blue) and elastin (F, H, EvG, black). Clusterin is undetectable in fibrotic lung fibroblasts forming and in cells covering fibroblastic foci (A), compared with strong staining of fibroblast-like cells in apparently non-fibrotic areas (B). Clusterin staining in macrophages, smooth muscle cells, endothelial cells and associated with elastic fibres appears consistent with that of clusterin staining in control lungs (D-E). IPF-specific increase in clusterin staining is located to larger areas of bronchial epithelial cells (C) and associated with thickened blood vessel walls (E) and extracellular matrix deposits (G) associated with strong staining for elastin (F, H). Different cell populations/structures are indicated by arrows; f - fibroblast-like cell, m - macrophage, he - hyperplastic epithelia cell, be-bronchial epithelial cell, en – endothelial cell, smc – smooth muscle cell, ef- elastic fibres. Scale bar represents 25 µm.

3.2.3 Clusterin associated with widespread elastin-rich deposits in IPF-lung

Consistent with control lung, clusterin staining was associated with vessel walls in lungs from IPF-patients (Figure 3.2E; EvG staining F). Additionally, clusterin also associated with amorphous elastin-rich deposits arising within fibrotic areas (Figure 3.2G; EvG staining H). Interestingly, those elastin-rich deposits were not located in fibroblastic foci, as examined by additional staining of serial sections of one representative fibroblastic focus in IPF-lung (Figure 3.4). Immunohistochemistry confirmed that clusterin is undetectable in areas of αSMA-positive fibrotic lung fibroblasts and surrounding matrix (Figure 3.4A, B). As demonstrated via EvG staining,

the matrix consisted predominantly of collagen (light red, EvG), while elastin (black, EvG) was only detectable in areas outside the focus, where αSMA expression was undetectable (Figure 3.4.C).

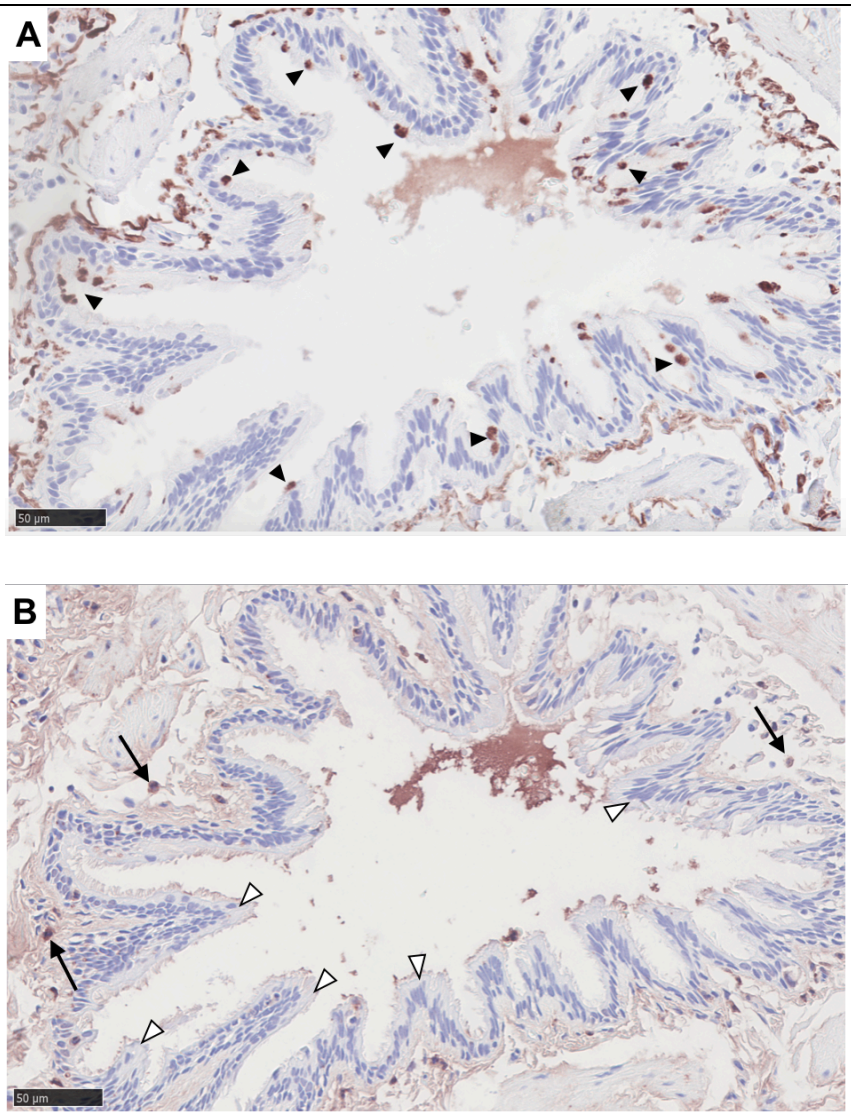

Figure 3.3 Clusterin staining associates with the bronchial epithelium and not with macrophages associated with the bronchial epithelium.

Immunohistochemical staining of serial sections of a representative bronchiole. Clusterin (A, brown, α/βchain AB: sc-8354, nuclei blue) staining is associated with bronchial epithelial cells (closed arrowheads. TGF-β_1 staining (B, brown, nuclei blue) did not co-localise with clusterin staining in bronchial epithelial cells (open arrow heads) but associated with interstitial macrophages (arrows). Clusterin and TGF-β_1 co-localise in the subepithelial matrix. Scale bar represents 50 µm.

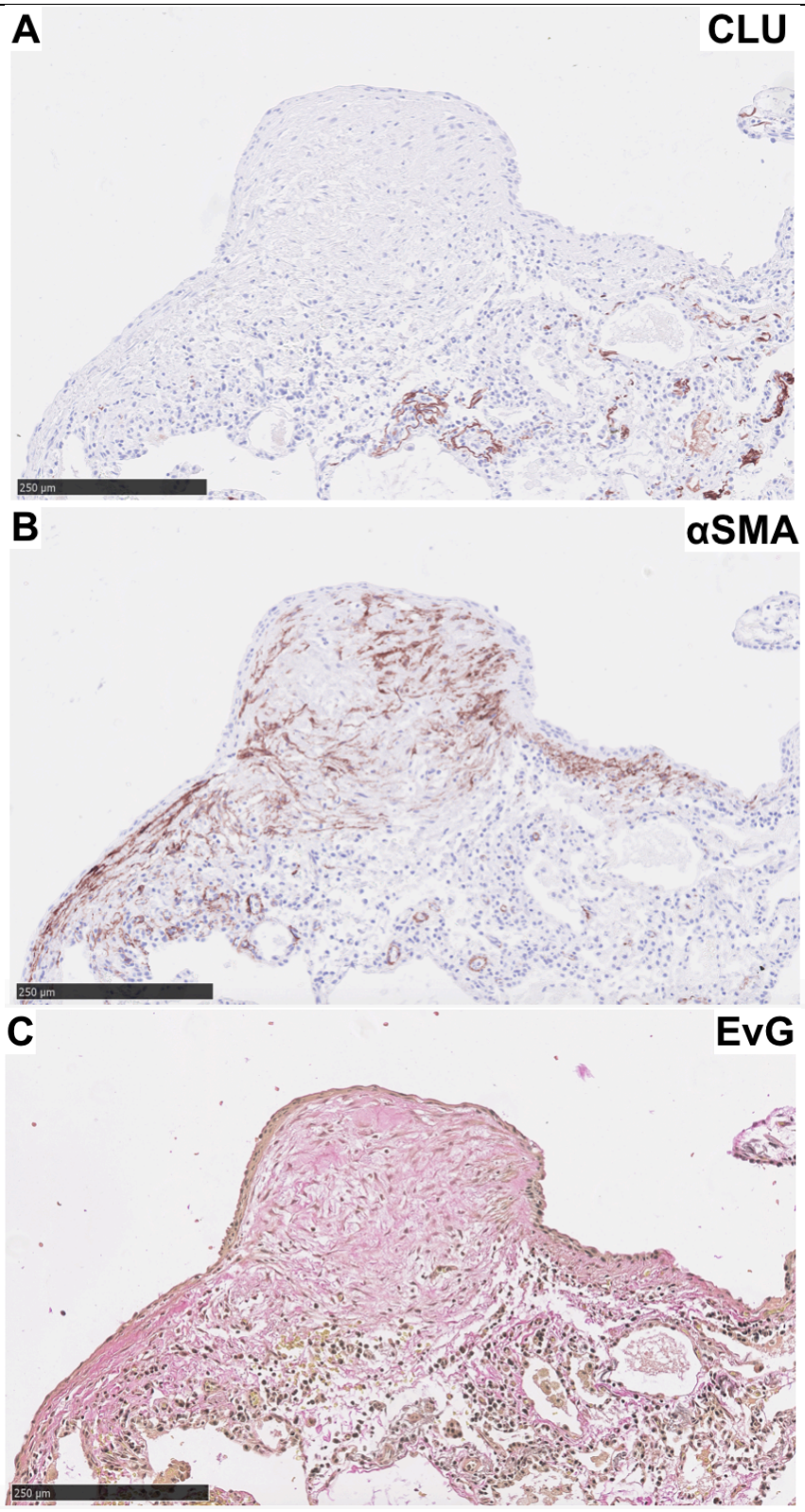

Figure 3.4 Undetectable clusterin in fibroblastic foci.

Immunohistochemical staining of clusterin (CLU in A, brown, nuclei - blue), αSMA (B, brown, nuclei – blue), C elastin (EvG, black) and collagen (EvG, light red) in serial sections of fibroblastic foci in IPF lung. Scale bar represents 250 µm.

3.2.4 Summary

The results in this section examine the expression of clusterin *in vivo* in human fibrotic and control tissue and explore changes in the immunohistochemical localisation of clusterin associated with key pro-fibrotic proteins αSMA and TGF-β_1. The main findings are;

- In normal lung clusterin staining associates with fibroblasts but is undetectable in fibroblasts associated with fibroblastic foci in IPF, particularly myofibroblasts expressing αSMA which were surrounded by high levels of deposited collagen.

- Clusterin staining co-localised with elastin staining in vessel walls of control and fibrotic lung and co-localised with elastin in extracellular matrix deposits, which were widely distributed across areas of fibrotic tissue. Elastin was not detectable in fibroblastic foci.

- In control lung tissue clusterin staining localised to sporadic areas of bronchial epithelial cells, but showed more extensive and intense staining in bronchial epithelial cells of IPF lungs.

- Weak or modest staining of clusterin in macrophages, smooth muscle cells and alveolar epithelial cells in IPF lung was comparable to that in control lung.

Together, the results in this section demonstrate a detailed analysis of clusterin distribution and expression in control lungs and outlines fibrosis-specific changes in control lung, which has not previously been described. These results suggest that a reduction of measurable clusterin in IPF-BALF may at least partly occur due to its association to elastin in widespread elastin deposits in fibrotic lungs. The results in this section further suggest that clusterin expression is down-regulated in fibrotic lung fibroblasts when compared with fibroblasts in control lungs. To validate these results and further assess the mechanisms contributing to a down-regulation of clusterin in IPF-BALF, the expression and regulation of clusterin was studied in fibroblasts isolated from control and fibrotic lungs *in vitro*.

3.3 *In vitro* assessment of clusterin expression in control and fibrotic lung fibroblasts and its regulation by TGF-β_1

3.3.1 *In vitro* expression and secretion of clusterin in control lung fibroblasts.

To validate the observations of different clusterin expression levels in fibroblasts from control and fibrotic lung, studies were conducted to assess clusterin expression and secretion *in vitro*. Clusterin expression and distribution in human lung fibroblasts has been previously described in the context of oxidative stress caused by cigarette smoke extract (Carnevali et al. 2006). Consistent with the report from Carnevali and colleagues, clusterin expression located to the cytoplasm and nucleus of control fibroblasts (Figure 3.5A). This result was further validated with different antibodies targeting the α- and/or the β-chain of clusterin (Figure 3.5B). It has been reported in other cell lines and lung fibroblasts that the protein size of clusterin varies depending on its level of maturation. Consistent with the report from Carnevali, Western blot analysis showed two clusterin bands of about 60 kDa and 40 kDa (Carnevali et al. 2006). Under reducing conditions, the mature, heterodimeric form of clusterin (76 – 80 kDa) is seen as 40 kDa band, separate α-chain and β-chain, reported to appear as bands at 36-39 kDa and 34-36 kDa (Figure 3.6A Blot 1), appears as double band in the cytoplasmic fraction. The 60 kDa band has been reported to represent the unglycosylated, uncleaved precursor form of the mature 76-80 kDa isoform and can only be found intracellularly, while the 34 – 39 kDa band (mature clusterin) is observed in the supernatant of primary lung fibroblasts (Figure 3.6A Blot 2).

Primary lung fibroblasts were routinely cultured in 10 % FBS in DMEM. In order to exclude the possibility that measurements of secretory clusterin are not originating from FBS, secretory clusterin cell culture medium alone or in the presence of primary fibroblast were measured. Results in Figure 3.6B show that the secretory clusterin value was very low in the culture medium containing FBS, while clusterin was measurable in cell supernatants of primary lung fibroblasts.

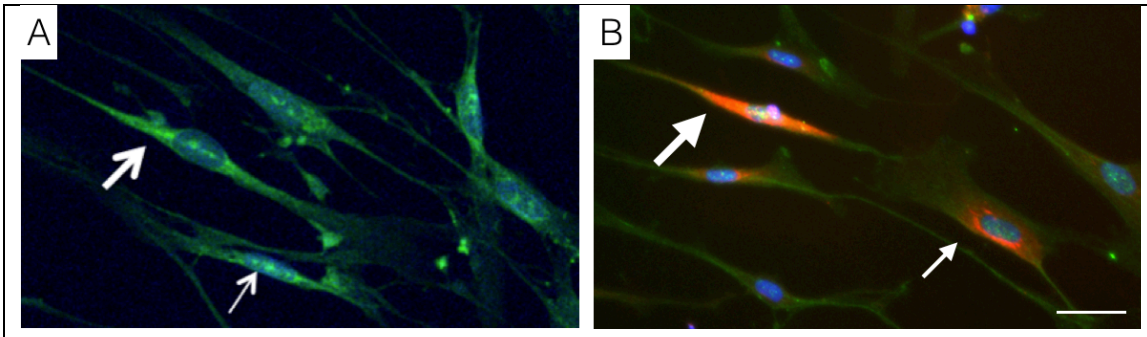

Figure 3.5 Clusterin expression in cytoplasm and perinuclear area of control lung fibroblasts *in vitro*.

Primary human lung fibroblasts were seeded at a density of 1 x 10^4 in chamber slide wells or 96-well plate wells and allowed to reach over 80 % confluence. Cells were serum-starved 18 hours, fixed in paraformaldehyde (A) or methanol (B) and stained for clusterin. DAPI (blue) was used to visualise the nucleus. For (A) a polyclonal anti-clusterin antibody as used against amino acids 120-449 (α-chain). For (B) a monoclonal antibody against amino acids 425-449 (α-chain, sc-5289, red) and a polyclonal antibody mapping near the N-terminus of clusterin (β-chain, green). Areas of co-localisation appear orange-red (large arrow). Clusterin localises to the cytoplasm (large arrow) and perinuclear area (small arrow) as visualised via confocal microscopy (A) or Image Xpress analysis (B). Scale bar 10µm.

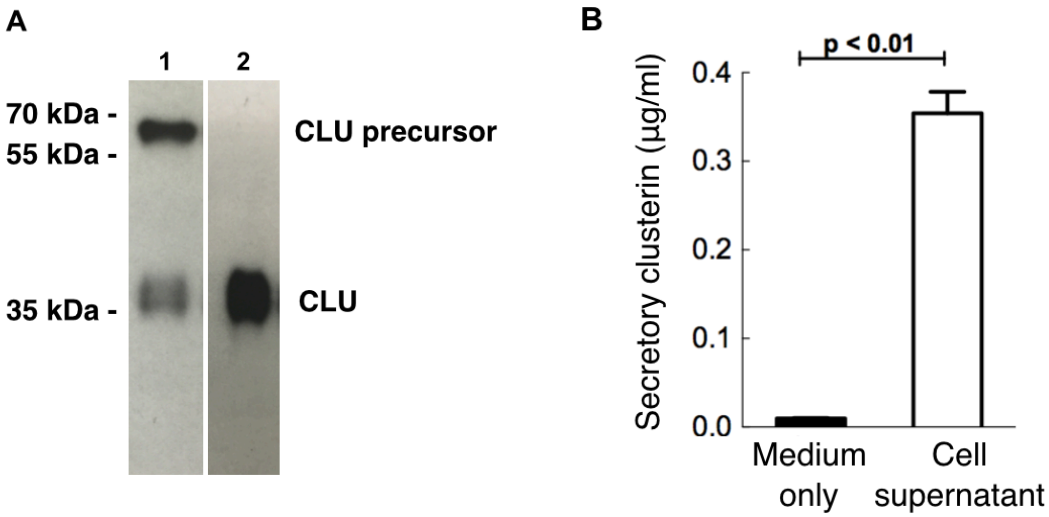

Figure 3.6 Primary lung fibroblasts derived from healthy lung tissue express and secrete detectable levels of clusterin.

Western blot analysis using an antibody detecting both α and β chain (α/βchain AB: sc-8354) shows clusterin protein expression in 10 µg whole cell lysates (Blot 1) and 20 µl cell supernatant (Blot 2) of primary lung fibroblasts cultured in T75 tissue culture flask as confluent monolayer. Under reducing conditions clusterin appears as a 60 kDa precursor and cleaved α and β subunits sized (34 - 39 kDa). (B) Clusterin in 50 µl culture medium (10 % (v/v) FBS in DMEM) without and with primary human lung fibroblasts.

3.3.2 Clusterin mRNA and protein levels in fibrotic fibroblasts compared with control fibroblasts *in vitro*.

To confirm the changes in clusterin expression observed in IPF lung (see section 3.2.1 and 3.2.2) the expression of clusterin in fibroblasts isolated from control and fibrotic lung was examined. Consistent with the immunohistochemical data, clusterin mRNA expression was reduced in fibrotic compared with control lung fibroblasts (Figure 3.7A microarray analysis). The differences were confirmed at protein level in representative donor fibroblast isolates assessed by protein array analysis (Figure 3.7B) and immunofluorescent staining (Figure 3.7C-E).

3.3.3 TGF-β_1 associates with areas of decreased clusterin expression in fibrotic lung.

TGF-β_1 is a major profibrotic mediator, which drives myofibroblast differentiation with up-regulation of αSMA and collagen expression. IPF lungs are characterised by increased levels of TGF-β_1 associated with the extracellular matrix and expressed by epithelial cells (Denney et al. 2015) and alveolar macrophages (Leppäranta et al. 2012). As described in Figure 3.8 there is a strong staining for TGF-β_1 associated with alveolar macrophages and the extracellular matrix (Henderson & Sheppard 2013b; Taipale et al. 1994). While previous studies suggest TGF-β_1 up-regulates clusterin expression in mammary epithelial cells (Itahana et al. 2007), there is little information on its effect on fibroblasts. To gain an overview of clusterin expression in TGF-β_1-rich areas of fibrotic lung immunohistochemical staining for TGF-β_1 and clusterin in fibroblastic foci in fibrotic lung was performed (see Figure 3.8). Results show that fibroblastic foci are rich in extracellular matrix-bound TGF-β_1 and myofibroblasts associated with these foci exhibit low clusterin expression. The inverse correlation of staining for TGF-β_1 and clusterin suggests a potential regulatory link between both proteins.

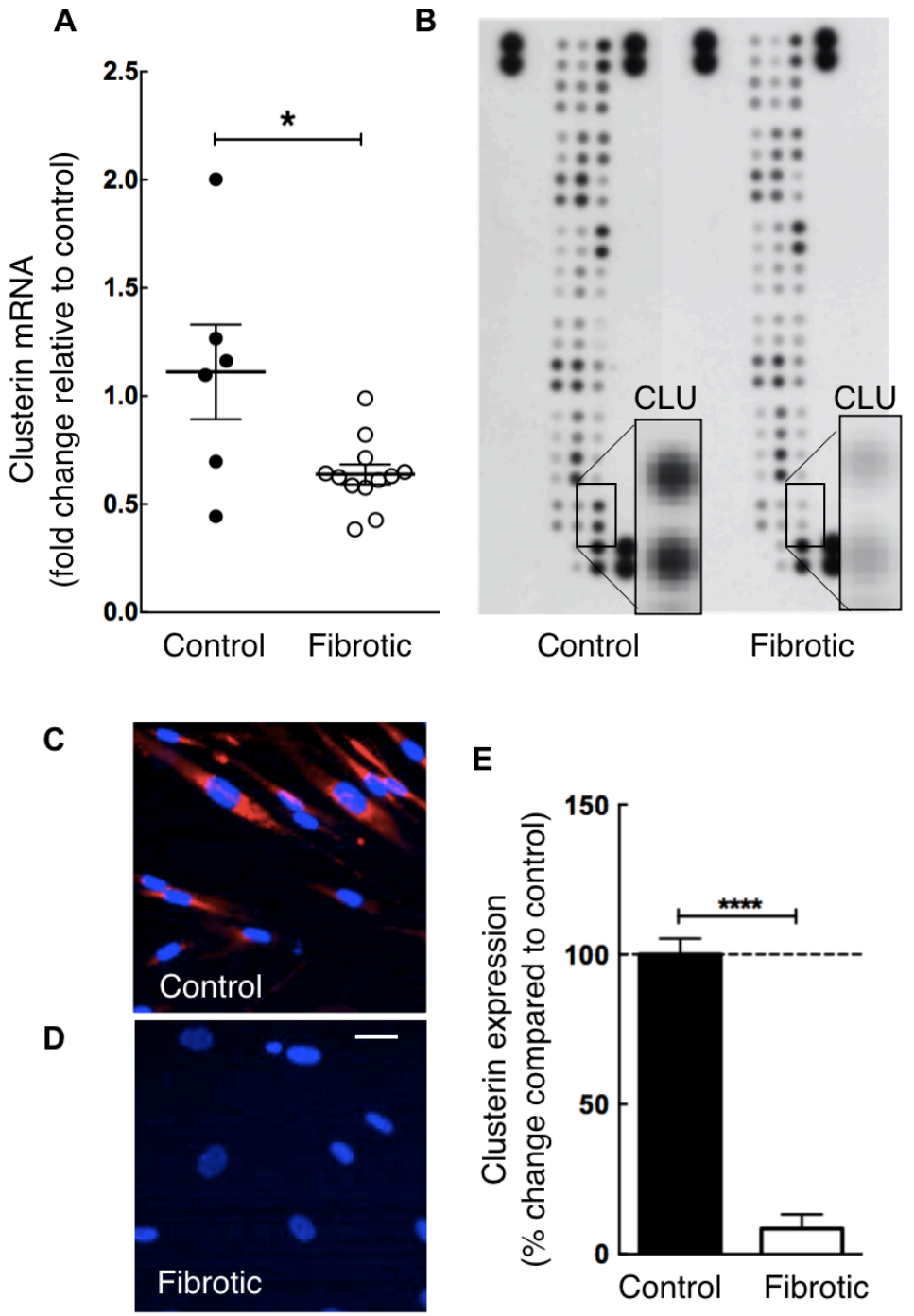

Figure 3.7 Clusterin mRNA and protein are decreased in fibrotic compared with control lung fibroblasts.

(A) Microarray mRNA analysis shows decreased clusterin gene expression in fibroblasts derived from IPF (n=5) and SSC (n=7) lungs (open circles) compared with controls (closed circles; n=6) *in vitro*. Proteome profiler array (B, performed by Dr. Toby Maher) and immunofluorescence staining (α-chain, sc-5289) of non-fibrotic and fibrotic fibroblasts (C) confirm low clusterin protein expression in fibrotic compared with control fibroblasts *in vitro*. (E) Quantification of panel (C, D) clusterin signal (pixel intensity) normalised to cell numbers per visual field (n=6). *$P < 0.05$, ****$P < 0.0001$; Scale bar in D represents 10 µm.

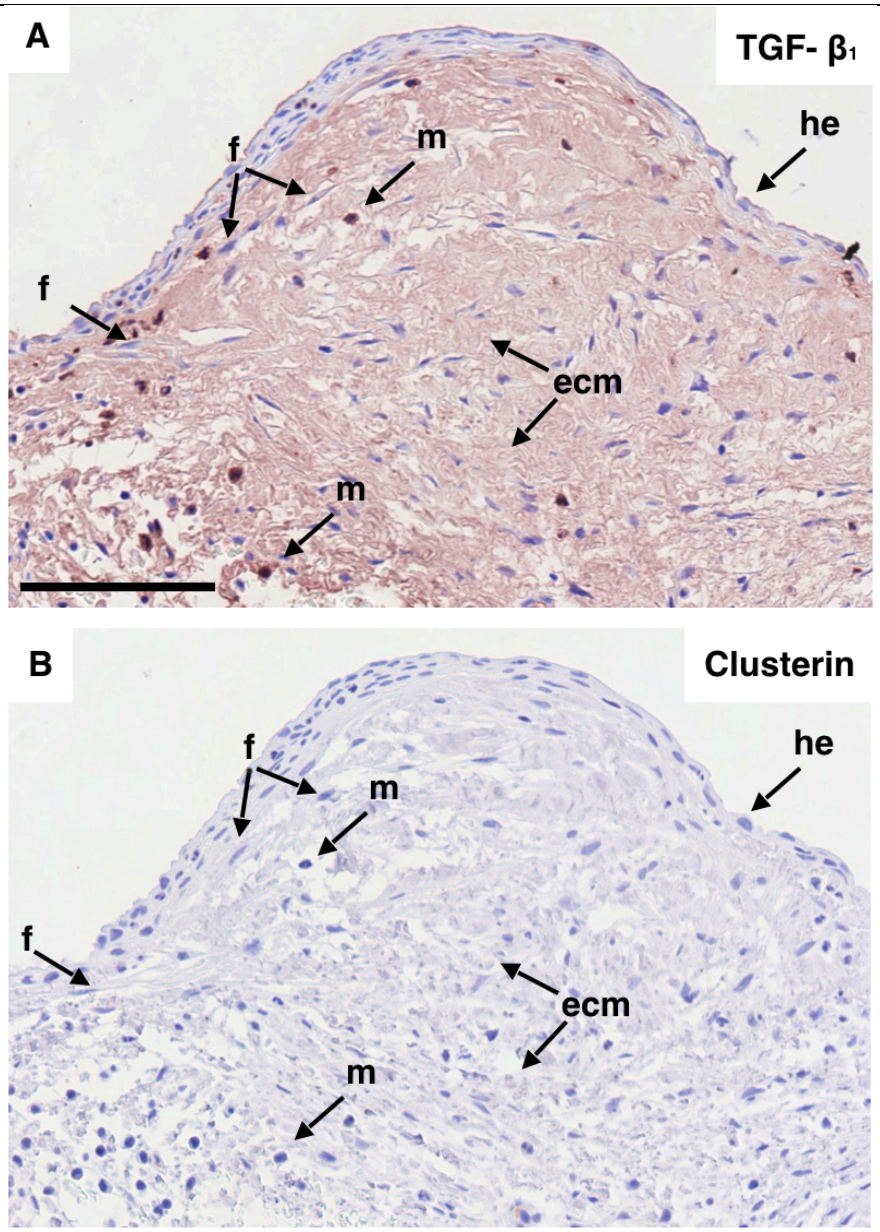

Figure 3.8 TGF-β_1 associates with areas of decreased clusterin expression in fibroblastic foci in fibrotic lung.

Representative images of TGF-β_1 staining (A, red/brown, nuclei blue) and clusterin staining (B, α/βchain AB: sc-8354, CLU red/brown, nuclei blue) in serial sections of fibroblastic foci in IPF-lung. While TGF-β_1 localises to ECM, fibroblasts and macrophages, staining for clusterin is weak or undetectable. f - fibroblast-like cell, m - macrophage, he - hyperplastic epithelia cell, ecm – extracellular matrix. Scale bar represents 100 µm.

3.3.4 TGF-β_1 down-regulates fibroblast clusterin mRNA and protein expression *in vitro*.

Results in the previous section showed that increased expression of TGF-β_1 co-localises with reduced expression of clusterin. While previous studies suggest TGF-β_1 up-regulates clusterin expression in epithelial cells (Itahana et al. 2007), there is little information on its effect on fibroblasts. It was therefore determined if TGF-β_1 regulates clusterin expression in control lung fibroblasts *in vitro*: Stimulation of control lung fibroblasts with TGF-β_1 (1 ng/ml, a dose which has been established to induce fibroblast differentiation (Tiggelman et al. 1997)) reduced clusterin mRNA levels in a time-dependent manner (Figure 3.9A). Clusterin expression began to decline by 4 hours and was significantly reduced by ≈ 77 % by 24 hours (Two-way ANOVA $p = 0.0051$). Clusterin down-regulation was maintained for at least 48 hours as confirmed by immunofluorescent staining (Figure 3.9C,D). Western blot analysis confirmed that clusterin levels are decreased in response to TGF-β_1 by 24 hours (Figure 3.9B) and TGF-β_1-induced fibroblast differentiation was confirmed by increased αSMA protein levels. Consistently, immunofluorescence analysis (Figure 3.9C-D) post TGF-β_1 stimulation, confirmed the down-regulation of clusterin by TGF-β_1.

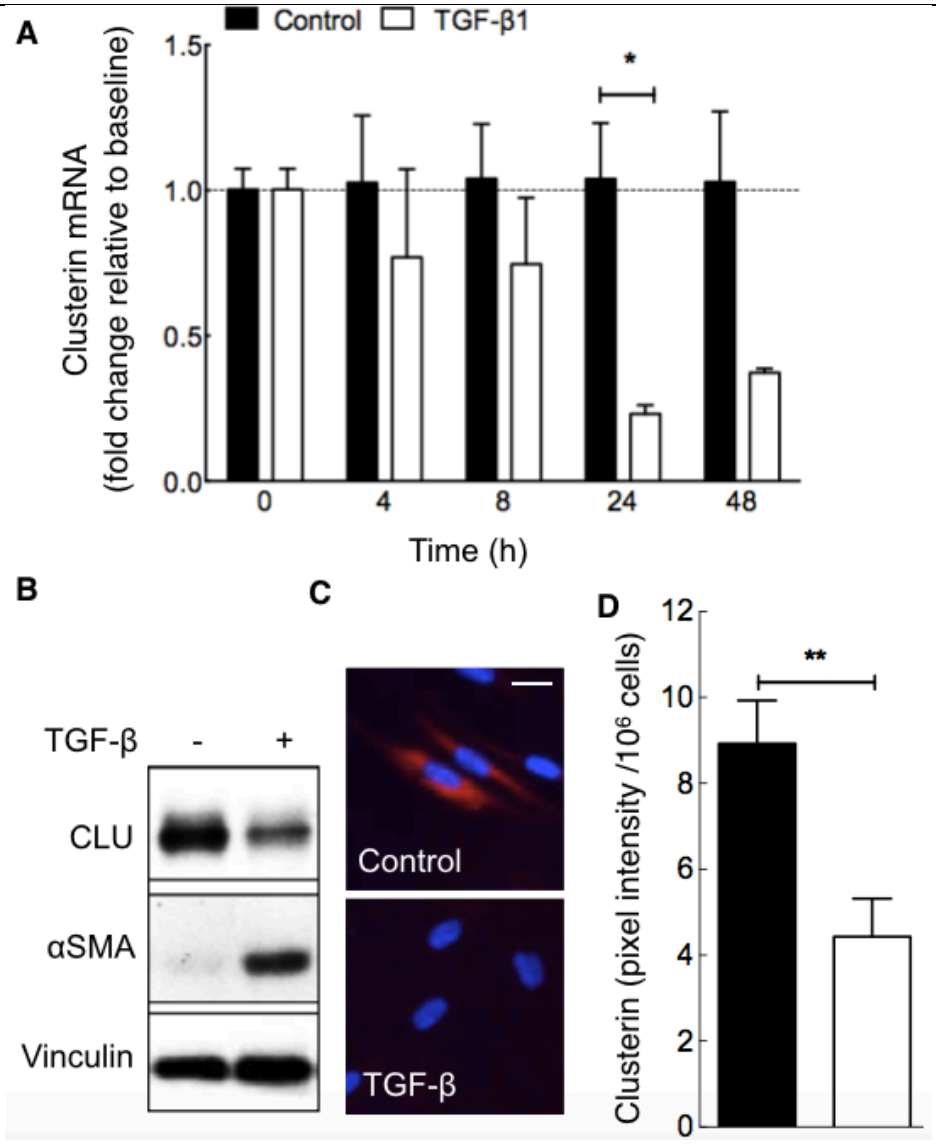

Figure 3.9 TGF-β_1 down-regulates fibroblast clusterin mRNA and protein expression *in vitro*.

(A) *In vitro* analysis of mRNA levels in TGF-β_1-stimulated (1 ng/ml) fibroblasts shows a time-dependent down-regulation of clusterin expression (n=3). Post TGF-β_1-stimulation (1 ng/ml) clusterin (CLU) protein levels are down-regulated compared with control as demonstrated via Western blot at 24 hours (B) and immunofluorescent staining at 48 hours (C, red, α-chain, sc-5289, nuclei - blue). (D) Quantification of fluorescent signal of panel C: clusterin signal (pixel intensity) was normalised to cell numbers per visual field and compared with control (n=6). **P* < 0.05, ***P* < 0.01.

3.3.5 Summary

This results section focuses on the expression of clusterin in association with profibrotic mediator TGF-β_1 in human fibrotic and control tissue. Modulatory effects of TGF-β_1 on clusterin expression have been assessed by analysis of mRNA and protein levels *in vitro*. The key findings are;

- *In vitro* studies confirm that control lung fibroblasts express and secrete high levels of clusterin.

- Consistent with findings in control and fibrotic lung fibroblasts *in vivo,* clusterin mRNA and protein are decreased in fibrotic compared with control lung fibroblasts.

- TGF-β_1 associated with areas of reduced clusterin expression in fibrotic lung.

- TGF-β_1 down-regulated clusterin mRNA and protein expression in lung fibroblasts *in vitro*.

In this section previous observations of reduced clusterin levels in fibrotic lung fibroblasts compared with controls were validated in *in vitro* studies. In addition, mechanisms contributing to a down-regulation in fibrotic lung fibroblasts were assessed *in vitro* studies with fibroblasts from control lung. This data suggests that reduced levels of clusterin in IPF-BALF could, at least in part be caused by a down-regulation of clusterin in response to TGF-β_1. However, the functional effects of a down-regulation of clusterin in lung fibroblasts remain unknown. Interestingly, TGF-β_1 down-regulated clusterin at a concentration, which induced fibroblast differentiation, as assessed by increased αSMA levels (Figure 3.9B). The next section will, therefore, address if the effects of TGF-β_1–induced fibroblast differentiation is dependent on clusterin down-regulation.

3.4 Effect of low clusterin expression on myofibroblast differentiation *in vitro*

TGF-β_1 is a key-mediator in pulmonary fibrosis and drives myofibroblast differentiation. Myofibroblasts express high levels of αSMA, exhibit a contractile phenotype as a result of increased stress fibre formation and secrete high levels of matrix proteins, e.g. collagen I. Results in the previous section 3.3 have demonstrated that TGF-β_1, down-regulates the expression of clusterin in lung fibroblasts, at a concentration and time, at which αSMA was increased. This section, therefore, investigates if the effect of TGF-β_1-induced fibroblast differentiation is dependent on its effects on clusterin expression. To begin to address this question, TGF-β_1-induced fibroblast - to myofibroblast differentiation was studied via increased αSMA expression and collagen deposition *in vitro*.

3.4.1 The effect of TGF-β_1 on αSMA protein expression and collagen I deposition under molecular crowding conditions.

Soluble procollagen levels can be measured in *in vitro* cultures using reverse-phase HPLC quantification of hydroxyproline, or by ELISA and Western blotting. However, the measurement of mature collagen is not possible without so-called molecular crowding conditions. Therefore, deposited collagen was measured via an immunocytofluorescence assay as described in section 2.14.1. To assess the degree of differentiation over time, αSMA protein levels were analysed in response to TGF-β_1 and compared with untreated controls (Figure 3.10A). As with previous experiments, fibroblasts were grown to confluence and serum-starved overnight. αSMA protein levels were assessed via Western blot analysis 18 – 72 hours post treatment with or without TGF-β_1 at 1 ng/ml. As Figure 3.10 demonstrates, αSMA expression was increased by approximately five-fold at 18 hours in response to TGF-β_1. By 48 hours αSMA protein levels were increased by just under ten-fold when compared with controls without administration of TGF-β_1 and increased further to over ten-fold by 72 hours. Based on these results subsequent experiments focussing on fibroblast differentiation were analysed at 48 or 72 hours.

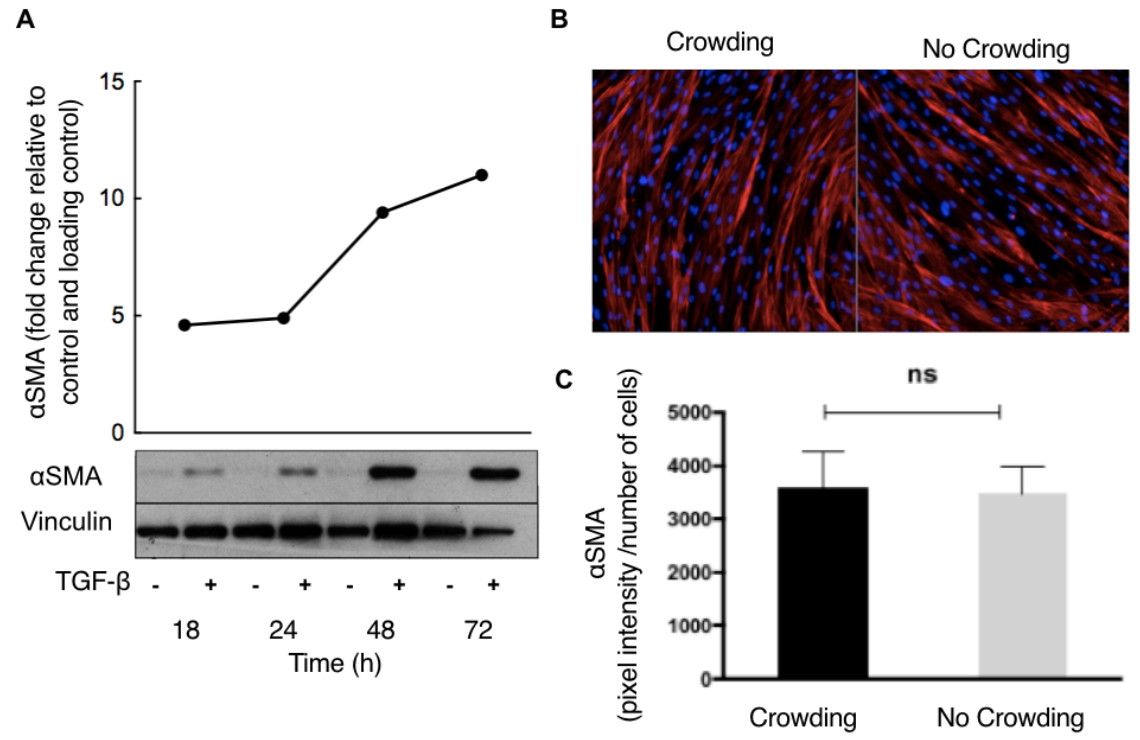

Figure 3.10 αSMA expression in response to TGF-β_1 over time and under crowding conditions.

Fibroblasts were grown to confluence, serum-starved with 0.4 % FBS in DMEM before treatment with and without TGF-β_1 (1 ng/ml) for 18-72 h. 10 μg of whole cell lysates were used for Western blot analysis (A, graph representative of three experiments). (B) Immunofluorescence staining for αSMA 72 h after TGF-β_1 –stimulation under crowding and no crowding conditions (quantification in C).

To confirm that changing tissue culture conditions do not affect the degree or course of differentiation, αSMA expression in response to TGF-β_1 under standard or under molecular crowding conditions was assesses at 72 hours (Figure 3.10B, C). At the endpoint measurement of 72 hours, molecular crowding conditions did not alter the course and levels of αSMA expression in response to TGF-β_1, when compared with non-crowding culture conditions. To confirm these results and to test the impact of different TGF-β_1 concentrations on both αSMA expression and collagen deposition, a dose response to TGF-β_1 was conducted at concentrations ranging from (0 pg/ml to 10 ng/ml) under molecular crowding conditions. Results in Figure 3.11A,C show collagen deposition was increased significantly (One-way ANOVA $p < 0.0001$) at 72 hours starting at a TGF-β_1 concentration of 0.1 ng/ml by a 44 ± 1.36 fold increase of collagen deposition when compared with controls without TGF-β_1.

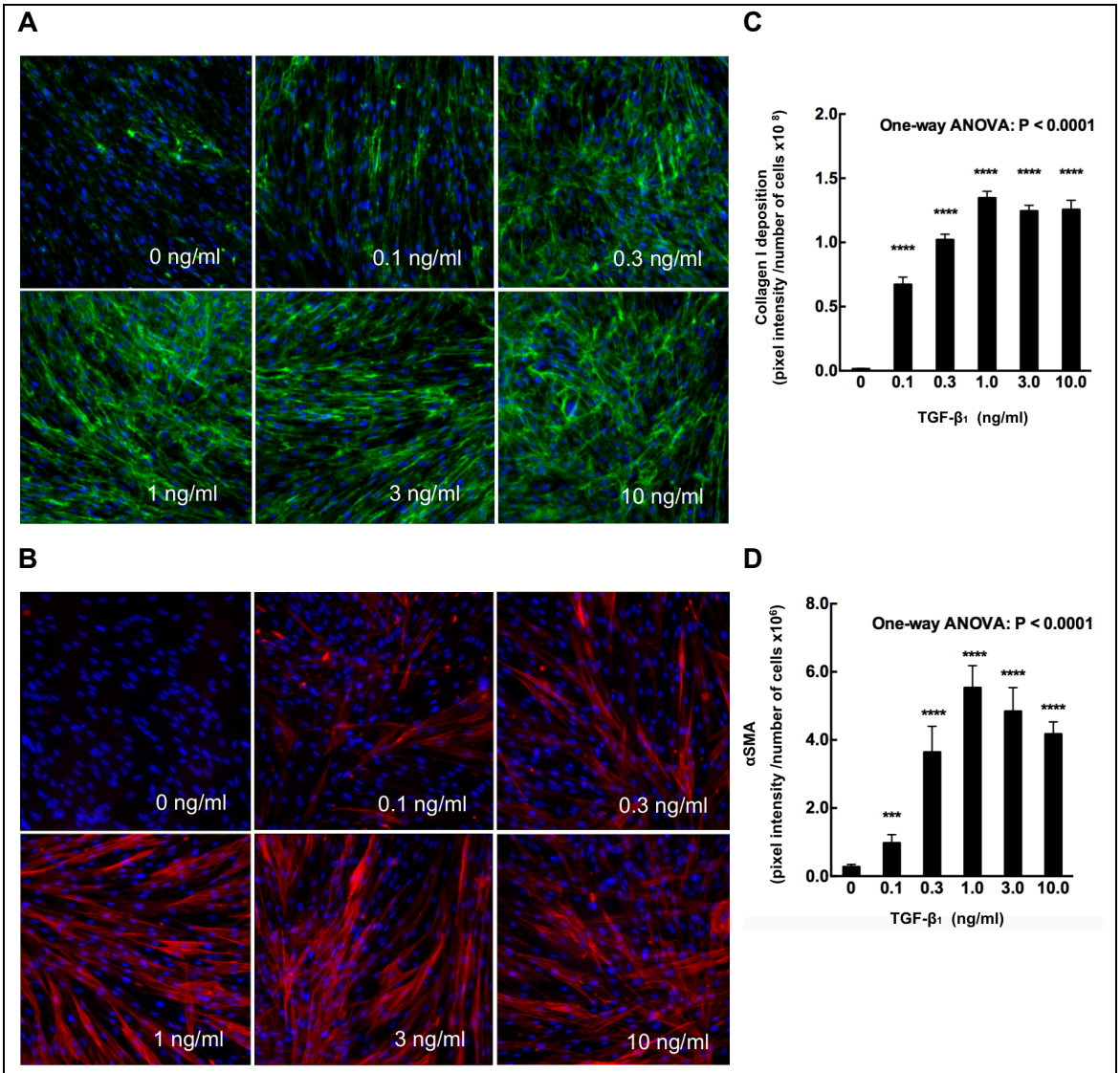

Figure 3.11 The effect of TGF-β_1 on αSMA expression and collagen I deposition under molecular crowding conditions.

Immunofluorescent staining of collagen I (A, collagen I green, nuclei blue) and αSMA (B, αSMA red, nuclei blue) 72 hours after TGF-β_1 stimulation (0 - 10ng/ml) under molecular crowding conditions (n=8). Quantification of the fluorescent signal (C for A and D for B): pixel intensity was normalised to cell numbers per visual field and compared with control respectively (8 technical replicates).

An increase by 89 ± 1.2 fold was measured for a TGF-β_1 concentration of 1 ng/ml and was not significantly different to the 83 ± 1.7 fold increase at a concentration of 10 ng/ml. Similarly, αSMA protein levels were significantly increased in response to TGF-β_1 (One-way ANOVA $p < 0.0001$) at 72 hours (Figure 3.11B,D). At a TGF-β_1 concentration of 0.1 ng/ml αSMA protein levels were increased by 3.5 ± 0.9 fold and were increased by 20.1 ± 2.4 fold at a concentration of 1 ng/ml when compared with untreated controls. Consistently, at a concentration of 10 ng/ml TGF-β_1 significantly increased αSMA protein expression by 15.2 ± 1.3 fold when compared with untreated controls.

3.4.2 siRNA targeting the clusterin gene reduces clusterin mRNA but not protein levels.

To begin to investigate the importance of clusterin in regulating TGF-β_1-induced myofibroblast differentiation, control fibroblasts were transfected with siRNA targeting the clusterin gene (section 2.8). Results in Figure 3.12A show that clusterin siRNA reduced the levels of measurable mRNA at 48 hours and 72 hours after targeting exon 7 of the clusterin gene: At 24 hours clusterin mRNA levels were reduced by 48 % in response to transfection with siRNA targeting the clusterin gene when compared with non-transduced controls and remained reduced up until 72 hours after transduction by 67 %, while transfection with non-silencing control siRNA did not significantly affect clusterin mRNA levels at 24, 48 and 72 hours when compared with non-transduced controls. However, protein levels were not reduced at those times (Figure 3.12.B). Consequently, in following studies in this thesis clusterin expression was modulated by an alternative, more stable gene silencing technique, using lentiviral shRNA (section 3.4.3).

3.4.3 Lentiviral shRNA- mediated clusterin knockdown in control lung fibroblasts.

A model of sustained clusterin knockdown based on small hairpin interference RNA (shRNA) was established as described in section 2.9. To exclude effects of transduction-induced changes, mock (non-silencing) shRNA-transduced fibroblasts were compared with untransduced controls. In such cases where there was no difference between untransduced controls and mock-transduced controls, only the results for mock-transduced fibroblasts are presented in this thesis. shRNA-induced clusterin knockdown compared with both mock-transduced and control was confirmed

for mRNA, protein and secretory clusterin (Figure 3.13). Figure 3.13A shows that clusterin mRNA levels were reduced in fibroblasts treated with shRNA targeting the clusterin gene when compared with controls. Clusterin mRNA levels were reduced to 4.6 % of mRNA levels observed with non-silencing controls. There was no significant difference between clusterin mRNA levels with non-silencing controls compared with non-transduced controls as assessed via qRT-PCR. Further ELISA analysis demonstrates that secretory clusterin levels are significantly reduced by 68.2 % to 0.11 ± 0.01 µg/ml with shRNA targeting clusterin gene expression when compared with non-transduced (0.35 ± 0.02 µg/ml) and non-silencing controls (0.38 ± 0.04 µg/ml) (Figure 3.13B). Clusterin knockdown by 92.5 % was further demonstrated by immunofluorescence (Figure 3.13D, E) and by western blotting (Figure 3.13C).

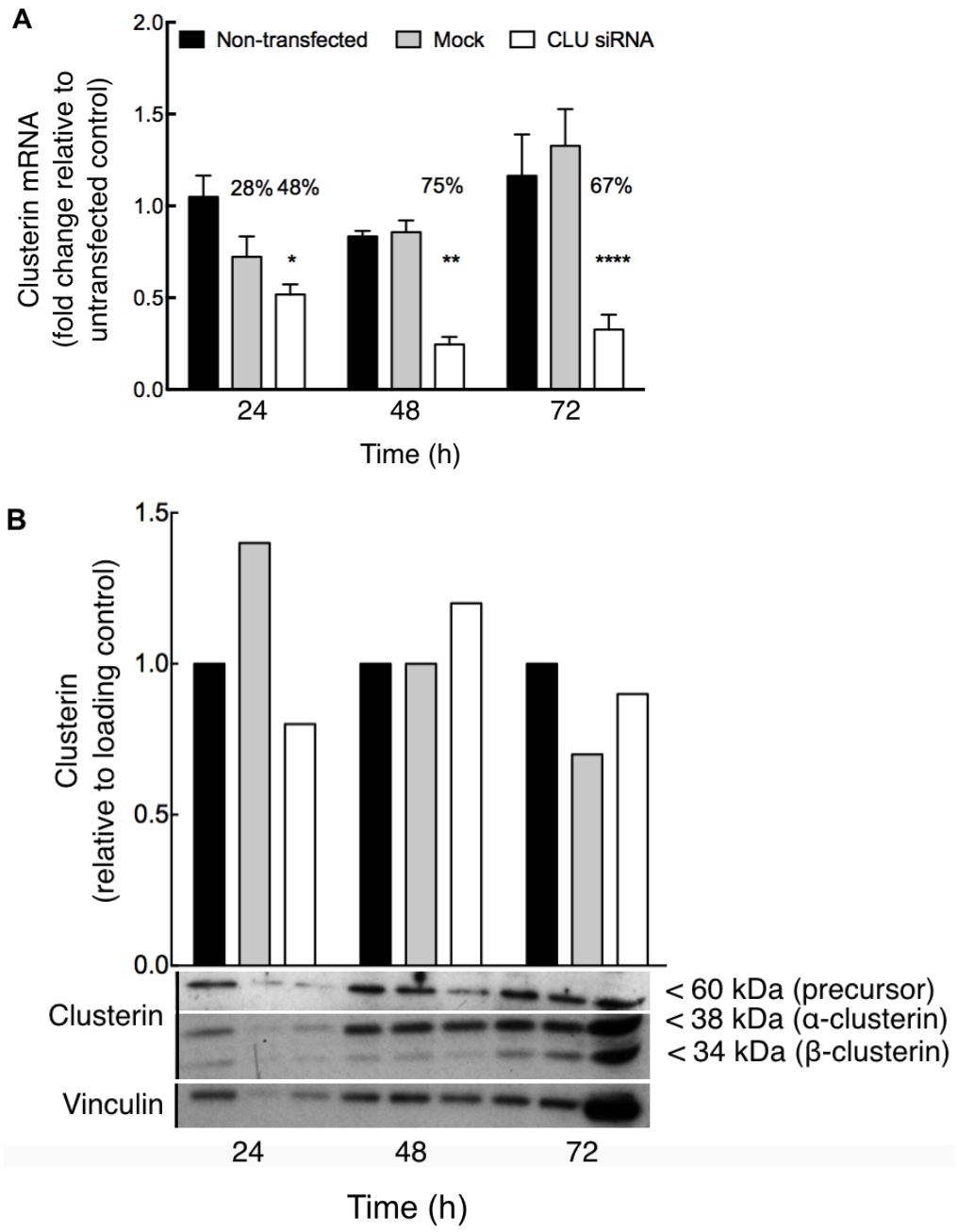

Figure 3.12 siRNA-mediated transfection of control lung fibroblasts down-regulated clusterin mRNA but not protein levels.

Fibroblasts were grown to 50 % confluence and transfected with siRNA targeting the clusterin gene or non-silencing siRNA or remained un-transfected. 24 -72 hours after transfection cells were lysed and clusterin mRNA and protein levels were assessed by qRT-PCR (A) and Western blot (B, α/βchain AB: sc-8354, semi-quantitative analysis). The mean ± SEM are shown for three experimental replicates for one representative cell line. This data is representative of two biological experiments; statistical significance was tested against clusterin expression of non-transduced cells. *P < 0.05, **P < 0.01, ****P < 0.0001.

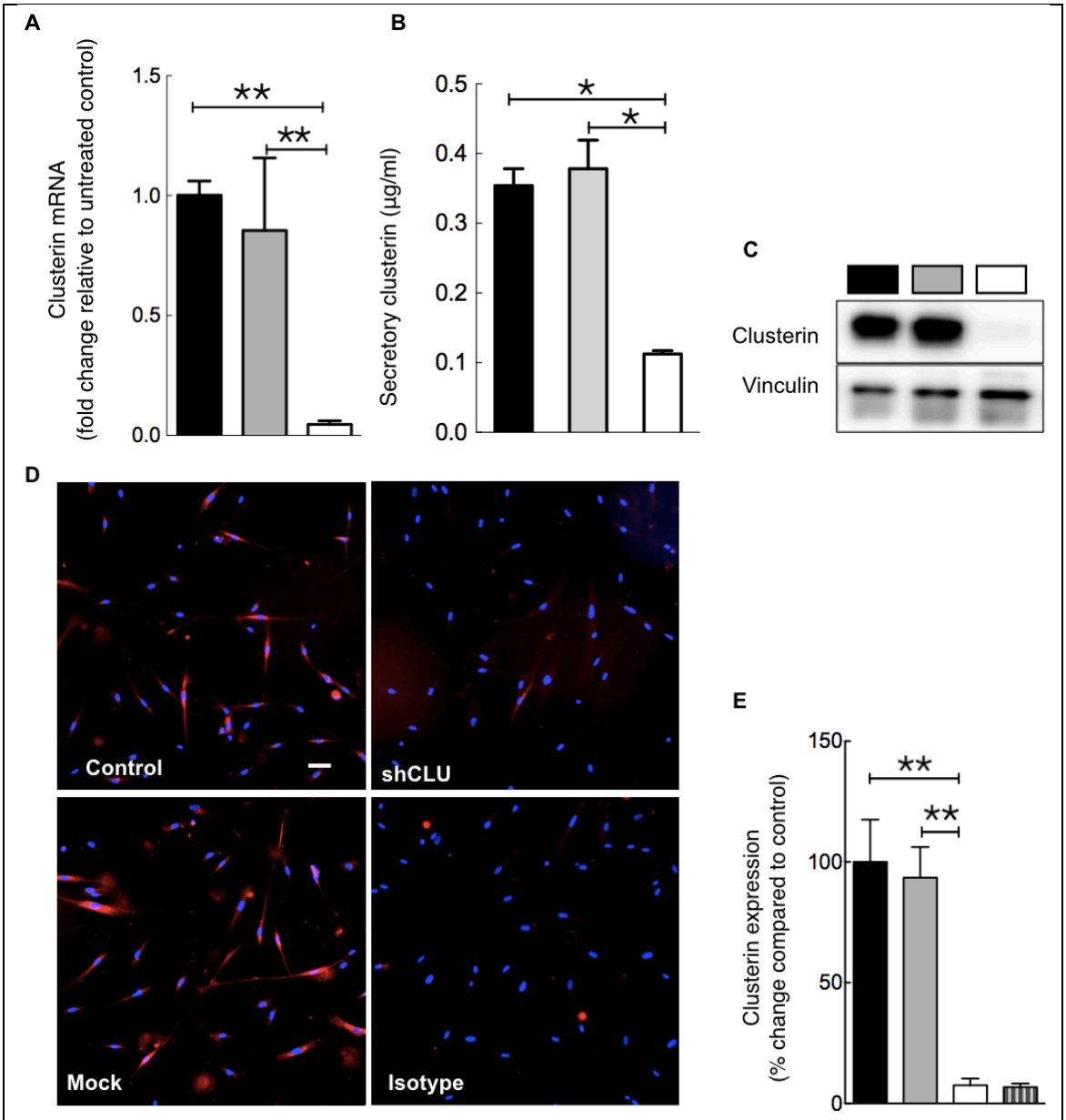

Figure 3.13 shRNA-modulated knockdown of clusterin in human normal lung fibroblast.

Clusterin gene and protein expression were silenced 48 hours post lentiviral transfection with shRNA targeting the clusterin gene (shCLU, open bars) compared with non-silencing (mock, grey bars) and non-transduced fibroblasts (control, black bars). qRT-PCR (A, n=3), ELISA of secretory clusterin (B), Western blot (C) and immunofluorescence staining (panel D, clusterin red (α-chain, sc-5289), nuclei - blue, n=3, quantitative analysis in E, isotype striped bar) confirmed low clusterin gene and protein expression in shCLU transfected fibroblasts. Scale bar in panel D represents 10 µm. *$P < 0.05$, **$P < 0.01$.

3.4.4 Effect of shRNA-mediated clusterin-deficiency on TGF-β_1-induced myofibroblast differentiation and collagen deposition.

In order to address whether clusterin-deficiency affects basal and TGF-β_1-induced αSMA and collagen mRNA and protein deposition, non-transduced control, mock-transduced and shRNA transduced clusterin-deficient fibroblasts were treated with or without TGF-β_1 (1 ng/ml) for 48 hours. Results in Figure 3.14 show that, although TGF-β_1 induced αSMA mRNA and protein in trend as assessed by qRT-PCR (Figure 3.14A) and Western blot analysis (Figure 3.14B), basal and induced αSMA levels did not show significant differences between control, mock and shCLU transduced fibroblasts. In detail αSMA mRNA were in trend induced by TGF-β_1 by 92.6 % for non-transduced shRNA, by 108,7 % for non-silencing shRNA and 89.9 % for shRNA targeting the clusterin gene.

As expected, TGF-β_1 significantly induced collagen I mRNA (Figure 3.14C) and protein deposition (Figure 3.15A,B) as assessed by qRT-PCR and immunofluorescent staining, respectively. However, there was no significant difference in response to TGF-β_1 between control, mock-transduced and shCLU fibroblasts. Which suggests that clusterin deficiency does not affect basal or TGF-β_1-induced collagen production. Collagen mRNA levels were increased by 9.5-fold for non-transduced shRNA and by 5.3-fold for non-silencing control and 4.8-fold for shRNA targeting the clusterin gene. Collagen deposition as assessed by fluorescence staining was increased by 2.07 ± 0.15 fold for non-transduced cells, 1.70 ± 0.28 fold for non-silencing shRNA induced cells and 1.94 ± 0.24 fold for fibroblasts transduced with shRNA targeting the clusterin gene (Figure 3.15B). The fold-increase in collagen deposition in response to TGF-β_1 was not significantly different between all groups although basal and TGF-β_1-induced deposited collagen levels diverged between clusterin deficient, mock and non-transduced fibroblasts.

This suggests that the observed TGF-β_1 induced down-regulation of clusterin is independent of its effect on myofibroblast differentiation, collagen synthesis, and deposition. The results are representative of two different experiments for fibroblasts from two donors.

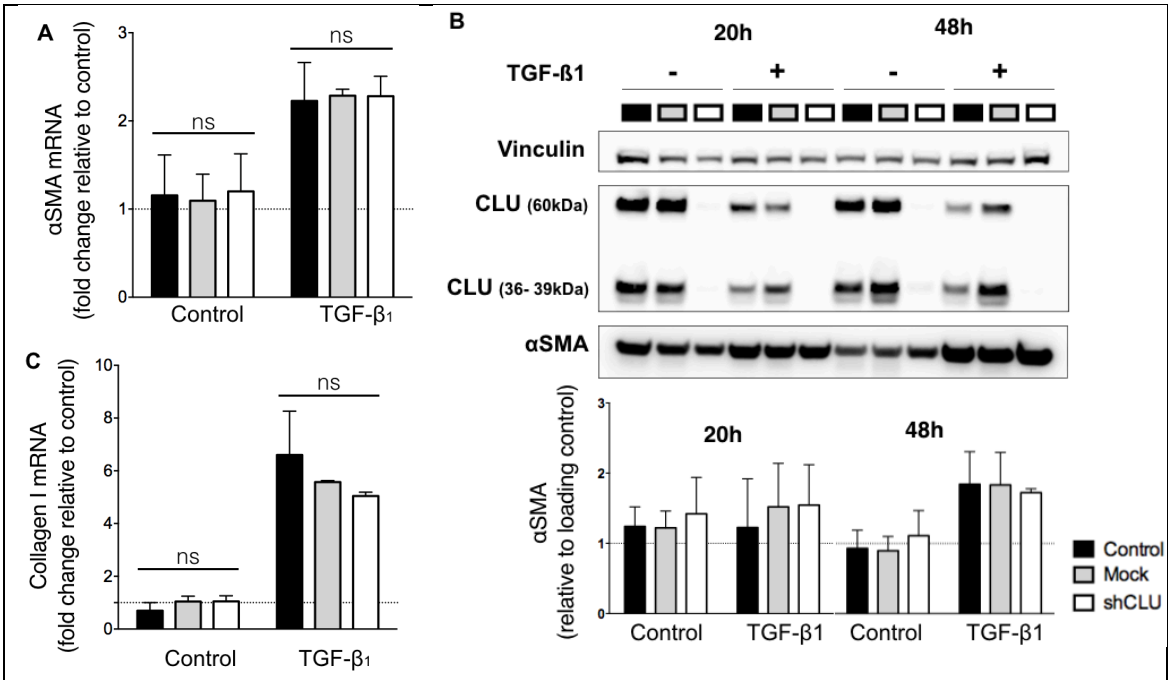

Figure 3.14 Effect of clusterin-deficiency on TGF-β_1-induced αSMA and collagen I mRNA and αSMA protein expression.

αSMA mRNA and protein and collagen mRNA levels were assessed in clusterin-deficient fibroblasts (open bars), mock-transduced (grey bars) and non-transduced control fibroblasts (black bars) 48 hours following TGF-β_1 stimulation (1ng/ml) and in untreated controls. qRT-PCR (A) and Western blot analysis (α-chain, sc-5289) (B) showed an increase of αSMA mRNA and protein post TGF-β_1 stimulation. Basal and increased levels of αSMA mRNA and protein, however, did not vary between clusterin-deficient, mock-transduced and control fibroblasts. Collagen mRNA (C) assessed by qRT-PCR was significantly increased in response to TGF-β_1. Although, basal and TGF-β_1 induced changes in collagen levels varied between clusterin-deficient, mock and control fibroblasts, the overall fold-increase in collagen mRNA levels did not significantly change between clusterin-deficient fibroblasts and control/mock fibroblasts. $^{**}P < 0.01$, $^{***}P < 0.001$, compared with untreated controls respectively.

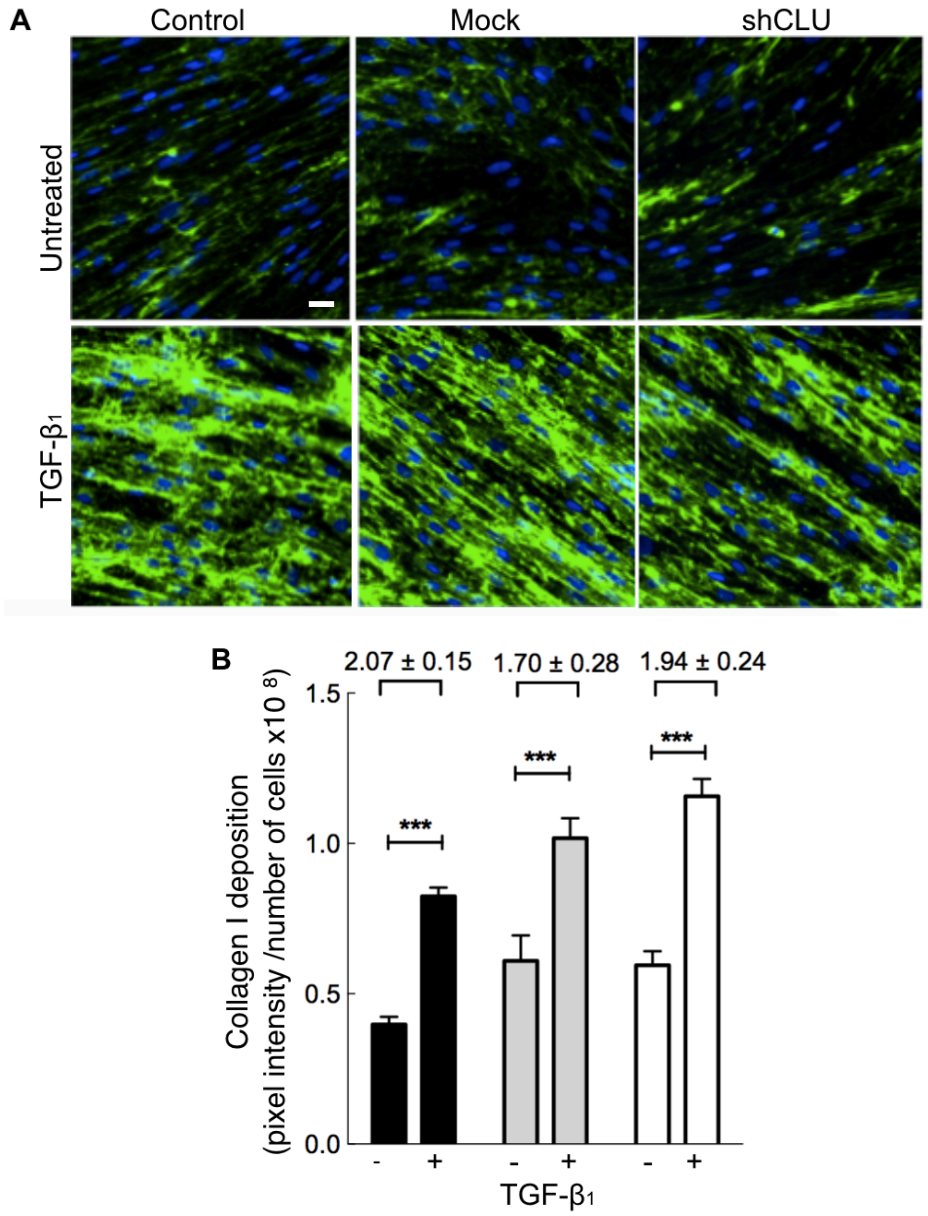

Figure 3.15 Effect of clusterin-deficiency on basal and TGF-β_1-induced collagen I deposition under molecular crowding conditions.

Clusterin-deficient fibroblasts (open bars), mock-transduced (grey bars) and non-transduced control fibroblasts (black bars) were grown to confluence, serum starved (0.4 % FBS) overnight. Ficoll, ascorbic acid and TGF-β_1 (1 ng/ml) were added for 48 hours. Collagen I deposition (A, B quantification) assessed by immunofluorescence staining was significantly increased in response to TGF-β_1. Although, basal and TGF-β_1 induced changes in collagen levels varied between clusterin-deficient mock and control fibroblasts, the overall fold-increase in collagen I deposition levels did not significantly change between clusterin-deficient fibroblasts and control/mock fibroblasts. Scale bar in A represents 10 µm. ***P < 0.001 compared with untreated controls respectively.

3.4.5 Summary

The results in this section have examined the consequences of clusterin gene silencing on TGF-β_1-induced lung fibroblast differentiation into myofibroblast. αSMA expression and collagen deposition were established as myofibroblast markers under standard and crowding cell culture conditions. The principle findings of these experiments are;

- Increasing αSMA protein expression in response to TGF-β_1 is time dependant and was increased by approximately 10-fold by 48 hours and 72 hours.

- Cell culture of lung fibroblasts under molecular crowding conditions demonstrated similar TGF-β_1 effects on αSMA protein expression compared with standard culture conditions at 72 hours.

- The effect of TGF-β_1 on control lung fibroblast collagen deposition and αSMA protein expression is dose dependent.

- Clusterin protein levels can be reduced by a stable knockdown of clusterin via shRNA, while transient gene silencing with siRNA resulted in a reduction of clusterin mRNA but not protein levels.

- Stable shRNA-induced clusterin-deficiency does not affect levels of basal or TGF-β_1-induced αSMA and collagen I mRNA and protein and collagen I deposition, when compared with untreated mock controls.

In summary, this section assessed the effect of low clusterin expression on TGF-β_1-induced fibroblast differentiation *in vitro*. The results presented in this section suggest that the TGF-β_1-induced downregulation of clusterin is independent of its effect on fibroblast differentiation. The next section will address if altered intra- or extracellular clusterin levels affect lung fibroblast migration.

3.5 Role of clusterin in modulating fibroblast migration *in vitro*

3.5.1 *In vitro* assessment of migration in clusterin-deficient fibroblasts compared with control fibroblasts in response to TGF-β_1 in a scratch assay.

Clusterin has been demonstrated to induce chemotaxis of human monocytes, murine macrophages (Kang et al. 2014) and porcine vascular smooth muscle cells (Millis et al. 2001). However, little is known about the role of clusterin in regulating migration of lung fibroblasts. To assess the effect of clusterin-deficiency on migration under basal conditions (0.4 % FBS in DMEM) or in response to TGF-β_1, a scratch assay was performed with non-transduced, mock-transduced and clusterin-deficient fibroblasts. For this purpose, cells were seeded in a 96-well plate and grown to confluence for 24 hours, as described in section 2.16. Subsequently, the cell monolayer was disrupted with a 96-needle device (Wound Maker™) creating a scratch of approximately 800 µm width in each well. In order to ensure that all detached cells are fully removed from the scratch area, needles in each well were moved up and down vertically in line with the scratch area three times. Detached cells were washed away, and cells in the wells remained untreated or were stimulated with TGF-β_1 (5 ng/ml) in 0.4 % FBS in DMEM.

Figure 3.16 demonstrates that under basal conditions the scratch was closed at similar time-points (non-transduced: 22 ± 2 hours, mock transduced 25.6 ± 2 hours and clusterin-deficient fibroblast 24 ± 2 hours, mean ± SEM) for all cell lines tested. Since there were no significant changes measurable between times of scratch closure of untransduced and mock-transduced cells, all subsequent experiments were conducted with mock-transduced fibroblasts as a control.

Interestingly, when TGF-β_1 was added to the culture medium after initiating the scratch the time needed for migrating cells to close the scratch increased in control fibroblast (from 25.6 ± 2 to 36 ± 2 hours). However, in clusterin-deficient fibroblasts the time required to close the scratch remained unchanged when compared with clusterin-deficient fibroblast without TGF-β_1 (27 ± 1.8 hours). This suggests that clusterin is important for a delay in migration in response to TGF-β_1.

Given the duration of the measurements of up to 48 hours, caution needs to be applied in interpreting differences between clusterin-deficient fibroblast and control fibroblast. At 48 hours migratory as well as proliferative effects in both cell lines may affect the duration of scratch closure. In order to limit proliferative effects, migration was assessed via directed transwell migration assays, which were limited to the duration of 19 hours (see next subsection, 3.5.2).

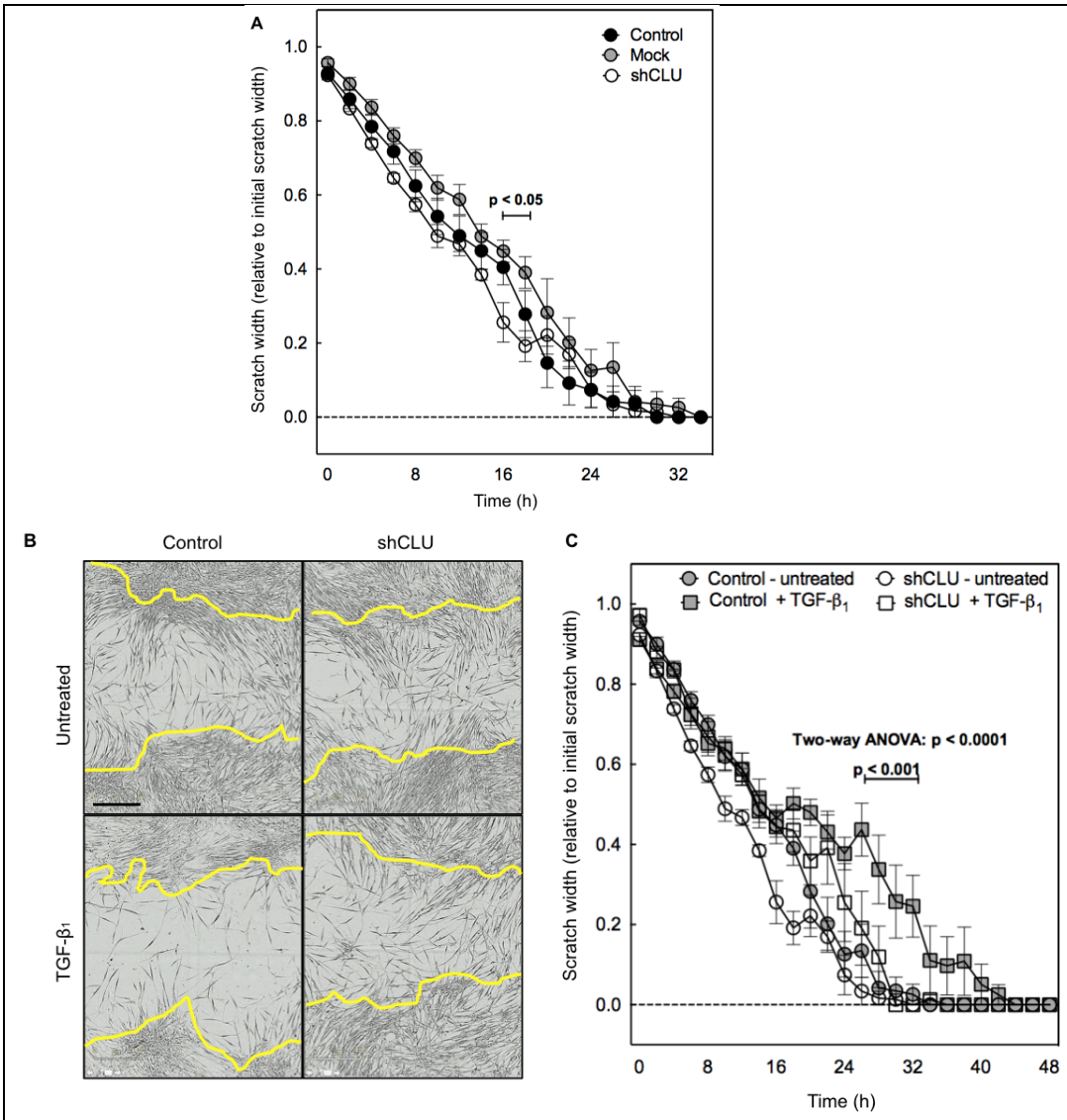

Figure 3.16 Migratory response of control and clusterin-deficient lung fibroblasts at baseline and in response to TGF-β_1.

Fibroblasts were seeded at 12 x 10^3 cells per well in a 96-well plate, grown to 80 % confluence and 800 µM wide scratches were applied via a 96-needle device. The migratory / proliferative response was captured 0 – 48 hours using phase-contrast microscopy. (A) Baseline migration did not vary between untransduced (control) fibroblasts, mock-transduced (mock) and clusterin-deficient (shCLU) lung fibroblasts. (B) Representative images of the scratch closure in control and clusterin-deficient fibroblasts at 28 hours (yellow lines: scratch edges at 0 h) in response to TGF-β_1 (5 ng/ml) compared with control (0.4% FBS in DMEM). (C) Time course demonstrating the decrease of scratch width in response to TGF-β_1 at 0 – 48 hours. The rate of scratch closure was defined as the scratch width at a particular time point divided by the initial scratch width. Data is representative of two individual experiments. Each point represents the mean +/- SEM of 6 replicates; scare bar in (B) 400 µm.

3.5.2 *In vitro* assessment of human lung fibroblast migration in response to PDGF-BB or TGF-β_1 in a Transwell® assay.

To determine the effect of clusterin-deficiency on migration in response to PDGF-BB or TGF-β_1 or exogenous clusterin, a transwell migration assay was established (Section 2.17). Previous reports demonstrated that PDGF-BB is one of the most potent inducers of fibroblast migration. Consistent with previous reports (Bonner et al. 1995; Osornio-Vargas et al. 1993; Tada et al. 2003), PDGF-BB significantly increased lung fibroblast migration and reached a maximal response at the lowest dose of 12.5 ng/ml (Figure 3.17A). At 25 ng/ml, an approximately 3 fold higher migration was induced when compared with un-stimulated controls. To assess the responsiveness of human lung fibroblasts to increasing cell numbers in combination with 25 ng/ml PDGF-BB or no PDGF-BB, experiments using fibroblasts derived from control lung tissue were undertaken (Figure 3.17C). Although, the yield of migrated cells could be increased at cell numbers larger than 50 x 10^3 cells/ well, a number of 50 x 10^3 cells/ well was chosen for all experiments presented here since this number of cells allowed the cells to adhere as monolayer to the transwell membrane. In addition, these results present evidence that the capacity to induce migration by 25 ng/ml PDGF-BB in fibroblast is not saturated at cell numbers over 50 x 10^3 cells/ well. In order to exclude the effect of increasing cell numbers as a consequence of proliferation in response to PDGF-BB (Blanc-Brude et al. 2001), while allowing maximal time for migration, the duration of this experiment was set to 18 h after addition of lung fibroblasts and stimuli to the upper chamber compartment of the transwell insert. In accordance with previous reports TGF-β_1 did not affect chemotaxis (Osornio-Vargas et al. 1993), as demonstrated in Figure 3.17D.

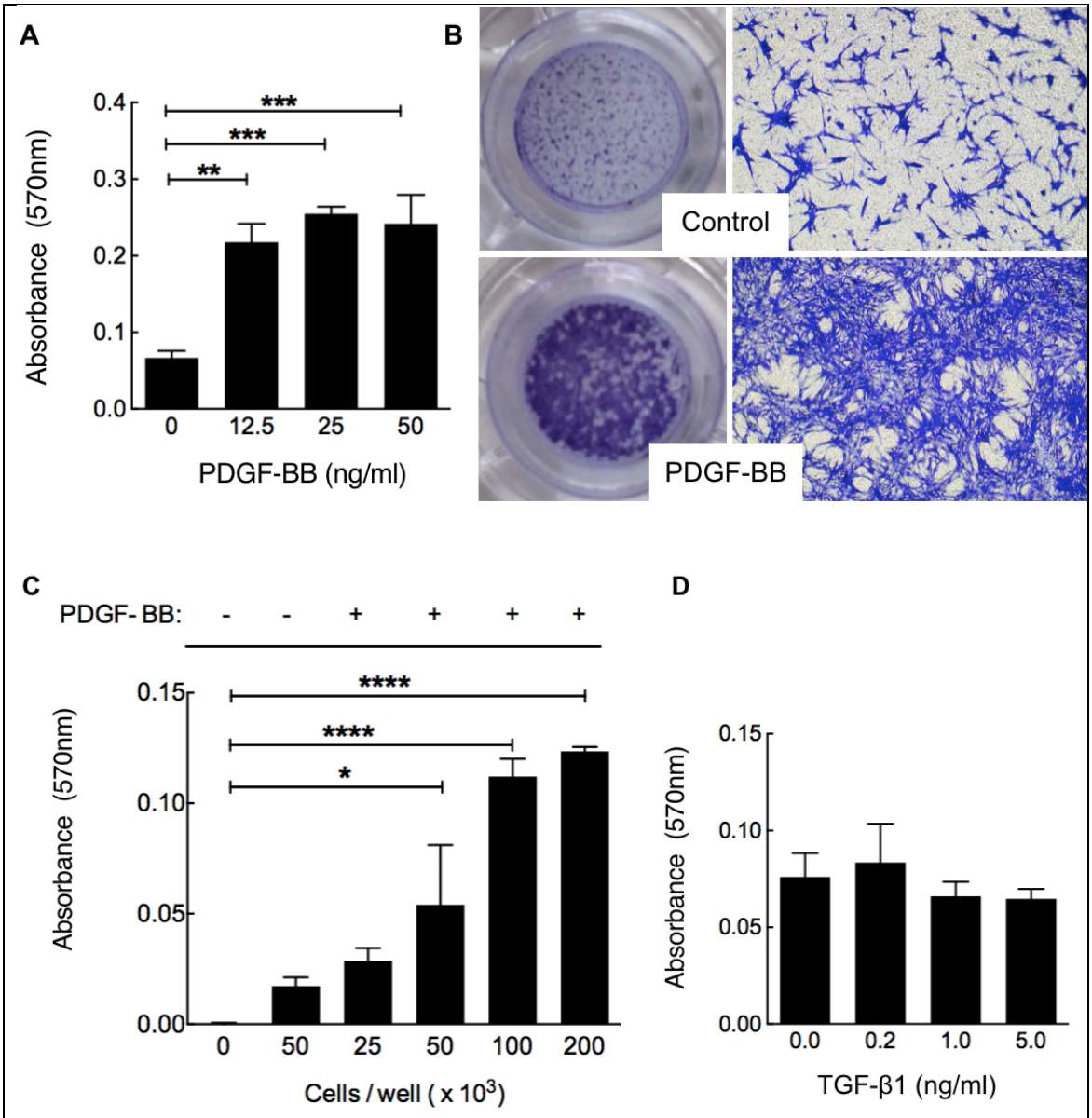

Figure 3.17 PDGF-BB induced fibroblast migration is concentration dependent.

Control fibroblasts were exposed to doubling doses of recombinant PDGF-BB from 0 - 50 ng/ml (A) for 18 hours in 0.4 % FBS in DMEM. (B) Representative bright field images of crystal violet-stained migratory fibroblasts on transwell polycarbonate membranes, showing a three fold change increase in migration in response to 25 ng/ml PDGF-BB compared with un-stimulated controls. (C) Shows that the number of cells that migrated through the membrane was dependent on the initial cell number seeded and could be induced by the addition of 25 ng/ml PDGF-BB. (D) Shows migratory response to TGF-β_1 in five fold increasing doses from 0 – 5 ng/ml. Quantification of migrated cells via crystal violet elution and spectrophotometric analysis of the absorbance at 570 nm. Data represent mean ± SEM of ≥ 2 independent experiments. *P < 0.05, **P < 0.01, ***P < 0.001, ****P < 0.0001.

3.5.3 Clusterin-deficiency or exogenous clusterin do not affect fibroblast basal and induced migration in control lung fibroblasts.

Since lung fibroblasts secrete clusterin (Figure 3.13B) at concentrations known to induce migration in other cell types the effects of clusterin-deficiency or addition of exogenous clusterin in lung fibroblast migration was examined. Transwell migration assays were conducted with control (mock-transduced), shRNA-mediated clusterin-deficient and fibrotic lung fibroblasts in response to PDGF-BB, TGF-β_1 or exogenous human plasma-derived clusterin. Results in Figure 3.18A show that exogenous clusterin did not affect chemotaxis in clusterin-deficient lung fibroblasts compared with controls. Furthermore, basal migration in clusterin-deficient and fibrotic lung fibroblasts did not differ when compared with untreated controls or in response to PDGF-BB and TGF-β_1. In the non-silencing shRNA group PDGF-BB induced migration by 3.9 ± 0.2 fold. In the group with shRNA targeting the clusterin gene migration in response to PDGF-BB was increased by 3.5 ± 0.0 fold. Together, these data suggest clusterin does not mediate chemotaxis in control or fibrotic lung fibroblasts *in vitro*.

3.5.4 Low clusterin expression or exogenous clusterin do not affect basal and induced migration in fibrotic lung fibroblasts.

To compare consequences of clusterin-deficiency on migration to those observed in fibrotic lung fibroblast with naturally low levels of clusterin (Figure 3.7) fibrotic lung fibroblast migration was assessed in response to PDGF-BB, TGF-β_1 or exogenous human plasma-derived clusterin and compared with fibroblast derived from control lung tissue (Figure 3.18B). Consistent with results derived with shRNA-induced clusterin-deficient fibroblasts, fibrotic lung fibroblast migration was not affected by exogenous clusterin. Furthermore, basal migration in fibrotic lung fibroblasts did not differ when compared with untreated controls or in response to PDGF-BB and TGF-β_1. Together, these data suggest clusterin does not mediate migration in control or fibrotic lung fibroblasts *in vitro*.

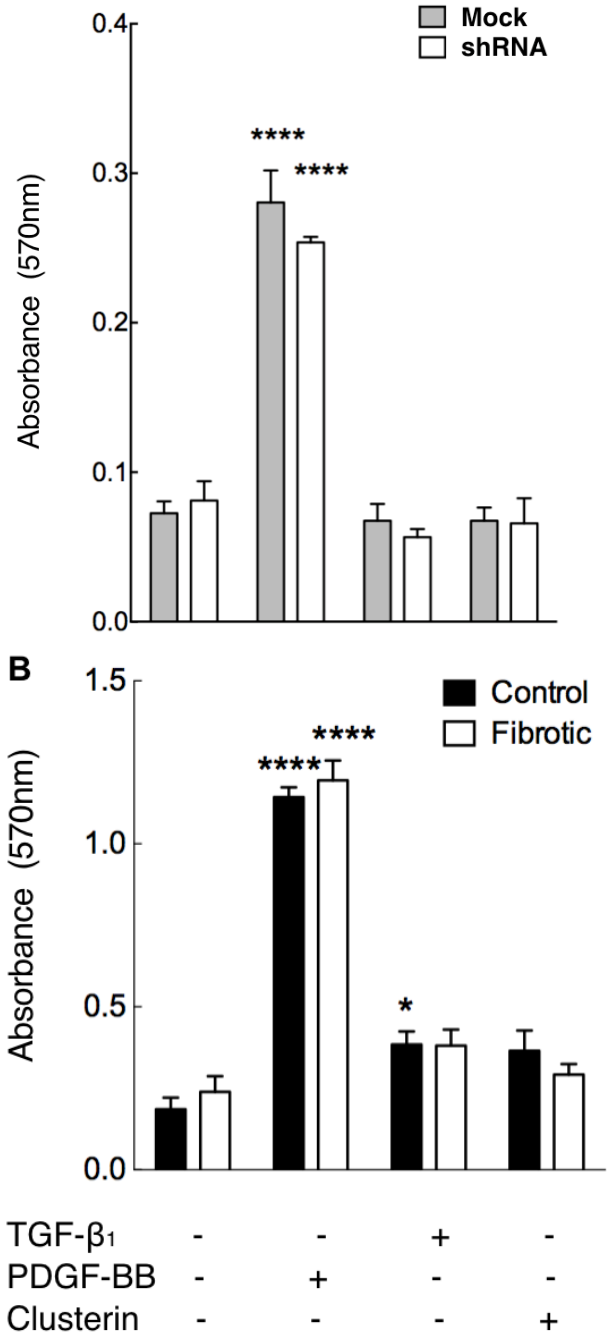

Figure 3.18 Exogenous clusterin and low intracellular clusterin do not affect lung fibroblast migration in control and fibrotic fibroblasts.

The migratory responses of mock-transduced and untransduced fibroblasts did not show significant differences, migratory responses of clusterin-deficient fibroblasts were compared with mock-controls only. Comparison of migratory response in mock-transduced (control) compared with shCLU deficient fibroblasts (A) and control fibroblasts to fibrotic lung fibroblasts (B) in response to no stimuli or PDGF-BB (25 ng/ml), TGF-β_1 (1 ng/ml) and exogenous, human plasma-derived clusterin (10 µg/ml). Quantification of migrated cells via violet elution and spectrophotometric analysis of the absorbance at 570nm. Data represent mean ± SEM of two independent experiments. *P < 0.05, ****P < 0.0001.

3.5.5 Summary

The results in this section examining the in vitro migratory response of clusterin-deficient control and fibrotic lung fibroblasts to basal, PDGF-BB, TGF-β_1 and exogenous clusterin demonstrate;

- The migratory response of control lung fibroblasts in response to PDGF-BB was increased at a concentration from 12.5 ng/ml by approximately 3-fold.

- The migratory response of control lung fibroblasts correlated with increased numbers of cells placed in the upper compartment of the transwell insert. A cell number of 50 x 10^3 cells resulted in a cell monolayer, covering the upper side of the transwell membrane.

- Exogenous clusterin did not affect chemotaxis in clusterin-deficient or fibrotic lung fibroblasts compared with controls.

- Basal migration in clusterin-deficient and fibrotic lung fibroblasts did not differ when compared with untreated controls or in response to PDGF-BB and TGF-β_1.

Effects observed in the scratch assay in response to TGF-β_1 are most likely not due to a difference in migration. An alternative hypothesis is that different effects on scratch closure in response to TGF-β_1 observed for clusterin-deficient fibroblasts compared with controls was due to altered proliferation. This possibility will be explored in the next section.

3.6 Role of clusterin in modulating fibroblast proliferation *in vitro*

Previous studies have indicated that clusterin promotes proliferation of renal tubular epithelial and vascular smooth muscle cells after injury (Nguan et al. 2014; Miyata et al. 2015). But the role of clusterin in regulating fibroblast proliferation remains unknown.

3.6.1 Clusterin-deficiency reduces the proliferative response in control fibroblasts.

To explore the impact of clusterin-deficiency on basal and induced proliferation, control, mock-transduced and clusterin-deficient fibroblasts were seeded in 96-well plates as described in section 2.14.3. After adhering overnight, and ensuring identical cell numbers per well among different groups for each experiment (Figure 3.19A, 4 x 10^3 cells / well), fibroblasts were exposed to increasing concentrations of serum, TGF-β_1 or PGE_2 and proliferation was quantified via DAPI staining as assessed by immunocytochemistry (detailed in section 2.14.2). Non-transduced and mock-transduced primary fibroblasts did not show a difference in their proliferative response. On this basis, results are shown for mock-transduced and clusterin-deficient cells only.
Data presented in Figure 3.19 and Figure 3.20 is expressed as percent change in cell numbers at a given time relative the cell numbers of controls for each time point. However, in the text this data is presented as absolute change in cell number per visual field (mean ± SEM).
Figure 3.19B shows that the rate of proliferation seen in response to serum was increased from 2.5 % serum in DMEM (Two way ANOVA $P < 0.0001$). The cell number of mock-transduced control cells per field (98.3 ± 4.43 cells mean ± SEM) was similar to cell numbers of clusterin-deficient fibroblasts (98.3 ± 3.16 cells mean ± SEM) after 72 hours in 0.4 % FBS in DMEM. High-serum significantly increased proliferation of mock-control and clusterin-deficient fibroblasts. However, the response to serum-induced proliferation was diminished by approximately 50 % in clusterin-deficient fibroblasts compared with controls (Figure 3.19B, mock 241,9 ± 9.71 and clusterin-deficient 169.65 ± 4.32; mean ± SEM) for 10 % FBS in DMEM. TGF-β_1 did not affect the proliferative response in control or clusterin-deficient fibroblasts (Figure 3.19C). In contrast, PGE_2 reduced proliferation in clusterin-deficient fibroblasts in trend compared with control (Figure 3.19D), resulting in 68.5 ± 0.76 (mock) versus 51.5 ± 3.49 cells (shCLU) per visual field (mean ± SEM) 48 hours after addition of 1 µM PGE_2. A summary of this data compared with the proliferative response is shown in Figure 3.20.

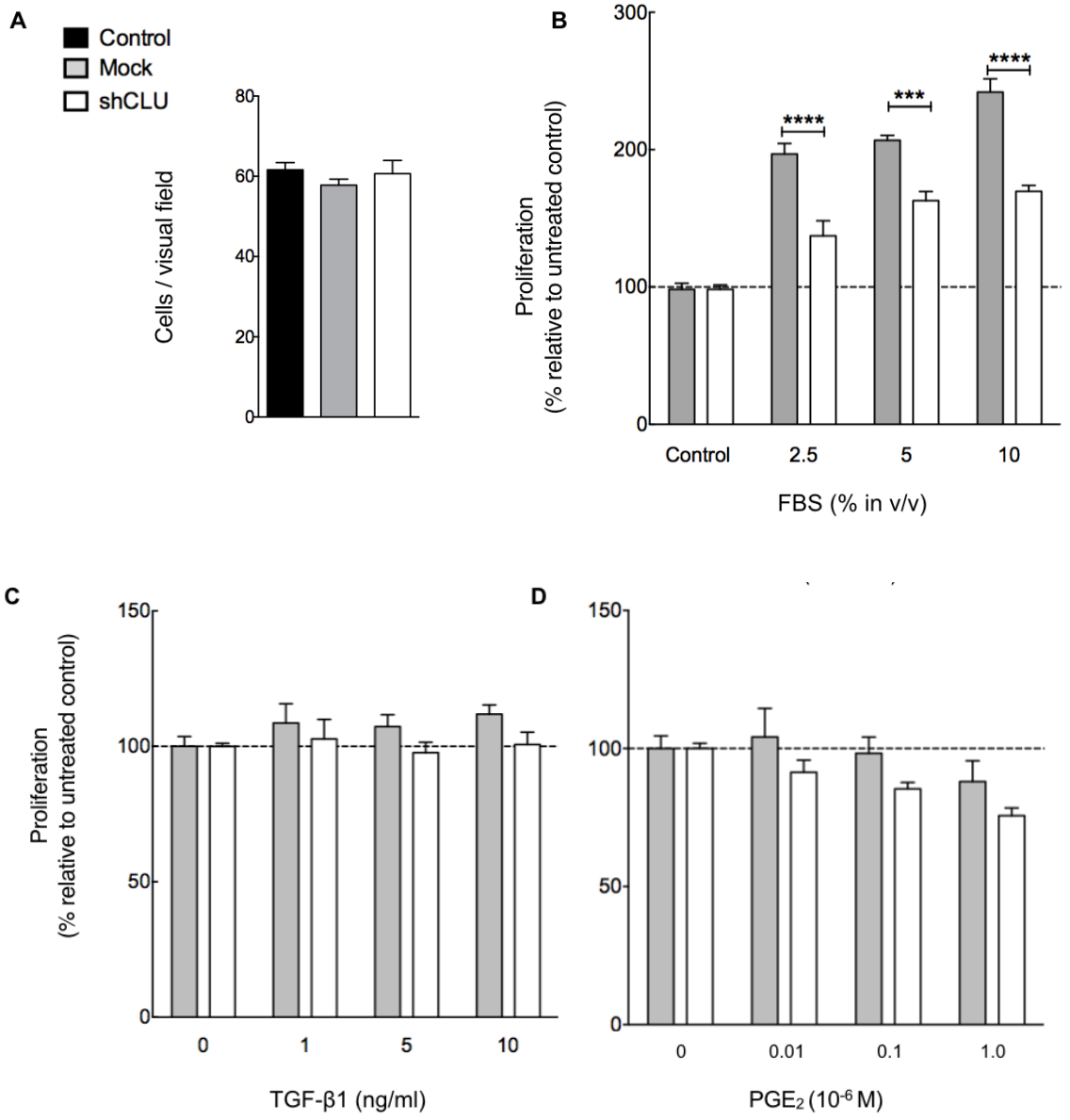

Figure 3.19 Effect of clusterin-deficiency on control lung fibroblast proliferation.

Clusterin-deficient (open bars), mock-transduced (grey bars) and non-transduced control lung fibroblasts (black bars) were seeded at a density of 4 x 10^3 cells per well in 96 well plates and allowed to adhere overnight in 0.4 % FBS in DMEM. Thereafter cell numbers were counted on a separate 96-well plate to ensure similar cell numbers among the groups (A). Cell numbers were assessed in four fields per well (n=6) by counting DAPI-positive nuclei in a high-throughput immunofluorescence assay. Proliferation in shRNA-mediated clusterin-deficient fibroblasts compared with controls was assessed in response to indicated concentrations of FBS (B), TGF-β_1 (C) and PGE_2 (D) at 48 hours (or 72 hours for FBS) in 0.4 % FBS in DMEM. Cell numbers were normalised to cell counts of low serum controls (0.4 % FBS in DMEM) and expressed as percent change in proliferation relative to control. Data represent mean ± SEM of three independent experiments. ***P < 0.001, ****P < 0.0001.

3.6.2 Exogenous clusterin does not affect lung fibroblast proliferation *in vitro.*

To determine if low intracellular or extracellular clusterin levels account for a reduced proliferative response in clusterin-deficient fibroblast, both mock-controls and clusterin-deficient fibroblast from control lungs were subjected to human plasma-derived clusterin for 48 hours. Interestingly, exogenous clusterin did not affect fibroblast proliferation in control or clusterin-deficient fibroblasts (Figure 3.20A). Together, these data suggest that endogenously generated intracellular clusterin but not exogenous clusterin is involved in promoting fibroblast proliferation.

3.6.3 Fibrotic lung fibroblasts display a hyperproliferative phenotype, despite low clusterin levels.

The response to the same mediators was also compared between control and fibrotic lung fibroblasts, which express low levels of clusterin (Figure 3.20B). Under low serum conditions (control 0.4% FBS in DMEM) control lung fibroblast numbers remained steady over time when comparing average cell numbers per visual field (0h: 70.5 ± 1.9 cells, 48 h 70.9 ± 2.5 and at 72 h 66.3 ± 4.2). By contrast numbers of fibroblasts from fibrotic lung increased under low serum conditions over time (0h: 85.1 ± 3.1 cells, 48 h 119.5 ± 1.8 and at 72 h 103.5 ± 5.5). However, in contrast to shRNA-mediated clusterin-deficient fibroblasts, naturally, clusterin-deficient fibrotic lung fibroblasts exhibited a greater proliferative response than controls.
At 48 hours, enhanced serum levels (10 % FBS in DMEM) increased cell numbers of fibroblasts from control lung from 121.4 ±1.9 cells/field when compared with numbers at low serum controls (70.9 ± 2.5). By contrast, numbers of fibroblast from fibrotic lung were increased from 119.5 ± 1.8 at low serum to 182.2 ± 2.6 at high serum conditions. This difference may be associated with changes in fibrotic lung fibroblasts unrelated to diminished clusterin expression. Moreover, fibrotic lung fibroblasts displayed a proliferative response to TGF-β_1 compared with untreated and non-fibrotic controls.

3.6.4 PGE_2 reduced measurable cell numbers of fibrotic lung fibroblasts and clusterin-deficient fibroblasts after 48 hours.

Consistent with shRNA-mediated clusterin-deficiency, PGE_2, but not exogenous clusterin, reduced measurable cell numbers of fibrotic lung fibroblasts 48 hours after administration of PGE_2 (Figure 3.19D and Figure 3.20A,B). After 48 hours of exposure to PGE_2 control fibroblasts numbers were reduced in trend to 111.5 ± 3.1 cells in the

presence of PGE_2 when compared with cell numbers of controls 121.4 ± 5.3. By contrast, this difference was significant for fibrotic lung fibroblasts, were cell numbers were reduced in the presence of PGE_2 146.6 ± 3.2 when compared with controls 182.2 ± 2.6 (Figure 3.20B).

Reduced cell numbers in response to PGE_2 may either be caused by reduced proliferation or induced apoptosis. To test if reduced cell numbers in response to PGE_2 do not only result from growth arrest (Fine & Goldstein 1987) but potentially from PGE_2-induced apoptosis, primary lung fibroblasts from control lung were subjected to increasing concentrations of PGE_2. Consistent with previous reports (Huang et al. 2009) in lung fibroblasts, PGE_2 induced apoptosis in a dose and time dependent manner (One way ANOVA P = 0.0326, Figure 3.21A). The data is expressed as percent change in apoptosis compared with baseline level of apoptosis for each time point (e.g. 19 hours 20.8 ± 1.17 %). Increasing doses and times of PGE_2 treatment resulted in a significant increase in apoptosis compared with untreated fibroblasts (Figure 3.21A, B).

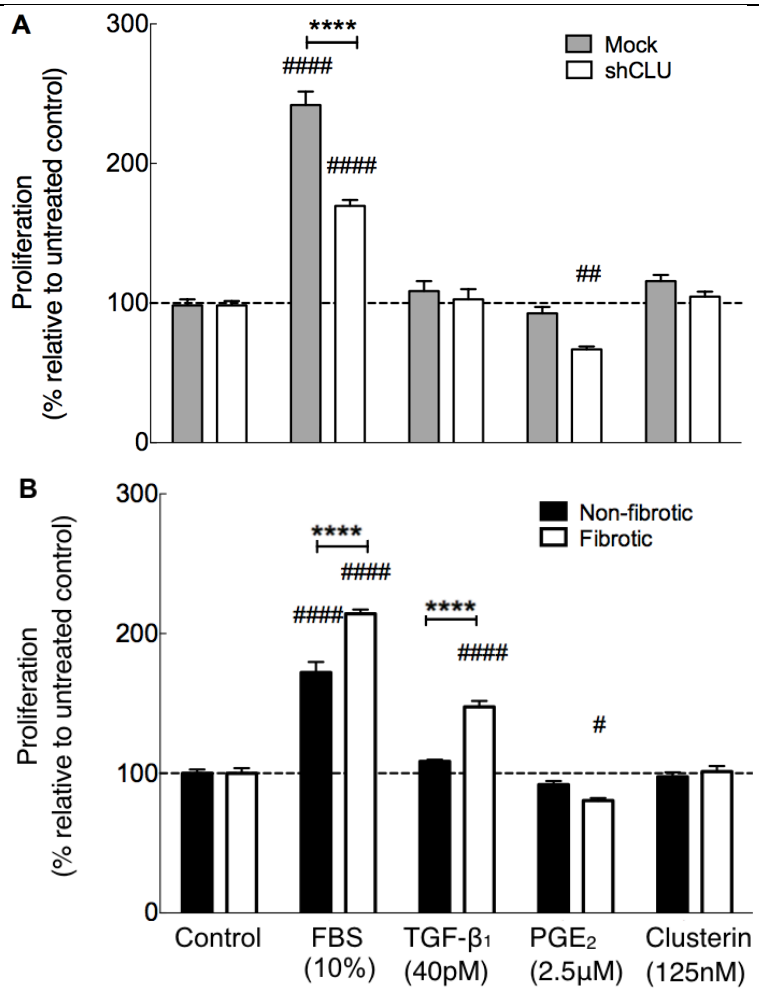

Figure 3.20 Effect of clusterin-deficiency on lung fibroblast proliferation.

Proliferation in shRNA-mediated clusterin-deficient fibroblasts (A) or fibrotic lung fibroblasts (B) compared with controls was assessed in response to the indicated stimuli for 48 hours (72 h for FBS) by counting DAPI-positive nuclei in a high-throughput immunofluorescence assay. Cell numbers were normalised to cell counts of low serum controls (0.4 % FBS in DMEM) and expressed as percent change in proliferation relative to control (n=6,). Significances compared with untreated controls are marked with (#) symbol and significances between controls vs. shCLU or non-fibrotic vs. fibrotic are indicated with (*). */# P < 0.05, **/ ## P < 0.01, ***/### P < 0.001, ****/#### P < 0.0001.

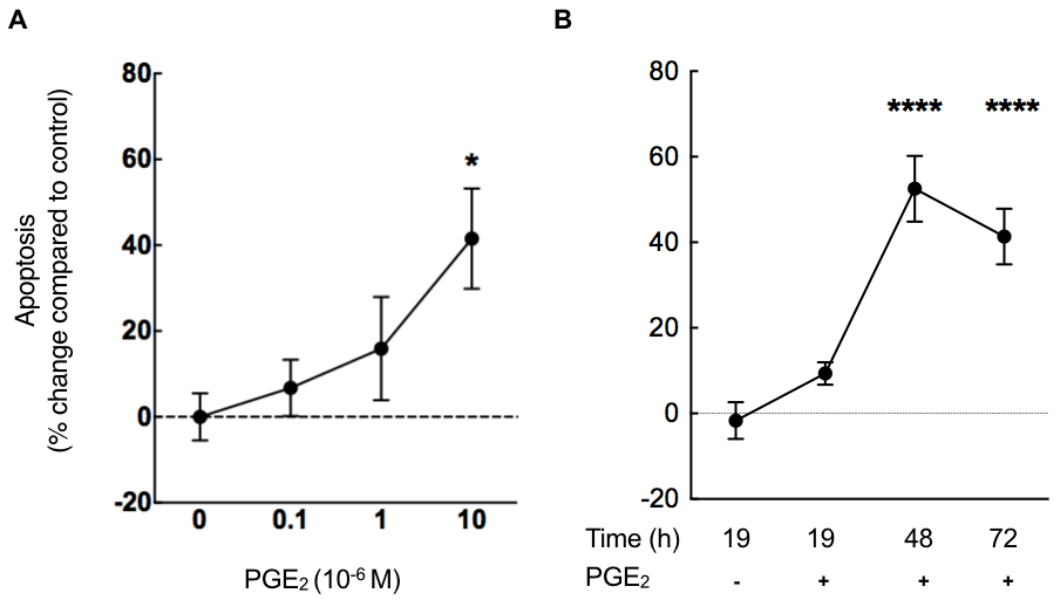

Figure 3.21 PGE_2 induced apoptosis is time and concentration dependent in control lung fibroblasts.

(A) Control fibroblasts were exposed to increasing doses of PGE_2 for 19 hours (B) for 19 hours to 72 hours at 10^{-6} M in 5 % FBS in DMEM. Apoptosis was determined by Annexin V/DAPI staining with FACS analysis. The data is expressed as change apoptosis compared with baseline level of apoptosis measured in untreated control cells for each time point. Each point represents the mean ± SEM (n=6). *P < 0.05, ****P < 0.0001 compared with untreated controls respectively.

3.6.5 Summary

The results in this section examining the *in vitro* proliferative response to high-serum, TGF-β_1 and PGE_2 in clusterin-deficient and fibrotic compared with control fibroblasts. The principle findings of these experiments are;

- Serum significantly increased proliferation of control and clusterin-deficient fibroblasts. In clusterin-deficient fibroblasts, serum-induced proliferation was diminished by approximately 50 % compared with controls.

- TGF-β_1 did not affect the proliferative response in control or clusterin-deficient fibroblasts.

- PGE_2 significantly reduced proliferation in clusterin-deficient and fibrotic fibroblasts compared with controls.

- Exogenous clusterin did not affect fibroblast proliferation in control, clusterin-deficient or fibrotic lung fibroblasts.

- Naturally, clusterin-deficient fibrotic lung fibroblasts exhibited a greater proliferative response to FBS than controls.

- Fibrotic lung fibroblasts displayed a proliferative response to TGF-β_1 compared with untreated and non-fibrotic controls.

- PGE_2 induces apoptosis in control lung fibroblasts in a dose and time dependent manner.

Together, this section suggests that in control lung fibroblasts clusterin-deficiency results in a decreased proliferative response, while exogenous clusterin did not affect proliferation. This suggests that intracellular rather than extracellular levels of clusterin are involved in regulating lung fibroblast proliferation. As TGF-β_1 did not affect fibroblast migration or proliferation it is still uncertain why TGF-β_1 delayed scratch closure in control but not in clusterin-deficient fibroblasts.

3.7 Role of clusterin lung fibroblast apoptosis

Clusterin has been associated with reduced apoptosis in prostate cancer cells (Zhang et al. 2005) and has been suggested to induce apoptosis in synoviocytes of RA joints (Devauchelle et al. 2006). In the present study, we sought to assess the role of clusterin in lung fibroblast apoptosis *in vitro* by investigating the effects of clusterin-deficiency and exogenous clusterin on FasL- induced apoptosis in control and fibrotic lung fibroblasts. We and others have previously demonstrated that fibrotic lung fibroblasts are more resistant to FasL-induced apoptosis when compared with control fibroblasts (Maher et al. 2010; Moodley et al. 2004). In order to determine the response of human lung fibroblasts to FasL-induced apoptosis, dose and time course experiments were conducted.

3.7.1 FasL- induced apoptosis of primary lung fibroblasts is dose dependent.

Fibroblasts were exposed to doubling concentrations of FasL from 25 ng/ml up to 200 ng/ml for 19 hours (Figure 3.22A) and apoptosis was quantified by Annexin V/ DAPI staining and flow cytometry as described in section 2.20. The proportion of apoptotic, untreated control cells was 24.17 ± 1.60 % (mean ± SEM). The proportion of apoptosis seen in response to FasL was dose dependent, increasing significantly in a near linear way with each dose doubling (One-way ANOVA = 0.0003).
At a dose of 100 ng/ml, FasL-induced apoptosis was increased by 31.31 ± 7.28 % when compared with untreated cells ($P < 0.01$), this rose to 48.98 ± 6.10 % at a FasL dose of 200 ng/ml ($P< 0.001$). On the basis of these results and previous studies in our lab a dose of 100 ng/ml (≈ 3.18 nM) was used for all subsequent experiments.

3.7.2 FasL- induced apoptosis of primary lung fibroblasts is time dependent.

Using a dose of FasL of 100 ng/ml, the effect of exposure to FasL on fibroblast apoptosis was determined at time points between 19 and 72 hours (Figure 3.22B). By 19 hours the number of apoptotic cells increased by 17.40 ± 5.28 % and increased further by 36.37 ± 7.86 % at 48 hours compared with untreated time matched cells. However, at 72 hours the proportion of apoptotic cells only increase by 4.99 ± 4.50 % when compared with time-matched untreated cells at 72 hours. A decreased rate of apoptotic cells in response to 72 hours FasL compared with 19 and 48 hour time-points may be caused by simultaneously induced fibroblast proliferation in response to FasL as demonstrated for fibroblast-like synoviocytes (Audo et al. 2014). To exclude

potential errors due to proliferative effects in subsequent experiments fibroblasts were exposed to FasL for 19 hours.

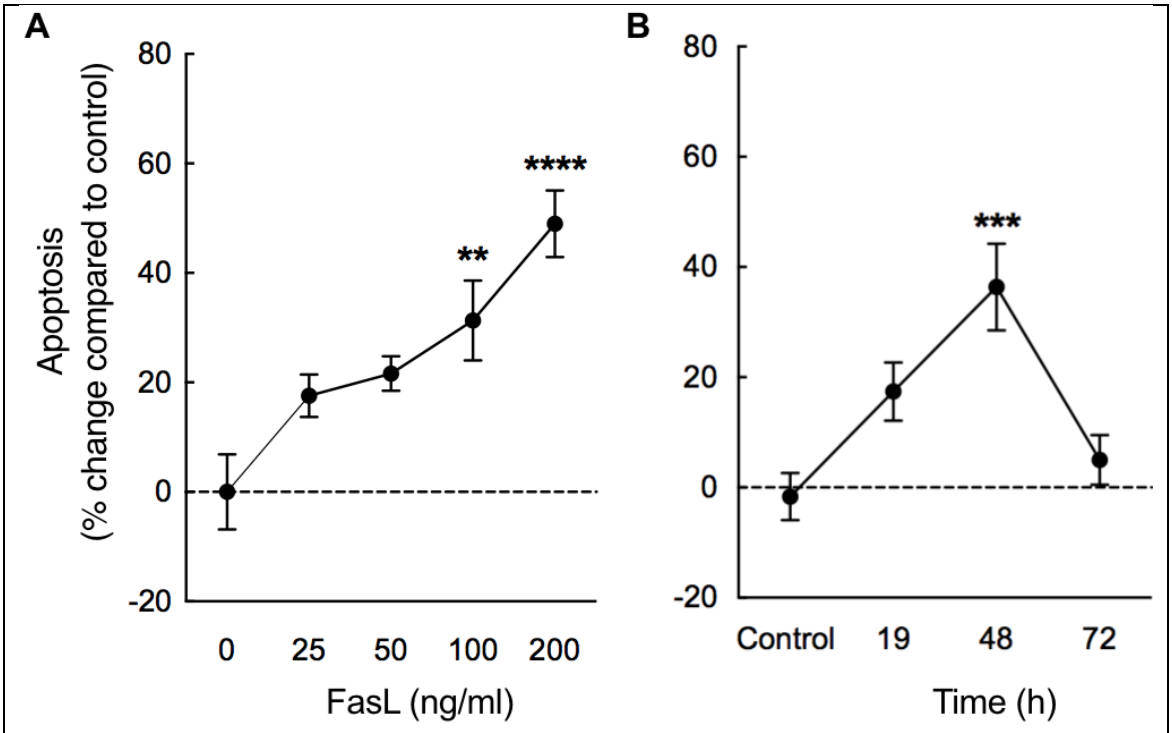

Figure 3.22 FasL-induced lung fibroblast apoptosis is concentration and time dependent.

(A) Control lung fibroblasts were exposed to doubling doses of recombinant human FasL from 25 - 200 ng/ml for 19 hours in 5 % FBS in DMEM; or to 100 ng/ml FasL for 19 -72 hours (B). Apoptosis was determined by Annexin V/DAPI staining with FACS analysis. The data is expressed as change in apoptosis compared with baseline level of apoptosis for each time point in untreated control cells (at 19 hours 24.17 ± 1.60 %). Each point represents the mean ± SEM of six experimental replicates. ***P < 0.001, ****P < 0.0001 compared with untreated controls respectively.

3.7.3 Effects of lentiviral transduction mediated clusterin-deficiency on basal and FasL- induced apoptosis.

To assess the importance of clusterin in mediating FasL-induced fibroblast apoptosis, clusterin-deficient fibroblasts were compared with mock transduced and non-transduced control lung fibroblasts. Clusterin-deficient fibroblasts, mock-transduced and non-transduced control lung fibroblasts were exposed to 100 ng/ml FasL for 19 hours as described in section 2.19. Data in Figure 3.23 are expressed as change in apoptosis compared with baseline level of apoptosis measured in untreated control cells (13.10 ± 0.33 %; mean ± SEM). As expected, treatment with FasL resulted in increased fibroblast apoptosis in control fibroblasts (by 21.58 ± 6.73 %) and in mock-transfected fibroblasts (by 40.54 ± 5.01 %; raw FACS data from representative fibroblast experiments are shown Appendix 3).
However, shRNA-mediated clusterin-deficient fibroblasts exhibited significantly higher basal rates of apoptosis (56.53 ± 8.52 %) than non-transduced and mock transduced fibroblasts. They also demonstrated an increased sensitivity to FasL-induced apoptosis (89.78 ± 9.21 %) compared with non–transduced ($p < 0.0001$) and mock-transduced ($p < 0.001$) fibroblasts. To explore if deficiency of extracellular or intracellular clusterin contributes to the differences seen in responsiveness to FasL, clusterin-deficient fibroblasts were exposed to extracellular clusterin (10 µg/ml) in the presence and absence of FasL and compared with relative levels of apoptosis in untreated control fibroblasts. Results shown in Figure 3.24 demonstrate that basal apoptosis in clusterin-deficient fibroblasts treated with exogenous clusterin (13.23 ± 3.39 %) tended to be lower than basal apoptosis levels of untreated control fibroblasts (17.16 ± 1.23 %) and that increased FasL-induced apoptosis could be overcome by administration of exogenous clusterin. These data suggest that exogenous or secreted clusterin protects lung fibroblasts from apoptosis *in vitro*.

3.7.4 Fibrotic fibroblasts are resistant to FasL-induced apoptosis and exogenous clusterin tends to reduce basal and FasL-induced apoptotic levels further.

In order to confirm that fibrotic lung fibroblasts used in this thesis are resistant to FasL-induced apoptosis, control and fibrotic lung fibroblast were treated with 0 - 200 ng/ml FasL for 19 hours. As previously described (Maher et al. 2010), Figure 3.25 demonstrates that fibrotic lung fibroblasts were more resistant to FasL-induced apoptosis than controls. Basal apoptosis in control (9.37 ± 0.63 %) and fibrotic (11.6 ±

0.69 %) lung fibroblasts was not significantly different. However, the proportion of apoptosis in fibrotic lung fibroblasts in response to 100 ng/ml FasL (68.3 ± 6.4 %) and to 200 ng/ml (118.9 ± 9.0 %) was significantly lower when compared with control lung fibroblasts (100 ng/ml: 212.3 ± 22.8 %, $p < 0.0001$ and 200 ng/ml: 265.2 ± 26.2 %, $p< 0.0001$). Since clusterin expression is reduced in IPF lung fibroblasts compared with controls, we sought to determine the effects of exogenous clusterin on apoptosis. In accordance with the protective effect of exogenous clusterin in control fibroblasts, we found that exogenous clusterin tended to reduce basal and FasL-induced apoptosis in fibrotic lung fibroblasts, but this was not statistically significant (Figure 3.26). This suggests that exogenous clusterin protects lung fibroblasts from apoptosis.

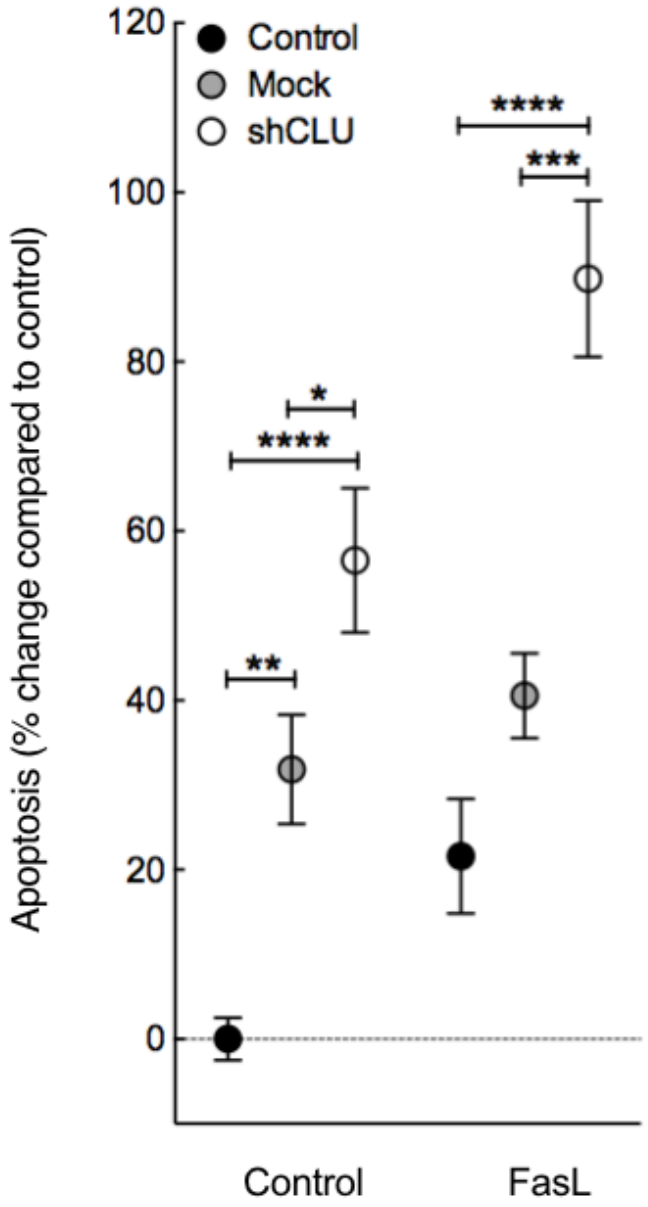

Figure 3.23 Clusterin-deficient fibroblasts are sensitised to basal and FasL-induced apoptosis.

Control lung fibroblasts (closed circle), mock-transduced (grey circle) and clusterin-deficient fibroblasts (open circle) were exposed to 100 ng/ml of FasL for 19 hours in 5 % FBS in DMEM. Apoptosis was determined by Annexin V/DAPI staining with FACS analysis. The data is expressed as change in apoptosis compared with baseline level of apoptosis in untreated control cells (13.10 ± 0.33 %). Each point represents the mean ± SEM of six experimental replicates. *P < 0.05, **P < 0.01 ***P < 0.001, ****P < 0.0001 compared with untreated un-transduced controls.

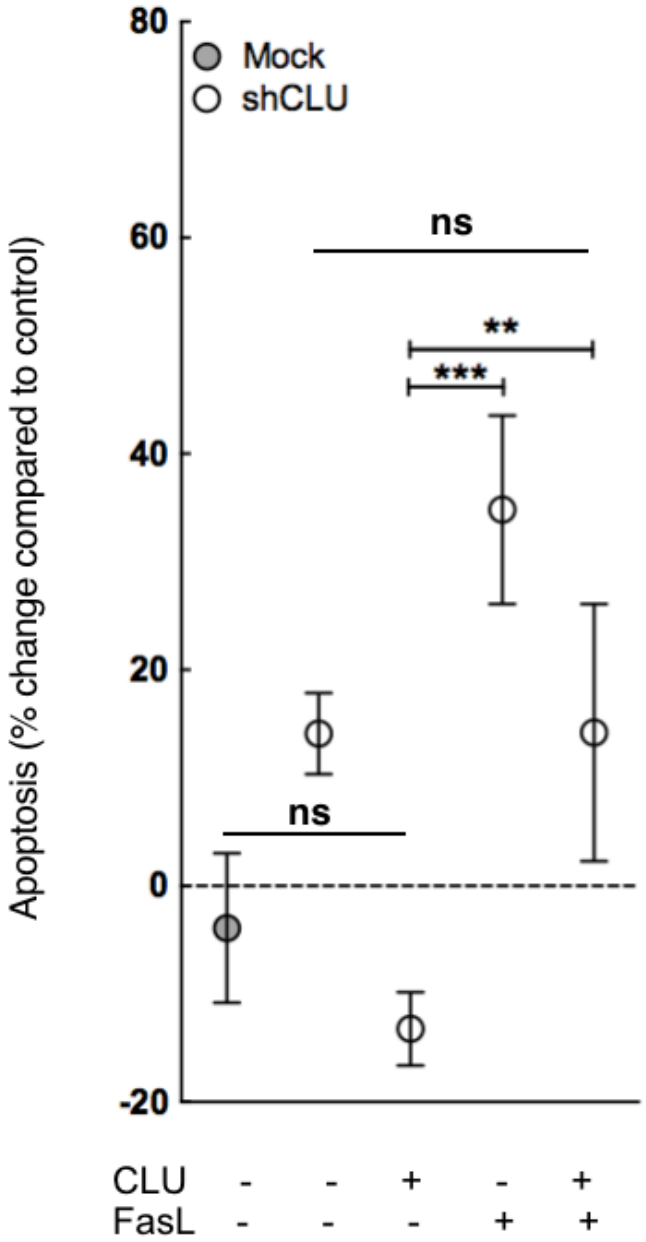

Figure 3.24 Increased sensitivity to basal and FasL-induced apoptosis is reversed by exogenous clusterin.

Control (grey circle) and clusterin-deficient fibroblasts (open circle) were exposed to 100 ng/ml of FasL for 19 hours in 5 % FBS in DMEM. Apoptosis was determined by Annexin V/DAPI staining with FACS analysis. The data is expressed as change in apoptosis compared with baseline level of apoptosis in untreated control cells (17.16 ± 1.23 %). Each point represents the mean ± SEM of five experimental replicates. $^{**}P < 0.01$ $^{***}P < 0.001$, compared with untreated controls.

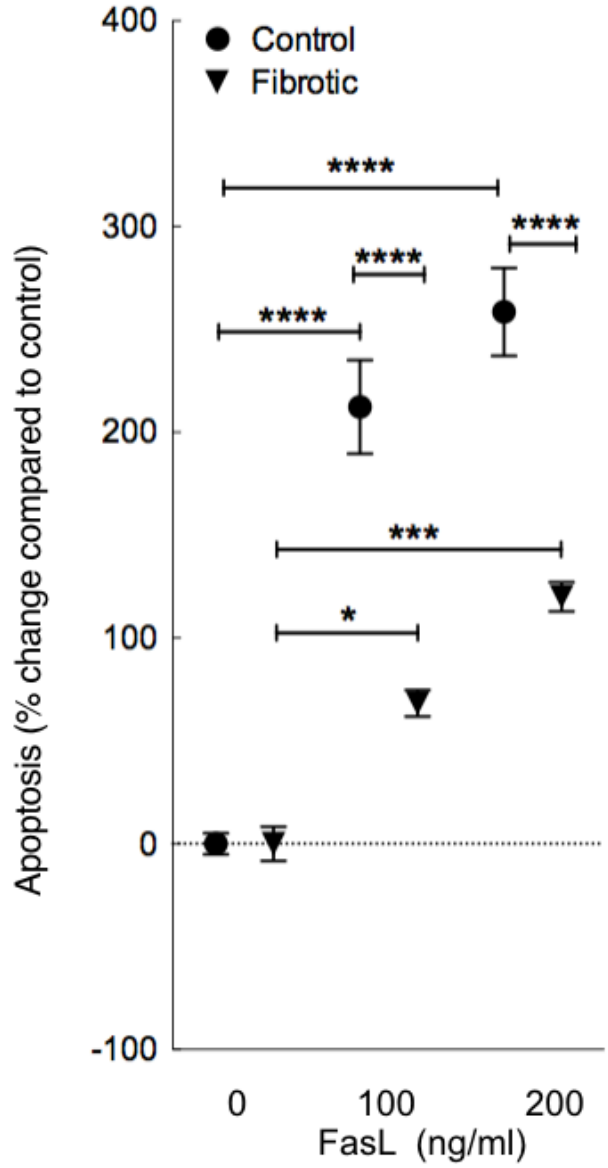

Figure 3.25 Fibrotic lung fibroblasts are resistant to FasL-induced apoptosis when compared with control lung fibroblasts.

Control lung fibroblasts (circle) and fibrotic lung fibroblasts (triangle) were exposed to 0 – 200 ng/ml of FasL (0 - 6 nM) for 19 hours in 5 % FBS in DMEM. Apoptosis was determined by Annexin V/DAPI staining with FACS analysis. The data is expressed as change in apoptosis compared with baseline level of apoptosis for each cell line. Basal apoptosis in control (9.37 ± 0.63 %) and fibrotic (11.6 ± 0.69 %) lung fibroblasts was not significantly different. Each point represents the mean ± SEM of five experimental replicates. *P < 0.05 ***P < 0.001, ****P < 0.0001compared with untreated controls.

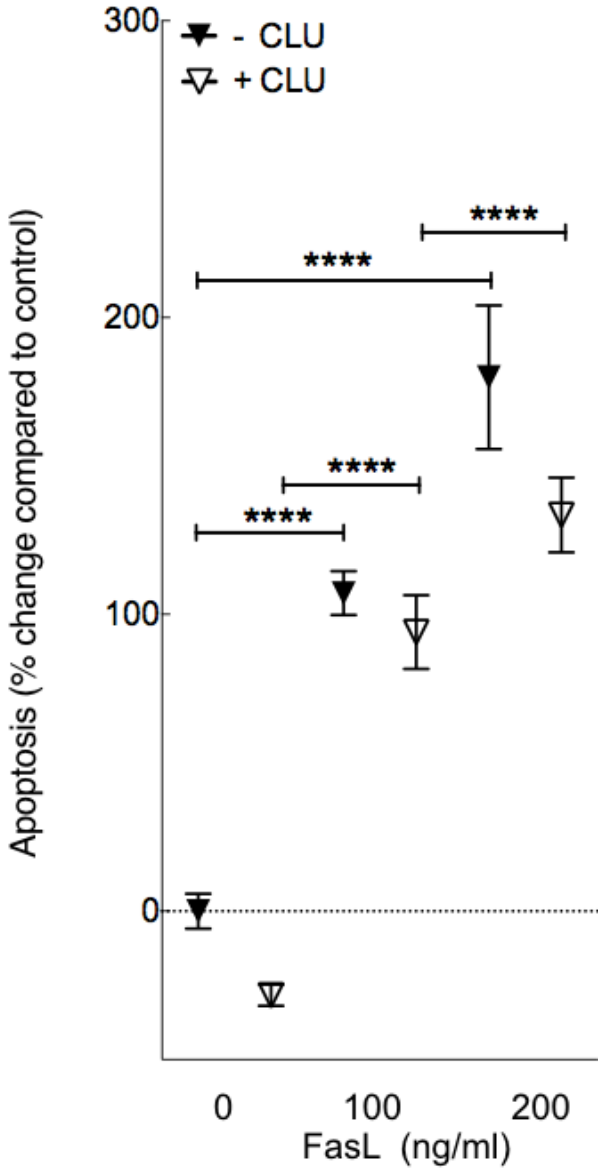

Figure 3.26 Exogenous clusterin reduces FasL-induced apoptosis in fibrotic fibroblasts.

Fibrotic lung fibroblasts were exposed to 0 - 200 ng/ml of FasL (3 - 6 nM) for 19 hours in the presence (open triangle) and absence (closed triangle) of exogenous clusterin (10 µg/ml). Apoptosis was determined by Annexin V/DAPI staining with FACS analysis. The data is expressed as change in apoptosis compared with baseline level of apoptosis (11.6 ± 0.69 %). Each point represents the mean ± SEM of five experimental replicates. ****$P < 0.0001$, compared with untreated controls, respectively.

3.7.5 Summary

The results in this section examined the *in vitro* apoptotic response to clusterin-deficiency in control and fibrotic lung fibroblasts in response to FasL compared with control lung fibroblast. The principle findings of these experiments demonstrate;

- The apoptotic response of control lung fibroblasts to FasL is dose-dependent with a measurable increase in apoptosis detectable at a FasL concentration of 25 ng/ml and continued to increase up to 200 ng/ml.

- FasL-induced apoptosis of control lung fibroblasts increases with the duration of FasL exposure up to 48 hours. At later times the assay is unstable (proliferation).

- Clusterin-deficient fibroblasts are sensitised to basal and FasL-induced apoptosis when compared with mock- and un-transduced controls.

- Increased sensitivity to apoptosis in clusterin-deficient lung fibroblasts can be overcome by administration of extracellular clusterin.

- Fibrotic lung fibroblasts are resistant to FasL-induced apoptosis when compared with fibroblasts derived from control lungs.

- In fibrotic lung fibroblasts, exogenous clusterin tends to reduce basal and FasL-induced apoptotic levels further.

In summary, this data suggests that clusterin-deficient fibroblasts are sensitised to basal and FasL-induced apoptosis, which could be overcome by exogenous clusterin. This suggests that exogenous clusterin protects against basal and FasL-induced apoptosis. Fibrotic lung fibroblasts were resistant to FasL-induced apoptosis when compared with control lung fibroblasts and exogenous clusterin tends to reduce FasL-induced apoptotic levels further.

3.8 *In vivo* LRP-2 receptor expression in normal and IPF lung.

LRP-2 (low-density lipoprotein-related protein 2), megalin or glycoprotein 330 has been identified as an endocytotic receptor for clusterin in polarised epithelial cell lines (Kounnas et al. 1995; Zlokovic et al. 1996; De et al. 2014). LRP-2 is expressed in primary alveolar epithelial cells in rodent lungs (Zheng et al. 1994; Kounnas et al. 1994) but the distribution of LRP-2 in the human lung has not previously been described. In addition, it is not known if LRP-2 receptor expression changes in the lungs of patients with pulmonary fibrosis. To assess the LRP-2 distribution in healthy and fibrotic lung tissue, immunohistochemistry was performed on control and IPF lung tissue as described in section 2.10. LRP-2 localisation on individual lung cell types was assessed by two independent reviewers.

In control lung tissue, LRP-2 localised strongly to alveolar monocytes/macrophages and weakly or moderately to bronchial epithelial cells (Figure 3.27A and Figure 3.28A). All other cell types, including epithelial, fibroblast-like and smooth muscle cells, showed low or undetectable staining for LRP-2. In IPF lung tissue immunohistochemical staining was similar to that of control lung tissue. In IPF lung LRP-2 staining localised to increased numbers of infiltrated macrophages and was predominantly localised to the cell surface of those cells (Figure 3.27B). Bronchial epithelial cells displayed a similar pattern of LRP-staining compared with control lungs while staining in fibroblast in fibrotic tissue was weak or undetectable (Figure 3.28B).

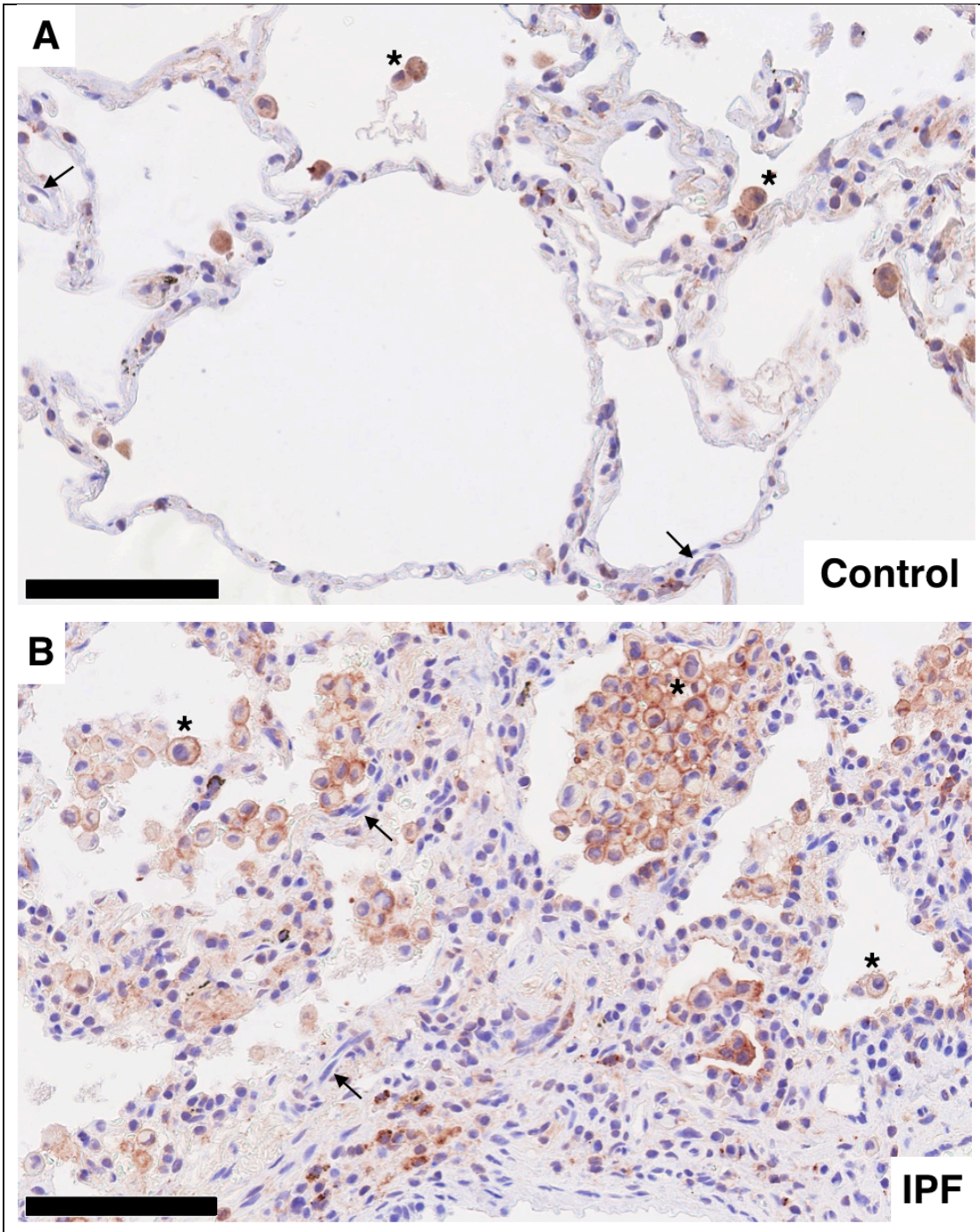

Figure 3.27 LRP-2 immunohistochemical localisation in normal and IPF lung.

Immunohistochemical staining for LRP-2 in paraffin-embedded sections of normal human lung (A) and IPF lung (B). Specific staining is red-brown, nuclei are counterstained blue with haematoxylin. In control lung, positive staining localised predominantly to alveolar macrophages (stars), while modest or undetectable staining was observed for fibroblast-like cells (arrows). In IPF lung positive LRP-2 signal localises to increased numbers of alveolar macrophages (stars) and is absent in fibroblasts (arrows). Scale bar represents 100 µm.

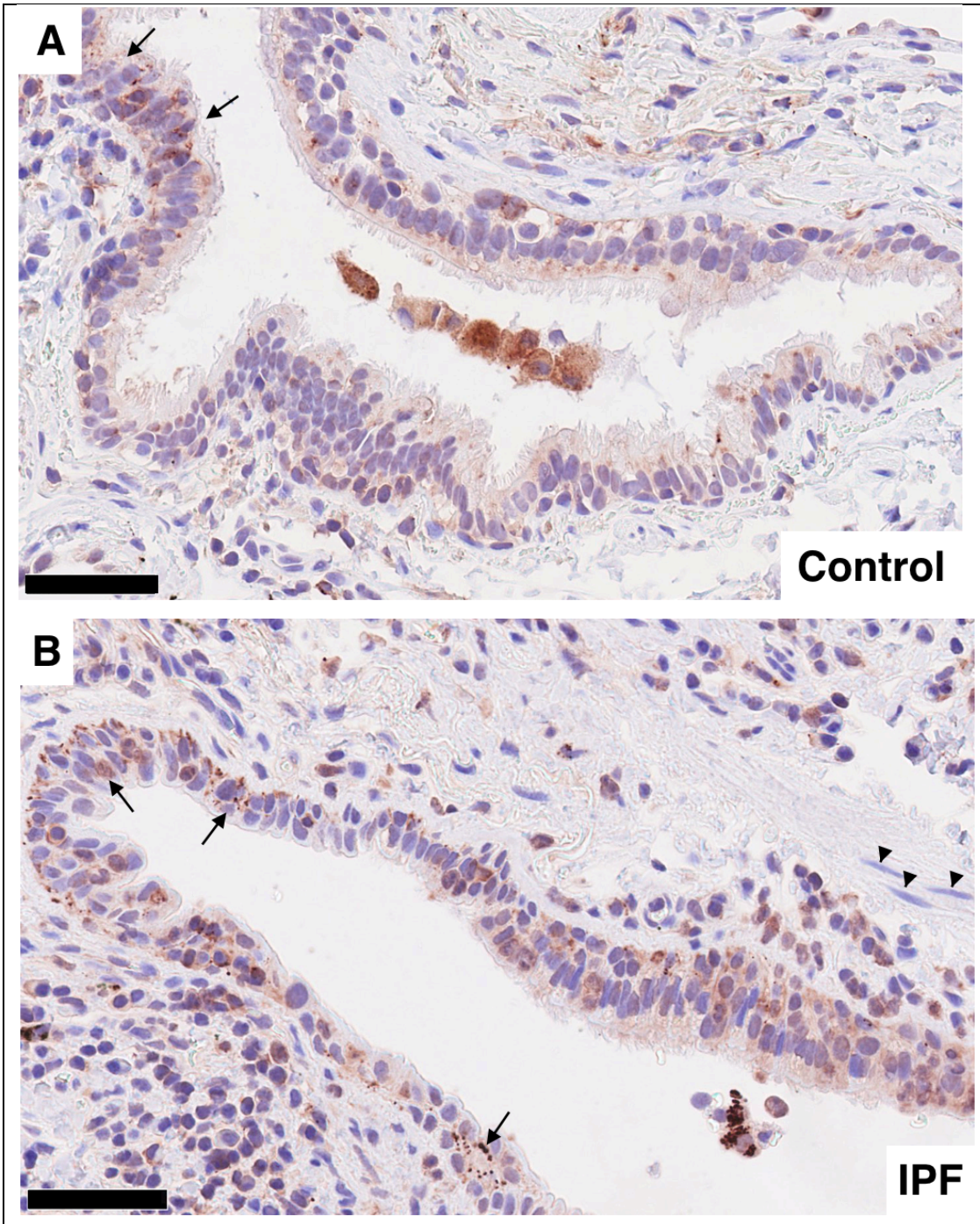

Figure 3.28 LRP-2 expression in bronchial epithelial cells of control and IPF lung tissue.

Immunohistochemical staining for LRP-2 in paraffin-embedded sections of normal human lung (A) and IPF lung (B). Specific staining is red-brown, nuclei are counterstained blue with haematoxylin. Staining for LRP-2 is similar in bronchial epithelial cells in control and fibrotic lung and located to the cytoplasm and displayed a mixed diffuse and punctate staining for LRP-2 in both control lung and fibrotic lung (arrows). Smooth muscle cells in fibrotic lung showed no detectable signal for LRP-2 (arrow head). Scale bar represents 50 µm.

3.9 *In vitro* assessment of the role of clusterin in modulating protein secretion in alveolar and blood-derived macrophages and bronchial epithelia cells.

3.9.1 Exogenous clusterin induces the secretion of pro-inflammatory cytokines/ chemokines and MMP-9 in human alveolar macrophages.

Pulmonary fibrosis has been associated with alternatively activated macrophages (Stahl et al. 2013; Mora et al. 2006), which express pro-fibrotic genes such as TGF-β_1, IGF-1 and PDGF (Wynes & Riches 2003; Gordon 2003; Wynn et al. 2011).
Further studies outline the significance of altered macrophage polarisation and their contribution to the onset and progression of pulmonary fibrosis (Murthy et al. 2015; Wermuth & Jimenez 2015).
Studies in murine macrophages have shown that clusterin induces TNFα secretion and the chemotactic migration of monocytes/macrophages (Y. J. Shim et al. 2012). However, the role of clusterin in modulating the phenotype and protein secretion of human alveolar macrophages is unknown. Similar to alveolar macrophages, bronchial epithelial cells secrete various cyto- and chemokines inducing migration and proliferation in fibroblasts, contributing to the progression of pulmonary fibrosis (Calabrese et al. 2005), but the effects of exogenous clusterin on the secretome of bronchial epithelial cells is still unknown.
This section focuses on the question whether the reduced availability of exogenous clusterin in IPF-BALF may affect the recruitment and phenotype of alveolar macrophages and the secretion of cytokines in bronchial epithelial cells. Having demonstrated that the LRP-2 receptor is highly expressed on the surface of alveolar macrophages and bronchial epithelial cells, the effect of exogenous clusterin on secreted pro- and anti-inflammatory proteins in alveolar macrophages and bronchial epithelial cells in mono- and co-culture were investigated *in vitro*. During the course of the research presented in this thesis, alveolar macrophages were isolated from one control donor in collaboration with Dr. Ben Calvert, however, bronchial epithelial explants for cell culture could not be established. Therefore, transformed human bronchial epithelial cells (BEAS-2B), developed by immortalization of normal human bronchial epithelial cells were used, on the basis that it has been demonstrated that BEAS-2B cells display many characteristics of bronchial epithelial cells. Furthermore, BEAS-2B cells are widely used in the *in vitro* investigation of bronchial cell behaviour (Park et al. 2015) and in pulmonary fibrosis research (Patel et al. 2015; Cabrera-Benítez et al. 2012).
To begin to investigate the effects of exogenous clusterin, human alveolar macrophages derived from a healthy control lung and BEAS-2B cells were (co-)

cultured as described in section 2.21 for 24 hours before being exposed to increasing concentrations of exogenous clusterin (1-5 µg/ml). This concentration was chosen on the basis of previous experiments with macrophages (Shim et al. 2011).

For all experiments, monocultures of each cell line were maintained on the same 96 well plate under the same conditions as the cell-co-culture. This was to control for effects resulting from the co-culture of alveolar macrophages with BEAS-2B cells.

The effects of exogenous clusterin on protein secretion in alveolar macrophages and BEAS-2B alone or in co-culture are demonstrated in Figure 3.29. Increasing doses of exogenous clusterin-induced the secretion of TNFα by ten-fold for 5 µg/ml exogenous clusterin (from 2.19 ± 0.28 pg/ml to 20.59 ± 1.32 pg/ml). This data is consistent with previous reports in murine Raw264.7 macrophages (Y. J. Shim et al. 2012) but has not been shown for human macrophages previously.

In addition, exogenous clusterin-induced the secretion of TNFα in BEAS-2B cells alone (from 0.3 ± 0.03 pg/ml to 18.02 ± 0.33 pg/ml) or in co-culture with alveolar macrophages (from 2.23 ± 2.43 pg/ml to 19.67 ± 0.13 pg/ml) as demonstrated in Figure 3.29A. Further analysis of chemotactic cytokine secretion in alveolar macrophages in response to exogenous clusterin show that MCP-1, MIP-1β, RANTES secretion is in trend induced in response to exogenous clusterin, which is has been previously reported in a model with Raw264.7 macrophages (Y. J. Shim et al. 2012). Furthermore and in accordance with findings in human monocytic cell line THP-1 and human primary monocytes MMP-9 secretion was induced by exogenous clusterin in alveolar macrophages (Shim et al. 2011). Together this data suggests that exogenous clusterin induces the secretion of pro-inflammatory TNFα and chemotactic cytokines. To confirm this and extend the cytokine profile of clusterin treated alveolar macrophages additional cytokines were analysed via luminex analysis. Similarly, to TNFα secretion, the secretion of other pro-inflammatory cytokines such as IL-6, IL-8 and IL-5 was increased in alveolar macrophages in response to increasing exogenous clusterin levels, while anti-inflammatory cytokine IL-1ra secretion remained stable in response to exogenous clusterin (Figure 3.29 B-F). The effects of clusterin on cytokines secretion was predominantly observed for alveolar macrophages in monoculture but were persistent for IL-8 and IL-6 in co-culture with BEAS-2B cells. However, no synergetic or additive effects on cytokine alteration was observed between BEAS-2B and alveolar macrophages. Ultimately, exogenous clusterin-induced changes in chemokine and cytokine secretion in BEAS-2B monocultures were limited to clusterin-induced TNFα secretion.

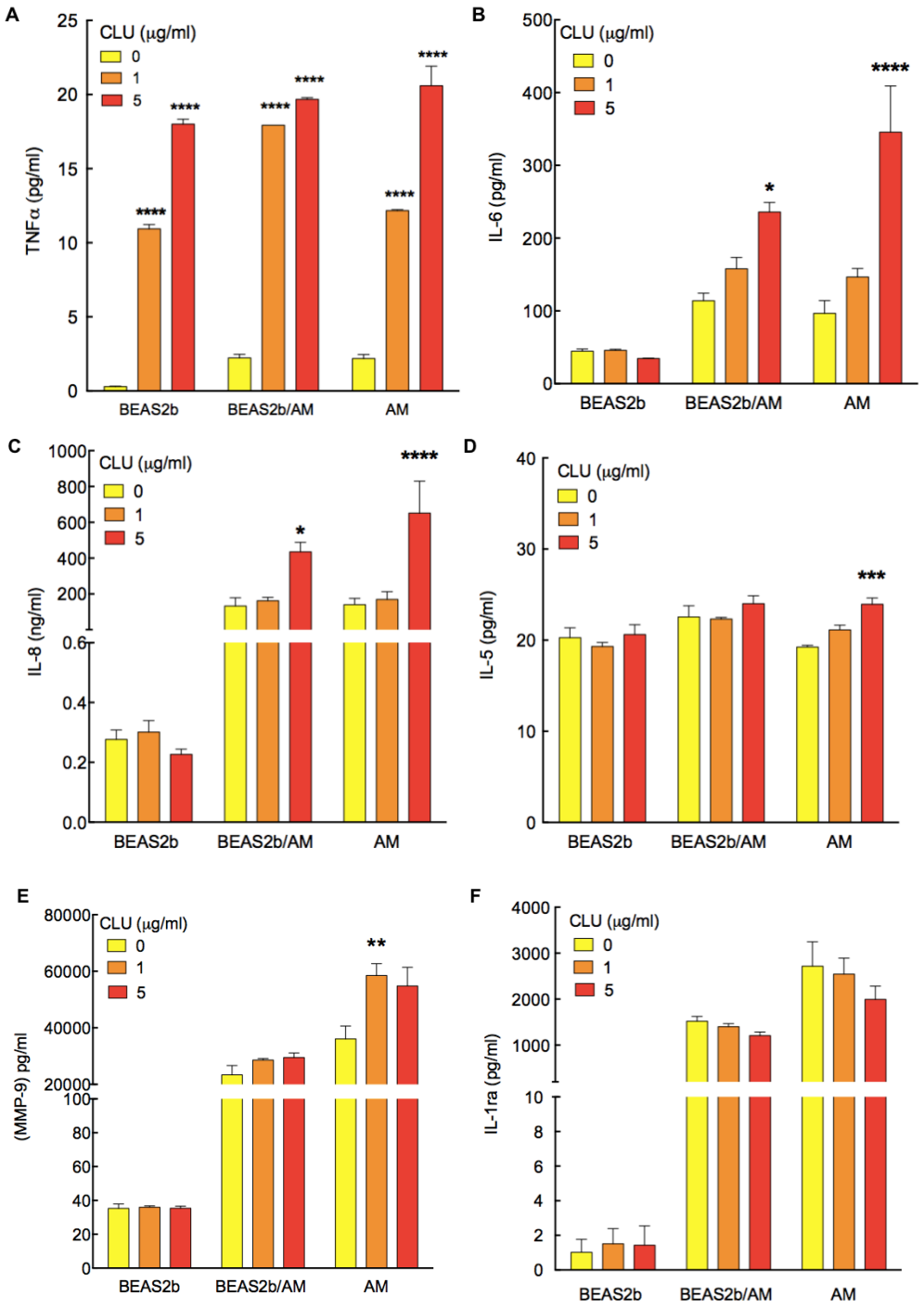

Figure 3.29 (continued over the page)

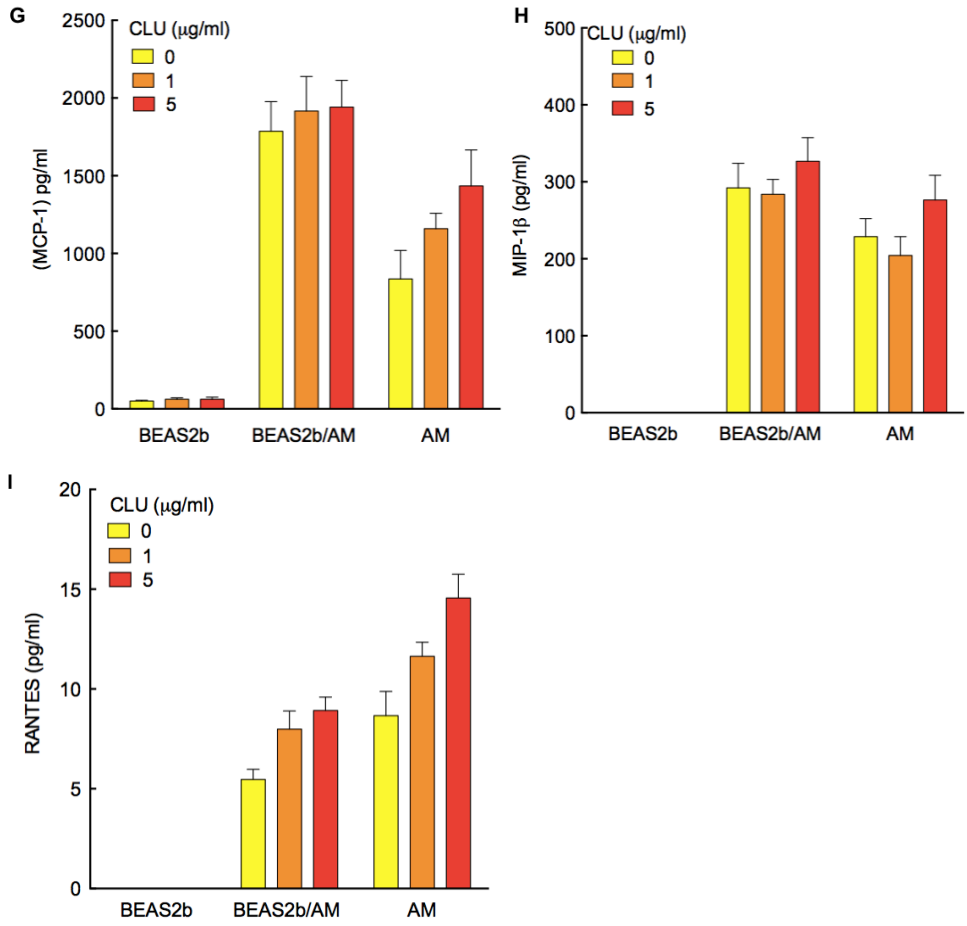

Figure 3.29 Exogenous clusterin induces the secretion of pro-inflammatory cytokines / chemokines and MMP-9 in alveolar macrophages in mono- or in co-culture with BEAS-2B cells.

BEAS-2B cells were cultured at 1 x 10^4 cells per well in a 96-well plate in medium containing 10 % FBS for 24 hours. Primary alveolar macrophages (AM) were added to wells containing BEAS-2B or seeded in empty wells for monoculture. Cells were then exposed to exogenous clusterin (1 - 5 µg/ml) for 24 hours. Cytokine, chemokine, and MMP-9 secretion were assessed via Luminex analysis. Bars represent the mean ± SEM of six experimental replicates. **P* < 0.05, ***P* < 0.01, ****P* < 0.001, *****P* < 0.0001, compared with untreated controls respectively.

Pulmonary administration of TNFα has been shown to reduce the fibrotic burden in mice with bleomycin-induced fibrosis (Redente et al. 2014). In this study, it was suggested that TNFα reduced the number and programming status of profibrotic, alternatively programmed macrophages. The findings in this section suggest that exogenous clusterin shifts the phenotype of alveolar macrophages, resulting in increased secretion of TNFα levels and other pro-inflammatory cyto- and chemokines.

3.9.2 Exogenous clusterin induces the secretion of pro-inflammatory cytokines/chemokines and MMP-9 in human-blood-derived macrophages.

The following subsection focuses on the effect of exogenous clusterin on macrophage programming. Due to a limitation in accessibility of human alveolar macrophages, subsequent studies were conducted with blood monocyte derived macrophages on the basis that alveolar macrophages, at least in part, originate *in vivo* from blood-derived monocytes (Landsman & Jung 2007). For this purpose, monocytes were isolated from human blood as described in section 2.21. Monocytes differentiated into macrophages in the presence of M-CSF (100 ng/ml) within four days. After 72 hours of treatment with 1 µg/ml exogenous clusterin supernatants were collected and analysed via luminex assay. The results outlined in Figure 3.30 highlight a number of changes in protein secretion observed in one donor following clusterin administration in M-CSF differentiated macrophages ("M0"). This experiment was repeated for two donors. Due to a high variability in donor responses, the observed data derived from two donors have not been presented in one graph. Results for the same method in a second donor are displayed in Appendix 4.

Consistent with results in alveolar macrophages (section 3.9) clusterin tends to induce the secretion of TNFα, IL-6, and MIP-1α and significantly induces the secretion of MMP-9 and IL-8 compared with untreated controls when administered to differentiated, unpolarised macrophages for 72 hours (red box in Figure 3.30). Although, the values for TNFα, IL-6, and MIP-1α are not significant in a two-way ANOVA presented with data obtained from "M1" polarised macrophages, the fold-increase in response to exogenous clusterin compared with no clusterin was as follows: For the donor displayed here, clusterin tended to induce measurable levels of TNFα from 1.8 ± 0.2 to pg/ml 10.8 ± 0.9 pg/ml and IL-6 from 38.6 ± 4.7 to 68.1 ± 19.2 pg/ml in unpolarised macrophages. Additionally, the secretory levels of MIP-1α were increased in trend from 35.4 ± 0.3 pg/ml to 72.0 ± 3.2 pg/ml in unpolarised macrophages. Secretory IL-8 was significantly increased by exogenous clusterin from 2671.7 ± 637.8 pg/ml to 15804.0 ± 487.1 pg/ml ($p < 0.01$) as well as MMP-9 from 275.9 ± 25.5 ng/ml to 815.3 ± 33.4 ng/ml. The data obtained from donor 2 (Appendix 4) are consistent with the data from donor 1 presented here, except for the results on MMP-9. In donor 2 exogenous clusterin did not increase the secretion of MMP-9 in unpolarised macrophages. Together, this data suggests that clusterin-induced the secretion of pro-inflammatory cytokines in unpolarised macrophages from two donors, but not for MMP-9. This data is preliminary and needs to be confirmed in a larger donor group for a wider range of clusterin concentrations (see section 3.9.3.).

To begin to investigate the potential role of exogenous clusterin in modulating between different induced polarisation states, macrophages were treated with LPS/IFNγ (10 ng/ml and 50 ng/ml) to polarize towards “M1” or IL-4 (20ng/ml) to polarize towards an “M2” phenotype for 72 hours, in the presence or absence of exogenous clusterin (1µg/ml). As expected, stimulation with LPS/IFNγ induced a “M1”-like phenotype in macrophages measurable by an induced secretion of pro-inflammatory cytokines, such as TNFα, IL-6, IL-8; MIP-1α. MMP-9 levels in response to LPS/IFNγ tended to decrease when compared with unpolarised “M0”-like macrophages in both donors (Figure 3.30, Appendix 4). Further analysis demonstrates that the presence of exogenous clusterin during the polarisation towards an “M1”-like phenotype does not alter the levels of pro-inflammatory cytokines when compared with “M1” controls without exogenous clusterin. MMP-9 levels in “M1”-like macrophages did not change in response to exogenous clusterin when compared to “M1”-like macrophages without clusterin.

Meanwhile, in macrophages that were polarised with IL-4 towards an “M2”-like phenotype, pro-inflammatory protein secretion was similar to that of un-polarised controls (Figure 3.30, Appendix 4). Besides, the presence of exogenous clusterin during the polarisation towards “M2”- phenotype did not alter pro-inflammatory cytokines and MMP-9 secretion significantly when compared with polarised controls without exogenous clusterin. Together, the present data suggests that exogenous clusterin induces the secretion of pro-inflammatory cytokines and MMP-9 in unpolarised macrophages, but did not revert or increase the secretion of those cytokines in the course of polarisation to towards an “M1” or “M2” phenotype.

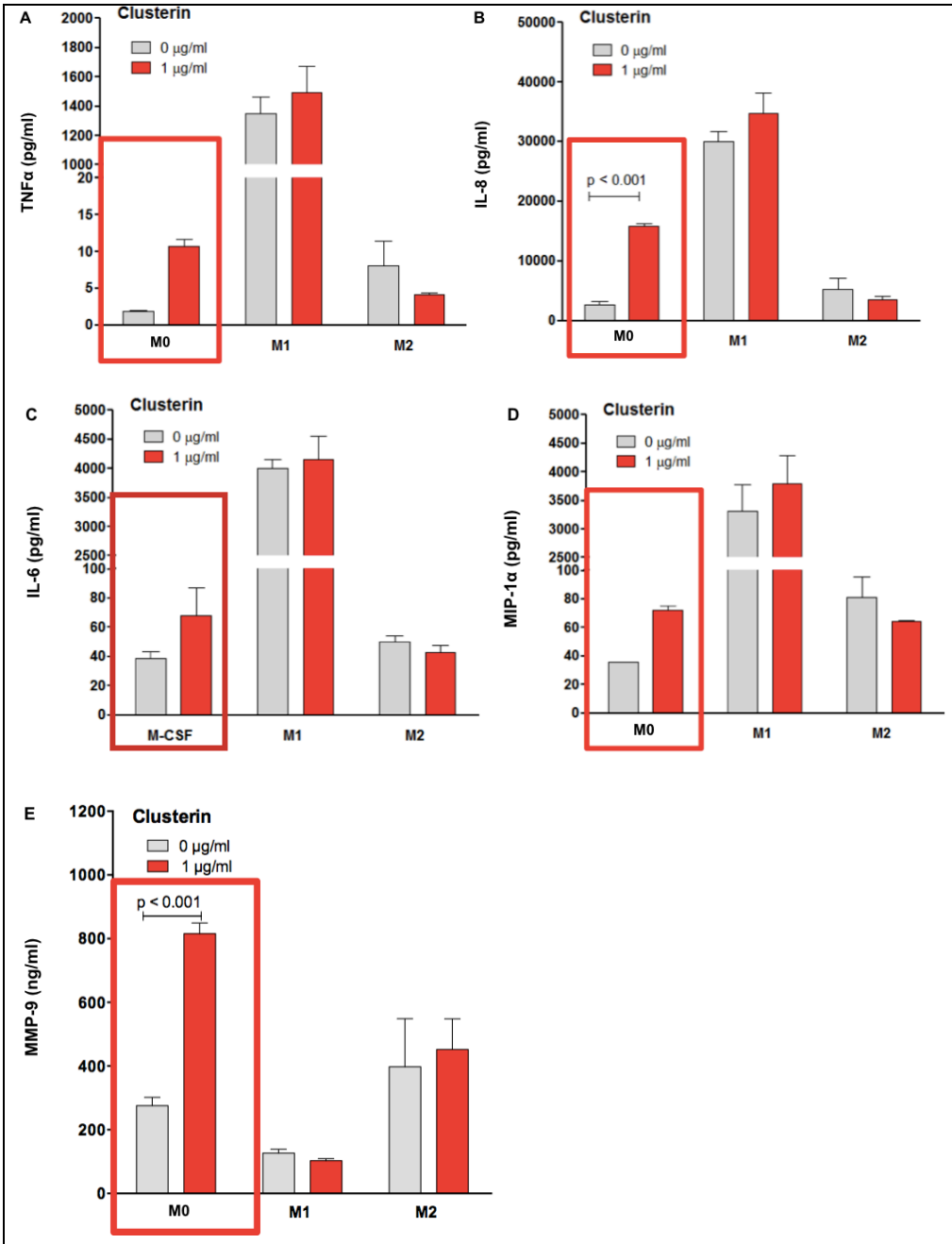

Figure 3.30 Donor 1: Effect of exogenous clusterin on cytokine and MMP-9 secretion during polarisation in blood-derived macrophages.

Human blood-derived $CD14^+$ cells were seeded into a 96 well plate (1 x 10^5 cells/well) and were allowed to differentiate into macrophages in the presence of M-CSF (100 ng/ml) for four days. Subsequently, cells were stimulated towards a "M1" phenotype with LPS / IFNγ (at 10 ng/ml for LPS and 50 ng/ml for IFNγ) or a "M2" phenotype with IL-4 (20 ng/ml) or remained untreated ("M0") in the presence and absence of human plasma-derived clusterin (1 µg/ml) for 72 hours. Cytokine, chemokine and MMP-9 secretion was assessed via Luminex analysis. Bars represent the mean ± SEM of three experimental replicates; significances compared with untreated controls respectively. Data were generated in a second donor and are displayed in Appendix 4.

3.9.3 Exogenous clusterin-induced alteration in cytokine and MMP-9 secretion in unpolarised macrophages is dose-dependent.

To begin to explore if the effects of clusterin on secreted proteins in unpolarised macrophages ("M0") are dose dependent, M-CSF differentiated macrophages from a third donor were stimulated with three-fold, six-point increasing concentrations of exogenous clusterin for 72 hours. To determine the effect on other cytokines/chemokines a 25-plex luminex assay was used to measure 25 proteins in cell supernatants simultaneously. Human plasma-derived clusterin mediated a dose-dependent increase in secretion of pro- and anti-inflammatory cytokines (Figure 3.31), chemotactic cytokines and MMP-9 (Figure 3.32) (One-way ANOVA MCP-1: $P= 0.0053$, MMP-9: $P = 0.0008$ and for all other $P< 0.0001$). Other secretory proteins were not detectable in response to low clusterin concentrations from but showed a trend towards an increase in response to higher concentrations of exogenous clusterin (IL-12 and IL-2R, Appendix 5). All other analytes were not detected in the cell supernatants (GM-CSF, IL-4, Eotaxin, MIG, IL-12, IL-17, IL-13, IL-7, IL-15, IFN-α, IL-5, IL-2, IFNγ). The levels of secreted TNFα were increased from 1.36 ± 0.40 pg/ml (mean ± SEM) to 150.68 ± 20.09 pg/ml following treatment with exogenous clusterin at the highest dose of 30 µg/ml.

This data was obtained from a third donor and consistent with trends of increase cytokine secretion observed with 1 µg/ml exogenous clusterin in donor 1 and 2 (section 3.9.2). Due to a significantly higher response with exogenous clusterin concentrations > 1 µg/ml observed in the third donor data presented in section 3.9.2 need to be validated using higher exogenous clusterin concentrations (5 µg/ml). Consecutive experiments were, therefore, conducted with an exogenous clusterin concentration of 5 µg/ml.

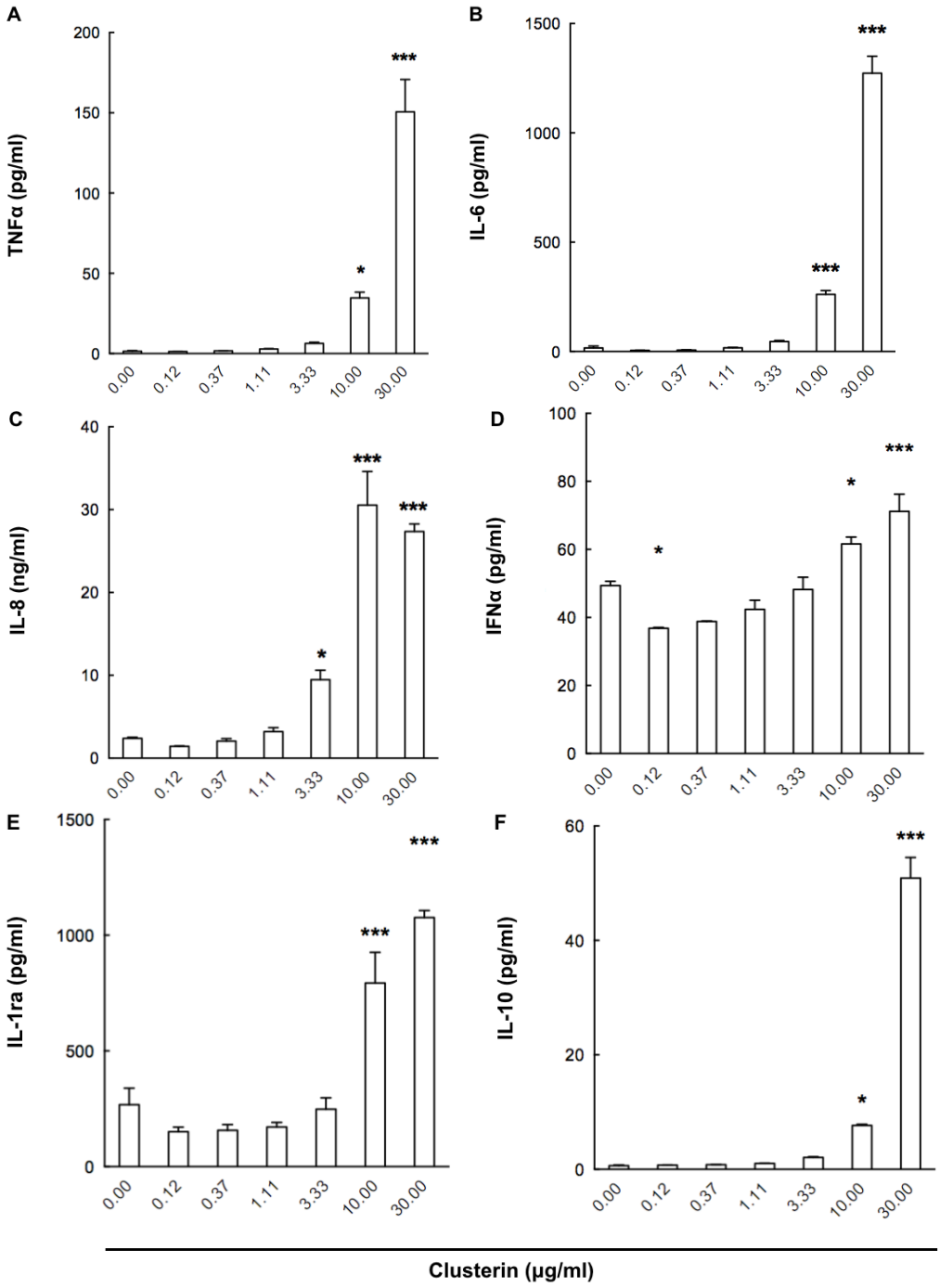

Figure 3.31 Donor 3: Exogenous clusterin-induced secretion of pro- and anti-inflammatory cytokines is concentration dependent.

Human blood-derived monocytes were seeded onto a 96-well plate (1 x 10^5 cells/well), differentiated to macrophages with M-CSF (100ng/ml) for four days and then exposed to human plasma-derived clusterin at three-fold increasing doses for 72 hours or remained untreated. Cytokine secretion was assessed via Luminex analysis. Bars represent the mean ± SEM of three experimental replicates; *P < 0.05, **P < 0.01, ***P < 0.001, ****P < 0.0001 compared with untreated controls.

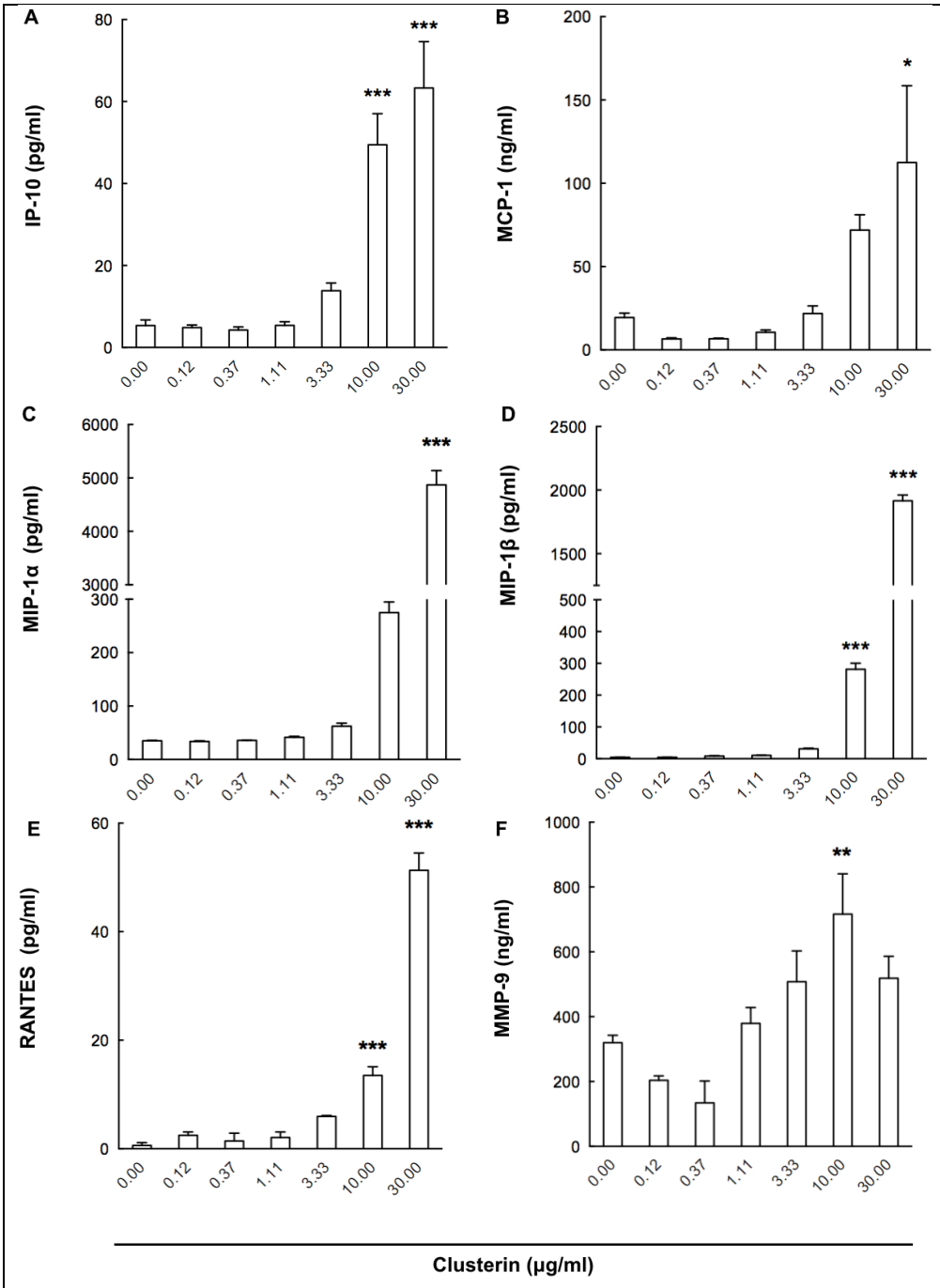

Figure 3.32 Exogenous clusterin-induced secretion of chemotactic cytokines and MMP-9 is concentration dependent.

Human blood-derived monocytes were seeded onto a 96-well plate (1 x 10^5 cells/well), differentiated to macrophages with M-CSF (100ng/ml) for four days and then exposed to human plasma-derived clusterin at three-fold increasing doses for 72 hours or remained untreated. Cytokine secretion was assessed via Luminex analysis. Bars represent the mean ± SEM of three experimental replicates; **P* < 0.05, ***P* < 0.01, ****P* < 0.001, *****P* < 0.0001 compared with untreated controls.

3.9.4 TNFα neutralising antibody attenuates the effect of induced cytokine secretion by exogenous clusterin in human blood-derived macrophages.

TNFα is considered to be a master cytokine in inflammation and is reportedly increased in patients with pulmonary fibrosis (Gauldie et al. 1993; Ziegenhagen et al. 1998), particularly by macrophages. *In vivo* studies in bleomycin-induced lung injury suggested that blocking TNFα signalling attenuates the development of fibrosis (Piguet et al. 2002; Zhang et al. 1997a; Ortiz et al. 1998; Oikonomou et al. 2006) . The importance of soluble TNFα in contributing to the pathogenesis of fibrosis may underlay its downstream induction of many cytokines and chemokines (Oikonomou et al. 2006; Zhang et al. 1997b), particularly in macrophages a central cell in the cytokine network of the lung (Scheule et al. 1992; Parameswaran & Patial 2010). To begin to explore if exogenous clusterin exerts its induction of pro-inflammatory cytokines in macrophages through autocrine/paracrine effects induced by increased levels of TNFα, a TNFα neutralising antibody experiment was conducted.

As a representative of pro-inflammatory cytokines IL-6 and for chemotactic cytokines MIP-1β was measured in the cell supernatant after 72 hours of exposure to exogenous clusterin (5 µg/ml) in the presence or absence of TNFα-neutralising antibody or matching isotype control (10 µg/ml). Consistent with previous results in sections 3.9 - 3.9.3, exogenous clusterin increased levels of secretory TNFα significantly (Figure 3.33A) by more than 40 fold, from 3.08 ± 0.36 pg/ml to 132.31 ± 11.40 pg/ml (mean ± SEM). As expected, no secreted TNFα was detectable in supernatants of macrophages with and without exposure to exogenous clusterin in the presence of TNFα neutralising antibody.

Consistent with the results observed for TNFα levels, IL-6 and MIP-1β levels were increased in response to exogenous clusterin (Figure 3.33B,C; $P < 0.0001$, IL-6: from 7.41 ± 2.85 to 358.75 ± 30.52 pg/ml and MIP-1β: from 21.52 ± 0.92 to 2786.81 ± 625.41 pg/ml). In the presence of TNFα-neutralising antibodies, this effect was attenuated by 98.06 ± 0.36 % for MIP-1β and 55.90 ± 4.06 % for IL-6 when compared with exogenous clusterin treated cells in the absence of neutralising antibodies ($P< 0.0001$). Ultimately, these preliminary data suggest that induced cytokine secretion, here examined for IL-6 and MIP-1β, is at least in part mediated through autocrine/paracrine effects of induced secretory TNFα in response to exogenous clusterin. However, this data needs to be confirmed experimentally with an isotype control, which does not alter cytokine levels when compared with untreated control. Unfortunately, the isotype control performed poorly since it did affect secretory TNFα in supernatants of macrophages exposed to isotype antibodies (in presence or absence

of exposure to exogenous clusterin), but demonstrated significantly different cytokine values when compared with untreated control in the presence of exogenous clusterin ($p < 0.0001$).

3.9.5 Polarisation towards an “M1” phenotype induces the secretion of clusterin in human blood-derived macrophages.

In this subsection, it was investigated whether levels of secretory clusterin are altered during activation of human blood-derived macrophages. To test this, human blood-derived macrophages were differentiated with M-CSF for four days and then subjected to LPS (10 ng/ml) and/or IFNγ (50 ng/ml) and IL-4 (20 ng/ml) for 72 hours. In accordance with immunohistochemical staining for clusterin in sections of healthy control lung (Figure 3.1), ELISA analysis demonstrated that M-CSF differentiated macrophages (“M0”) secrete low levels of clusterin (0.53 ± 0.12 ng/ml, mean ± SEM, Figure 3.34). Interestingly, secretory clusterin levels increased upon activation with LPS and further increased when LPS and IFNγ were combined (19.69 ± 0.52 ng/ml, mean ± SEM, Figure 3.34). In contrast, secretory clusterin levels were not altered when macrophages were polarised towards an “M2” phenotype with IL-4 when compared with untreated control cells (Figure 3.34).

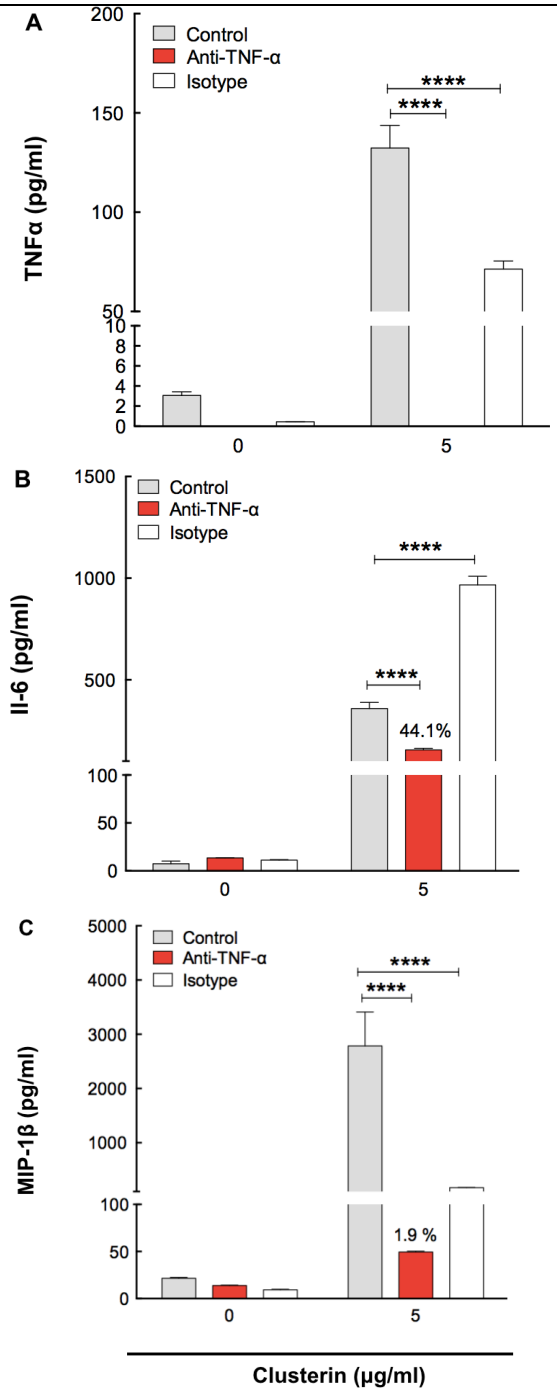

Figure 3.33 TNFα neutralising antibody attenuates the effect of exogenous clusterin on induced cytokine secretion.

Human blood-derived monocytes were seeded onto a 96-well plate (1 x 10^5 cells/well), differentiated to macrophages with M-CSF (100 ng/ml) for four days and then exposed to human plasma-derived clusterin (5 µg/ml) in the presence or absence of TNFα neutralising antibody, isotype control (10 µg/ml) or remained untreated. IL-6 and MIP-1β secretion was assessed via Luminex analysis. Bars represent the mean ± SEM of three experimental replicates; ****$P < 0.0001$ compared with untreated controls.

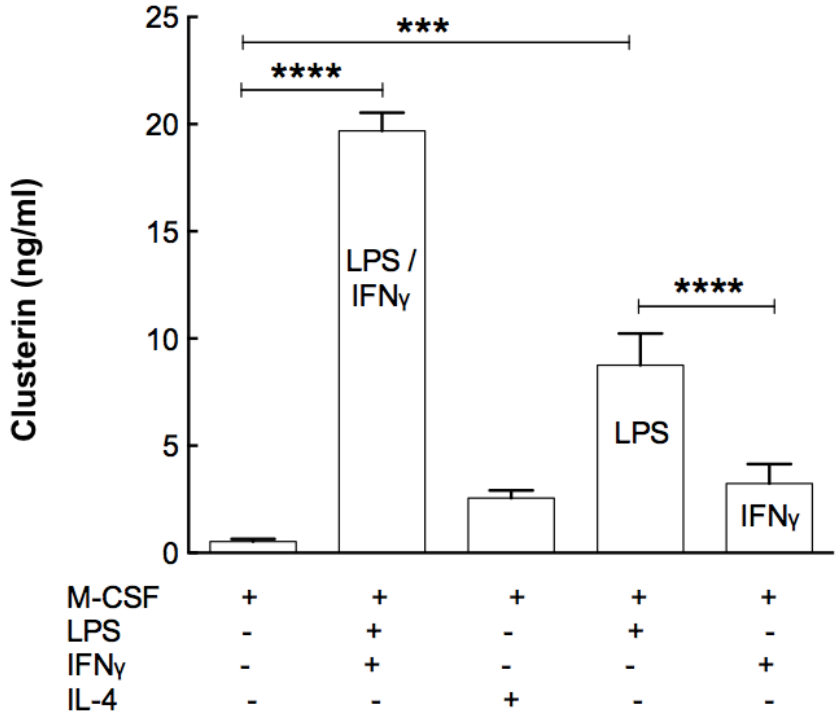

Figure 3.34 Macrophage activation with LPS and/or IFNγ induces the secretion of clusterin.

Human blood-derived monocytes were seeded onto a 96-well plate (1 x 10^5 cells/well), differentiated to macrophages with M-CSF (100ng/ml) for four days and then exposed to LPS (10 ng/ml) and/or IFNγ (50 ng/ml) or IL-4 (20 ng/ml) for 72 hours. Clusterin secretion was assessed via ELISA analysis. Bars represent the mean ± SEM of three experimental replicates; ****$P < 0.0001$ compared to untreated controls.

3.9.6 Summary

The experiments reported in this section have explored the production and *in vitro* effects of exogenous clusterin on pro-inflammatory and anti-inflammatory cytokine/ chemokine secretion in primary alveolar, blood-derived macrophages and BEAS-2B cells. The principle findings reported in this section are;

- Clusterin receptor LRP-2 localises to bronchial epithelial cells in control lung. Alveolar macrophages of control lung tissue express clusterin receptor LRP-2 on the cell surface.

- Localisation and intensity of LRP-2 in IPF lung tissue is similar to that of control lung. However in fibrotic lung LRP-2 was located to increased numbers of alveolar macrophages.

- Exogenous clusterin induces the secretion of TNFα in alveolar macrophages, in bronchial epithelial cells (BEAS-2B) and in co-culture of both cell types.

- Exogenous clusterin induces the secretion of TNFα, pro-inflammatory cytokines/chemokines and MMP-9 in human blood derived, unpolarised macrophages.

- Exogenous clusterin does, however, not alter protein secretion during the polarisation towards an “M1” or “M2” phenotype, when polarised in the presence of LPS/IFNγ or IL-4.

- The induction of pro-and anti-inflammatory cytokines by exogenous clusterin in human blood-derived macrophages is dose dependent. TNFα neutralising antibody attenuates the effect of exogenous clusterin on induced cytokine secretion.

- Polarisation towards an “M1” phenotype induces the secretion of clusterin in human blood-derived macrophages. This may provide an autocrine feedback loop to induce “M1” polarisation in unpolarised “M0” macrophages.

4 Discussion

4.1 Overview

The development of pulmonary fibrosis is incompletely understood. Although aberrant injury repair mechanisms, with persistence of increased numbers of fibroblast/myofibroblast cells driving excess production of extracellular matrix proteins, are considered to be central to its pathogenesis (McAnulty 2007). It is, therefore, essential to understand the mechanisms, which contribute to the development of fibrosis. Protein signatures of IPF-BALF may provide new insights into mechanisms associated with altered proteins linked to disease pathology. Clusterin, a multifunctional protein, has been identified as one of 15 proteins reduced in BALF of IPF patients when compared with healthy controls (T. H. Kim et al. 2010). Clusterin is ubiquitously expressed and has been reported to regulate multiple cell functions of fundamental importance both inside and outside cells (Kapron et al. 1997; Carnevali et al. 2006).

To date there is little information on the distribution and role of clusterin in the normal human lung, the study from Kim et al. is currently the only report that adumbrates an association of clusterin with the pathology of pulmonary fibrosis. Interestingly, in other human disease and animal models up or down-regulation of clusterin was associated with diminution or enhancement of fibrogenesis respectively: In human liver fibrosis clusterin was one of the top five markers with the highest reliability to change expression between the early stages and more advanced hepatic fibrosis (Gangadharan, Bapat, Rossa, Robin Antrobus, et al. 2012). Furthermore, clusterin-deficient mice exhibited accelerated renal fibrosis in response to unilateral ureteral obstruction, when compared with wild type-mice (Jung et al. 2012). In addition, clusterin has been suggested to act as a primary cellular defence mechanism against progressive injury associated with progressive intestinal fibrosis in dogs (Greer et al. 2006). However, the localisation of clusterin in normal and fibrotic lung, the mechanisms contributing to its down-regulation in IPF-BALF and its role in the normal lung as well as in the pathogenesis of pulmonary fibrosis have not been investigated. These observations led to the generation of the hypothesis examined in this thesis; **that clusterin plays an important role in normal human lung homoeostasis and changes in clusterin distribution and expression may be protective against the pathogenesis of pulmonary fibrosis.**

To begin to address this hypothesis clusterin distribution was examined in human control and IPF lung tissue. This study immunohistochemically examined the expression and localisation of clusterin in normal and fibrotic human lung. This analysis demonstrated that in human control lung clusterin associated with fibroblast-like cells, bronchial epithelial cells and elastin in vessel walls. To question disease relevance, staining for clusterin in fibrotic lung was performed and compared with intensity and staining pattern in normal lung tissue. Strikingly, this analysis demonstrated weak or undetectable clusterin staining of fibroblasts in fibrotic regions but not in morphologically normal areas of fibrotic lung. Utilising fibroblast isolated from control and fibrotic lungs this observation was validated *in vitro*: Messenger and protein expression analysis confirmed that clusterin levels were decreased in fibrotic lung fibroblasts compared with controls. Further *in vitro* analysis revealed that TGF-β_1 is capable of down-regulating clusterin expression in control fibroblasts, as demonstrated by mRNA, immunocytochemistry and western blot analysis. Since TGF-β_1 mediates the differentiation of fibroblasts to myofibroblasts (Desmoulière et al. 1993), it was investigated if TGF-β_1-mediated myofibroblast differentiation is dependant on TGF-β_1-induced clusterin down-regulation. However, shRNA-mediated down-regulation of clusterin did not affect TGF-β_1-induced fibroblast differentiation assessed by αSMA expression, collagen I expression and deposition. Since there was no evidence for a role of clusterin in fibroblast differentiation, other fibroblast functions in response to altered intracellular and extracellular clusterin were addressed: In IPF several lines of evidence demonstrate that uncontrolled fibroblast accumulation is at least partly due to enhanced fibroblast migration (Suganuma et al. 1995; Sakai & Andrew M Tager 2013), proliferation (Calabrese et al. 2005; Khalil et al. 2005a) and fibroblast/myofibroblast resistance to apoptosis (Maher et al. 2010; Moodley et al. 2004).

Based on the characteristic pattern of staining and differences observed in fibrotic lung the functional effects of clusterin on human lung fibroblast proliferation, migration and apoptosis *in vitro* in fibroblasts isolated from control and fibrotic lung were investigated. To model the effects of clusterin-deficiency in lung fibroblasts, fibroblasts from one control lung were isolated and clusterin messenger RNA and protein expression was stably silenced via shRNA-mediated knockdown targeting clusterin mRNA. Although this procedure was performed for fibroblasts from another control lung, the affects of clusterin-deficiency on fibroblast differentiation and function were only studied in cells derived from one donor. These studies provide first insights into clusterin dependent effects in lung fibroblasts and were established to model for the effects of clusterin in this cell type. Administration of human plasma-derived clusterin was used to model changes in secretory clusterin levels. Clusterin has been previously reported to

promote proliferation of epithelial and vascular smooth muscle cells after injury (Nguan et al. 2014; Miyata et al. 2015). To study if clusterin is involved in regulating fibroblast proliferation of control and fibrotic lung fibroblasts, cell proliferation in response to proliferative and anti-proliferative stimuli was assessed via a DAPI-cell count based proliferation assay. High-throughput fluorescence analysis of DAPI stained nuclei showed that shRNA-induced clusterin-deficiency decreased fibroblast proliferation in response to serum, suggesting that clusterin is involved in regulating fibroblast proliferation. In contrast, fibrotic lung fibroblasts with low clusterin levels exhibited a hyperproliferative phenotype compared with non-fibrotic control fibroblasts that express higher levels of clusterin. Differences in the proliferative response in control compared with fibrotic lung fibroblasts may be unrelated to diminished clusterin expression. Consistent with previous studies in our group and others (Maher et al. 2010; Moodley et al. 2004), FACS analysis demonstrated that fibroblasts isolated from fibrotic lung tissue were resistant to FasL-induced apoptosis when compared with control lung fibroblasts. Additionally, results in this thesis suggest that shRNA-mediated down-regulation of clusterin-induced basal and FasL-induced apoptosis in control fibroblasts, which was overcome by addition of exogenous clusterin. This supports that clusterin is involved in protecting lung fibroblasts from basal and FasL-induced apoptosis. Interestingly, when assessing the effects of exogenous clusterin on FasL-induced apoptosis; it became evident that exogenous clusterin tended to further potentiate resistance to apoptosis in fibrotic lung fibroblasts. This suggests that the down-regulation of clusterin in IPF fibroblasts may be a physiologically appropriate, but insufficient, response of these cells intended to limit the development of an environment favouring unopposed fibroproliferation.

Apart from a fibrosis-specific alteration in clusterin expression in fibrotic lung fibroblasts, immunohistochemical staining demonstrated that clusterin staining was associated with amorphous elastin-rich deposits, a characteristic hallmark within fibrotic regions in IPF (Parra et al. 2007). Future studies would be necessary to confirm the cause for this association, but the current literature suggests that clusterin, known to act as extracellular chaperone, may prevent protein aggregation or clearance of defective or degraded elastin (Janig et al. 2007; Poon et al. 2002; Bartl et al. 2001). While clusterin was sporadically expressed in bronchial epithelial cells of normal adult lung; clusterin staining was both more frequent and intense in IPF lungs. The increased expression of clusterin in the bronchial epithelium in IPF may be a reflection of epithelial stress/injury or, alternatively, a component of the aberrant re-expression of development genes that occurs in IPF (Selman et al. 2008).

Alveolar macrophages express clusterin receptor LRP2, suggesting that these cells are responsive to altered clusterin levels in the lung. *In vitro* studies with human alveolar and blood-derived macrophages, demonstrate that exogenous clusterin induces the secretion of pro-inflammatory cytokines/chemokines, including TNFα. Reduced levels of secretory clusterin in IPF may potentially promote the polarisation towards an "M2" macrophage phenotype, which has been shown to contribute to the pathogenesis of IPF (Stahl et al. 2013; Schupp et al. 2015; Keane 2008; Byrne et al. 2016).

In summary, the results presented in this thesis support the notion that in lungs of patients with IPF reduced clusterin is at least partly, due to a combination of TGF-β_1-mediated down-regulation of fibroblast synthesis and increased binding to elastin. This appears to represent an appropriate but insufficient response to limit fibroproliferation.
In IPF elastin-associated clusterin may exert its chaperoning activity in order to contribute to the quality control of extracellular matrix proteins. Additionally, *in vitro* experiments with alveolar and blood-derived macrophages demonstrated that macrophages are polarised towards an "M1-like" phenotype in response to human plasma-derived clusterin. In turn, reduced levels of secretory clusterin in the fibrotic lung may, therefore, benefit a polarisation towards "M2-like" macrophages, which produce pro-fibrotic mediators, including TGF-β_1, resulting in further reduction of secretory clusterin by lung fibroblasts and progression of pulmonary fibrosis.

Ultimately, this suggests that the alterations of clusterin distribution and expression in fibrotic lung are a protective mechanism against the progression of fibrosis in the lung. However, further studies are required to fully understand the complex biology of clusterin in normal human lung and its role in the pathogenesis of pulmonary fibrosis. The following sections will discuss these findings and their implications in more detail.

4.2 Clusterin expression in control and fibrotic lung

To our knowledge, this is the first comprehensive demonstration of clusterin expression in normal compared with fibrotic lung. Although analysis of clusterin expression in bronchial biopsy specimens of smokers and non-smokers has been reported previously (Carnevali et al. 2006), a detailed analysis of clusterin expression and distribution in the human lung has not been performed. Carnevali and colleagues showed that clusterin was mildly expressed in sections of bronchial biopsy specimens and immunostaining was markedly increased in the submucosa of biopsy specimens obtained from active smokers (Carnevali et al. 2006). Carnevali et al. conclude in their report, that clusterin may have a protective effect in the airways of smokers. This report, however, did not outline the cell specific clusterin expression and potential implications in cell function. Furthermore, fibrosis relevant changes in clusterin distribution in the human lung remain unreported. Consequently, immunohistochemical staining was performed to address in detail how clusterin is distributed in the normal compared with fibrotic lung.

Immunohistochemical analysis revealed that clusterin staining was sporadically associated with bronchial epithelial cells in normal adult lung (section 3.2.1,Figure 3.1B) but was more extensive in lung tissue from IPF patients (Figure 3.2C). Previous reports indicated that in rodents, clusterin is expressed embryologically in the lung epithelium during branching morphogenesis (French et al. 1993; Nyeng et al. 2008; Zheng et al. 2013) but is not expressed in post-developmental or healthy adult bronchial epithelium (Nyeng et al. 2008; Zheng et al. 2013). Infection and injury have been reported to induce the expression of clusterin in bronchial epithelium (Zheng et al. 2013), epithelium of other organs including the ileum of Crohn's disease patients (Gassler et al. 2001) and in experimental kidney injury (Jung et al. 2012) where clusterin is thought to be protective. The increased expression of clusterin in the bronchial epithelium in IPF may, therefore, reflect epithelial stress/injury or, alternatively, a component of the aberrant re-expression of development genes that occurs in IPF (Selman et al. 2008).

4.2.1 Clusterin is associated with elastin in the lung.

Immunolocalisation of clusterin clearly demonstrated its association with elastin in vessel walls (section 3.2.3). Staining was increased in IPF lung and was also observed in amorphous elastin-rich deposits within fibrotic regions (Figure 3.2E-H). Elastin

deposition has previously been shown to be increased in IPF lungs compared with controls (Rozin et al. 2005; Enomoto et al. 2013), but there is also evidence for increased levels of neutrophil elastase- and MMP7-mediated elastin degradation in IPF (Jacob H Kristensen et al. 2015; J H Kristensen et al. 2015). The increase of elastin in the IPF lung has been suggested to be a process of “fibroelastosis”; a process in which a reactivation of elastin synthesis follows increased elastin destruction in disease. However, this elastin synthesis occurs in a disordered manner, contributing to a distortion of the alveolar architecture (Rozin et al. 2005). Consequently, increased abundant accumulation of elastic fibres in fibrotic areas of the lungs of patients with IPF has been associated with poor prognosis (Enomoto et al. 2013). Enomoto and colleagues suggested that mechanisms preventing the aberrant accumulation of elastic fibres in the lung might present a therapeutic target in fibrotic disease.

Clusterin has previously been found to associate with elastin in the human photo-aged skin (Janig et al. 2007), cirrhotic liver (Aigelsreiter et al. 2009) and exfoliation syndrome (Zenkel & Schlötzer-Schrehardt 2014) but has not previously been observed in association with elastic fibres in patients with pulmonary fibrosis. Several potential explanations have been proposed for the association of clusterin with elastin. Clusterin, like small heat shock proteins, is a molecular chaperone which, through hydrophobic interactions, is able to bind and stabilise partially folded, stressed proteins and long-lived protein intermediates that slowly aggregate, including elastin, shielding and preventing their precipitation (Janig et al. 2007; Poon et al. 2002). Alternatively, clusterin may contribute to the clearance of defective and degraded elastin via megalin/gp330 receptor-mediated endocytosis (Bartl et al. 2001; Janig et al. 2007). Further studies would be necessary to determine the precise role of the association of clusterin with elastin in normal and fibrotic lung. Unfortunately, in the context of this, thesis it did not prove to be possible to further study the association of clusterin with elastin.

4.2.2 Clusterin expression in lung fibroblasts.

Immunohistochemical clusterin staining of control and fibrotic lungs presented in this thesis provides evidence for a strong staining of clusterin in fibroblasts in the alveolar septum of normal human lung (Figure 3.1, section 3.2.1). Similar staining was observed in apparently normal areas of IPF lung but in fibrotic regions staining for clusterin was weak or undetectable, especially in fibroblasts/myofibroblasts in fibroblastic foci (section 3.2.2). Furthermore, weak clusterin staining was associated with areas of strong TGF-β_1 staining and αSMA positive cells (Figure 3.4 and Figure 3.8). This observation is in accordance with findings in clusterin-deficient mice, in which αSMA-positive myofibroblasts were more frequent when compared with wild-type mice (Jung et al. 2012). However, the functional role of clusterin in lung fibroblasts and the mechanisms by which it is regulated remain unknown. Potential mechanisms for the regulation of clusterin and its role in mediating pro-fibrotic cell functions were investigated in control lung fibroblasts and compared with effects on fibrotic lung fibroblasts and are discussed in the following sections.

4.3 *In vitro* assessment of clusterin expression in human control and fibrotic lung fibroblasts and its regulation by TGF-β_1.

In order to verify if changes in clusterin expression between control and fibrotic lung fibroblasts are preserved *in vitro,* clusterin expression was assessed in fibroblasts isolated from control and fibrotic lung. Preliminary data obtained by Dr Toby Maher via protein array analysis suggested that clusterin is detectable at high levels in control but not in fibrotic lung fibroblasts (Figure 3.7B). Dr Maher emphasised that changes in relative clusterin protein levels were the most prominent difference between control and fibrotic lung fibroblasts compared with other proteins on the apoptosis array. In order to verify this preliminary data, microarray, RT-qPCR and immunofluorescence analysis were performed to determine clusterin mRNA and protein expression in control compared with fibrotic lung fibroblasts. Overall, clusterin expression analysis *in vitro* confirmed that fibrotic lung fibroblasts express lower clusterin levels when compared with fibroblast isolated from control lung (Figure 3.7). This is consistent with immunohistochemical observations discussed in section 4.2, where fibroblasts/myofibroblasts in IPF lung, predominantly fibroblast forming fibroblastic foci demonstrated reduced staining of clusterin when compared with fibroblasts derived from normal lung.

In the course of this thesis, Dr Nisha Kanda established a 3D spheroid model with fibroblasts from control and fibrotic lung and analysed the expression profile for spheroids in both groups via microarray analysis. Amongst others, clusterin expression was significantly down-regulated in spheroids formed by fibrotic lung fibroblasts compared with ones that were formed by control lung fibroblasts (10 cell lines each, $p = 0.023$), and verified the data generated *in vivo* via immunohistochemistry and *in vitro* culture (section 3.2 and 3.3). In response to this finding, further investigations focused on the mechanism by which, clusterin may be reduced in fibrotic lung fibroblasts.

To elucidate a potential mechanism by which clusterin may be regulated in lung fibroblasts, regulatory mechanisms of clusterin in other cell types were reviewed. TGF-β_1 has been previously reported to up-regulate clusterin expression in mammary epithelial cells, where clusterin expression was suggested as functionally important for epithelial cell differentiation (Itahana et al. 2007). Similarly, TGF-β_1 is a major profibrotic mediator, which drives myofibroblast differentiation and excessive collagen deposition in pulmonary fibrosis (Fernandez & Eickelberg 2012; Scotton & Chambers 2007).

To explore potential regulatory effects of TGF-β_1 on clusterin expression *in vitro*, control fibroblasts were exposed to a dose of 1 ng/ml (40 pM) TGF-β_1, which is known to stimulate myofibroblast differentiation as demonstrated in section 3.4.1 and previous reports (Tiggelman et al. 1997; Guo et al. 2009; Evans et al. 2016). Exposure of control lung fibroblasts to TGF-β_1 resulted in a significant down-regulation of clusterin expression over time, with a significant decrease in clusterin mRNA at 24 hours after exposure to TGF-β_1 and persistent down-regulation of clusterin protein was maintained until at least 48 hours as demonstrated via immunofluorescence and Western blot analysis (see section 3.3.4.). This data is in contrast with previous studies in epithelial cells in which TGF-β_1 has been reported to up-regulate clusterin expression (Itahana et al. 2007; Wegrowski et al. 1999) and suggests that the effects of TGF-β_1 on clusterin expression are cell and tissue specific. It is noticeable that TGF-β_1 at a concentration that is known to induce myofibroblast differentiation was sufficient to reduce clusterin expression. It was, therefore, of importance to clarify whether the pro-fibrotic effects of TGF-β_1 induced myofibroblast differentiation are mediated by down-regulation of clusterin in lung fibroblasts.

4.4 *In vitro* assessment of the effects of clusterin-deficiency on fibroblast differentiation

Under normal physiological conditions in response to lung injury, fibroblasts differentiate to myofibroblast as part of a proliferative phase during normal wound healing (Darby et al. 2014). Myofibroblasts exhibit a contractile phenotype as a result of increased stress fibre formation and secrete high levels of ECM proteins, such as collagen type I, in order to enable contraction and to strengthen the wound (Darby et al. 2014). Phenotypically, myofibroblasts are an intermediate cell type between fibroblasts and smooth muscle cells and can be identified by the expression of increased levels of αSMA (Desmoulière et al. 1993; Skalli et al. 1986). Myofibroblasts become most abundant in the proliferation phase during wound healing, and progressively undergo apoptosis during the resolution phase, which signals the onset of the maturation phase for normal functional tissue (Horowitz & Thannickal 2006). Dysregulation of the wound repair-response can result in uncontrolled myofibroblast accumulation, fundamentally contributing to the development of fibrosis (Desmouliere et al. 2005; Gabbiani 2003; Hinz et al. 2001). To date, the mechanisms that involve aberrant myofibroblast differentiation and accumulation are incompletely understood and key mediators orchestrating these processes, are a focus of research (Chambers 2008).

In order to assess the role of clusterin in myofibroblast differentiation, control fibroblasts were genetically modified to downregulate clusterin expression. An overexpression of clusterin in control lung fibroblasts was not induced since previous literature suggested that clusterin overexpression induces apoptosis within 24h in fibroblast-like synoviocytes (Devauchelle et al. 2006). Consequently, clusterin silencing seemed to be a suitable model to study multiple cell functions.

As described in this thesis, transfection with siRNA targeting the clusterin gene significantly reduced clusterin mRNA but not protein levels in lung fibroblasts (see section 3.4.2). One potential explanation for an impaired knock-down of clusterin protein levels via siRNA could be that clusterin half-life is increased, when clusterin associates with a wide range of other proteins, including GRP78, which at least in part may be responsible for a persistence of clusterin protein over time (Li et al. 2013). The half-life of secretory clusterin was significantly prolonged via overexpression of secretory clusterin interaction partner GRP78 (424 hours), suggesting that GRP78, a member of the HSP70 family, contributes to clusterin stability (Li et al. 2013). While the reason for an impaired clusterin protein knock-down via siRNA remains unknown, functional consequences of clusterin-deficiency *in vitro* were assessed via stable shRNA-mediated knockdown of clusterin in control lung fibroblasts.

Additionally, for this thesis, previously made observations on TGF-β_1-induced αSMA expression and collagen I deposition in human lung fibroblasts were verified *in vitro*. TGF-β_1 dose and time responses were studied, and αSMA expression was analysed via fluorescence microscopy and Western blotting (Figure 3.11B and Figure 3.10A). Consistent with previous results in the literature, TGF-β_1 induced αSMA expression at a dose of 1 ng/ml in human lung fibroblasts (Desmoulière et al. 1993), as demonstrated in section 3.4.1. Reassuringly, the time-response experiment at this concentration resulted in a maximal αSMA protein expression by 48 hours (Figure 3.10A), as previously described (Thannickal et al. 2003). In order to assess collagen deposition *in vitro* a so-called "scar in a jar" assay was established in our laboratories, according to the procedure first described by Chen and colleagues (Chen et al. 2009). Although basal collagen production/deposition is expected in lung fibroblasts as a homeostatic process to maintain the normal structure and function of the lung tissue, it is noteworthy that relatively high collagen deposition was observed at baseline, in control and clusterin-deficient fibroblasts (section 3.4.4.), similarly to studies performed by Chen et al. This may underlay an effect of autocrine TGF-β_1 secretion by lung fibroblasts (Kelley et al. 1991) or an effect induced by "matrix" stiffness since the fibroblasts were grown on plastic tissue culture dishes (Petersen et al. 2012). Similarly to αSMA expression collagen deposition was dependant on increasing TGF-β_1 concentrations at 72 hours as demonstrated via immunocytochemistry analysis in section 3.4.4 (Figure 3.11A). Collagen deposition in response to TGF-β_1 appeared to reach a maximum at 1 ng/ml and did not increase beyond these levels at a concentration higher than 1 ng/ml.
On this basis, subsequent myofibroblast experiments were performed using a concentration of TGF-β_1 of 1 ng/ml for 48 hours in 0.4 % FBS in DMEM, to assess the consequences of clusterin-deficiency on TGF-β_1-induced myofibroblast differentiation. Although, basal and TGF-β_1-induced changes in collagen I levels varied between clusterin-deficient, mock-transduced and control fibroblasts, the overall fold-increase in collagen mRNA and deposition levels did not significantly change (Figure 3.14). Figure 3.14 demonstrated that TGF-β_1 down-regulated clusterin expression at 20 hours and 48 hours (Figure 3.14B), which is consistent with changes described in section 3.3.4. Consistent with results for collagen and αSMA mRNA basal and TGF-β_1 induced αSMA protein and collagen deposition did not vary between control mock-transduced and clusterin-deficient lung fibroblasts (Figure 3.14C and Figure 3.15).

In conclusion, results in section 3.4.4 show that shRNA-mediated down-regulation of clusterin did not affect basal or TGF-β_1-induced fibroblast differentiation, as assessed by αSMA expression, collagen I expression and deposition when compared with mock-

and untransduced controls. This suggests that the TGF-β_1-induced down-regulation of clusterin is independent of its effects on fibroblast to myofibroblast differentiation. These results are consistent with two independent experiments in fibroblasts from one control lung cell line and model for the effects of clusterin-deficiency in lung fibroblasts. Additional studies in lung fibroblasts from other control lung donors would be required to prove reproducibility in fibroblasts from other donors. These findings contrast with reports in smooth muscle cells where clusterin has been suggested to be involved in phenotypic modulation and differentiation (Liu et al. 2015; Moulson & Millis 1999). Furthermore, a reduction in clusterin expression was associated with increased αSMA expression in smooth muscle cells (Orlandi et al. 2005). Other studies in renal tubular epithelium-like cells, suggested that TGF-β_1-induced type I collagen expression was reduced in a dose-dependent manner when clusterin was overexpressed (Jung et al. 2012). Moreover, Jung and colleagues reported that type I collagen and αSMA protein were induced in response to renal injury in clusterin-deficient mice compared with wild-type controls (Jung et al. 2012). The contradictory effects of clusterin-deficiency on αSMA expression and collagen deposition in lung fibroblast could point towards tissue or model specific effects and underline once again the complexity of clusterin biology.

4.5 Consequences of altered clusterin expression on migration in control and fibrotic lung fibroblasts

Fibroblasts play a key role in mediating tissue remodelling after injury and are rapidly recruited to the wound site. *In vitro* studies with fibroblasts from fibrotic regions compared with fibroblasts from healthy lung suggest that fibrotic lung fibroblasts display increased migratory activity (Suganuma et al. 1995). Furthermore, it has been shown that fibrotic lung fibroblasts close wounds faster than fibroblasts from healthy lung as assessed in co-culture with A549 epithelial cells *in vitro* (Prasad et al. 2014). Fibroblast migration may, therefore, play a role in the pathogenesis of pulmonary fibrosis leading to increased fibroblast accumulation in fibrotic areas. There is currently little known about the pathway that is accountable for the invasive migratory phenotype in fibrotic lung fibroblasts compared with control lung fibroblasts. White et al. suggested that $\alpha_4\beta_1$ integrin signalling induces a migratory phenotype in fibrotic lung fibroblasts, inducing tissue invasion in *in vitro* models (White et al. 2003). A more recent study from Chen et al. demonstrated that matrix stiffness regulates increased basement membrane invasion by myofibroblasts via mechanosensing integrin $\alpha_6\beta_1$ (H. Chen et al. 2016b). Clusterin has been demonstrated to be involved in the regulation of migration

in many cell types, including macrophages and lung cancer cells *in vitro* (Y.-J. Shim et al. 2012; C.-Y. Cheng et al. 2012). Yet the role of clusterin in lung fibroblast migration is unexplored. In this thesis, the effects of clusterin-deficiency or exogenous clusterin on lung fibroblast migration were determined via scratch closing assay and transwell migration assay analysis. The limitations of these assays are, however, that they do not allow a definitive separation between fibroblast migration and proliferation. Results in Figure 3.16 show that basal scratch closure in 0.4 % FBS in DMEM did not vary between control, mock-transduced and clusterin-deficient-fibroblasts. This was assessed by the time that control, mock-transduced and clusterin-deficient fibroblasts needed to close an 800 µm wide scratch in six wells of a 96-well plate. Since the time needed to close the scratch was not significantly different in non-transduced and mock-transduced fibroblasts, subsequent scratch assay experiments with clusterin-deficient fibroblasts were compared with mock-transduced controls. In the light of previous studies, it was interesting to assess the time of scratch closure in response to TGF-β_1: Studies with rat lung fibroblasts have demonstrated that TGF-β_1 does not regulate migration (Osornio-Vargas et al. 1993). Contrarily, TGF-β_1 has been described to be a potent chemoattractant for dermal fibroblasts (Arnold E Postlethwaite et al. 1987). Here, the effects of scratch closure in clusterin-deficient and control lung fibroblasts are discussed: Up until about 16 - 24 hours after disrupting the monolayer mock-transduced and clusterin-deficient fibroblasts fill the scratch area at a similar rate (Figure 3.16). From 16 - 24 hours the rate at which the scratch closure occurs is divergent with TGF-β_1-treated cells closing the scratch more slowly in control but not in clusterin-deficient cells. This observation was confirmed in two independent experiments via scratch assay analysis and suggests that clusterin is essential in TGF-β_1-induced delayed scratch closure. One possible explanation for this is that TGF-β_1 induces the differentiation into myofibroblasts but this seems unlikely since it was already demonstrated in this thesis that clusterin deficiency does not affect TGF-β_1-induced myofibroblast differentiation. One explanation for this divergence could be that at 16 - 24 hours cells mock-transduced and clusterin-deficient lung fibroblasts differ in their proliferation rate, resulting in divergent numbers of fibroblasts contributing to the scratch closure. One limitation of this scratch assay is that scratch closure is likely mediated by a combination of fibroblast migration and proliferation and a TGF-β_1-induced delay in scratch closure may be caused by proliferative or migratory effects. The duration of this assay was up to 42 hours before the scratch was closed by all fibroblasts groups. Since the relative scratch closure was only divergent after 16 hours it seems more likely that the effect was related to changes in proliferation since this would be expected to start to show and effect at around 24 hours. To address this, an

alternative assay had to be established, to reduce potential effects of varying proliferation between cell groups to focus on the migratory response in response to altered clusterin expression. Therefore, same conditions were applied in a transwell assay, but the experiment was limited to 19 hours to limit proliferative effects in 0.4 % FBS in DMEM.

In contrast, results derived in two independent experiments obtained via transwell assay showed that TGF-β_1 at concentrations ranging from 0-5 ng/ml did not affect the number of control lung fibroblasts that had migrated through the transwell membrane pores within 19 hours (Figure 3.17D). A possible reason for these contrasting results obtained in scratch assay and transwell assays may be related to different endpoints between both assays. In the presence of TGF-β_1 human fibroblasts have been demonstrated to form nodules over time (Xu et al. 2007). This has been observed in some wells in the scratch assay videos (< 96 hours). TGF-β_1-induced nodule formation could reduce the number of lung fibroblasts free to migrate towards the scratch area contributing to the scratch closure. It is, therefore, challenging to assess lung fibroblast migration in response to TGF-β_1 over a longer period of time. In order to allow enough time for the lung fibroblasts to migrate through the transwell membrane but limit nodule formation and proliferation, transwell analysis with mock-transduced and clusterin-deficient lung fibroblasts was performed for only 19 hours. At 19 hours no nodule formation was observed microscopically. These conditions were, therefore, used to assess the migratory response of clusterin-deficient lung fibroblasts compared to mock-transduced controls. Results in (Figure 3.18A) demonstrate that the number of cells that had migrated through the transwell membrane was not significantly different for clusterin-deficient fibroblasts when compared to mock-transduced controls. Together, this suggests that clusterin-deficiency does not effect fibroblast migration in response to TGF-β_1 when compared with controls.

Secretory clusterin has previously been shown to increase migration of macrophages at doses form 0 - 4 µg/ml (Y. J. Shim et al. 2012) but decreased migration in vascular smooth muscle cells (Millis et al. 2001). To begin to examine the effects of exogenous clusterin on migration in control and clusterin-deficient lung fibroblasts, the number of migrated cells in response to 10 µg/ml exogenous clusterin was assessed. Similar to results with TGF-β_1, the migratory response in mock-transduced and clusterin-deficient fibroblasts was not altered in the presence of exogenous clusterin (10 µg/ml) although lower concentrations than 10 µg/ml have been shown to induce migration of

macrophages (Y.-J. Shim et al. 2012). These results suggest that exogenous clusterin may not be involved in regulating lung fibroblast migration *in vitro*.

To test the migratory response of clusterin-deficient fibroblasts at a higher magnitude the effects of pro-migratory PDGF-BB were tested in mock-transduced and clusterin-deficient fibroblasts. As demonstrated in section 3.5.2 a PDGF-BB concentration of 25 ng/ml increased the migratory response by approximately three-fold in control fibroblasts compared with a response without PDGF-BB (Figure 3.17). This concentration has been already established in migration studies with lung fibroblasts (Bonner et al. 1991; Panzhinskiy et al. 2012). Figure 3.18A demonstrates that clusterin-deficiency did not significantly result in altered numbers of migrated cells in response to PDGF-BB compared with controls. This suggests that reduced intracellular clusterin levels do not affect the migratory response in lung fibroblasts.

In conclusion, data generated via transwell assay (Figure 3.18) appears to focus on migratory effects and limit proliferative effects. Analysis via transwell assays and suggests that clusterin-deficiency (intracellular) and exogenous clusterin are not involved in regulating basal, TGF-β_1 or PDGF-BB induced migration *in vitro*. An increased duration of endpoints (<96 hours) when assessing fibroblast migration, pointed towards divergent proliferation that may have had an effect on the duration that was needed to close the scratch area.
In order to investigate if clusterin-deficiency has an effect on fibroblast proliferation, in response to PDGF-BB and TGF-β_1, the consequences of altered clusterin expression on proliferation of control and fibrotic lung fibroblasts were studied *in vitro*, and results are discussed in section 4.6.

4.6 Consequences of altered clusterin expression in control and fibrotic lung fibroblasts on proliferation

Besides increased fibroblast migration, enhanced proliferation has been suggested to be one of the causes for increased fibroblast and myofibroblast accumulation in fibrotic disease (Mio et al. 1992), particularly in response to TGF-β_1 (Chambers et al. 2003). In contrast, PGE_2 has previously been shown to reduce proliferation in human lung fibroblasts (McAnulty et al. 1997; Keerthisingam et al. 2001).
To begin to explore the role of clusterin in regulating proliferation, the proliferative response to serum, TGF-β_1, PGE_2 and exogenous clusterin in clusterin-deficient and

fibrotic lung fibroblast was compared with controls. For this purpose, cell numbers were assessed over time (48 - 96 hours) by counting DAPI-stained nuclei in a high-throughput fluorescence assay (section 2.14.3). For each experiment, as well as all other experiments in this thesis that are cell number sensitive, initially seeded cell numbers for each group were assessed and checked for equal numbers (an example is given in Figure 3.19). Increasing cell numbers over time were compared with cell numbers of controls (0.4 % FBS in DMEM) for each time-point and changes expressed as percent change relative to controls. As expected for control lung fibroblasts increasing serum concentrations induced proliferation in both control and clusterin-deficient lung fibroblasts (Two-way ANOVA $P < 0.0001$) at 72 hours (Figure 3.19B). Therefore, FBS concentrations and the endpoint of 72 hours provide a good magnitude of effects to explore the effects of clusterin-deficiency on proliferation.
Nonetheless, Figure 3.19 demonstrates that the response to serum-induced proliferation was diminished by approximately 50 % in clusterin-deficient fibroblasts compared with controls. This suggests that clusterin is involved in regulating fibroblast proliferation since clusterin-deficiency reduces the proliferative response to serum *in vitro*. These results are consistent with findings in two other independent experiments using fibroblasts derived from one donor and are in accordance with reports of clusterin promoting proliferation in VSMC *in vitro* (Miyata et al. 2015).

To further explore the role of clusterin in fibroblast proliferation, the proliferative response to PGE_2 was examined in mock-transduced and clusterin-deficient lung fibroblasts. PGE_2 concentrations from 0 - 1 µM reduced cell numbers in control lung fibroblast in trend but this was not significant (Figure 3.19D). At a higher concentration (2.5 µM) PGE_2 reduced the cell numbers of clusterin-deficient fibroblasts significantly when compared to fibroblasts from control lung fibroblasts ($p < 0.05$, Figure 3.20A). A reason for the reduction in cell numbers in response to PGE_2 could be PGE_2 induced growth arrest, which has been reported previously (Fine & Goldstein 1987). The data in Figure 3.20A suggests that clusterin-deficient lung fibroblasts are sensitised to PGE_2-induced growth arrest when compared to controls. Another explanation for reduced cell numbers in response to PGE_2 could be the induction of apoptosis by PGE_2 as previously reported for lung fibroblasts (Huang et al. 2009). A preliminary study via FACS analysis in line with this hypothesis (section 3.6.4, Figure 3.21A, B), supports that decreased cell numbers in response to PGE_2 may be a consequence of PGE_2-induced apoptosis as assessed in fibroblasts from control lung. In control lung fibroblasts PGE_2 induced apoptosis at a concentration of 1 µM at 48 h ($p< 0.0001$) (Figure 3.21). Although PGE_2-induced apoptosis was not studied for clusterin-deficient

lung fibroblast in line with this thesis the section 4.7 will address if clusterin-deficiency is associated with increased lung fibroblast apoptosis.

Furthermore, the proliferative response to altered exogenous clusterin levels was studied in clusterin-deficient and control lung fibroblasts. As has been shown in line with this work, lung fibroblasts secrete clusterin (Figure 3.6 and Figure 3.13) and may, therefore, impact on proliferation levels by increased clusterin secretion. The results in Figure 3.20A, however, suggest that secretory clusterin does not affect fibroblast proliferation in control or clusterin-deficient fibroblasts since cell counts were not altered in response to exogenous clusterin. Ultimately, this data suggests that intracellular rather than secretory/ exogenous clusterin regulates fibroblast proliferation.

In contrast, fibroblasts derived from IPF lung with reduced clusterin expression (as demonstrated in section 3.3.2), exhibited a hyperproliferative phenotype compared with non-fibrotic control fibroblasts that express higher levels of clusterin (Figure 3.20B). The reason for this is not known but is likely due to a potential dominance of clusterin-independent, pro-proliferative mechanisms in fibrotic lung fibroblasts, resulting in enhanced proliferation despite low clusterin expression. For example, the inability of fibrotic lung fibroblasts to up-regulate COX-2 and subsequently $PGE_{2,}$ which is a potent inhibitor of fibroblast proliferation, in response to TGF-β_1 (Maher et al. 2010), results in TGF-β_1-induced PDGF expression and enhanced proliferation of fibrotic lung fibroblasts (McAnulty et al. 1997). This would be consistent with the results presented here.

Together, the results in this section suggest that clusterin-deficient fibroblasts and fibrotic lung fibroblasts with naturally low clusterin expression display reduced proliferation in response to PGE_2 when compared with baseline conditions. This observation may be due to the anti-proliferative effects of PGE_2 as outlined earlier (McAnulty et al. 1997), but this observation could also be justified by pro-apoptotic properties of PGE_2. The observations outlined in this section suggest that clusterin-deficiency may affect lung fibroblast apoptosis. Consecutive studies focused, therefore, on the effect of clusterin-deficiency on basal and FasL-induced apoptosis.

4.7 Consequences of altered clusterin expression in control and fibrotic lung fibroblasts on apoptosis

In IPF several lines of evidence demonstrate that uncontrolled fibroblast accumulation is at least partly due to fibroblast/myofibroblast resistance to apoptosis (Maher et al. 2010; Moodley et al. 2004). Detailed studies have demonstrated that human lung fibroblasts from fibrotic lung are resistant to Fas-mediated apoptosis when compared with fibroblasts derived from normal lung (Tanaka et al. 2002). Additional studies have shown that fibroblast apoptosis could be induced via administration of FasL (Moodley et al. 2004; Bühling et al. 2005). FasL through the binding of Fas (CD95) is a potent inducer of the extrinsic apoptosis pathway (Moodley et al. 2004; Maher et al. 2010; Bühling et al. 2005). Of interest for the subject of this thesis is that it has previously been demonstrated that down–regulation of clusterin in rheumatoid arthritis (RA), was associated with synovial fibroblast resistance to FasL-mediated apoptosis (García et al. 2010) and that transgenic overexpression of clusterin in RA synovial fibroblasts promotes apoptosis (Devauchelle et al. 2006).

It was, therefore, investigated whether clusterin-deficiency contributes to the resistance of fibrotic lung fibroblasts to basal and FasL-induced apoptosis. For these studies, recombinant FasL was used. In order to optimise the experimental procedure and establish detectable levels of basal and FasL-induced apoptosis, preliminary studies were performed and dose response and time course studies were conducted. These studies showed that recombinant FasL, induced apoptosis in a time and dose-dependent manner (Figure 3.22). All experiments were performed in 5 % serum in DMEM to enhance apoptotic levels in response to FasL when compared to 10 % serum and keep basal apoptosis levels low when compared to no serum in the culture medium. Moreover, no significant evidence of cell necrosis or cell apoptosis was observed under basal conditions (5 % serum in DMEM) as verified by inverted light microscopic analysis. FasL-induced apoptosis was measurable 19 hours after administration of FasL (Figure 3.22B), providing a sufficient magnitude of inducible apoptosis to study the effect of clusterin-deficiency on basal and FasL-induced apoptosis when compared with controls. By contrast, the 72-hour endpoint after exposure to FasL was not suitable for these studies since apoptotic levels were comparable with baseline apoptosis levels (Figure 3.22B). This may be due to a proliferative effect in response to FasL, consistent with previous reports in fibroblast-like synoviocytes (Audo et al. 2014). In addition, FasL concentrations from 100 ng/ml induced apoptosis levels significantly, as demonstrated in Figure 3.22A. Based on the combined results of all preliminary experiments subsequent fibroblast apoptosis

experiments were carried out with 100 or 200 ng/ml FasL for 19 hours in 5 % serum in DMEM, conditions which show a full magnitude of effects sufficient to examine the effects of clusterin-deficiency and exogenous clusterin on fibroblast apoptosis.
The *in vitro* studies presented here showed that unlike in synovial fibroblasts, shRNA-mediated down-regulation of clusterin-induced basal and FasL-induced apoptosis in control fibroblasts (Figure 3.23) when compared with mock-transduced and non-transduced controls. Furthermore, it was demonstrated that the increase in basal and FasL-induced apoptosis seen with low clusterin expression could be overcome by addition of exogenous clusterin (Figure 3.24). Interestingly, it has been previously described that secretory clusterin-induced resistance to apoptosis in hepatocellular carcinoma cells by activating the Akt pathway (Xiu et al. 2013a), in prostatic cells (Ammar & Closset 2008) and in VSMC, where exogenous clusterin protected against H_20_2-induced apoptosis (Liu et al. 2015). Conversely, it has been shown in VSMC, that anti-clusterin antibodies induced apoptosis (Miwa et al. 2004).

Together data presented in this thesis suggests, that clusterin is involved in regulating lung fibroblasts apoptosis *in vitro*. This data was reproducible and was consistent with two other independent experiments. It is, however, noticeable that although significant, levels of FasL-induced apoptosis were relatively low when compared to basal apoptosis levels. One example is that FasL-induced 20 % more apoptosis when compared to basal apoptotic levels (13.10 ± 0.33 % basal apoptosis in Figure 3.23), which equates to 2.62 % increase with FasL. It is, therefore, questionable if the full magnitude of apoptotic effects by FasL was reached for this set of experiments. The following studies focused on the effects of low clusterin in fibrotic lung fibroblasts when compared to control lung fibroblasts. These studies confirmed the previously reported resistance of fibrotic lung fibroblasts to FasL-induced apoptosis when compared with control fibroblasts (Figure 3.25). Furthermore, exogenous clusterin tended to further potentiate this resistance to apoptosis (Figure 3.26) in fibroblasts derived from fibrotic lung. Together, these *in vitro* studies suggest that clusterin is protective against basal and FasL-induced apoptosis in normal and fibrotic lung fibroblasts *in vitro*. Although clusterin protects against apoptosis in control fibroblasts, low clusterin in fibrotic lung fibroblasts does not seem to contribute to increased sensitivity to apoptosis in fibrotic lung fibroblasts. Fibrotic lung fibroblasts were resistant to FasL-induced apoptosis despite low clusterin levels *in vitro*. However, these findings are in contrast to the effects of clusterin in synovial fibroblasts apoptosis, further supporting the notion that the effects of clusterin are cell and tissue dependent.

4.8 The distribution of LRP-2 receptors in human control and fibrotic lung.

Reduced levels of secretory clusterin in IPF-BALF suggest that fibrosis-specific changes include a decreased availability of secretory clusterin in the lung. To further investigate which pulmonary cells are potentially affected by low levels of secretory clusterin, clusterin receptor expression in control and fibrotic lung was assessed. Clusterin has been reported to associate with a wide range of receptors, and it has been shown that the complex formation with other proteins results in internalisation of clusterin in cells expressing these receptors (Leeb et al. 2014; Kang et al. 2016). Clusterin receptor lipoprotein-related protein 2 (LRP2) or megalin, an endocytotic receptor for multiple ligands with signalling potential, has been described to be expressed in many absorptive epithelial cells, predominantly in the kidney (Kaseda et al. 2007), but its role in the human lung is incompletely understood. To date reports about LRP2 in the human lung point towards expression in Type II pneumocytes (Lundgren et al. 1997). Willnow and colleagues reported that lungs of new-born LRP2 knockdown mice were characterised by thickened alveolar walls and poor lung inflation, suggesting that clusterin receptor LRP-2 plays a crucial role in pulmonary inflation and alveolar expansion (Willnow et al. 1996). In keeping with these reports, it is likely that lung inflation and surfactant production in Type II alveolar cells are dependant on LRP2 pathways (Fisher & Howie 2006). Interestingly, LRP2 has been suggested to be down-regulated by TGF-β_1 in proximal-tubule-derived opossum kidney cells, and to play a role in clusterin-dependent clearance of cellular debris in non-professional phagocytes via endocytosis (Hermey et al. 2001; Gekle et al. 2003). Gekle and colleagues, therefore, suggest that endocytosis in other tissues than the kidney may also be reduced in response to elevated TGF-β_1. To date fibrosis related changes of LRP2 expression are unexplored.

To assess the expression of LRP-2 in control and fibrotic lungs in detail, a monoclonal antibody targeting human LRP2 was used for immunohistochemical staining. The results presented in this thesis (section 3.8) show that LRP2 associated with bronchial epithelial cells, while staining was considerably weaker in alveolar epithelial cells (including Type II pneumocytes). Bronchial epithelial cells in IPF lung displayed a similar LRP2-staining pattern when compared with bronchial epithelial cells in control lungs while staining in fibroblasts in control and fibrotic tissue was weak or undetectable (Figure 3.28). Consistent with previous results in fibrotic liver (Pieper-Fürst et al. 2011), macrophages were associated with strong LRP2 staining both control and fibrotic lung. However, LRP2 staining in macrophages was not altered in control or fibrotic lung, merely the number of infiltrated monocytes/macrophages was

increased in fibrotic compared with control lung. LRP2 expression localised predominantly to the cell membrane of macrophages, which suggests that LRP-2 acts as receptor for clusterin-induced signalling, as described in neuronal cells (Gil et al. 2013). The effect of exogenous clusterin on the macrophage phenotype in human lungs is, however, incompletely understood.

4.9 Effect of exogenous clusterin on protein secretion in alveolar or blood-derived macrophages in co-culture with bronchial epithelial cells.

Results presented in this thesis suggest that macrophages and bronchial epithelial cells express high levels of clusterin receptor LRP2. Due to high LRP2 expression in bronchial epithelial cells and alveolar macrophages, these cells are likely to respond to altered levels of secretory clusterin in the lung. Altered secretory clusterin levels, such as they were described for pulmonary fibrosis may, therefore, impact on these cell types affecting phenotype or protein expression levels. The effects of exogenous clusterin on protein secretion in alveolar or blood-derived macrophages as well as bronchial epithelial cells are incompletely understood.

Bronchial epithelial cells and alveolar macrophages present the frontline physical barrier and defence to confront environmental toxins and pathogens and play a key role in mounting an immune response via the production of pro-inflammatory cytokines and chemokines responsible for the recruitment and activation of immune cells in the lung (Hong et al. 2016; Murthy et al. 2015). In contrast alternatively activated alveolar macrophages regulate mechanisms that contribute to repair in response to injury-induced inflammation. Similar to T cells, macrophages exert divergent functions by switching between phenotypically distinct subpopulations: Macrophages that mediate inflammation have been classified as “M1”-like whereas macrophages with tissue remodelling/pro-fibrotic activity have been classified as “M2”-like and are defined by their expression of cell markers and the secretion of pro- or anti-inflammatory cytokines (Wermuth & Jimenez 2015). For simplicity reasons traditional macrophage polarisation termini were used within this thesis, despite the acknowledgement that macrophage polarisation is highly dynamic and can result in intermediate polarisation states with increased plasticity as reported in many *in vitro* studies (N. Wang et al. 2014; Hussell & Bell 2014b; Aggarwal et al. 2014).

As eluded to earlier in this thesis, multiple sources of evidence suggest that alternatively activated (“M2”-like) macrophages are linked to progression of pulmonary fibrosis (Murthy et al. 2015; Stahl et al. 2013; Mora et al. 2006; Wynes & Riches 2003;

Gordon 2003; Wynn et al. 2011). This is because “M2” macrophages secrete pro-fibrotic mediators, while pro-inflammatory (“M1”-like) macrophages have been suggested to oppose these effects in mice (He et al. 2013). It is, therefore, important to understand if secretory clusterin affects the polarisation state of alveolar macrophages. To identify potential links of altered secretory clusterin levels with the pathogenesis of fibrosis, the effect of clusterin on alveolar macrophage phenotype in co-culture with bronchial epithelial cells was explored. A co-culture with bronchial epithelial cells was essential since it allows the definition of potential immunomodulatory effects of clusterin in both cell types individually and in co-culture, considering crosstalk between both cell types, such as they occur under physiological conditions in the lung.

To study the immunomodulatory effects of clusterin, a possible endotoxin contamination of the used human plasma-derived clusterin had to be ruled out, since it is known that endotoxins modulate the production and secretion of pro-inflammatory cytokines by macrophages (at concentrations > 0.5 ng/ml) (Morris et al. 1992). Supplier information of the human plasma-derived clusterin used in experiments for this thesis declares a low contamination risk with endotoxin (< 1.0 EU/µg or < 0.1 to 0.2 ng endotoxin/mL) according to the criteria for industry leading proteins[6]. An endotoxin contamination of human plasma-derived clusterin product seems, therefore, unlikely.

As reported in the results section 3.9, exogenous human plasma-derived clusterin-induced the secretion of TNFα by 24 hours in both human alveolar macrophages and bronchial epithelial cells (Figure 3.29). Clusterin has previously been reported to induce the secretion of TNFα in murine macrophages (Y.-J. Shim et al. 2012), but this has not been previously reported for human (alveolar) macrophages or bronchial epithelial cells. TNFα is a pleiotropic cytokine, demonstrated to be involved in the pathogenesis of pulmonary fibrosis (Freeburn et al. 2005). TNFα is a key mediator of inflammatory cell recruitment to sites of alveolar injury and induces the production of pro-inflammatory cytokines by monocytes and neutrophils (Tracey & Cerami 1994; Freeburn et al. 2005). There are several lines of evidence that suggest that TNFα plays a role in driving profibrotic processes: TNFα has been demonstrated to induce proliferation and collagen deposition in lung fibroblasts (Piguet et al. 1990). Furthermore, overexpression of TNFα in murine lung caused fibrosing alveolitis (Miyazaki et al. 1995) and cytokines orchestrated by TNFα have been suggested to amplify the inflammatory response and drive the progression to fibrosis (Zhang et al.

[6] http://www.ebioscience.com/knowledge-center/functional-activity/animal-free-recombinant-proteins/endotoxin-effects.htm

1997b; Oikonomou et al. 2006). In contrast, a more recent study suggests that TNFα contributes to the resolution of established pulmonary fibrosis in mice via a mechanism involving reduced numbers and programming status of profibrotic macrophages (Redente et al. 2014). Moreover, it has been described that basal resistance of lung fibroblasts and myofibroblasts to Fas-induced apoptosis is overcome by sensitization with TNFα (Frankel et al. 2006). Together, these observations indicate the complex nature of TNFα in controlling the homoeostasis between inflammatory and repair responses, with opposing effects on the development and progression of pulmonary fibrosis.

In addition to the secretion of TNFα, the effects on chemotactic cytokine secretion in response to clusterin were investigated in human alveolar macrophages and blood-derived macrophages as described in detail in section 3.9.2. A screening of secretory, fibrosis-relevant chemokines in response to secretory clusterin has demonstrated that MCP-1, MIP-1β and RANTES secretion was induced in blood-derived MCSF-differentiated macrophages (Figure 3.32). This observation was in trend reproducible for alveolar macrophages at 24 hours (Figure 3.29). It is noteworthy that experiments in blood-derived macrophages were conducted at higher clusterin doses and exposure time and that these studies are preliminary studies, which require further optimisation.

A possible explanation for similar but unmatched results in alveolar and blood-derived macrophages could lie in duration that clusterin was exposed to these cells. While changes in blood-derived macrophages were observed at 72 hours in response to clusterin, the effects might have been not fully evolved at 24 hours as studied for alveolar macrophages. Future studies should, therefore, focus on the effects of clusterin on chemokine secretion in alveolar macrophages derived from a control donor lung over time. It is well established, that CC chemokines, such as MCP-1, MIP-1β and RANTES, are associated with the expression of adhesion molecules and the recruitment of inflammatory cells to the lung (Antoniades et al. 1992; Iyonaga et al. 1994; Car et al. 1994; Kodama et al. 1998; Suga et al. 1999). Having demonstrated that exogenous clusterin induces chemotactic cytokine secretion by blood-derived macrophages, this *in vitro* study suggests that clusterin may induce the recruitment of macrophages and other immune cells *in vivo*.

To further explore the immunomodulatory effects of secretory clusterin on macrophages and bronchial epithelial cells, additional analysis of secreted pro- and anti-inflammatory cytokines in response to exogenous clusterin was performed. Consistent with induced TNFα secretion and chemokines, pro-inflammatory cytokines were elevated in supernatants of alveolar macrophages (IL-6, IL-8, IL-5, Figure 3.29)

and blood-derived unpolarised macrophages (IL-6, IL-8, IFNα, Figure 3.31). Similarly to measurements for TNFα, exogenous clusterin-induced the secretion of IL-6 and IL-8 by alveolar macrophages in co-culture with bronchial epithelial cells. However, clusterin did not induce these cytokines in monocultures of bronchial epithelial cells, which could indicate that the induced cytokines derived from alveolar macrophages in co-culture with bronchial epithelial cells in this *in vitro* model. By contrast, clusterin stimulated the secretion of anti-inflammatory cytokines, IL-1ra and IL-10, together with predominantly pro-inflammatory cytokines (Figure 3.31). IL-10 and IL-1ra are both potent anti-inflammatory molecules that curtail the production of inflammatory cytokines during infection or tissue damage (Freeburn et al. 2005; Herold et al. 2011; Lech & Anders 2013). Consistent with previous studies of macrophage treatment with LPS (Chanteux et al. 2007), an induction of anti-inflammatory cytokines with pro-inflammatory cytokines suggests a biphasic cytokine release in response to clusterin. It has been previously suggested that pro- and anti-inflammatory cytokines are released by functional divergent alveolar macrophage subsets in disease (Morales-Nebreda et al. 2015; Hussell & Bell 2014b; Aggarwal et al. 2014). Furthermore, TNFα has been shown to stimulate IL-10 production, a potential negative feedback mechanism to regulate its expression (Wanidworanun & Strober 1993). In conclusion, clusterin induces a biphasic, predominantly pro-inflammatory cytokine release in both alveolar and blood-derived macrophages. A shift in the cytokine and chemokine profile in alveolar and blood-derived macrophages may underlay a potential effect of clusterin on polarisation, which would be relevant for multiple macrophage-dependent pathologies, including pulmonary fibrosis. To begin to explore if secretory clusterin affects macrophage polarisation the effects of exogenous clusterin during M1 or M2 polarisation were studied in MCSF differentiated blood-derived macrophages. Preliminary data in MCSF-differentiated macrophages from two blood donors demonstrated that LPS/IFNγ induced predominantly pro-inflammatory cytokines such as TNFα, IL-8, IL-6, MIP-1α as expected (Donor 1: Figure 3.30, Donor 2 Appendix 4). However, the level of LPS/IFNγ induced cyto- and chemokines was not altered when clusterin was present during polarisation. Although reproducibility of these results has to be demonstrated in additional donors, this data suggests that clusterin does not alter polarisation in the context of “M1”polarisation with LPS/IFNγ. Similarly, “M2-like” polarisation with IL-4 was not altered in the presence of clusterin. When comparing the effects of clusterin on the cytokine profile of unpolarised blood-derived macrophages the responses in three donors were in trend similar but also dependant on the overall responsiveness of individual cell isolate. In donor 3 TNFα, IL-8, IL-6 and IFNα were significantly elevated in response to 10 µg/ml clusterin (Figure 3.31). By contrast, donor

1 and 2 demonstrated a trend towards the induction of pro-inflammatory cytokines TNFα, IL-8, IL-6 and MIP-1α for a concentration of 1 µg/ml exogenous clusterin (Donor 1: Figure 3.30, Donor 2 Appendix 4). An explanation for this may be that higher concentrations than 1 µg/ml exogenous clusterin are required to induce a response. Another explanation could be that donor 3 was a low responder to pro-inflammatory stimuli, which is why a high clusterin concentration of 10 µg/ml was required to induce an effect. Moreover, MMP-9 response to clusterin varied in all tree donors: MMP-9 secretion was significantly induced in donor 3 (Figure 3.31) by 10 µg/ml clusterin and in donor 1 by 1 µg/ml clusterin (Figure 3.30). However, there was no difference observed for donor 2 (Appendix 4). It is remarkable that basal MMP-9 secretion in unpolarised macrophages from donor 2 was increased when compared with cells from donor 1 and 3. Overall this preliminary data suggests that secretory clusterin induces a pro-inflammatory, macrophage phenotype, similar but with a lower magnitude to that of "M1-like" in unpolarised blood-derived macrophages *in vitro*. In order to fully understand the magnitude of the effect of exogenous clusterin on the secretory protein profile of unpolarised macrophages, further studies are required in cell isolates from additional donors. Future *in vitro* studies should, therefore, focus on the effect of increasing clusterin concentrations on multiple donors, with a varying range of responsiveness to pro-inflammatory stimuli.

To begin to understand the mechanisms that are involved in clusterin mediated polarisation towards an pro-inflammatory, "M1-like" phenotype", the role of TNFα in mediating these changes was assessed. TNFα, a "master regulator" of pro-inflammatory cytokine production (Maini et al. 1995) could be upregulated or the bioavailability increased by clusterin. To address this, clusterin mediated effects were studied in the presence of anti-TNFα antibodies (section 3.9.4). Consistent with earlier studies presented in this thesis, clusterin-induced the secretion of representative pro-inflammatory cytokines (IL-6) and chemokines (MIP-1β). However, in the presence of anti-TNFα antibodies, this effect was significantly reduced (Figure 3.33). Whether this is due to a clusterin-induced enhanced availability of membrane-bound TNFα or secretory TNFα or induced expression and secretion remains unknown. The location of TNFα was suggested to be relevant in the context of fibrotic disease in mice: A study in bleomycin-induced fibrosis in mice suggested that transmembrane TNFα expression is sufficient to elicit an inflammatory response, but was incompetent in initiating a fibrotic phase of the disease, while soluble TNFα was shown to be essential for the development of fibrotic lesions (Oikonomou et al. 2006). Secretory clusterin may play a

role in regulating these processes, and future studies should focus on whether clusterin affects TNFα expression, localisation within the cell or its bioavailability.

In following studies it was assessed if “M1”- or “M2”-like polarised macrophages secrete different levels of secretory clusterin. To address this, monocytes from two different donors were differentiated and polarised into “M1-like” or “M2-like” macrophages or remained untreated (“M0-like”) and clusterin secretion was assessed after 72 hours via ELISA. The data suggest that “M0-like” macrophages secrete low clusterin levels (Figure 3.34). This was expected given that macrophages in control and fibrotic lung were associated with low clusterin staining in immunohistochemical analysis (Figure 3.2 and Figure 3.8). Interestingly, macrophages exposed to pro-inflammatory stimuli (LPS/IFNγ or LPS alone) increased the secretion of clusterin significantly, while IFNγ and IL-4 did not significantly alter clusterin secretion. Although this is only preliminary data, reproduced in two donors the induction of clusterin secretion in pro-inflammatory macrophages may provide a positive feedback loop, ensuring that in the event of inflammation clusterin secretion is induced in those macrophages. Moreover, clusterin secretion was also induced in trend in response to an “M2-like” polarisation, even though this was not significant.
In summary, the present preliminary data suggests that secretory clusterin induces a pro-inflammatory response in macrophages. Additionally, LPS/IFNγ activated, pro-inflammatory “M1-like” macrophages secrete increased levels of clusterin when compared with unpolarised controls. Although this data was derived *in vitro* and requires validation in a higher number of donors, this mechanism may provide a positive clusterin-dependent feedback loop keeping secretory clusterin levels increased, which in turn could result in further polarisation towards a pro-inflammatory “M1-like” macrophage phenotype.

Taken together these observations suggest that reduced availability of secretory clusterin, as it is observed during the development of pulmonary fibrosis, may impede a clusterin-induced pro-inflammatory “M1”-like phenotype in macrophages favouring a shift towards polarisation of pro-fibrotic, alternatively activated “M2”-like macrophages.
This hypothesis is supported by immunohistochemical studies in this thesis, which show that alveolar macrophages in fibrotic lung tissue express low levels of clusterin (Figure 3.2D and Figure 3.8B), as it has been shown to be the case for “M2-like” or unpolarised macrophages (Figure 3.34). This may be relevant for the pathogenesis of pulmonary fibrosis since it has been reported that acute exacerbation of IPF is linked to a shift towards M2 phenotype (Schupp et al. 2015), but the underlying mechanism as

to why M2 shift appears in IPF remains unknown. Additional evidence for the importance of a shift towards M2 macrophages in the development of pulmonary fibrosis has been demonstrated previously (Prasse et al. 2006; Mora et al. 2006). As suggested by Schupp and colleagues, a shift towards M2 populations could be induced through the context of a wound healing response uncontrolled in on-going repair processes (Schupp et al. 2015). Prasse and colleagues propose that alveolar macrophages from patients with pulmonary fibrosis display a phenotype of alternatively activated macrophages, promoting a positive feedback loop with lung fibroblasts to create and maintain a profibrotic milieu (Prasse et al. 2006).

Alternatively activated, “M2”-like macrophages produce and secrete fibrogenic mediators, including TGF-β_1 (Fadok et al. 1998) and inversely, TGF-β_1 has been suggested to mediate alternative macrophage activation (Gong et al. 2012). This is consistent with TGF-β_1 positive macrophages in fibrotic lung sections as observed in Figure 3.8., supporting previous reports stating that human fibrotic lung tissue is characterised by TGF-β_1 -positive, “M2-like” macrophages.

In keeping with these reports, it may be possible that reduced clusterin levels contribute to an impaired pro-inflammatory “M1-like” shift that would oppose “M2-like” driven pro-fibrotic effects. In response to elevated TGF-β_1 in the fibrotic lung, clusterin secretion, such as it has been demonstrated for lung fibroblasts (Figure 3.13) could be further reduced by TGF-β_1, creating a vicious circle of low secretory clusterin and alternatively activated macrophages perpetuating pulmonary fibrosis.

.

4.10 Summary, conclusions and future directions.

4.10.1 Summary

The aim of this thesis was to investigate if clusterin plays an important role in normal human lung and whether alterations of clusterin are relevant to the pathogenesis of pulmonary fibrosis. The results presented in this thesis provide insights into the distribution, expression, and function of clusterin in normal lung and compare these with lungs from patients with IPF.

Immunohistochemical analysis demonstrated that clusterin co-localised with elastin in vessel walls and additionally with amorphous elastin deposits in fibrotic lung. This suggests that reduced levels of clusterin in IPF-BALF (T. H. Kim et al. 2010) are, at least partly, due to increased binding to elastin. Although future studies would be necessary to confirm the cause for the association of clusterin to elastin in fibrotic tissue, reduced clusterin expression in the lung may limit its extracellular chaperoning activity contributing to dysregulated deposition of elastin, a mechanism that has previously been described for UV-aged human skin (Janig et al. 2007).

The work presented here showed for the first time that clusterin was strongly associated with fibroblasts in control lung tissue, but was undetectable in fibroblasts in fibrotic regions of lungs from patients with pulmonary fibrosis, as verified in *in vitro* studies. TGF-β_1 has been shown to down-regulate clusterin expression in control fibroblasts but the down-regulation of clusterin by TGF-β_1 was shown to be independent of its effect on fibroblast-to-myofibroblast transition. Further studies were conducted to assess the effect of clusterin-deficiency in control lung fibroblast on migration, proliferation, and apoptosis, which were compared with results from fibrotic lung fibroblast with low clusterin expression. These data, demonstrate that clusterin is involved in regulating fibroblast proliferation and apoptosis *in vitro*. Down-regulation of clusterin in fibrotic lung fibroblasts may be at least partly due to increased TGF-β_1 and could, therefore, represent an appropriate but insufficient response to limit proliferation and reduce the resistance to apoptosis, the main cause for the development and progression of pulmonary fibrosis.

Furthermore, while clusterin was sporadically expressed in bronchial epithelial cells of the normal adult lung, clusterin staining was both more frequent and intense in IPF lungs. An increase in clusterin expression in IPF bronchial epithelial cells may be

induced by epithelial stress/injury or, alternatively, a component of the aberrant re-expression of development genes that occurs in IPF (Selman et al. 2008).
This thesis also illustrated some intriguing, novel findings, advocating that clusterin may play a role in modulating macrophages towards a pro-inflammatory phenotype: Preliminary studies demonstrated that exogenous clusterin-induced the secretion of pro-inflammatory cyto- and chemokines, most notably TNFα, potentially opposing "M2-like" driven pro-fibrotic macrophage responses, relevant for the development of pulmonary fibrosis.

Ultimately, these results provide support for the initial hypothesis, suggesting that clusterin plays an important homeostatic role in normal human lung. Clusterin expression and function were highly tissue and cell dependent, underlining once more the complex biology of multifunctional protein clusterin, in a novel context of human lung. Up- or down-regulation of clusterin in macrophages, epithelial cells and fibroblasts, partly by TGF-$\beta_{1,}$ may contribute to tissue homoeostasis in normal lung and the protection against the development of pulmonary fibrosis.

4.10.2 Conclusions

Figure 4.1 concludes how clusterin may be involved in regulating cell homoeostasis in control lung and outlines how changes in clusterin affect different cell types and suggests how these changes may be involved in processes that protect against the development of lung fibrosis.

1) In the normal lung (A) clusterin associated with elastin in vessel walls. Secretory clusterin levels are measurable in solutes from the lower respiratory tract (BALF) (T. H. Kim et al. 2010). In fibrotic lung (B) clusterin associates with elastin in vessel walls and additionally with amorphous elastin deposits in fibrotic lung, potentially reducing secretory clusterin levels in lung solutes as suggested by reduced secretory clusterin in IPF-BALF (T. H. Kim et al. 2010).

2) In healthy lung (A) secretory clusterin is available in the solutes from the lower respiratory tract and may regulate the homoeostasis of pro-inflammatory ("M1"-like) and pro-fibrotic ("M2"-like) macrophages: Clusterin has been shown to induce the secretion of pro-inflammatory cytokines such as TNFα by alveolar macrophages. Pro-inflammatory, "M1"-like macrophages increase the secretion of clusterin and contribute at least in part to homeostatic levels of secretory

clusterin in control lung. In fibrotic lung (B) low secretory clusterin levels potentially result in a shift towards profibrotic “M2-like” macrophages with increased secretion of TGF-β_1 and reduced secretion of clusterin.

3) In normal lung, TGF-β_1 is increased in large amounts upon normal wound healing to promote fibroblast to myofibroblast differentiation. Under homeostatic conditions TGF-β_1 levels are low when compared with levels in fibrotic lung and TGF-β_1-induced fibroblast to myofibroblast differentiation occurs in a controlled manner. In fibrotic lung TGF-β_1 levels are enhanced, partly due to induced secretion by profibrotic “M2”-like macrophages. Increased levels of TGF-β_1 promote uncontrolled myofibroblasts differentiation with excessive extracellular matrix deposition. Down-regulation of clusterin in fibrotic lung fibroblasts may provide a mechanism to antagonise proliferation and resistance to apoptosis and may therefore provide a protective mechanism against further progression of the disease. In turn, reduced intracellular clusterin in fibrotic lung fibroblasts may at least in part further contribute to reduce secretory clusterin levels in fibrotic lung accelerating profibrotic processes.

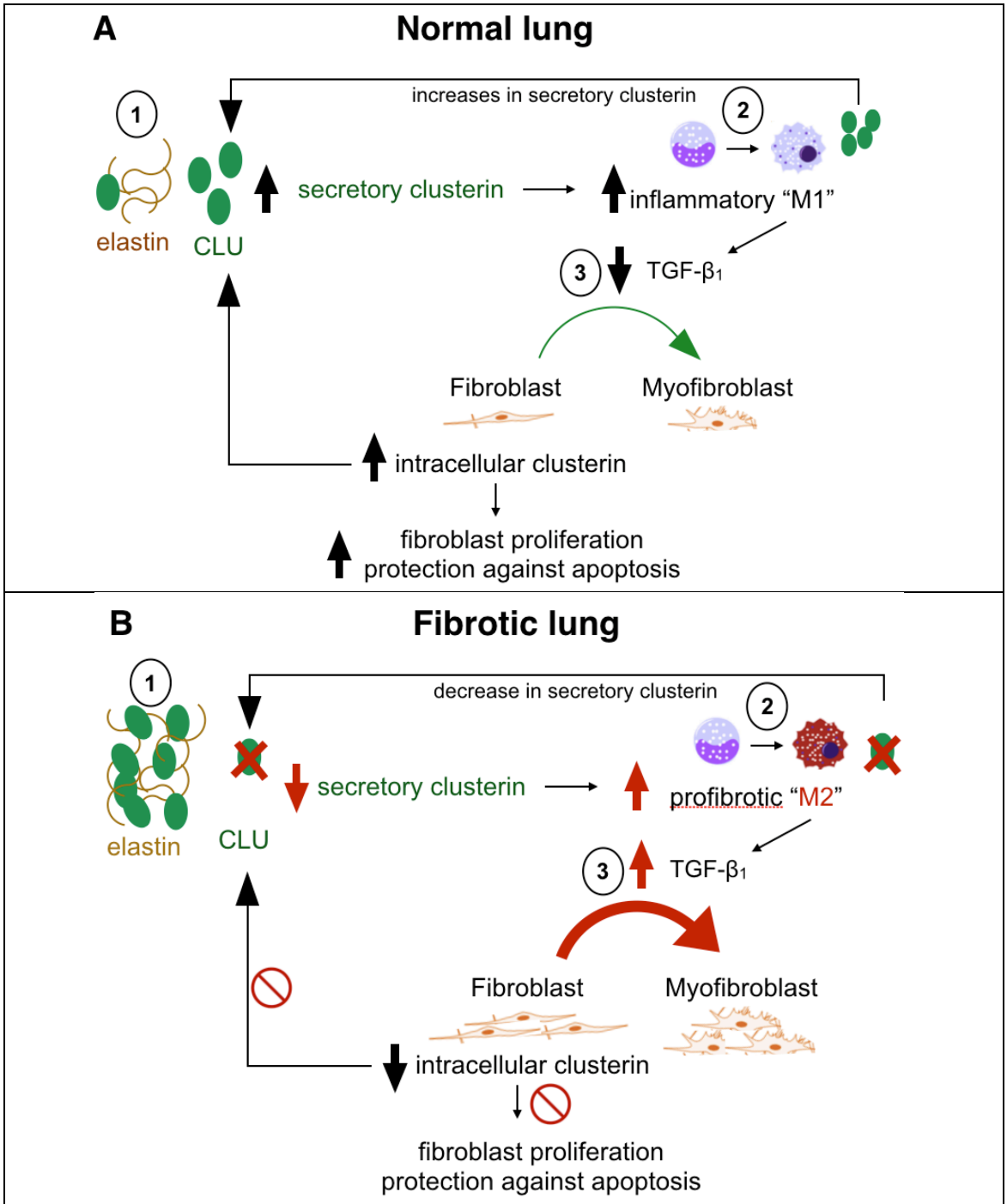

Figure 4.1 Schematic overview of potential protective effects of clusterin against the development of pulmonary fibrosis. Continued over the page.

Figure 4.1 **Schematic overview of potential protective effects of clusterin against the development of pulmonary fibrosis.**
(A) In normal lung clusterin associates with elastin in vessel walls and secretory clusterin is involved in regulating the homoeostasis of pro-inflammatory and profibrotic cytokine secretion by inducing a pro-inflammatory macrophage phenotype in the lung. A controlled number of alternatively activated ("M2"- like) macrophages secrete relatively low levels of TGF-β_1, which results in controlled myofibroblast differentiation compared with fibrotic lungs. In control lung clusterin is expressed and secreted by fibroblasts and promotes fibroblast proliferation and protects against apoptosis. Clusterin secretion by lung fibroblasts contributes at least in part to secretory clusterin levels regulating homeostatic processes in control lung. (B) In fibrotic lung clusterin associates with amorphous elastin deposits, measurable secretory clusterin is reduced in fibrotic lung (T. H. Kim et al. 2010), potentially resulting in reduced secretion of pro-inflammatory cytokines by "M1"-like macrophages and a shift towards "M2"-like profibrotic macrophages that secrete high levels of TGF-β_1. Increased levels of TGF-β_1 induce myofibroblast differentiation and excessive extracellular matrix deposition. Fibroblasts isolated from fibrotic lung show down-regulated intracellular clusterin to potentially limit fibroproliferation, further contributing to reduced levels of secretory clusterin in fibrotic lung.

4.10.3 Future directions

Immunohistochemical studies presented in this thesis suggest that clusterin is differentially expressed in various cell types in the lung and that this expression pattern is altered in fibrotic lung. Although, the reduction of clusterin in fibrotic lung fibroblasts compared with fibroblasts from control lung has been demonstrated for various donors (five IPF and seven SSc patients compared with six controls), functional consequences of reduced clusterin expression *in vitro* have only been studied in representative control and fibrotic lung fibroblasts. Future *in vitro* studies are required to test if findings presented in this thesis are reproducible for fibroblasts from multiple donors. Furthermore, additional data generated in control and fibrotic lung fibroblast overexpressing clusterin could verify the results regarding the functional role of clusterin presented here.
Additional studies with LRP2 blocking antibodies would elucidate if the clusterin-dependent secretion of pro-inflammatory cytokines and chemokines is mediated by an interaction of clusterin with its receptor LRP2.

Moreover, these *in vitro* studies could be complemented with studies in bleomycin-induced fibrosis in clusterin-deficient compared with wild type mice. This *in vivo* model would provide insight into changes of clusterin expression throughout the development

of pulmonary fibrosis in mice. In addition, this model would deliver multiple insights into the role of clusterin in regulating cell and tissue homoeostasis in mice: Firstly define the effects of depleted secretory clusterin on extracellular matrix quality control, particularly with respect to the protection against elastin accumulation and aggregation in interstitial elastin deposits. Secondly, investigate if the absence of secretory clusterin induces a shift towards profibrotic “M2”-like macrophages accelerating a profibrotic environment e.g. via enhanced TGF-β_1 secretion. Thirdly, assess if the overall tissue distortion by excessive fibroblast/myofibroblast accumulation is increased in clusterin-deficient mice with and without bleomycin-induced fibrosis. Moreover, explore if profibrotic and pro-inflammatory chemokines/chemokines are induced in murine BALF to establish the effects of clusterin-deficiency on cytokine profile in mice. Further studies of the mechanisms underlying clusterin effects on cell homoeostasis and matrix quality control in mice, may enhance our understanding of its role in human control and fibrotic lung.

Preliminary *in vitro* studies presented in this thesis assessed the effects of altered secretory clusterin on human macrophage phenotype modulation. These studies should be reproduced in a larger donor cohort, including cell isolates from donors with a low and high responder profile to pro-inflammatory stimuli. This would further contribute to the understanding of a potential modulation of macrophage populations by clusterin in the context of health and disease.
Together, future *in vitro* and *in vivo* studies would further enhance our understanding of the role of clusterin in tissue homoeostasis in normal lung, and how alterations in clusterin distribution and expression may protect against or promote the development of pulmonary fibrosis.

5 References

Van Aarsen, L.K. et al., 2008. Antibody-mediated blockade of integrin alpha v beta 6 inhibits tumor progression in vivo by a transforming growth factor-beta-regulated mechanism. *Cancer research*, 68(2), pp.561–70.

Adds, J., Larkcom, E. & Miller, R., 2001. The pulmonary system. In *Respiratory and coordination*. London: Nelson Thornes Ltd, p. 138.

Aggarwal, N.R., King, L.S. & Alessio, 2014. Diverse macrophage populations mediate acute lung inflammation and resolution. *American Journal of Physiology*, 21224.

Aigelsreiter, A. et al., 2009. Clusterin expression in cholestasis, hepatocellular carcinoma and liver fibrosis. *Histopathology*, 54(5), pp.561–70.

Akers, I.A. et al., 2000. Mast cell tryptase stimulates human lung fibroblast proliferation via protease-activated receptor-2. *American Journal of Physiology - Lung Cellular and Molecular Physiology*, 278, pp.L193–L201.

Alberts, B. et al., 2014. *Molecular Biology of the Cell, Sixth Edition* 6th ed., Garland Science.

Ammar, H. & Closset, J.L., 2008. Clusterin activates survival through the phosphatidylinositol 3-kinase/Akt pathway. *The Journal of biological chemistry*, 283(19), pp.12851–61.

Antonelou, M.H. et al., 2011. Apolipoprotein J / Clusterin Is a Novel Structural Component of Human Erythrocytes and a Biomarker of Cellular Stress and Senescence. *PLoS ONE*, 6(10), pp.1–10.

Antoniades, H.N. et al., 1992. Expression of monocyte chemoattractant protein 1 mRNA in human idiopathic pulmonary fibrosis. *Proceedings of the National Academy of Sciences of the United States of America*, 89(12), pp.5371–5.

Antoniades, H.N. et al., 1990. Platelet-derived growth factor in idiopathic pulmonary fibrosis. *The Journal of clinical investigation*, 86(October), pp.1055–64.

Araya, J. et al., 2006. Integrin-mediated transforming growth factor-beta activation regulates homeostasis of the pulmonary epithelial-mesenchymal trophic unit. *The American journal of pathology*, 169(2), pp.405–415.

ATS/ERS, 2002. International Multidisciplinary Consensus Classification of the Idiopathic Interstitial Pneumonias. *Am J Respir Crit Care Med*, 165, pp.277–304.

Audo, R. et al., 2014. Distinct effects of soluble and membrane-bound Fas ligand on fibroblast-like synoviocytes from rheumatoid arthritis patients. *Arthritis and Rheumatology*, 66(12), pp.3289–3299.

Bailey, R.W. et al., 2002. Heat shock-initiated apoptosis is accelerated and removal of damaged cells is delayed in the testis of clusterin/ApoJ knock-out mice. *Biology of reproduction*, 66(4), pp.1042–1053.

Balestro, E. et al., 2016. Immune Inflammation and Disease Progression in Idiopathic Pulmonary Fibrosis. *PloS one*, 11(5), p.e0154516.

Bartl, M.M. et al., 2001. Multiple receptors mediate apoJ-dependent clearance of cellular debris into nonprofessional phagocytes. *Experimental cell research*, 271(1), pp.130–41.

Baumgartner, K.B. et al., 1997. Cigarette smoking: a risk factor for idiopathic pulmonary fibrosis. *American journal of respiratory and critical care medicine*, 155(1), pp.242–8.

Bettuzzi, S. et al., 2002. Clusterin (SGP-2) transient overexpression decreases proliferation rate of SV40-immortalized human prostate epithelial cells by slowing down cell cycle progression. *Oncogene*, 21(27), pp.4328–4334.

Bettuzzi, S. & Rizzi, F., 2009. Chapter 5: Nuclear CLU (nCLU) and the fate of the cell. *Advances in cancer research*, 104, pp.59–88.

Bitterman, P.B. et al., 1986. Modulation of alveolar macrophage-driven fibroblast proliferation by alternative macrophage mediators. *Journal of Clinical Investigation*, 77(3), pp.700–708.

Blanc-Brude, O.P. et al., 2001. Factor Xa is a fibroblast mitogen via binding to effector-cell protease receptor-1 and autocrine release of PDGF. *American journal of physiology. Cell physiology*, 281(2), pp.C681–C689.

Bonner, J.C. et al., 1991. Differential proliferation of rat lung fibroblasts induced by the platelet-derived growth factor-AA, -AB, and -BB isoforms secreted by rat alveolar macrophages. *American journal of respiratory cell and molecular biology*, 5(6), pp.539–547.

Bonner, J.C. et al., 1995. Transforming growth factor beta 1 downregulates the platelet-derived growth factor alpha-receptor subtype on human lung fibroblasts in vitro. *Am J Respir Cell Mol Biol*, 13, pp.496–505.

Borok, Z. et al., 1991. Augmentation of Functional Prostaglandin E Levels on the Respiratory Epithelial Surface by Aerosol Administration of Prostaglandin E. *American Review of Respiratory Disease*, 144(5), pp.1080–1084.

Bottoms, S.E. et al., 2010. Tgf-Beta isoform specific regulation of airway inflammation and remodelling in a murine model of asthma. *PloS one*, 5(3), p.e9674.

Bozyk, P.D. & Moore, B.B., 2011. Prostaglandin E2 and the pathogenesis of pulmonary fibrosis. *American journal of respiratory cell and molecular biology*, 45(3), pp.445–52.

Bringardner, B. et al., 2008. The role of inflammation in the pathogenesis of idiopathic pulmonary fibrosis. *Antioxidants & Redox Signaling*, 10(2), pp.287–302.

Brown, P.D. et al., 1990. Physicochemical activation of recombinant latent transforming growth factor-beta's 1, 2, and 3. *Growth factors (Chur, Switzerland)*, 3, pp.35–43.

Brummelkamp, T.R., Bernards, R. & Agami, R., 2002. A system for stable expression of short interfering RNAs in mammalian cells. *Science (New York, N.Y.)*, 296, pp.550–553.

Bühling, F. et al., 2005. Altered expression of membrane-bound and soluble CD95/Fas contributes to the resistance of fibrotic lung fibroblasts to FasL induced apoptosis. *Respiratory research*, 6, p.37.

Burkey, B.F., DeSilva, H. V & Harmony, J.A., 1991. Intracellular processing of apolipoprotein J precursor to the mature heterodimer. *Journal of lipid research*, 32(6), pp.1039–48.

Busse, W.W. & Lemanske, R.F., 2001. Asthma. *N Engl J Med*, 344(5).

Byrne, A.J., Maher, T.M. & Lloyd, C.M., 2016. Pulmonary Macrophages: A New Therapeutic Pathway in Fibrosing Lung Disease. *Trends in Molecular Medicine*, 22(4), pp.303–316.

Byun, K. et al., 2014. Clusterin/ApoJ enhances central leptin signaling through Lrp2-mediated endocytosis. *EMBO reports*, 15(7), pp.801–8.

Cabrera-Benítez, N.E. et al., 2012. Mechanical stress induces lung fibrosis by epithelial–mesenchymal transition. *Critical Care Medicine*, 40(2), pp.510–517.

Calabrese, F. et al., 2005. Idiopathic interstitial pneumonias Primum movens: Epithelial, endothelial or whatever. In Sarcoidosis Vasculitis and Diffuse Lung Diseases. Suppl 1:S15-23

Camelo, A. et al., 2014. The epithelium in idiopathic pulmonary fibrosis: Breaking the barrier. *Frontiers in Pharmacology*, 4, pp.1–11.

Car, B.D. et al., 1994. Elevated IL-8 and MCP-1 in the bronchoalveolar lavage fluid of patients with idiopathic pulmonary fibrosis and pulmonary sarcoidosis. *Am.J Respir Crit Care Med*, 149(1073–449X), pp.655–659.

Carnevali, S. et al., 2006. Clusterin decreases oxidative stress in lung fibroblasts exposed to cigarette smoke. *American journal of respiratory and critical care medicine*, 174(4), pp.393–9.

Castelino, F. V & Varga, J., 2010. Interstitial lung disease in connective tissue diseases: evolving concepts of pathogenesis and management. *Arthritis research & therapy*, 12(4), p.213.

Castranova, V. et al., 1988. The alveolar type II epithelial cell: A multifunctional pneumocyte. *Toxicology and Applied Pharmacology*, 93(3), pp.472–483.

Chambers, R.C., 2008. Abnormal wound healing responses in pulmonary fibrosis: focus on coagulation signalling. *European Respiratory Review*, 17(109), pp.130–137.

Chambers, R.C. et al., 2003. Global expression profiling of fibroblast responses to transforming growth factor-beta1 reveals the induction of inhibitor of differentiation-1 and provides evidence of smooth muscle cell phenotypic switching. *The American journal of pathology*, 162(2), pp.533–546.

Chang, W. et al., 2010. SPARC Suppresses Apoptosis of Idiopathic Pulmonary Fibrosis Fibroblasts through Constitutive Activation of Catenin. *Journal of Biological Chemistry*, 285(11), pp.8196–8206.

Chanteux, H. et al., 2007. LPS induces IL-10 production by human alveolar macrophages via MAPKinases- and Sp1-dependent mechanisms. *Respiratory research*, 8(1), p.71.

Charnay, Y. et al., 2012. Clusterin in neurological disorders: molecular perspectives and clinical relevance. *Brain research bulletin*, 88(5), pp.434–43.

Chen, C.Z. & Raghunath, M., 2009. Focus on collagen: in vitro systems to study fibrogenesis and antifibrosis state of the art. *Fibrogenesis & tissue repair*, 2(1), p.7.

Chen, C.Z.C. et al., 2009. The Scar-in-a-Jar: studying potential antifibrotic compounds from the epigenetic to extracellular level in a single well. *British journal of pharmacology*, 158(5), pp.1196–209.

Chen, H. et al., 2016a. Mechanosensing by the α6-integrin confers an invasive fibroblast phenotype and mediates lung fibrosis. *Nature Communications*, 7, p.12564.

Chen, H. et al., 2016b. Mechanosensing by the α6-integrin confers an invasive fibroblast phenotype and mediates lung fibrosis. *Nature Communications*, 7, p.12564.

Chen, H.-C., 2005. Boyden chamber assay. *Methods in molecular biology (Clifton, N.J.)*, 294, pp.15–22.

Chen, X. et al., 2016. miRNA-378 reverses chemoresistance to cisplatin in lung adenocarcinoma cells by targeting secreted clusterin. *Scientific Reports*, 6(November 2014), p.19455.

Cheng, C.Y. et al., 2012. Regulation of chemosensitivity and migration by clusterin in non-small cell lung cancer cells. *Cancer Chemotherapy and Pharmacology*, 69(1), pp.145–154.

Chilosi, M., Poletti, V. & Rossi, A., 2012. The pathogenesis of COPD and IPF: Distinct horns of the same devil? *Respiratory Research*, 13(1), p.3.

Chou, T.-Y. et al., 2009. Clusterin silencing in human lung adenocarcinoma cells induces a mesenchymal-to-epithelial transition through modulating the ERK/Slug pathway. *Cellular signalling*, 21(5), pp.704–11.

Chuquimia, O.D. et al., 2013. Alveolar epithelial cells are critical in protection of the respiratory tract by secretion of factors able to modulate the activity of pulmonary macrophages and directly control bacterial growth. *Infection and Immunity*, 81(1), pp.381–389.

Churchill, L. et al., 1989. Cyclooxygenase metabolism of endogenous arachidonic acid by cultured human tracheal epithelial cells. *The American review of respiratory disease*, 140, pp.449–459.

Clark, R.A., 1991. The Communality of Cutaneous Wound Repair and Lung Injury. *Chest*, 99(3), pp.57–60.

Clark, R.A.F., 1996. *The molecular and cellular biology of wound repair*, Springer.

Clarke, D.L. et al., 2013. Matrix regulation of idiopathic pulmonary fibrosis: the role of enzymes. *Fibrogenesis & tissue repair*, 6(1), p.20.

Coker, R.K. et al., 1997. Transforming growth factors-b1, -b2, and -b3 stimulate fibroblast procollagen production in vitro but are differentially expressed during bleomycin-induced lung fibrosis. *Am J Pathol*, 150(3), pp.981–991.

Conte, E. et al., 2014. Effect of pirfenidone on proliferation, TGF-beta -induced myofibroblast differentiation and fibrogenic activity of primary human lung fibroblasts. *European Journal of Pharmaceutical Sciences*, 58(1), pp.13–19.

Cool, C.D. et al., 2006. Fibroblast foci are not discrete sites of lung injury or repair: The fibroblast reticulum. *American Journal of Respiratory and Critical Care Medicine*, 174(6), pp.654–658.

Corrin, B. et al., 1994. Immunohistochemical localization of transforming growth factor-beta 1 in the lungs of patients with systemic sclerosis, cryptogenic fibrosing alveolitis and other lung disorders. *Histopathology*, 24(2), pp.145–150.

Craig, V.J. et al., 2015. Matrix metalloproteinases as therapeutic targets for idiopathic pulmonary fibrosis. *American Journal of Respiratory Cell and Molecular Biology*, 53(5), pp.585–600.

Crystal, R.G. et al., 2008. Airway epithelial cells: current concepts and challenges. *Proc Am Thorac Soc*, 5(7), pp.772–777.

Crystal, R.G. et al., 1976. Idiopathic pulmonary fibrosis. Clinical, histologic, radiographic, physiologic, scintigraphic, cytologic, and biochemical aspects. *Annals of Internal Medicine*, 85(6), pp.769–788.

Cutroneo, K.R. et al., 2007. Therapies for bleomycin induced lung fibrosis through regulation of TGF-beta1 induced collagen gene expression. *Journal of cellular physiology*, 211(3), pp.585–9.

Daccord, C. & Maher, T., 2016. Recent advances in idiopathic pulmonary fibrosis. *Tuberc Respir Dis (Seoul)*, 74(1), pp.1–6.

Darby, I.A. et al., 2014. Fibroblasts and myofibroblasts in wound healing. *Clinical, Cosmetic and Investigational Dermatology*, 7, pp.301–311.

Datta, A., Scotton, C.J. & Chambers, R.C., 2011. Novel therapeutic approaches for pulmonary fibrosis. *British Journal of Pharmacology*, 163, pp.141–172.

David Kaminsky, 2011. *Netter Collection of Medical Illustrations: Respiratory System* 2nd ed., Elsevier Health Sciences.

De, S., Kuwahara, S. & Saito, A., 2014. The endocytic receptor megalin and its associated proteins in proximal tubule epithelial cells. *Membranes*, 4(3), pp.333–335.

Denney, L. et al., 2015. Pulmonary Epithelial Cell-Derived Cytokine TGF-β1 Is a Critical Cofactor for Enhanced Innate Lymphoid Cell Function. *Immunity*, 43(5), pp.945–958.

Desmoulière, A. et al., 1995. Apoptosis mediates the decrease in cellularity during the transition between granulation tissue and scar. *The American journal of pathology*, 146(1), pp.56–66.

Desmoulière, A. et al., 1993. Transforming growth factor-beta 1 induces alpha-smooth muscle actin expression in granulation tissue myofibroblasts and in quiescent and growing cultured fibroblasts. *The Journal of cell biology*, 122(1), pp.103–111.

Desmouliere, A., Chaponnier, C. & Gabbiani, G., 2005. Tissue repair, contraction, and the myofibroblast. *Wound.Repair Regen.*, 13(1), pp.7–12.

Devauchelle, V. et al., 2006. Characterization and functional consequences of underexpression of clusterin in rheumatoid arthritis. *Journal of immunology (Baltimore, Md. : 1950)*, 177(9), pp.6471–9.

Doonan, F. & Cotter, T.G., 2008. Morphological assessment of apoptosis. *Methods*, 44, pp.200–204.

Dumont, P. et al., 2002. Overexpression of apolipoprotein J in human fibroblasts protects against cytotoxicity and premature senescence induced by ethanol and tert-butylhydroperoxide. *Cell stress & chaperones*, 7(1), pp.23–35.

Dunsmore, S.E. & Rannels, D.E., 1996. Extracellular matrix biology in the lung. *The American journal of physiology*, 270(1 Pt 1), pp.L3–L27.

E. B. Meltzer, P.W.N., 2008. Idiopathic pulmonary fibrosis. *Orphanet Journal of Rare Disease*, 345(7), pp.517–525.

Eaton, D.C. et al., 2004. Regulation of Na+ channels in lung alveolar type II epithelial cells. *Proceedings of the American Thoracic Society*, 1(1), pp.10–6.

Egan, J.J. et al., 1995. Epstein-Barr virus replication within pulmonary epithelial cells in cryptogenic fibrosing alveolitis. *Thorax*, 50(12), pp.1234–9.

Elbashir, S.M. et al., 2001. Duplexes of 21-nucleotide RNAs mediate RNA interference in cultured mammalian cells. *Nature*, 411(6836), pp.494–498.

Elias, J.A. et al., 1985. Human alveolar macrophage inhibition of lung fibroblast growth. A prostaglandin-dependent process. *The American review of respiratory disease*, 131(1), pp.94–9.

Enomoto, N. et al., 2013. Amount of elastic fibers predicts prognosis of idiopathic pulmonary fibrosis. *Respiratory Medicine*, 107(10), pp.1608–1616.

Enomoto, N. et al., 2006. Quantitative analysis of fibroblastic foci in usual interstitial pneumonia. *Chest*, 130(1), pp.22–29.

Evans, I.C. et al., 2016. Epigenetic Regulation of Cyclooxygenase-2 by methylation of c8orf4 in Pulmonary Fibrosis. *Clinical Science*, 4, pp.575–586.

Fadok, V. a et al., 1998. Macrophages That Have Ingested Apoptotic Cells In Vitro Inhibit Proinflammatory Cytokine Production Through Autocrine / Paracrine Mechanisms Involving TGF-beta. *Society*, 80206(28).

Fairweather, M. et al., 2015. Celecoxib inhibits early cutaneous wound healing. *Journal of Surgical Research*, 194(2), pp.717–724.

Falke, L.L. et al., 2015. Diverse origins of the myofibroblast—implications for kidney fibrosis. *Nature reviews. Nephrology*, 11(4), pp.233–44.

Fernandez, I.E. & Eickelberg, O., 2012. The Impact of TGF-β on Lung Fibrosis: From Targeting to Biomarkers. *Proceedings of the American Thoracic Society*, 9(3), pp.111–116.

Fine, A. & Goldstein, R.H., 1987. The effect of PGE2 on the activation of quiescent lung fibroblasts. *Prostaglandins*, 33(6), pp.903–913.

Fisher, C.E. & Howie, S.E.M., 2006. The role of megalin (LRP-2/Gp330) during development. *Developmental biology*, 296, pp.279–97.

Flaherty, K.R. et al., 2003. Fibroblastic foci in usual interstitial pneumonia: idiopathic versus collagen vascular disease. *Am.J.Respir.Crit Care Med.*, 167(10), pp.1410–1415.

Frankel, S.K. et al., 2006. TNF-beta sensitizes normal and fibrotic human lung fibroblasts to Fas-induced apoptosis. *American Journal of Respiratory Cell and Molecular Biology*, 34(20), pp.293–304.

Frantz, C., Stewart, K.M. & Weaver, V.M., 2010. The extracellular matrix at a glance. *Journal of cell science*, 123, pp.4195–4200.

Freeburn, R.W., Armstrong, L. & Millar, A.B., 2005. Cultured alveolar macrophages from patients with idiopathic pulmonary fibrosis (IPF) show dysregulation of lipopolysaccharide-induced tumor necrosis factor-beta (TNF-beta) and interleukin-10 (IL-10) inductions. *European Cytokine Network*, 16(1), pp.5–16.

French, L.E. et al., 1993. Murine Clusterin: Molecular cloning and mRNA localization of a gene associated with epithelial differentiation process during embryogenesis. *Journal of Cell Biology*, 122(5), pp.1119–1130.

Fu, Y. et al., 2015. Lentivirus-mediated shRNA interference of clusterin blocks proliferation, motility, invasion and cell cycle in the ovarian cancer cells. *Journal of ovarian research*, 8, p.59.

Fujii, T. et al., 2002. Interaction of alveolar macrophages and airway epithelial cells following exposure to particulate matter produces mediators that stimulate the bone marrow. *American Journal of Respiratory Cell and Molecular Biology*, 27(1), pp.34–41.

Fukuda, Y. et al., 1995. Significance of early intra-alveolar fibrotic lesions and integrin expression in lung biopsy specimens from patients with idiopathic pulmonary fibrosis. *Hum Pathol*, 26(1), pp.53–61.

Gabbiani, G., 2003. The myofibroblast in wound healing and fibrocontractive diseases. *J.Pathol.*, 200(4), pp.500–503.

Gangadharan, B., Bapat, M., Rossa, J., Antrobus, R., et al., 2012. Discovery of novel biomarker candidates for liver Fibrosis in Hepatitis C patients: A preliminary study. *PLoS ONE*, 7(6).

Gangadharan, B., Bapat, M., Rossa, J., Antrobus, R., et al., 2012. Discovery of novel biomarker candidates for liver Fibrosis in Hepatitis C patients: A preliminary study. *PLoS ONE*, 7(6).

García, S. et al., 2010. Akt activity protects rheumatoid synovial fibroblasts from Fas-induced apoptosis by inhibition of Bid cleavage. *Arthritis Research & Therapy*, 12.

Gassler, N. et al., 2001. Expression of clusterin in Crohn's disease of the terminal ileum. *Histology and Histopathology*, 16(3), pp.755–762.

Gauldie, J., Jordana, M. & Cox, G., 1993. Cytokines and pulmonary fibrosis. *Thorax*, 48(9), pp.931–5.

Gekle, M. et al., 2003. Transforming growth factor-β1 reduces megalin- and cubilin-mediated endocytosis of albumin in proximal-tubule-derived opossum kidney cells. *The Journal of Physiology*, 552(2), pp.471–481.

Gil, S.Y. et al., 2013. Clusterin and LRP2 are critical components of the hypothalamic feeding regulatory pathway. *Nature Communications*, 4(May), pp.1862–1869.

Girton, R. a, Sundin, D.P. & Rosenberg, M.E., 2002. Clusterin protects renal tubular epithelial cells from gentamicin-mediated cytotoxicity. *American Journal of Physiology - Renal Physiology*, 282, pp.F703–F709.

Goffin, J.M. et al., 2006. Focal adhesion size controls tension-dependent recruitment of alpha-smooth muscle actin to stress fibers. *The Journal of cell biology*, 172, pp.259–268.

Gong, D. et al., 2012. TGFβ signaling plays a critical role in promoting alternative macrophage activation. *BMC immunology*, 13, p.31.

Gordon, S., 2003. Alternative activation of macrophages. *Nat Rev Immunol*, 3(1), pp.23–35.

Gordon, S.B. & Read, R.C., 2002. Macrophage defences against respiratory tract infections The immunology of childhood respiratory infections. *British medical bulletin*, 61(1), pp.45–61.

Greenlee, K.J., Werb, Z. & Kheradmand, F., 2007. Matrix metalloproteinases in lung: multiple, multifarious, and multifaceted. *Physiological reviews*, 87(1), pp.69–98.

Greer, A.K. et al., 2006. Gene expression analysis in a canine model of X-linked Alport syndrome. *Mammalian Genome*, 17(9), pp.976–990.

Gribbin, J. et al., 2006. Incidence and mortality of idiopathic pulmonary fibrosis and sarcoidosis in the UK. *Thorax*, 61(11), pp.980–5.

Gross, T.J. & Hunninghake, G.W., 2001. Idiopathic pulmonary fibrosis. *N.Engl.J.Med.*, 345(7), pp.517–525.

Grotendorst, G.R., Soma, Y., et al., 1989. EGF and TGF-alpha are potent chemoattractants for endothelial cells and EGF-like peptides are present at sites of tissue regeneration. *Journal of cellular physiology*, 139, pp.617–623.

Grotendorst, G.R., Smale, G. & Pencev, D., 1989. Production of transforming growth factor beta by human peripheral blood monocytes and neutrophils. *Journal of cellular physiology*, 140, pp.396–402.

Guo, W. et al., 2009. Abrogation of TGF-beta1-induced fibroblast-myofibroblast differentiation by histone deacetylase inhibition. *American journal of physiology. Lung cellular and molecular physiology*, 297(5), pp.L864-70.

Hamilton, L.M. et al., 2001. The bronchial epithelium in asthma--much more than a passive barrier. *Monaldi Arch Chest Dis*, 56(1), pp.48–54.

Hampel, B. et al., 2005. Apoptosis resistance of senescent human fibroblasts is correlated with the absence of nuclear IGFBP-3. *Aging cell*, 4(6), pp.325–330.

Han, M.K. et al., 2008. Sex differences in physiological progression of idiopathic pulmonary fibrosis. *Eur.Respir.J.*, 31(6), pp.1183–1188.

Hance, A.J., Bradley, K. & Crystal, R.G., 1976. Lung collagen heterogeneity. Synthesis of type I and type III collagen by rabbit and human lung cells in culture. *The Journal of clinical investigation*, 57(1), pp.102–11.

Haschek, W.M. & Rousseau, C.G., 1997. *Fundamentals of Toxicologic Pathology*, Elsevier.

He, C. et al., 2013. Accelerated development of pulmonary fibrosis via Cu,Zn-superoxide dismutase-induced alternative activation of macrophages. *Journal of Biological Chemistry*, 288(28), pp.20745–20757.

Heller, A.R. et al., 2003. Clusterin protects the lung from leukocyte-induced injury. *Shock (Augusta, Ga.)*, 20(2), pp.166–170.

Hempel, S.L., Monick, M.M., He, B., et al., 1994. Synthesis of prostaglandin H synthase-2 by human alveolar macrophages in response to lipopolysaccharide is inhibited by decreased cell oxidant tone. *The Journal of biological chemistry*, 269, pp.32979–32984.

Hempel, S.L., Monick, M.M. & Hunninghake, G.W., 1994. Lipopolysaccharide induces prostaglandin H synthase-2 protein and mRNA in human alveolar macrophages and blood monocytes. *The Journal of clinical investigation*, 93, pp.391–396.

Henderson, N.C. & Sheppard, D., 2013a. Integrin-mediated regulation of TGF-beta in fibrosis. *Biochimica et Biophysica Acta - Molecular Basis of Disease*, 1832(7), pp.891–896.

Henderson, N.C. & Sheppard, D., 2013b. Integrin-mediated regulation of TGFβ in fibrosis. *Biochimica et Biophysica Acta - Molecular Basis of Disease*, 1832, pp.891–896.

Henry, M.T. et al., 2002. Matrix metalloproteinases and tissue inhibitor of metalloproteinase-1 in sarcoidosis and IPF. *The European respiratory journal : official journal of the European Society for Clinical Respiratory Physiology*, 20(5), pp.1220–1227.

Hermey, G. et al., 2001. Multiple Receptors Mediate apoJ-Dependent Clearance of Cellular Debris into Nonprofessional Phagocytes. *Exp Cell Res*, 279, pp.130–141.

Herold, S., Mayer, K. & Lohmeyer, J., 2011. Acute Lung Injury: How Macrophages Orchestrate Resolution of Inflammation and Tissue Repair. *Frontiers in Immunology*, 2(November), pp.1–13.

Herzog, E.L., Mathur, A., Tager, A.M., et al., 2014. Interstitial Lung Disease Associated With Systemic Sclerosis and Idiopathic Pulmonary Fibrosis: How Similar and Distinct? *Arthritis Rheumatology*, 4(164), pp.1967–1978.

Herzog, E.L., Mathur, A. & Tager, A.M., 2014. Interstitial Lung Disease Associated With Systemic Sclerosis and Idiopathic Pulmonary Fibrosis. *NIH Public Access*, 18(8),

pp.1199–1216.

Hinz, B. et al., 2001. Alpha-smooth muscle actin expression upregulates fibroblast contractile activity. *Mol.Biol.Cell*, 12(9), pp.2730–2741.

Hinz, B. et al., 2007. The Myofibroblast. *The American Journal of Pathology*, 170(6), pp.1807–1816.

Hinz, B., 2010. The myofibroblast: Paradigm for a mechanically active cell. *Journal of Biomechanics*, 43(1), pp.146–155.

Hodge, S. et al., 2002. Up-regulation of production of TGF-β and IL-4 and down-regulation of IL-6 by apoptotic human bronchial epithelial cells. *Immunology and Cell Biology*, 80, pp.537–543.

Hong, G.H. et al., 2016. Clusterin Modulates Allergic Airway Inflammation by Attenuating CCL20-Mediated Dendritic Cell Recruitment. *The Journal of Immunology*, 196, pp.2021–2030.

van den Hoogen, F. et al., 2013. 2013 classification criteria for systemic sclerosis: an American college of rheumatology/European league against rheumatism collaborative initiative. *Annals of the rheumatic diseases*, 72(11), pp.1747–55.

Horowitz, J.C., Martinez, F.J. & Thannickal, V.J., 2012. NIH Public Access. , 6(3), pp.201–210.

Horowitz, J.C. & Thannickal, V.J., 2006. Epithelial-mesenchymal interactions in pulmonary fibrosis. *Seminars in respiratory and critical care medicine*, 27(6), pp.600–12.

Hostettler, K.E. et al., 2008. Airway epithelium-derived transforming growth factor-beta is a regulator of fibroblast proliferation in both fibrotic and normal subjects. *Clinical and experimental allergy : Journal of the British Society for Allergy and Clinical Immunology*, 38(8), pp.1309–17.

Hsieh, S.-Y. et al., 2005. Dys-regulation of clusterin in human hepatoma is not associated with tumorigenesis but is secondary to cell response to external stresses. *Molecular carcinogenesis*, 43(2), pp.100–7.

Huang, S.K. et al., 2014. Lung fibroblasts from patients with idiopathic pulmonary fibrosis exhibit genome-wide differences in DNA methylation compared to fibroblasts from nonfibrotic lung. *PloS one*, 9(9), p.e107055.

Huang, S.K. et al., 2009. Prostaglandin E2 induces fibroblast apoptosis by modulating multiple survival pathways. *The FASEB journal : official publication of the Federation of American Societies for Experimental Biology*, 23(12), pp.4317–4326.

Humphreys D.T et al., 1997. Effects of clusterin overexpression on TNFalpha and TGFbeta - mediated death of L929 cells. [Biochemistry. 1997] - PubMed - NCBI.

Biochemistry, pp.15233–15243.

Hussell, T. & Bell, T.J., 2014a. Alveolar macrophages: plasticity in a tissue-specific context. *Nature reviews. Immunology*, 14(2), pp.81–93.

Hussell, T. & Bell, T.J., 2014b. Alveolar macrophages: plasticity in a tissue-specific context. *Nature reviews. Immunology*, 14(February), pp.81–93.

Hutchinson, J. et al., 2015. Global incidence and mortality of idiopathic pulmonary fibrosis: A systematic review. *European Respiratory Journal*, 46(3), pp.795–806.

Hwang, S. et al., 2013. Far-infrared radiation inhibits proliferation, migration, and angiogenesis of human umbilical vein endothelial cells by suppressing secretory clusterin levels. *Cancer letters*.

Imhof, A. et al., 2006. Sustained astrocytic clusterin expression improves remodeling after brain ischemia. *Neurobiology of disease*, 22(2), pp.274–83.

Inomata, M. et al., 2014. Pirfenidone inhibits fibrocyte accumulation in the lungs in bleomycin-induced murine pulmonary fibrosis. *Respiratory research*, 15, p.16.

Irving, W.L., Day, S. & Johnston, I.D., 1993. Idiopathic pulmonary fibrosis and hepatitis C virus infection. *The American review of respiratory disease*, 148(6 Pt 1), pp.1683–1684.

Itahana, Y. et al., 2007. Regulation of clusterin expression in mammary epithelial cells. *Experimental cell research*, 313, pp.943–51.

Iyonaga, K. et al., 1994. Monocyte chemoattractant protein-1 in idiopathic pulmonary fibrosis and other interstitial lung diseases. *Human pathology*, 25(5), pp.455–63.

Jagirdar, J. et al., 1997. Immunohistochemical localization of transforming growth factor beta isoforms in asbestos-related diseases. *Environmental health perspectives*, 105 Suppl, pp.1197–1203.

Janig, E. et al., 2007. Clusterin associates with altered elastic fibers in human photoaged skin and prevents elastin from ultraviolet-induced aggregation in vitro. *The American journal of pathology*, 171(5), pp.1474–1482.

Jeong, S. et al., 2012. Interaction of clusterin and matrix metalloproteinase-9 and its implication for epithelial homeostasis and inflammation. *The American journal of pathology*, 180(5), pp.2028–39.

Jin, G. & Howe, P.H., 1999. Transforming growth factor beta regulates clusterin gene expression via modulation of transcription factor c-Fos. *European journal of biochemistry / FEBS*, 263(2), pp.534–542.

Jordana, M. et al., 1994. Immune-inflammatory functions of fibroblasts. *The European respiratory journal : official journal of the European Society for Clinical Respiratory Physiology*, 7, pp.2212–2222.

July, L. V et al., 2004. Nucleotide-based therapies targeting clusterin chemosensitize

human lung adenocarcinoma cells both in vitro and in vivo. *Molecular cancer therapeutics*, 3(3), pp.223–232.

Jun, H.-O. et al., 2011. Clusterin protects H9c2 cardiomyocytes from oxidative stress-induced apoptosis via Akt/GSK-3β signaling pathway. *Experimental & molecular medicine*, 43(1), pp.53–61.

Jung, G.-S. et al., 2012. Clusterin attenuates the development of renal fibrosis. *Journal of the American Society of Nephrology*, 23(1), pp.73–85.

Kamio, K. et al., 2005. Promoter analysis and aberrant expression of the MUC5B gene in diffuse panbronchiolitis. *American Journal of Respiratory and Critical Care Medicine*, 171(9), pp.949–957.

Kang, B.H. et al., 2014. Clusterin stimulates the chemotactic migration of macrophages through a pertussis toxin sensitive G-protein-coupled receptor and Gβγ-dependent pathways. *Biochemical and Biophysical Research Communications*, 445, pp.645–650.

Kang, S.-W. et al., 2005. Clusterin interacts with SCLIP (SCG10-like protein) and promotes neurite outgrowth of PC12 cells. *Experimental cell research*, 309(2), pp.305–15.

Kang, S.S. et al., 2016. Identification of plexin A4 as a novel clusterin receptor links two Alzheimer's disease risk genes. *Human molecular genetics*.

Kapron, J.T. et al., 1997. Identification and characterization of glycosylation sites in human serum clusterin. *Protein science : a publication of the Protein Society*, 6(10), pp.2120–33.

Kaseda, R. et al., 2007. Megalin-mediated endocytosis of cystatin C in proximal tubule cells. *Biochemical and Biophysical Research Communications*, 357(4), pp.1130–1134.

Kasper, M. & Haroske, G., 1996. Alterations in the alveolar epithelium after injury leading to pulmonary fibrosis. *Histology and Histopathology*, 11(2), pp.463–483.

Katzenstein, A.L.A., Mukhopadhyay, S. & Myers, J.L., 2008. Diagnosis of usual interstitial pneumonia and distinction from other fibrosing interstitial lung diseases. *Human Pathology*, 39(9), pp.1275–1294.

Katzenstein, a L., 1985. Pathogenesis of "fibrosis" in interstitial pneumonia: an electron microscopic study. *Human pathology*, 16(10), pp.1015–1024.

Keane, M.P., 2008. The role of chemokines and cytokines in lung fibrosis. *European Respiratory Review*, 17(109), pp.151–156.

Keerthisingam, C.B. et al., 2001. Cyclooxygenase-2 deficiency results in a loss of the anti-proliferative response to transforming growth factor-beta in human fibrotic lung fibroblasts and promotes bleomycin-induced pulmonary fibrosis in mice. *The*

American journal of pathology, 158(4), pp.1411–1422.

Kelley, J. et al., 1991. Cytokine signaling in lung: transforming growth factor-beta secretion by lung fibroblasts. *The American journal of physiology*, 260, pp.L123–L128.

Khalil, N. et al., 1991. Increased production and immunohistochemical localization of transforming growth factor-beta in idiopathic pulmonary fibrosis. *American journal of respiratory cell and molecular biology*, 5(2), pp.155–162.

Khalil, N. et al., 2005a. Proliferation of pulmonary interstitial fibroblasts is mediated by transforming growth factor-beta1-induced release of extracellular fibroblast growth factor-2 and phosphorylation of p38 MAPK and JNK. *Journal of Biological Chemistry*, 280, pp.43000–43009.

Khalil, N. et al., 2005b. Proliferation of pulmonary interstitial fibroblasts is mediated by transforming growth factor-beta1-induced release of extracellular fibroblast growth factor-2 and phosphorylation of p38 MAPK and JNK. *The Journal of biological chemistry*, 280(52), pp.43000–9.

Khalil, N. et al., 1996. TGF-beta 1, but not TGF-beta 2 or TGF-beta 3, is differentially present in epithelial cells of advanced pulmonary fibrosis: an immunohistochemical study. *American journal of respiratory cell and molecular biology*, 14, pp.131–138.

Kim, B.M. et al., 2006. Clusterin induces differentiation of pancreatic duct cells into insulin-secreting cells. *Diabetologia*, 49(2), pp.311–20.

Kim, H.-J. et al., 2009. Protective role of clusterin/apolipoprotein J against neointimal hyperplasia via antiproliferative effect on vascular smooth muscle cells and cytoprotective effect on endothelial cells. *Arteriosclerosis, thrombosis, and vascular biology*, 29(10), pp.1558–64.

Kim, J.-S. et al., 2006. Transforming growth factor-beta1 regulates macrophage migration via RhoA. *Blood*, 108(6), pp.1821–9.

Kim, J.H. et al., 2010. Protective effect of clusterin from oxidative stress-induced apoptosis in human retinal pigment epithelial cells. *Investigative ophthalmology & visual science*, 51(1), pp.561–566.

Kim, T.H. et al., 2010. Role of Lung Apolipoprotein A-I in Idiopathic Pulmonary Fibrosis Antiinflammatory and Antifibrotic Effect on Experimental Lung Injury and Fibrosis. *American Journal of Respiratory and Critical Care Medicine*, 182, pp.633–642.

King, T.E. et al., 2014. A phase 3 trial of pirfenidone in patients with idiopathic pulmonary fibrosis. *The New England journal of medicine*, 370(22), pp.2083–92.

King, T.E. et al., 2001. Predicting survival in idiopathic pulmonary fibrosis: scoring system and survival model. *American journal of respiratory and critical care*

medicine, 164(7), pp.1171–1181.

King Jr., T.E., Pardo, A. & Selman, M., 2011. Idiopathic pulmonary fibrosis. *Lancet*, 378(9807), pp.1949–1961.

Kirszbaum, L., Bozas, S.E. & Walker, I.D., 1992. SP-40,40, a protein involved in the control of the complement pathway, possesses a unique array of disulphide bridges. *FEBS letters*, 297(1–2), pp.70–6.

Kistler, K.D. et al., 2014. Lung transplantation in idiopathic pulmonary fibrosis: a systematic review of the literature. *BMC pulmonary medicine*, 14(1), p.139.

Klahr, S. & Morrissey, J.J., 1997. Comparative study of ACE inhibitors and angiotensin II receptor antagonists in interstitial scarring. *Kidney Int.Suppl*, 63, pp.S111–S114.

Kodama, N. et al., 1998. Expression of RANTES by bronchoalveolar lavage cells in nonsmoking patients with interstitial lung diseases. *American Journal of Respiratory Cell and Molecular Biology*, 18(4), pp.526–531.

Kolodsick, J.E. et al., 2003. Prostaglandin E2 inhibits fibroblast to myofibroblast transition via E. prostanoid receptor 2 signaling and cyclic adenosine monophosphate elevation. *Am.J.Respir.Cell Mol.Biol.*, 29(5), pp.537–544.

Korfei, M. et al., 2008. Epithelial endoplasmic reticulum stress and apoptosis in sporadic idiopathic pulmonary fibrosis. *American journal of respiratory and critical care medicine*, 178, pp.838–846.

Kounnas, M.Z. et al., 1995. Identification of Glycoprotein 330 as an Endocytic Receptor for Apolipoprotein J/Clusterin. *The Journal of biological chemistry*, 270(June 2), pp.13070–13075.

Kounnas, M.Z. et al., Immunological localization of glycoprotein 330, low density lipoprotein receptor related protein and 39 kDa receptor associated protein in embryonic mouse tissues. *In vivo (Athens, Greece)*, 8(3), pp.343–51.

Kozel, B.A. et al., 2006. Elastic Fiber Formation: A Dynamic View of Extracellular Matrix Assembly Uning Timer Reporters. *Journal of cellular physiology*, 207(1), pp.12–22.

Kreuter, M. et al., 2015. Pharmacological Treatment of Idiopathic Pulmonary Fibrosis: Current Approaches, Unsolved Issues, and Future Perspectives. *BioMed Research International*, 2015.

Kristensen, J.H. et al., 2015. Levels of circulating MMP-7 degraded elastin are elevated in pulmonary disorders. *Clinical Biochemistry*, p48.

Kristensen, J.H. et al., 2015. Serological assessment of neutrophil elastase activity on elastin during lung ECM remodeling. *BMC Pulmonary Medicine*, 15, p.53.

Kropski, J.A. et al., 2013. Genetic studies provide clues on the pathogenesis of idiopathic pulmonary fibrosis. , 17, pp.9–17.

Kuhn, C. & McDonald, J.A., 1991. The roles of the myofibroblast in idiopathic pulmonary fibrosis. Ultrastructural and immunohistochemical features of sites of active extracellular matrix synthesis. *The American journal of pathology*, 138(5), pp.1257–65.

Kumar, R.K. et al., 1996. Epithelial cell-derived transforming growth factor-beta in bleomycin-induced pulmonary injury. *International journal of experimental pathology*, 77(3), pp.99–107.

Kwon, H.-S. et al., 2014. Clusterin expression level correlates with increased oxidative stress in asthmatics. *Annals of allergy, asthma & immunology : official publication of the American College of Allergy, Asthma, & Immunology*, 112, pp.217–21.

Lakins, J.N. et al., 2006. Evidence That Clusterin Has Discrete Chaperone and Ligand Binding Sites. *Biochemistry*, 41, pp.282–291.

Lakins, J.N. et al., 2002. Evidence that clusterin has discrete chaperone and ligand binding sites. *Biochemistry*, 41(1), pp.282–91.

Lama, V. et al., 2002. Prostaglandin E2 synthesis and suppression of fibroblast proliferation by alveolar epithelial cells is cyclooxygenase-2-dependent. *American Journal of Respiratory Cell and Molecular Biology*, 27(6), pp.752–758.

Landsman, L. & Jung, S., 2007. Lung Macrophages Serve as Obligatory Intermediate between Blood Monocytes and Alveolar Macrophages. *The Journal of Immunology*, 179(6), pp.3488–3494.

Last, J.A. & Reiser, K.M., 1984. Collagen biosynthesis. *Environ.Health Perspect.*, 55, pp.169–177.

Laurent, G.J. & McAnulty, R.J., 1983. Protein metabolism during bleomycin-induced pulmonary fibrosis in rabbits. In vivo evidence for collagen accumulation because of increased synthesis and decreased degradation of the newly synthesized collagen. *Am Rev Respir Dis*, 128(1), pp.82–88.

Law, G.L. & Griswold, M.D., 1994. Activity and form of sulfated glycoprotein 2 (clusterin) from cultured Sertoli cells, testis, and epididymis of the rat. *Biology of reproduction*, 50(3), pp.669–79.

Lawson, W.E. et al., 2008. Endoplasmic reticulum stress in alveolar epithelial cells is prominent in IPF: association with altered surfactant protein processing and herpesvirus infection. *American journal of physiology. Lung cellular and molecular physiology*, 294, pp.L1119–L1126.

Leask, A. & Abraham, D.J., 2004. TGF-beta signaling and the fibrotic response. *FASEB journal : official publication of the Federation of American Societies for Experimental Biology*, 18(7), pp.816–27.

Lech, M. & Anders, H.J., 2013. Macrophages and fibrosis: How resident and infiltrating

mononuclear phagocytes orchestrate all phases of tissue injury and repair. *Biochimica et Biophysica Acta - Molecular Basis of Disease*, 1832, pp.989–997.

Leeb, C., Eresheim, C. & Nimpf, J., 2014. Clusterin is a ligand for apolipoprotein E receptor 2 (ApoER2) and very low density lipoprotein receptor (VLDLR) and signals via the Reelin-signaling pathway. *The Journal of biological chemistry*, 289(7), pp.4161–72.

Leibovich, S.J. & Ross, R., 1975. The role of the macrophage in wound repair. A study with hydrocortisone and antimacrophage serum. *The American journal of pathology*, 78(1), pp.71–100.

Lemjabbar, H. et al., 1999. Overexpression of alveolar macrophage gelatinase B (MMP-9) in patients with idiopathic pulmonary fibrosis: effects of steroid and immunosuppressive treatment. *American journal of respiratory cell and molecular biology*, 20(5), pp.903–13.

Leppäranta, O. et al., 2012. Regulation of TGF-β storage and activation in the human idiopathic pulmonary fibrosis lung. *Cell and Tissue Research*, 348(3), pp.491–503.

Li, H. et al., 2010. Clusterin immunoexpression and its clinical significance in patients with non-small cell lung cancer. *Lung*, 188(5), pp.423–431.

Li, J. et al., 2012. Stable Knockdown of Clusterin by Vector-Based RNA Interference in a Human Breast Cancer Cell Line Inhibits Tumour Cell Invasion and Metastasis. *Journal of International Medical Research*, 40(2), pp.545–555.

Li, J. & Huang, Y., 2013. The Evaluation of Cognitive Impairment and Relevant Factors in Patients with Chronic Obstructive Pulmonary Disease. pp.98–105.

Li, M.O. et al., 2006. Transforming growth factor-beta regulation of immune responses. *Annual review of immunology*, 24, pp.99–146.

Li, N. et al., 2013. GRP78 regulates clusterin stability, retrotranslocation and mitochondrial localization under ER stress in prostate cancer, Ocogene (November 2011), pp.1933–1942.

Li, X. et al., 2004. Apoptosis in lung injury and remodeling. *Journal of applied physiology (Bethesda, Md. : 1985)*, 97(4), pp.1535–42.

Li, Y.J. et al., 2010. Prostaglandin E2 inhibits human lung fibroblast chemotaxis through disparate actions on different E-prostanoid receptors. *American Journal of Respiratory Cell and Molecular Biology*, 44(1), pp.99–107.

Liu, X. et al., 2015. Secretory clusterin is upregulated in rats with pulmonary arterial hypertension induced by systemic-to-pulmonary shunts and exerts important roles in pulmonary artery smooth muscle cells. *Acta Physiologica*, 213, pp.505–518.

Livak, K.J. & Schmittgen, T.D., 2001. Analysis of relative gene expression data using real-time quantitative PCR and the 2(-Delta Delta C(T)) Method. *Methods (San*

Diego, Calif.), 25(4), pp.402–8.

Loveman, E. et al., 2015. The clinical effectiveness and cost-effectiveness of treatments for idiopathic pulmonary fibrosis: a systematic review and economic evaluation. *Health technology assessment (Winchester, England)*, 19(20).

Lovgren, A.K. et al., 2011. beta-Arrestin Deficiency Protects Against Pulmonary Fibrosis in Mice and Prevents Fibroblast Invasion of Extracellular Matrix. *Sci.Transl.Med.*, 3(74), p.74.

Lundgren, S. et al., 1997. Tissue Distribution of Human gp330/Megalin, a Putative Ca2+ sensing protein. *the Journal of Histochemistry and Cytochemistry*, 45, pp.383–392.

Lynch, J.P. et al., 2016. Idiopathic Pulmonary Fibrosis : Epidemiology , Clinical Features , Prognosis , and Management. *Semin Respir Crit Care Med*, pp.331–57.

Ma, G. et al., 2015. sCLU regulates cisplatin chemosensitivity of lung cancer cells in vivo. *World journal of surgical oncology*, 13, p.80.

Maher, T.M. et al., 2010. Diminished prostaglandin E2 contributes to the apoptosis paradox in idiopathic pulmonary fibrosis. *American journal of respiratory and critical care medicine*, 182(1), pp.73–82.

Maher, T.M., 2013. PROFILEing idiopathic pulmonary fibrosis: Rethinking biomarker discovery. *European Respiratory Review*, 22, pp.148–152.

Maher, T.M. & Wells, A.U., 2008. Optimal treatment for idiopathic pulmonary fibrosis. *Thorax*, 63(12), p.1120-1121.

Maher, T.M., Wells, A.U. & Laurent, G.J., 2007. Idiopathic pulmonary fibrosis: Multiple causes and multiple mechanisms? *European Respiratory Journal*, 30(5), pp.835–839.

Maini, R.N. et al., 1995. Beneficial effects of tumour necrosis factor-alpha (TNF-alpha) blockade in rheumatoid arthritis (RA). *Clinical and experimental immunology*, 101(2), pp.207–12.

Manoury, B. et al., 2007. Influence of early neutrophil depletion on MMPs/TIMP-1 balance in bleomycin-induced lung fibrosis. *International Immunopharmacology*, 7(7), pp.900–911.

Martinez, F.O. et al., 2008. Macrophage activation and polarization. *Frontiers in bioscience.* 13(4), pp.453–61.

Martinez, F.O. & Gordon, S., 2014. The M1 and M2 paradigm of macrophage activation: time for reassessment. *F1000prime reports*, 6, p.13.

Martinez, F.O., Helming, L. & Gordon, S., 2009. Alternative activation of macrophages: an immunologic functional perspective. *Annual review of immunology*, 27, pp.451–83.

Marzolo, M.P. & Farfán, P., 2011. New insights into the roles of megalin/LRP2 and the regulation of its functional expression. *Biological Research*, 44, pp.89–105.

McAnulty, R.J., 2007. Fibroblasts and myofibroblasts: Their source, function and role in disease. *The International Journal of Biochemistry & Cell Biology*, 39(4), pp.666–671.

McAnulty, R.J. et al., 1997. Indomethacin suppresses the anti-proliferative effects of transforming growth factor-beta isoforms on fibroblast cell cultures. *Biochemical Journal*, 321, pp.639–643.

Meltzer, E.B. & Noble, P.W., 2008. Idiopathic pulmonary fibrosis. *Orphanet Journal of Rare Disease*, 345(7), pp.517–525.

Micallef, L. et al., 2012. The myofibroblast, multiple origins for major roles in normal and pathological tissue repair. *Fibrogenesis & tissue repair*, 5 Suppl 1(Suppl 1), p.S5.

Michel, D. et al., 1997. Stress-induced transcription of the clusterin/apoJ gene. *The Biochemical journal*, (Pt 1), pp.45–50.

Millis, J. et al., 2001. Clusterin regulates vascular smooth muscle cell nodule formation and migration. *Journal of cellular physiology*, 186(2), pp.210–9.

Min, B.H. et al., 1998. Transient expression of clusterin (sulfated glycoprotein-2) during development of rat pancreas. *Journal of Endocrinology*, 158(1), pp.43–52.

Mio, T. et al., 1992. Proliferative characteristics of fibroblast lines derived from open lung biopsy specimens of patients with IPF (UIP). *Chest*, 102(3), pp.832–837.

Miwa, Y. et al., 2004. Involvement of clusterin in 15-deoxy-delta12,14-prostaglandin J2-induced vascular smooth muscle cell differentiation. *Biochemical and biophysical research communications*, 319(1), pp.163–8.

Miyata, M. et al., 2001. Apolipoprotein J/Clusterin Is Induced in Vascular Smooth Muscle Cells After Vascular Injury. *Circulation*, 104(12), pp.1407–1412.

Miyata, M. et al., 2015. Muscle Cells After Vascular Injury. *Circulation*, 104, pp.1407–1413.

Miyazaki, Y. et al., 1995. Expression of a tumor necrosis factor-beta transgene in murine lung causes lymphocytic and fibrosing alveolitis: A mouse model of progressive pulmonary fibrosis. *Journal of Clinical Investigation*, 96(1), pp.250–259.

Miyazono, K. et al., 1991. A role of the latent TGF-beta 1-binding protein in the assembly and secretion of TGF-beta 1. *The EMBO journal*, 10(5), pp.1091–101.

Moises Selman, L. & Barrios, R., 1991. Potential role of proteases in pulmonary fibrosis. *Interstitial Pulmonary Diseases*, CRC Press.

Moodley, Y.P. et al., 2004. Comparison of the morphological and biochemical changes

in normal human lung fibroblasts and fibroblasts derived from lungs of patients with idiopathic pulmonary fibrosis during FasL-induced apoptosis. *The Journal of pathology*, 202(February), pp.486–495.

Moon, H.-G. et al., 2015. Lung epithelial cell-derived extracellular vesicles activate macrophage-mediated inflammatory responses via ROCK1 pathway. *Cell death & disease*, 6, p.e2016.

Moore, B.B. et al., 2014. Inflammatory leukocyte phenotypes correlate with disease progression in idiopathic pulmonary fibrosis. *Frontiers of medicine*, 1(56).

Mora, A.L. et al., 2006. Activation of alveolar macrophages via the alternative pathway in herpesvirus-induced lung fibrosis. *American Journal of Respiratory Cell and Molecular Biology*, 35(4), pp.466–473.

Morales-Nebreda, L. et al., 2015. The heterogeneity of lung macrophages in the susceptibility to disease. *European Respiratory Review*, 24(137), pp.505–509.

Morgan, T.E. et al., 1995. Clusterin expression by astrocytes is influenced by transforming growth factor beta 1 and heterotypic cell interactions. *Journal of neuroimmunology*, 58(1), pp.101–10.

Morishima, Y. et al., 2001. Triggering the induction of myofibroblast and fibrogenesis by airway epithelial shedding. *American Journal of Respiratory Cell and Molecular Biology*, 24(1), pp.1–11.

Morris, D.D. et al., 1992. Endotoxin-induced production of interleukin 6 by equine peritoneal macrophages in vitro. *American Journal of Veterinary Research*, 53(8), pp.1298–1301.

Moulson, C.L. & Millis, a J., 1999. Clusterin (Apo J) regulates vascular smooth muscle cell differentiation in vitro. *Journal of cellular physiology*, 180(January), pp.355–364.

Muhammad, L.A. & Saad, F., 2015. The role of clusterin in prostate cancer: treatment resistance and potential as a therapeutic target. *Expert review of anticancer therapy*, 15(9), pp.1049–61.

Munger, J.S. et al., 1999. The integrin alpha v beta 6 binds and activates latent TGF beta 1: a mechanism for regulating pulmonary inflammation and fibrosis. *Cell*, 96(3), pp.319–328.

Murthy, S. et al., 2015. Alternative activation of macrophages and pulmonary fibrosis are modulated by scavenger receptor, macrophage receptor with collagenous structure. *FASEB Journal*, 29(8), pp.3527–3536.

Mutsaers, S.E. et al., 1997. Mechanisms of tissue repair: From wound healing to fibrosis. *International Journal of Biochemistry and Cell Biology*, 29, pp.5–17.

Mydlarz, W. et al., 2014. Clusterin Is a Gene-Specific Target of microRNA-21 in Head

and Neck Squamous Cell Carcinoma. *Clinical cancer research : an official journal of the American Association for Cancer Research*, pp.868–877.

Myers, J.L. & Katzenstein, A.L.A., 1988. Epithelial necrosis and alveolar collapse in the pathogenesis of usual interstitial pneumonia. *Chest*, 94(6), pp.1309–1311.

Narayan, P. et al., 2011. The extracellular chaperone clusterin sequesters oligomeric forms of the amyloid-β1−40 peptide. *Nature Structural & Molecular Biology*, 19, pp.79–83.

Navaratnam, V. et al., 2011. The rising incidence of idiopathic pulmonary fibrosis in the UK. *Thorax*, 66(6), pp.462–467.

Nguan, C.Y.C. et al., 2014. Promotion of cell proliferation by clusterin in the renal tissue repair phase after ischemia-reperfusion injury. *American journal of physiology. Renal physiology*, 306(7), pp.724–733.

Nicholson, A.G. et al., 2002. The relationship between individual histologic features and disease progression in idiopathic pulmonary fibrosis. *American Journal of Respiratory and Critical Care Medicine*, 166(2), pp.173–177.

Niu, Z. et al., 2012. Small interfering RNA targeted to secretory clusterin blocks tumor growth , motility , and invasion in breast cancer. , 44(12), pp.991–998.

Nizard, P. et al., 2007. Stress-Induced Retrotranslocation of Clusterin / ApoJ into the Cytosol. , (1), pp.554–565.

Noble, P.W., Barkauskas, C.E. & Jiang, D., 2012. Pulmonary fibrosis: patterns and perpetrators. *J.Clin.Invest*, 122(8), pp.2756–2762.

Nyeng, P. et al., 2008. FGF10 maintains distal lung bud epithelium and excessive signaling leads to progenitor state arrest, distalization, and goblet cell metaplasia. *BMC developmental biology*, 8, p.2.

Oikonomou, N. et al., 2006. Soluble TNF mediates the transition from pulmonary inflammation to fibrosis. *PLoS ONE*, 1(1).

Olczyk, P., Mencner, L. & Komosinska-Vassev, K., 2014. The Role of the Extracellular Matrix Components in Cutaneous Wound Healing. *BioMed research international*, 2014, p.747584.

Osornio-Vargas, A. et al., 1993. Early passage rat lung fibroblasts do not migrate *in vitro* to transforming growth factor beta. *Rapid communication*. 6, pp 6-9.

Orlandi, A. et al., 2005. Modulation of clusterin isoforms is associated with all-trans retinoic acid-induced proliferative arrest and apoptosis of intimal smooth muscle cells. *Arteriosclerosis, Thrombosis, and Vascular Biology*, 25, pp.348–353.

Ortiz, L.A. et al., 1998. Expression of TNF and the necessity of TNF receptors in bleomycin-induced lung injury in mice. *Experimental lung research*, 24(6), pp.721–743.

Osornio-Vargas, A.R. et al., 1993. Early-passage rat lung fibroblasts do not migrate in vitro to transforming growth factor beta. *Rapid Communication*, (6), pp.6–9.

Panzhinskiy, E. et al., 2012. Hypoxia induces unique proliferative response in adventitial fibroblasts by activating PDGFbeta receptor-JNK1 signalling. *Cardiovascular Research*, 95(3), pp.356–365.

Parameswaran, N. & Patial, S., 2010. Tumor Necrosis Factor- a signaling in macrophages. *NIH Public Access*, 48(Suppl 2), pp.1–6.

Pardo, A. & Selman, M., 2012. Role of matrix metaloproteases in idiopathic pulmonary fibrosis. *Fibrogenesis & tissue repair*, 5(Suppl 1), p.S9.

Park, S., Mathis, K.W. & Lee, I.K., 2013. The physiological roles of apolipoprotein J/clusterin in metabolic and cardiovascular diseases. *Reviews in endocrine & metabolic disorders*. pp 45-53.

Park, Y. hee et al., 2015. Human bronchial epithelial BEAS-2B cells, an appropriate in vitro model to study heavy metals induced carcinogenesis. *Toxicology and Applied Pharmacology*, 287(3), pp.240–245.

Parra, E.R. et al., 2007. Abnormal deposition of collagen/elastic vascular fibres and prognostic significance in idiopathic interstitial pneumonias. *Thorax*, 62(5), pp.428–37.

Patel, A.S. et al., 2015. Epithelial cell mitochondrial dysfunction and PINK1 are induced by transforming growth factor- beta1 in pulmonary fibrosis. *PLoS ONE*, 10(3), pp.1–14.

Penn, J.W., Grobbelaar, A.O. & Rolfe, K.J., 2012. The role of the TGF-β family in wound healing, burns and scarring: a review. *International journal of burns and trauma*, 2(1), pp.18–28.

Petersen, A. et al., 2012. The Impact of Substrate Stiffness and Mechanical Loading on Fibroblast-Induced Scaffold Remodeling. *Tissue Engineering Part A*, 18(17–18), pp.1804–1817.

Petropoulou, C. et al., 2001. Clusterin/apolipoprotein J is a novel biomarker of cellular senescence that does not affect the proliferative capacity of human diploid fibroblasts. *FEBS letters*, 509(2), pp.287–297.

Pieper-Fürst, U. et al., 2011. Expression of the megalin C-terminal fragment by macrophages during liver fibrogenesis in mice. *Biochimica et Biophysica Acta - Molecular Basis of Disease*, 1812(12), pp.1640–1648.

Pierce, E.M. et al., 2007. Idiopathic pulmonary fibrosis fibroblasts migrate and proliferate to CC chemokine ligand 21. *The European respiratory journal*, 29(6), pp.1082–93.

Piguet, P.F. et al., 2002. Tumor necrosis factor/cachectin plays a key role in bleomycin-

induced pneumopathy and fibrosis. *Journal of Experimental Medicine*, 170, pp.655–663.

Piguet, P.F., Grau, G.E. & Vassalli, P., 1990. Subcutaneous perfusion of tumor necrosis factor induces local proliferation of fibroblasts, capillaries, and epidermal cells, or massive tissue necrosis. *The American journal of pathology*, 136(1), pp.103–10.

Plataki, M. et al., 2005. Expression of apoptotic and antiapoptotic markers in epithelial cells in idiopathic pulmonary fibrosis. *Chest*, 127(1), pp.266–274.

Poon, S. et al., 2000. Clusterin is an ATP-independent chaperone with very broad substrate specificity that stabilizes stressed proteins in a folding-competent state. *Biochemistry*, 39(51), pp.15953–60.

Poon, S. et al., 2002. Clusterin is an extracellular chaperone that specifically interacts with slowly aggregating proteins on their off-folding pathway. *FEBS Letters*, 513(2–3), pp.259–266.

Postlethwaite, A.E. et al., 1987. Stimulation of the chemotactic migration of human fibroblasts by transforming growth factor beta. *Journal of Experimental Medicine*, 165(I), pp.251–256.

Prasad, S., Hogaboam, C.M. & Jarai, G., 2014. Deficient repair response of IPF fibroblasts in a co-culture model of epithelial injury and repair. *Fibrogenesis & tissue repair*, 7(1), p.7.

Prasse, A. et al., 2006. A vicious circle of alveolar macrophages and fibroblasts perpetuates pulmonary fibrosis via CCL18. *American Journal of Respiratory and Critical Care Medicine*, 173(7), pp.781–792.

Prochnow, H. et al., 2013. Non-secreted clusterin isoforms are translated in rare amounts from distinct human mRNA variants and do not affect Bax-mediated apoptosis or the NF-κB signaling pathway. *PloS one*, 8(9), p.e75303.

Puglisi, S. et al., 2016. What We Know About the Pathogenesis of Idiopathic Pulmonary Fibrosis. *Seminars in respiratory and critical care medicine*, 37(3), pp.358–67.

Rafii, R. et al., 2013. A review of current and novel therapies for idiopathic pulmonary fibrosis. *J.Thorac.Dis.*, 5(1), pp.48–73.

Raghu, G. et al., 2011. An Official ATS/ERS/JRS/ALAT Statement: Idiopathic pulmonary fibrosis: Evidence-based guidelines for diagnosis and management. *American Journal of Respiratory and Critical Care Medicine*, 183, pp.788–824.

Raghu, G. et al., 2006. Incidence and prevalence of idiopathic pulmonary fibrosis. *Am.J.Respir.Crit Care Med.*, 174(7), pp.810–816.

Reddy, K.B., Karode, M.C., et al., 1996. Interaction of transforming growth factor beta

receptors with apolipoprotein J/clusterin. *Biochemistry*, 35, pp.309–314.

Reddy, K.B., Jin, G., et al., 1996. Transforming growth factor β (TGFβ)-induced nuclear localization of apolipoprotein J/clusterin in epithelial cells. *Biochemistry*, 35(95), pp.6157–6163.

Redente, E.F. et al., 2014. Tumor necrosis factor-a accelerates the resolution of established pulmonary fibrosis in mice by targeting profibrotic lung macrophages. *American Journal of Respiratory Cell and Molecular Biology*, 50(4), pp.825–837.

Reinhardt, A.K. et al., 2005. Quantification of collagen and proteoglycan deposition in a murine model of airway remodelling. *Respiratory research*, 6, p.30.

Reisfeld, R.A., Lewis, U.J. & Williams, D.E., 1962. Disk electrophoresis of basic proteins and peptides on polyacrylamide gels. *Nature*, 195, pp.281–3.

Rennard, S.I., Togo, S. & Holz, O., 2006. Cigarette smoke inhibits alveolar repair: a mechanism for the development of emphysema. *Proceedings of the American Thoracic Society*, 3(8), pp.703–8.

Richeldi, L. et al., 2014. Efficacy and Safety of Nintedanib in Idiopathic Pulmonary Fibrosis - ProQuest. *The New England Journal of Medicine*, pp.2071–82.

Richeldi, L., 2016. How we will diagnose IPF in the future. QJM, (July), pp.1–3.

Risau, W. et al., 1992. Platelet-derived growth factor is angiogenic in vivo. *Growth factors*, 7(4), pp.261–266.

Rizzi, F., Coletta, M. & Bettuzzi, S., 2009. Chapter 2: Clusterin (CLU): From one gene and two transcripts to many proteins. *Advances in cancer research*, 104, pp.9–23.

Rodriguez-Menocal, L. et al., 2012. Stimulation of skin and wound fibroblast migration by mesenchymal stem cells derived from normal donors and chronic wound patients. *Stem Cells Transl Med*, March, pp.221–229.

Röszer, T.I., 2015. Understanding the mysterious M2 macrophage through activation markers and effector mechanisms. *Mediators of Inflammation*, 2015, pp.16–18.

Rosenberg, E. & Silkensen, J., 1995. Clusterin: physiologic and pathophysiologic considerations. *The international journal of biochemistry & cell biology*, 2725(95), pp.633–645.

Royce, S.G. et al., 2009. Effect of extracellular matrix composition on airway epithelial cell and fibroblast structure: implications for airway remodeling in asthma. *Annals of allergy, asthma & immunology : official publication of the American College of Allergy, Asthma, & Immunology*, 102(3), pp.238–246.

Rozin, G.F. et al., 2005. Collagen and elastic system in the remodelling process of major types of idiopathic interstitial pneumonias (IIP). *Histopathology*, 46(4), pp.413–421.

Sakai, N. & Tager, A.M., 2013. Fibrosis of two: Epithelial cell-fibroblast interactions in

pulmonary fibrosis. *Biochimica et Biophysica Acta - Molecular Basis of Disease*, 1832(7), pp.911–921.

Sanders, Y.Y. et al., 2008. Thy-1 promoter hypermethylation: A novel epigenetic pathogenic mechanism in pulmonary fibrosis. *American Journal of Respiratory Cell and Molecular Biology*, 39(5), pp.610–618.

Santilli, G., Aronow, B.J. & Sala, A., 2003. Essential requirement of apolipoprotein J (clusterin) signaling for IkappaB expression and regulation of NF-kappaB activity. *The Journal of biological chemistry*, 278(40), pp.38214–9.

Sarasa-Renedo, A. & Chiquet, M., 2005. Mechanical signals regulating extracellular matrix gene expression in fibroblasts. In *Scandinavian Journal of Medicine and Science in Sports*. pp. 223–230.

Sarrazy, V. et al., 2011. Mechanisms of pathological scarring: Role of myofibroblasts and current developments. *Wound Repair and Regeneration*, 19(SUPPL. 1).

Scheule, R.K. et al., 1992. Bleomycin stimulation of cytokine secretion by the human alveolar macrophage. *American Journal of Physiology*, 262(4 Pt 1), pp.L386-91.

Schupp, J.C. et al., 2015. Macrophage activation in acute exacerbation of idiopathic pulmonary fibrosis. *PLoS ONE*, 10(1), pp.1–11.

Scotton, C.J. et al., 2009. Increased local expression of coagulation factor X contributes to the fibrotic response in human and murine lung injury. *J.Clin.Invest*, 119(9), pp.2550–2563.

Scotton, C.J. & Chambers, R.C., 2007. Molecular targets in pulmonary fibrosis: the myofibroblast in focus. *Chest*, 132(4), pp.1311–21.

Selman, M. et al., 2001. Idiopathic pulmonary fibrosis: prevailing and evolving hypotheses about its pathogenesis and implications for therapy. *Annals of internal medicine*, 134(2), pp.136–51.

Selman, M. & Pardo, A., 2006. Role of epithelial cells in idiopathic pulmonary fibrosis: from innocent targets to serial killers. *Proceedings of the American Thoracic Society*, 3, pp.364–372.

Selman, M., Pardo, A. & Kaminski, N., 2008. Idiopathic pulmonary fibrosis: Aberrant recapitulation of developmental programs? *PLoS Medicine*, 5(3), pp.0373–0380.

Shannan, B. et al., 2006. Challenge and promise: roles for clusterin in pathogenesis, progression and therapy of cancer. *Cell Death Differ*, 13(1), pp.12–19.

Shannon, J.M. & Hyatt, B.A., 2004. Epithelial-mesenchymal interactions in the developing lung. *Annual review of physiology*, 66, pp.625–645.

Shi, H. et al., 2013. Knockdown of clusterin inhibits the growth and migration of renal carcinoma cells and leads to differential gene expression. *Molecular Medicine Reports*, 8(1), pp.35–40.

Shi, M. et al., 2011. Latent TGF-β structure and activation. *Nature*, 474(7351), pp.343–349.

Shi, Y. & Massague, J., 2003. Mechanisms of TGF-beta signaling from cell membrane to the nucleus. *Cell*, 113(6), pp.685–700.

Shifren, A. et al., 2012. Mechanisms of remodeling in asthmatic airways. *Journal of allergy*, 2012, p.316049.

Shim, Y.-J. et al., 2011. Clusterin induces matrix metalloproteinase-9 expression via ERK1/2 and PI3K/Akt/NF-κB pathways in monocytes/macrophages. *Journal of leukocyte biology*, 90(4), pp.761–9.

Shim, Y.J. et al., 2012. Clusterin induces the secretion of TNF-a and the chemotactic migration of macrophages. *Biochemical and Biophysical Research Communications*, 422, pp.200–205.

Shin, Y.J. et al., 2006. Clusterin enhances proliferation of primary astrocytes through extracellular signal-regulated kinase activation. *Neuroreport*, 17(18), pp.1871–5.

Shin, Y.J. et al., 2009. Protective effect of clusterin on oxidative stress-induced cell death of human corneal endothelial cells. *Molecular vision*, 15(December), pp.2789–2795.

Silkensen, J.R., Schwochau, G.B. & Rosenberg, M.E., 1994. The role of clusterin in tissue injury. *Biochemistry and cell biology*, 72(11–12), pp.483–8.

Simionescu, M., 1980. Ultrastructural organization of the alveolar-capillary unit. *Ciba Foundation symposium*, 78, pp.11–36.

Singer, A.J. & Clark, R.A., 1999. Cutaneous wound healing. *The New England journal of medicine*, 341(10), pp.738–46.

Sinno, H. & Prakash, S., 2013. Complements and the wound healing cascade: an updated review. *Plastic surgery international*, 2013, p.146764.

Skalli, O. et al., 1986. A monoclonal antibody against alpha-smooth muscle actin: a new probe for smooth muscle differentiation. *The Journal of cell biology*, 103(6 Pt 2), pp.2787–96.

Sol, I.S. et al., 2016. Relationship between sputum clusterin levels and childhood asthma. *Clinical and experimental allergy : journal of the British Society for Allergy and Clinical Immunology*, 46(5), pp.688–95.

Solomon, J.J. et al., 2013. Scleroderma lung disease. *European respiratory review : an official journal of the European Respiratory Society*, 22(127), pp.6–19.

Song, E. et al., 2000. Influence of Alternatively and Classically Activated Macrophages on Fibrogenic Activities of Human Fibroblasts. *Cellular Immunology*, 204(1), pp.19–28.

Speer, M.C. et al., 2011. A Common MUC5B Promoter Polymorphism and Pulmonary

Fibrosis. *The New England journal of medicine*, 364, pp.1503–1512.

Stahl, M. et al., 2013. Lung collagens perpetuate pulmonary fibrosis via CD204 and M2 macrophage activation. *PLoS ONE*, 8(11), pp.1–10.

Stewart, E.M. et al., 2007. Effects of glycosylation on the structure and function of the extracellular chaperone clusterin. *Biochemistry*, 46(5), pp.1412–22.

Strieter, R.M. et al., 2009. The role of circulating mesenchymal progenitor cells, fibrocytes, in promoting pulmonary fibrosis. *Trans. Am. Clin. Climatol. Assoc.*, 120(0065–7778 (Print) LA–eng PT–Journal Article PT–Research Support, Non–U.S. Gov't SB–IM), pp.49–59.

Striz, I. et al., 2001. Cell-cell contacts with epithelial cells modulate the phenotype of human macrophages. *Inflammation*, 25(4), pp.241–246.

Suga, M. et al., 2000. Characteristic elevation of matrix metalloproteinase activity in idiopathic interstitial pneumonias. *American Journal of Respiratory and Critical Care Medicine*, 162(5), pp.1949–1956.

Suga, M. et al., 1999. Clinical significance of MCP-1 levels in BALF and serum in patients with interstitial lung diseases. *Eur Respir J*, 14(2), pp.376–382.

Suganuma, H. et al., 1995. Enhanced migration of fibroblasts derived from lungs with fibrotic lesions. *Thorax*, 50, pp.984–989.

Swertfeger, D.K. et al., 1996. Apolipoprotein J/clusterin induction in myocarditis: A localized response gene to myocardial injury. *The American journal of pathology*, 148(6), pp.1971–1983.

Tada, H. et al., 2003. Increased binding and chemotactic capacities of PDGF-BB on fibroblasts in radiation pneumonitis. *Radiation research*, 159, pp.805–811.

Taipale, J. et al., 1994. Latent transforming growth factor-beta 1 associates to fibroblast extracellular matrix via latent TGF-beta binding protein. *The Journal of cell biology*, 124(January), pp.171–181.

Tamada, M., Sheetz, M.P. & Sawada, Y., 2004. Activation of a signaling cascade by cytoskeleton stretch. *Developmental Cell*, 7(5), pp.709–718.

Tanaka, T. et al., 2002. Resistance to Fas-mediated apoptosis in human lung fibroblast. *The European respiratory journal*, 20(2), pp.359–368.

Tao, F. & Kobzik, L., 2002. Lung macrophage-epithelial cell interactions amplify particle-mediated cytokine release. *American Journal of Respiratory Cell and Molecular Biology*, 26(4), pp.499–505.

Thannickal, V.J. et al., 2004. Mechanisms of pulmonary fibrosis. *Annu.Rev.Med.*, 55, pp.395–417.

Thannickal, V.J. et al., 2003. Myofibroblast differentiation by transforming growth factor-b1 is dependent on cell adhesion and integrin signaling via focal adhesion

kinase. *Journal of Biological Chemistry*, 278(14), pp.12384–12389.

Thomas-salgar, S. & Albert, J., 1994. Clusterin Expression in Differntiating Smooth Muscle Cells.

Thompson, H.G. et al., 2006. Epithelial-derived TGF-beta2 modulates basal and wound-healing subepithelial matrix homeostasis. *Am. J. Physiol. Lung Cell Mol. Physiol.*, pp.L1277–L1285.

Tiggelman, A.M. et al., 1997. Transforming growth factor-beta-induced collagen synthesis by human liver myofibroblasts is inhibited by alpha2-macroglobulin. *Journal of hepatology*, 26(6), pp.1220–8.

Tobin, R.W. et al., 1998. Increased prevalence of gastroesophageal reflux in patients with idiopathic pulmonary fibrosis. *American journal of respiratory and critical care medicine*, 158(6), pp.1804–1808.

Tomasek, J.J. et al., 2002. Myofibroblasts and mechano-regulation of connective tissue remodelling. *Nature reviews. Molecular cell biology*, 3(5), pp.349–63.

Torday, J.S. & Rehan, V.K., 2003. Mechanotransduction determines the structure and function of lung and bone: a theoretical model for the pathophysiology of chronic disease. *Cell biochemistry and biophysics*, 37(3), pp.235–246.

Townsley, M.I., 2013. Structure and composition of pulmonary arteries, capillaries and veins. *Compr Physiology*, pp.675–709.

Tracey, K.J. & Cerami, A., 1994. Tumor necrosis factor: a pleiotropic cytokine and therapeutic target. *Annu Rev Med*, 45, pp.491–503.

Travis, W.D. et al., 2013. An official American Thoracic Society/European Respiratory Society statement: Update of the international multidisciplinary classification of the idiopathic interstitial pneumonias. *American Journal of Respiratory and Critical Care Medicine*, 188(6), pp.733–748.

Trawinska, M.A., Rupesinghe, R.D. & Hart, S.P., 2016. Patient considerations and drug selection in the treatment of idiopathic pulmonary fibrosis. *Therapeutics and Clinical Risk Management*, 12, pp.563–574.

Troakes, C. et al., 2016. Clusterin expression is upregulated following acute head injury and localizes to astrocytes in old head injury. *Neuropathology*.

Trougakos, I.P., 2013. The Molecular Chaperone Apolipoprotein J / Clusterin as a Sensor of Oxidative Stress : Implications in Therapeutic Approaches – A Mini-Review. Gerontology,(59), pp 514-523.

Trougakos, I.P. & Gonos, E.S., 2006. Regulation of clusterin / apolipoprotein J , a functional homologue to the small heat shock proteins , by oxidative stress in ageing and age-related diseases. , 40(December), pp.1324–1334.

Tschumperlin, D.J. et al., 2003. Mechanical stress triggers selective release of fibrotic

mediators from bronchial epithelium. *American Journal of Respiratory Cell and Molecular Biology*, 28(2), pp.142–149.

Turner-Warwick, M., 1998. In search of a cause of cryptogenic fibrosing alveolitis (CFA): one initiating factor or many? *Thorax*, 53 Suppl 2(Suppl 2), pp.S3-9.

Uh, S.T. et al., 1998. Morphometric analysis of insulin-like growth factor-I localization in lung tissues of patients with idiopathic pulmonary fibrosis. *American journal of respiratory and critical care medicine*, 158(5 Pt 1), pp.1626–35.

Varga, J. & Abraham, D., 2007. Systemic sclerosis: a prototypic multisystem fibrotic disorder. *The Journal of clinical investigation*, 117(3), pp.557–567.

Van Der Velden, V.H.J., Savelkoul, H.F.J. & Versnel, M.A., 1998. Bronchial epithelium: Morphology, function, and pathophysiology in asthma. *European Cytokine Network*, 9(4), pp.585–597.

Viard, I. et al., 1999. Clusterin gene expression mediates resistance to apoptotic cell death induced by heat shock and oxidative stress. *The Journal of investigative dermatology*, 112(3), pp.290–296.

Wang, N., Liang, H. & Zen, K., 2014. Molecular mechanisms that influence the macrophage M1-M2 polarization balance. *Frontiers in Immunology*, 5(NOV), pp.1–9.

Wang, X. et al., 2014. Clusterin plays an important role in clear renal cell cancer metastasis. *Urologia internationalis*, 92(1), pp.95–103.

Wang, X. et al., 2015. Effects of down-regulation of clusterin by small interference RNA on human acute myeloid leukemia cells. *International Journal of Clinical and Experimental Medicine*, 8(11), pp.20925–20931.

Wanidworanun, C. & Strober, W., 1993. Predominant role of tumor necrosis factor-alpha in human monocyte IL-10 synthesis. *J.Immunol.*, 151(12), pp.6853–6861.

Ward, H.E. & Nicholas, T.E., 1984. Alveolar type I and type II cells. *Australian and New Zealand journal of medicine*, 14(5 Suppl 3), pp.731–4.

Wardlaw, A.J. et al., 1989. Leukotrienes, LTC4 and LTB4, in bronchoalveolar lavage in bronchial asthma and other respiratory diseases. *The Journal of Allergy and Clinical Immunology*, 84(1), pp.19–26.

Wegrowski, Y. et al., 1999. Transforming growth factor beta-1 up-regulates clusterin synthesis in thyroid epithelial cells. *Experimental cell research*, 247(2), pp.475–483.

Wermuth, P.J. & Jimenez, S.A., 2015. The significance of macrophage polarization subtypes for animal models of tissue fibrosis and human fibrotic diseases. *Clinical and translational medicine*, 4, p.2.

White, E.S. et al., 2003. Integrin alpha4beta1 regulates migration across basement

membranes by lung fibroblasts: A role for phosphatase and tensin homologue deleted on chromosome 10. *American Journal of Respiratory and Critical Care Medicine*, 168(4), pp.436–442.

Whitsett, J.A. & Alenghat, T., 2015. Respiratory epithelial cells orchestrate pulmonary innate immunity. *Nature immunology*, 16(1), pp.27–35.

Williamson, J.D., Sadofsky, L.R. & Hart, S.P., 2015. The pathogenesis of bleomycin-induced lung injury in animals and its applicability to human idiopathic pulmonary fibrosis. *Experimental Lung Research*, 41(2), pp.57–73.

Wollin, L. et al., 2015. Mode of action of nintedanib in the treatment of idiopathic pulmonary fibrosis. *European Respiratory Journal*, 45(5), pp.1434–1445.

Willis, B.C. et al., 2005. Induction of epithelial-mesenchymal transition in alveolar epithelial cells by transforming growth factor-beta1: potential role in idiopathic pulmonary fibrosis. *The American journal of pathology*, 166(5), pp.1321–32.

Willnow, T.E. et al., 1996. Defective forebrain development in mice lacking gp330/megalin. *Proceedings of the National Academy of Sciences of the United States of America*, 93(16), pp.8460–8464.

Wilson, M., 2000. Clusterin is a secreted mammalian chaperone. *Trends in Biochemical Sciences*, 25(3), pp.95–98.

Wilson, M.S. & Wynn, T. a, 2009. Pulmonary fibrosis: pathogenesis, etiology and regulation. *Mucosal immunology*, 2(2), pp.103–21.

Wong, P. et al., 1993. Genomic organization and expression of the rat TRPM-2 (clusterin) gene, a gene implicated in apoptosis. *The Journal of biological chemistry*, 268(7), pp.5021–31.

Wong, P. et al., 1994. Molecular characterization of human TRPM-2/clusterin, a gene associated with sperm maturation, apoptosis and neurodegeneration. *European journal of biochemistry / FEBS*, 221(3), pp.917–25.

Worthington, J.J., Klementowicz, J.E. & Travis, M. a, 2011. TGFβ: a sleeping giant awoken by integrins. *Trends in biochemical sciences*, 36(1), pp.47–54.

Wyatt, A.R. et al., 2011. Clusterin facilitates in vivo clearance of extracellular misfolded proteins. *Cellular and molecular life sciences : CMLS*, 68(23), pp.3919–31.

Wynes, M.W. & Riches, D.W.H., 2003. Induction of macrophage insulin-like growth factor-I expression by the Th2 cytokines IL-4 and IL-13. *Journal of immunology*, 171(7), pp.3550–9.

Wynn, T. a, Ph, D. & Barron, L., 2011. Macrophages: Master Regulators of Inflammation and Fibrosis. *Semin Liver Dis.*, 30(3), pp.245–257.

Xiu, P. et al., 2013. Secretory clusterin contributes to oxaliplatin resistance by activating Akt pathway in hepatocellular carcinoma. , 104(3), pp.375–382.

Xu, J. & Clark, R.A.F., 1996. Extracellular matrix alters PDGF regulation of fibroblast integrins. *Journal of Cell Biology*, 132(1–2), pp.239–249.

Xu, M. et al., 2015. Clusterin silencing sensitizes pancreatic cancer MIA-PaCa-2 cells to gmcitabine via regulation of NF-kB/Bcl-2 signaling. *International journal of clinical and experimental medicine*, 8(8), pp.12476–86.

Xu, Q. et al., 2007. In vitro models of TGF- beta -induced fibrosis suitable for high-throughput screening of antifibrotic agents. *American Journal of Physiology. Renal Physiology*, 293(May 2007), pp.F631–F640.

Yamamoto, Y. et al., 2015. siRNA lipid nanoparticle potently silences clusterin and delays progression when combined with androgen receptor cotargeting in enzalutamide-resistant prostate cancer. *Clinical Cancer Research*, 21(21), pp.4845–4855.

Yan, Y. et al., 2013a. RNA interference-mediated secretory clusterin gene silencing inhibits proliferation and promotes apoptosis of human non-small cell lung cancer cells. *Hepato-Gastroenterology*, 60(122), pp.70–75.

Yanaba, K. et al., 2012. A possible contribution of elevated serum clusterin levels to the inhibition of digital ulcers and pulmonary arterial hypertension in systemic sclerosis. *Archives of dermatological research*, 304(6), pp.459–63.

Yang, C. et al., 2000. Nuclear clusterin/XIP8, an x-ray-induced Ku70-binding protein that signals cell death. Proc Natl Acad Sci USA, 97(11), pp.5907–5912.

Yang, I. V, 2012. Epigenomics of idiopathic pulmonary fibrosis Review. Epigenomics, 4, pp.195–203.

Yang, I. V. & Schwartz, D.A., 2015. Epigenetics of idiopathic pulmonary fibrosis. *Translational Research*, 165(1), pp.48–60.

Yi, E.S. et al., 1996. Platelet-derived growth factor causes pulmonary cell proliferation and collagen deposition in vivo. *The American journal of pathology*, 149(2), pp.539–48.

Yu, Q. & Stamenkovic, I., 2000. Cell surface-localized matrix metalloproteinase-9 proteolytically activates TGF-beta and promotes tumor invasion and angiogenesis. *Genes and Development*, 14(2), pp.163–176.

Zenkel, M. & Schlötzer-Schrehardt, U., 2014. The composition of exfoliation material and the cells involved in its production. *Journal of Glaucoma*, 23(8 Suppl 1), pp.S12-4.

Zhang, B. et al., 2014. siRNA-directed clusterin silencing promotes cisplatin antitumor activity in human non-small cell lung cancer xenografts in immunodeficient mice. *European review for medical and pharmacological sciences*, 18(11), pp.1595–601.

Zhang, F. et al., 2016. TGF-β induces M2-like macrophage polarization via SNAIL-

mediated suppression of a pro-inflammatory phenotype. *Oncotarget*.

Zhang, H. et al., 2005. Clusterin inhibits apoptosis by interacting with activated Bax. *Nature cell biology*, 7(9), pp.909–15.

Zhang, H.Y. et al., 1996. Lung fibroblast alpha-smooth muscle actin expression and contractile phenotype in bleomycin-induced pulmonary fibrosis. *The American journal of pathology*, 148, pp.527–537.

Zhang, K. et al., 1997a. TNF-alpha-mediated lung cytokine networking and eosinophil recruitment in pulmonary fibrosis. *Journal of immunology (Baltimore, Md. : 1950)*, 158(2), pp.954–959.

Zhang, X. & Mosser, D.M., 2008. Macrophage activation by endogenous danger signals. *Journal of Pathology*, 214(2), pp.161–178.

Zhao, C. et al., 2010. Involvement of type II pneumocytes in the pathogenesis of chronic obstructive pulmonary disease. *Respiratory medicine*, 104(10), pp.1391–5.

Zheng, D. et al., 2013. A cellular pathway involved in clara cell to alveolar type II cell differentiation after severe lung injury. *PLoS ONE*, 8(8), p.e71028.

Zheng, G. et al., 1994. Organ distribution in rats of two members of the low-density lipoprotein receptor gene family, gp330 and LRP/alpha 2MR, and the receptor-associated protein (RAP). *The journal of histochemistry and cytochemistry : official journal of the Histochemistry Society*, 42(4), pp.531–542.

Zhou, W. et al., 2010. Loss of clusterin expression worsens renal ischemia-reperfusion injury. *American journal of physiology. Renal physiology*, 298(30), pp.F568–F578.

Zhou, Y. et al., 2010. Thy-1-integrin alphav beta5 interactions inhibit lung fibroblast contraction-induced latent transforming growth factor-beta1 activation and myofibroblast differentiation. *J.Biol.Chem.*, 285(29), pp.22382–22393.

Ziegenhagen, M.W. et al., 1998. Increased expression of proinflammatory chemokines in bronchoalveolar lavage cells of patients with progressing idiopathic pulmonary fibrosis and sarcoidosis. *J Investig Med*, 46(5), pp.223–231.

Zlokovic, B. V et al., 1996. Glycoprotein 330/megalin: probable role in receptor-mediated transport of apolipoprotein J alone and in a complex with Alzheimer disease amyloid beta at the blood-brain and blood-cerebrospinal fluid barriers. *Proceedings of the National Academy of Sciences of the United States of America*, 93(9), pp.4229–4234.

Appendix

Microarray			
Disease	**Gender**	**Lung area of tissue collection**	**Age**
Control			
0198	F	Normal tissue distal to tumour resection	69
0798	F	Normal tissue distal to tumour resection	73
0898	F	Normal tissue distal to tumour resection	33
0998	M	Peripheral lung, Donor died from stroke	55
0307	M	Normal tissue distal to tumour resection	N/A
CTR6	F		54
IPF			
0208	F	Peripheral biopsy tissue from area identified as fibrotic by CT	61
0308	M	Peripheral biopsy tissue from area identified as fibrotic by CT	58
0508	M	Peripheral biopsy tissue from area identified as fibrotic by CT	77
0406	F	Peripheral biopsy tissue from area identified as fibrotic by CT	73
0507	F	Peripheral biopsy tissue from area identified as fibrotic by CT	64
SSC			
SSC1	M	Peripheral biopsy tissue	47
SSC2	F	Peripheral biopsy tissue	56
SSC3	F	Peripheral biopsy tissue	49
SSC4	F	Peripheral biopsy tissue	53
SSC5	F	Peripheral biopsy tissue	56
SSC6	F	Peripheral biopsy tissue	48
SSC7	F	Peripheral biopsy tissue	57

In vitro work			
Disease	**Gender**	**Lung area of tissue collection**	**Age**
Control			
0898	F	Normal tissue distal to tumour resection	33
0998	M	Peripheral lung, Donor died from stroke	55
0109	N/A	Normal tissue distal to tumour resection	N/A
IPF			
0207	M	Peripheral tissue from transplant lung	54

Histology			
Disease	**Gender**	**Lung area of tissue collection**	**Age**
Control			
AD01_09_02	N/A	Normal tissue distal to tumour resection	N/A
0307	N/A	Normal tissue distal to tumour resection	N/A
AD 02_09_02	N/A	Normal tissue distal to tumour resection	N/A
IPF			
0207	M	Peripheral tissue from transplant lung	54
0508	M	Peripheral biopsy tissue from area identified as fibrotic by CT	77
0304	M	Peripheral tissue from transplant lung	47

Appendix 1 Table of patient information

Patient information regarding disease state, sex, age and lung area grouped into methods used.

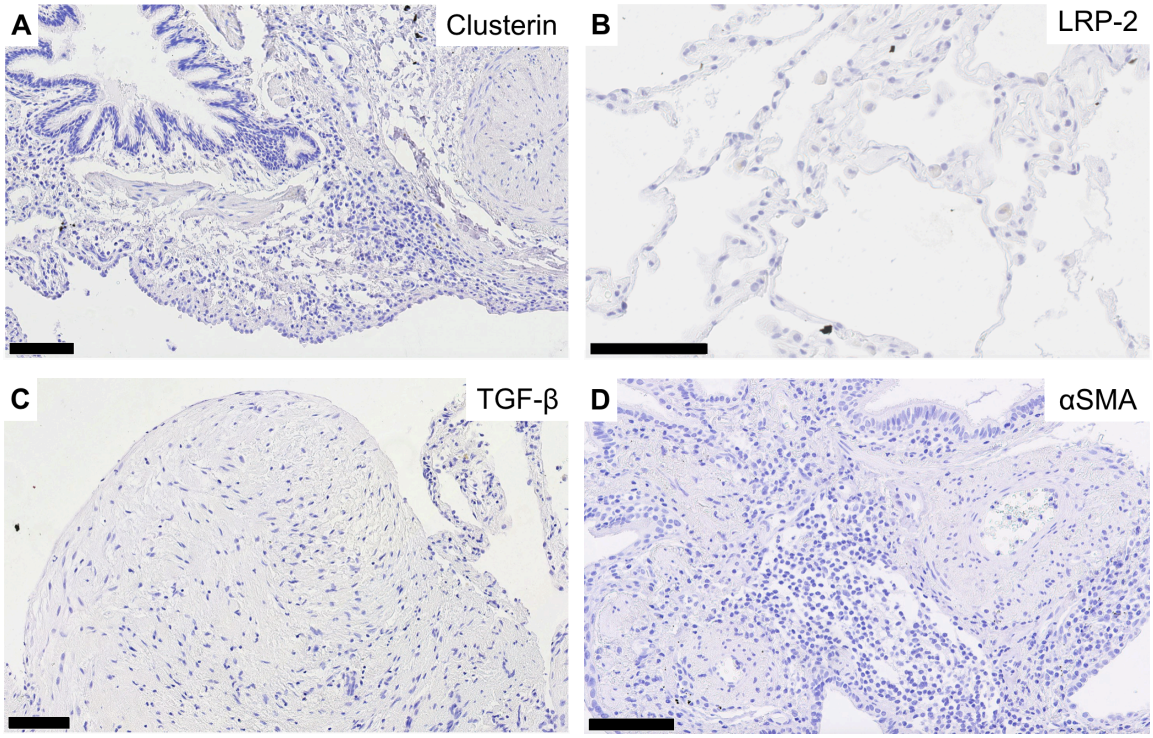

Appendix 2 Negative controls for immunohistochemistry in human lung tissue sections.

Sections were incubated with isotype IgG or IgG_1 in place of primary antibody – antibody species matched primary antibody species. No positive staining was observed with any of the negative controls. Abbreviations; LRP-2 – low-density lipoprotein-related protein 2. Scale bar represents 100 µm.

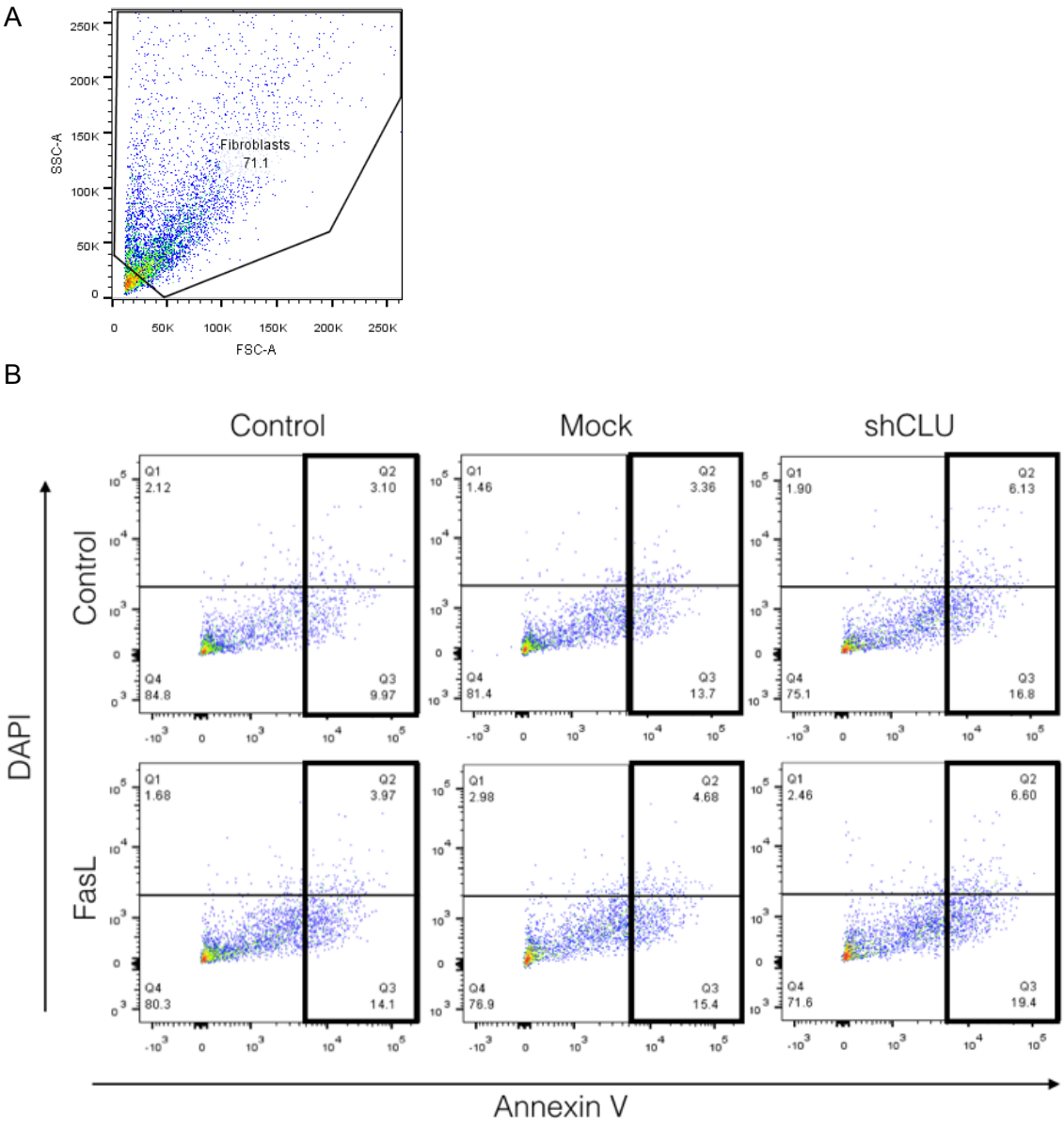

Appendix 3 Example of Flow cytometry data derived from fibroblast apoptosis experiment.

(A) For FACS analysis fibroblasts were gated on forward scatter (FSC-A) and side scatter (SSC-A) characteristics to exclude cell debris. (B) Shows representative plots from an experiment performed in quintuplicate using control, mock-transduced and clusterin-deficient control lung fibroblasts exposed to FasL (100 ng/ml) for 19 hours compared with untreated controls. Apoptosis was determined by Annexin V (AV) and DAPI staining followed by FACS analysis. Cells in the lower left quadrant (Q4) are $AV^-/DAPI^-$ and are alive. Cells in the lower right quadrant (Q3) are $AV^+/DAPI^-$ and are apoptotic. Cells in the upper right quadrant (Q2) are $AV^+/DAPI^+$ and are late apoptotic or necrotic. Plots presented correspond to the data shown in Figure 3.23 for early apoptotic cells only ($AV^+/DAPI^-$ and $AV^+/DAPI^+$ - black frame).

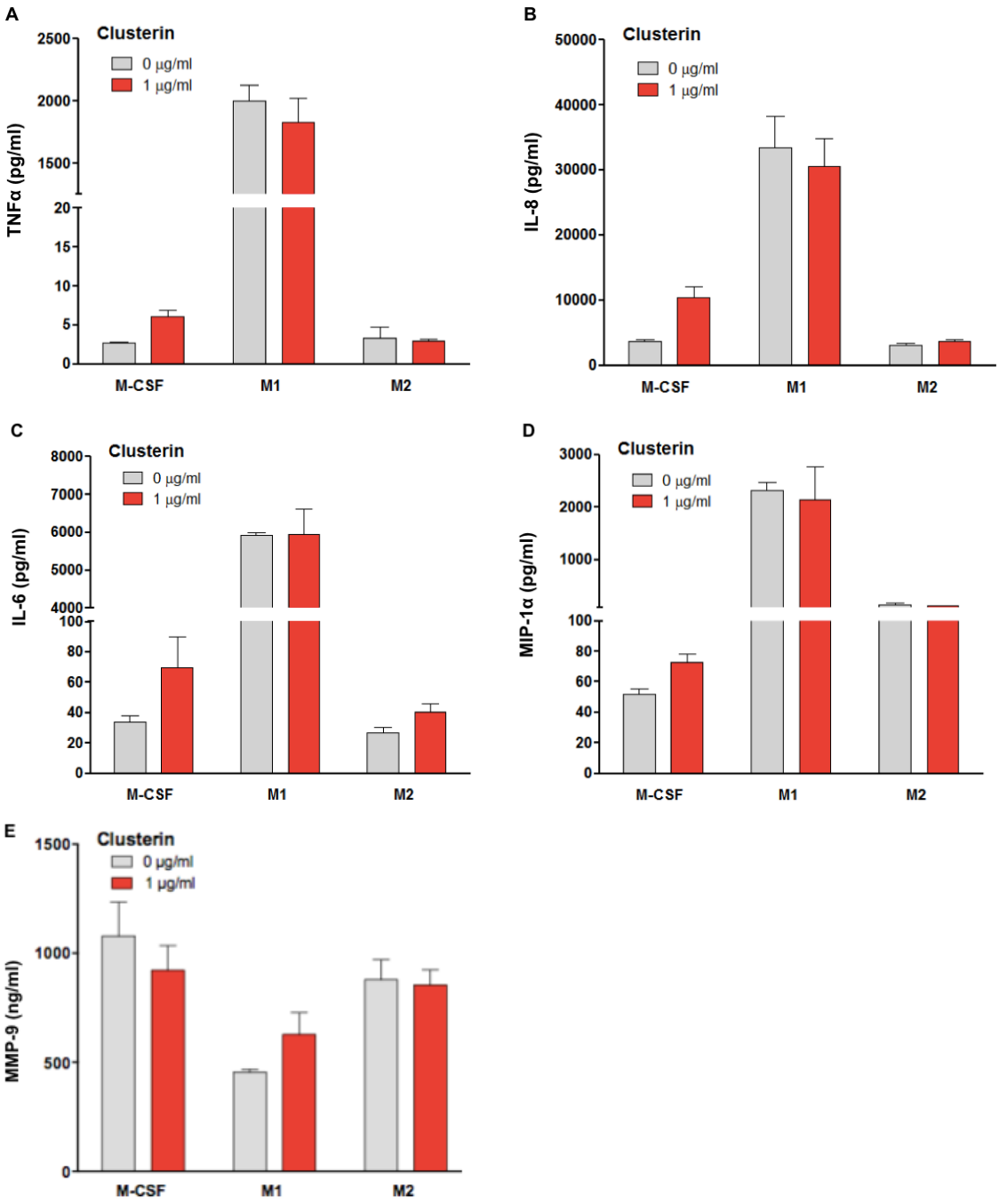

Appendix 4 Donor 2: Effect of exogenous clusterin on cytokine and MMP-9 secretion during polarisation in blood-derived macrophages.

Human blood-derived $CD14^+$ cells were seeded into a 96 well plate (1 x 10^5 cells/well) and were allowed to differentiate into macrophages in the presence of M-CSF (100 ng/ml) for four days. Subsequently, cells were stimulated towards a “M1” phenotype with LPS / IFNγ (at 10 ng/ml for LPS and 50 ng/ml for IFNγ) or a “M2” phenotype with IL-4 (20 ng/ml) or remained untreated (“M0”) in the presence and absence of human plasma-derived clusterin (1 µg/ml) for 72 hours. Cytokine, chemokine and MMP-9 secretion was assessed via Luminex analysis. Bars represent the mean ± SEM of three experimental replicates; significances compared with untreated controls respectively.

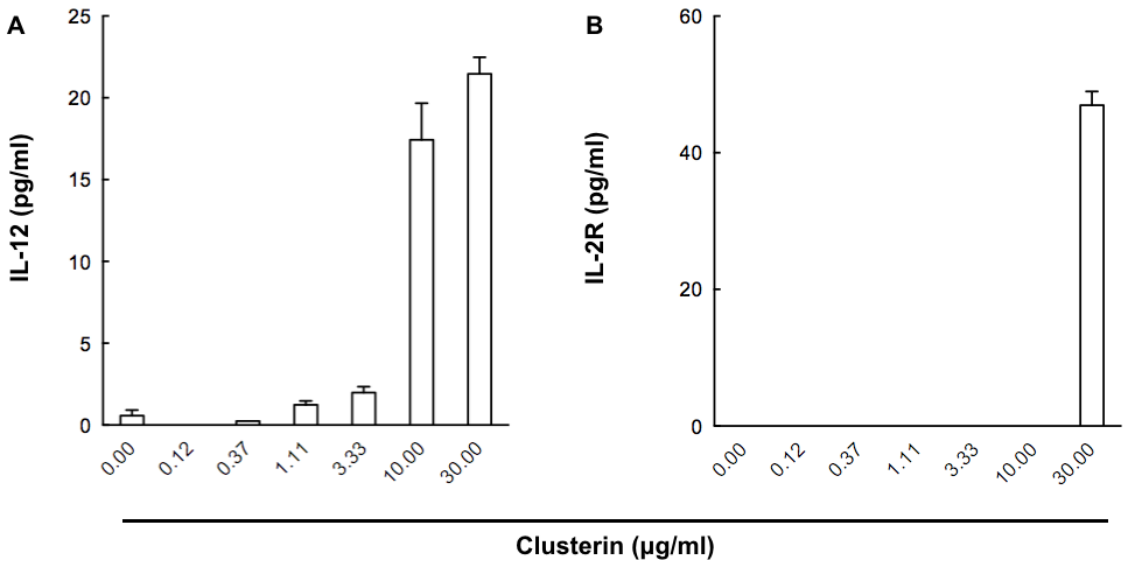

Appendix 5 IL-12 and IL-2R levels are measurable in supernatants of blood-derived macrophages in response to high concentrations of exogenous clusterin.

Human blood-derived macrophages were seeded onto a 96-well plate (1 x 10^5 cells/well), differentiated with M-CSF (100ng/ml) for four days and then exposed to human plasma-derived clusterin at three-fold increasing doses for 72 hours or remained untreated. IL-12 and IL-2R secretion was assessed via Luminex analysis. Bars represent the mean ± SEM of three experimental replicates. One–way ANOVA analysis could not be performed due to immeasurable levels of IL-12 and IL-2R at low concentrations of exogenous clusterin.

Paper, posters and awards

Paper

- Korsen M, Bragado Alonso S, Peix L, Bröker BM, Dressel A. (2015) Cladribine Exposure Results in a Sustained Modulation of the Cytokine Response in Human Peripheral Blood Mononuclear Cells. PLoS One. 2015 Jun 18;10(6):e0129182.

- Peix L, Evans IC, Pearce DR, Simpson JK, Maher TM, McAnulty RJ (in preparation). The yin and yang of clusterin: Diverse functions promote and protect against the development of pulmonary fibrosis.

Poster

- Poster presentation at CRAFT Symposium (GSK, Stevenage). January 2014
- Poster presentation at the 18th International Colloquium on Lung and Airway Fibrosis (ICLAF; Canada). September 2014
- Poster presentation at CRAFT Symposium (GSK, Stevenage). July 2015
- Poster presentation at the American Thorax Society Conference (ATS; California). May 2016
- Poster presentation at the 19th International Colloquium on Lung and Airway Fibrosis (ICLAF; Ireland). September 2016.

Prizes and Awards

- MPhil/Ph.D. Highest mark for MPhil/ Ph.D. upgrade talk in the basic science category (2014).
- Travel award: ICLAF (Canada). September 2014
- Travel award: ATS (USA). May 2016
- Travel award: ICLAF (Ireland). September 2016
- Travel Fellowship from “Action for Pulmonary Fibrosis” (May 2016).